Engineering of Natural Cartilage Substitution Biomaterials

Hazel Louise Fermor

Submitted in accordance with the requirements for the degree of Doctor of Philosophy

The University of Leeds

Faculty of Biological Sciences

September 2013

The candidate confirms that the work submitted is his/her own, except where work which has formed part of jointly-authored publications has been included. The contribution of the candidate and the other authors to this work has been explicitly indicated below. The candidate confirms that appropriate credit has been given within the thesis where reference has been made to the work of others.

Chapter 3 is based on a joint authorship publication, Fermor, H.L., McLure, S.W.D., Taylor, S.D., Russell, S.L., Williams, S., Fisher, J., Ingham, E. Biological, biochemical and biomechanical characterisation of articular cartilage from the porcine, bovine and ovine hip and knee. Bio-Medical Materials and Engineering. In press. As the lead author the candidate was responsible for the laboratory work, analysis and writing of the paper. McLure, S.W.D. and Taylor, S.D. were responsible for laboratory work relating to the biomechanical testing of specific animal osteochondral tissues as indicated in Table 3.1. The contributions of the co-authors included discussions on experimental design of the study, critique and proof reading of the manuscript and obtaining funding for the study.

Acknowledgements

First and foremost I would like to express my sincere gratitude to my supervisor, Professor Eileen Ingham. She has shown great kindness and patience throughout the last four years, without her knowledge and wisdom this work would not have been possible. She is an incredible mentor and a true inspiration. I would also like to thank my co-supervisors Professor John Fisher CBE, Dr Sophie Williams and Dr Serena Russell, for their guidance and for their assistance with all things engineering. Their hard work is very much appreciated.

I would also like to thank all members of the iMBE for their support both academically and socially, they have made my time studying towards this PhD very enjoyable. Special thanks go out to Dr Simon Taylor and Dr Stuart McLure for their assistance with biomechanical testing and to the wonderful people of office 6.64, Carly Taylor, Caroline Gough and Nic Gowland.

My family have provided a constant source of support and without their encouragement I would not be here today. I thank them from the bottom of my heart. Words cannot express the appreciation I have for my incredible husband, Dan. His love and patience have been invaluable and his support both emotionally and academically has enabled me to achieve all that I have so far. Thank you for putting up with my constant ramblings, theories and stupid questions.

I would like to dedicate this work to my Grandmothers, Dorothy and Ivy and also to my beautiful Nephew, Lucas who all sadly passed away during the course of this study.

Abstract

Cartilage lesions cause pain and a loss of joint motion, and if not repaired will further degenerate into an osteoarthritic state. Currently the only treatment options for end stage osteoarthritis are total joint replacements, which are not preferable for younger or more active patients. Early intervention therapies to repair initial cartilage damage and stem the progression of osteoarthritis are thought to be a more favourable treatment option in appropriate cases. It is hypothesised that an acellular xenogeneic osteochondral scaffold could be used in mosaicplasty-like operations to provide an immunocompatible, off-the-shelf biomaterial for osteochondral lesion repair, retaining the same natural composition, structure and function as native cartilage.

Initial characterisation of cartilages from different species (pig, cow and sheep) and joint regions of the hip and knee revealed differences in cartilage biology, biochemistry and biomechanics. Osteochondral tissues from skeletally immature porcine medial condyles were selected along with mature bovine femoral groove tissues as source materials for decellularisation, primarily based on cartilage thickness and glycosaminoglycan (GAG) content.

Bovine osteochondral pins were subject to a number of decellularisation protocols and were shown to be successfully decellularised following use of a water pik to remove bone marrow, four cycles of freeze-thaw (two of which were in a hypotonic buffer with protease inhibitors), two cycles of hypotonic buffer followed by incubation in 0.1 % (w/v) SDS with protease inhibitors and treatment with nucleases and sterilisation with 0.1 % (v/v) peracetic acid. The process removed all whole cell nuclei, as visualised by histology and reduced cartilage DNA content per cartilage dry weight to 39 $ng.mg^{-1}$. However, the process removed 99% of GAGs and resulted in reduced biomechanical properties.

Porcine osteochondral pins were fully decellularised following use of the above process with one cycle of incubation in hypotonic buffer and 0.1 % (w/v) SDS in hypotonic buffer. Cartilage DNA content was reduced by 98% and the osteochondral tissues contained no visible cell nuclei. Cartilage GAG content was reduced by 60 %. Further alterations to the protocol to improve GAG retention revealed cartilage damage; histologically appearing highly porous and having greatly increased water content and almost

complete GAG loss. A comprehensive investigation was conducted to identify the cause of the damage, however no protocol could be developed which completely eradicated cartilage damage.

Further characterisation of acellular bovine osteochondral scaffolds showed that a low concentration of SDS remained in the bone, and that this had cytotoxic effects when incubated in contact with BHK cells. Further washes in PBS were added to the protocol to remove excess SDS, however this increased washing led to damage of the bovine cartilage, as seen previously in porcine osteochondral decellularisation.

Finally, the decellularisation process was applied to whole porcine condyles in which the ratio of cut edge to cartilage area was minimised and minimal damage to the decellularised cartilage was seen. In summary, the complex microstructure of cartilage has been shown to be surprisingly fragile *ex vivo* and a novel approach to the development of clinically relevant acellular osteochondral grafts is required; however significant advances have been made in the current study.

Table of Contents

List of Tables

List of Figures

List of Abbreviations

ACI	Autologous chondrocyte implantation
ACL	Anterior cruciate ligament
ADAMTS	A disintegrin and a metalloprotease with thrombospondin motifs
AMCI	Autologous matrix induced chondrogenesis
ANOVA	Analysis of variance
APC	Antigen presenting cell
ATP	Adenosine triphosphate
BHK	Baby hamster kidney
BMP	Bone morphogenic protein
BSA	Bovine serum albumen
BSE	Bovine spongiform encephalopathy
CDMP	Cartilage-derived morphogenic protein
CHAPS	3-[(3-cholamidopropyl)dimethylammonio]-1-propanesulfonate
CILP	Cartilage intermediate layer protein
CL	Confidence level
CMP	Cartilage matrix protein
COMP	Cartilage oligomeric matrix protein
CPM	Counts per minute
CS	Chondroitin sulphate
CTGF	Connective tissue growth factor
DABCO	1,4-diazobicyclo-(2, 2, 2)-octane
DAPI	4’,6-diamidino-2-phenylindole
DMB	1,9- dimethylemethylene blue
DMEM	Dulbecco’s modified Eagle’s medium

DMSO	Dimethyl sulphoxide
DNA	Deoxyribonucleic acid
DNase	Deoxyribonuclease
ECM	Extracellular matrix
EDTA	Ethylenediaminetetraacetic acid
ELISA	Enzyme-linked immunosorbent assay
FBS	Foetal bovine serum
FE	Finite element
FGF	Fibroblast growth factor
GAG	Glycosaminoglycan
Gal	Galactose
GalNAc	N-acetylgalactosamine
GlcUA	Glucuronate
GMEM	Glasgow’s minimal essential media
H&E	Haematoxylin and eosin
HA	Hyaluronan (hyaluronic acid)
HAS	Hyaluronan synthase
HGF	Hepatocyte growth factor
HLA	Human leukocyte-associated
ICRS	International cartilage repair society
IFN	Interferon
IGD	Interglobular domain
IGF	Insulin-like growth factor
IL	Interleukin
KS	Keratan sulphate
LIF	Leukaemia inhibitory factor
LP	Link protein
LPS	Lipopolysaccharide
LVDT	Linear variable differential transducer

MACI	Matrix assisted chondrocyte Implantation
MHC	major histocompatibility complex
MMP	Matrix metalloproteinase
MRI	Magnetic resonance imaging
MSD	Minimum significant difference
NBF	Neutral buffered formalin
NO	Nitric oxide
OA	Osteoarthritis
OSM	Oncostatin M
PAA	Peracetic acid
PAR	Protease-activated receptor
PAS	Periodic acid and Schiff’s reagent
PBS	Phosphate buffered saline
PCL	Posterior cruciate ligament
PCL	poly (ε-caprolactone)
PEGDA	Poly(ethylene glycol) diacrylate
PERV	Porcine endogenous retrovirus
PGA	Polyglycolic acid
PLA	Polylactic acid
PVA	Polyvinyl alcohol
RNA	Ribonucleic acid
RNase	Ribonuclease
SAL	Surface amorphous layer
SDC	Sodium deoxycholate
SDS	Sodium dodecyl sulphate
SIS	Small intestinal submucosa
SLRP	Small leucine-rich repeat protein
SZP	Superficial zone protein
TBS	Tris buffered saline

TGF	Transforming growth factor
TNF	Tumour necrosis factor
TPB	Tryptone phosphate broth
TSE	Transmissible spongiform encephalopathys
VAS	Visual analogue scale
α-gal	Galactose α1-3 galactose

Chapter 1
Introduction

1.1 General introduction

Osteoarthritis (OA) is a major public health concern, causing high levels of morbidity within the population and posing a large socioeconomic burden (Brooks, 2006). It is the most common disease affecting joints, and is characterised by irreversible progressive articular cartilage damage leading to joint failure (Herrero-Beaumont *et al.*, 2009). Increasingly, OA is being recognised as a disease of the entire joint. Initial injury to the cartilage itself or other joint tissues such as ligaments can affect load distribution and friction during joint articulation, this abnormal activity leads to progressive erosion of the cartilage and malalignment of the joint resulting in further damage, including damage to the muscles and tissue inflammation (Felson, 2009).

It is clear from the progressive nature of the disease that initially minor cartilage surface damage can lead to a much greater physiological disorder. Therefore early intervention treatments are crucial to prevent or delay the development of debilitating OA, and avoid end stage treatments such as total joint replacement. There are currently a number of therapies available to treat initial cartilage lesions, however these are often ineffective, only having short-term therapeutic benefit or causing difficulties such as donor site morbidity. Considering these therapies, it is proposed that a new tissue engineered approach may provide a better treatment option.

.

1.2 Anatomy

1.2.1 The hip joint (acetabulofemoral)

The hip joint (Figure 1.1) is commonly affected by OA, as a load bearing joint, the surface cartilage is exposed to high mechanical stress leading to wear. Here the acetabulum of the pelvis articulates with the head of the femur through a synovial 'ball and socket' joint allowing for flexion, extension and rotation. The articulating surfaces of the acetabulum and femoral head are lined with hyaline cartilage which reduces friction allowing the joint to function. The hemi-spherical femoral head is held in the acetabulum by a fibrocartilaginous labrum lip which extends past the bony element of the acetabulum.

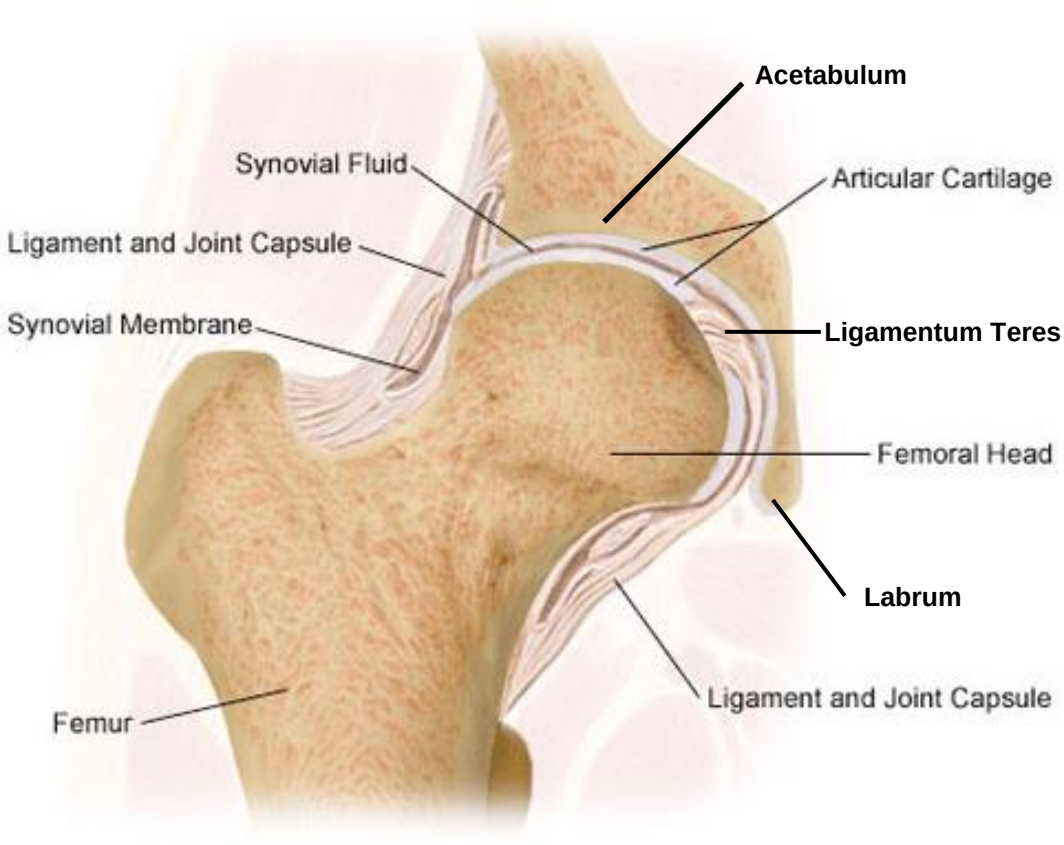

Figure 1.1 The hip joint. Diagram entailing the main features of the joint. Figure adapted from http://www.noc.nhs.uk/hipandknee/information/hip/joint-anatomy.aspx.

The synovial membrane and fibrous capsule are attached to the femoral neck (zona orbicularis) and the labrum encasing the femoral head and acetabulum, they contain synovial fluid which provides lubrication and cushioning for the joint. The capsule along with one intracapsular (ligamentum teres) and three extracapsular ligaments (iliofemoral, ishiofemoral and pubofemoral) provide mechanical stability for the joint (Gray, 2000; Sinnatamby, 2006).

1.2.2 The knee joint

The knee joint (Figure 1.2) is the largest synovial joint in the body. An effective 'hinge' joint, it allows for flexion and extension, as well as slight rotation in some positions. It is a complex joint which articulates between a) the femur and the patella, via a sellar joint whereby the patella slides through the patellofemoral grove, and b) the tibio-femoral joint, which articulates the medial and lateral condyles of the femur with the tibial plateau; these interactions are partially divided by the two menisci. The condyles of the femur and the tibial plateau are, like the articular surfaces of the hip joint, lined by hyaline cartilage, allowing reduced friction. The medial and lateral menisci are composed of fibrocartilage, which has different biological and mechanical properties from hyaline cartilage, allowing it to cushion the joint effectively.

The joint is surrounded by an articular capsule which is composed of a strong fibrous membrane lined by the synovial membrane. The capsule is attached to the cartilage margins on both the femur and the tibia and to the head of the fibula The presence of a suprapatellar bursa anteriorly on the femur results in the joint capsule being attached more proximally than the cartilage. As with the hip joint, the capsule provides stability to the joint, and encloses the synovial fluid which provides lubrication for the joint. Ligaments act alongside the capsule to provide stability to the joint by limiting movement. Intracapsular ligaments include the anterior (ACL) and posterior cruciate ligaments (PCL), injury to which may often result in damage to cartilage, leading to OA (Felson & Zhang, 1998). The

transverse ligament, anterior and posterior meniscofemoral and the meniscotibial ligaments are also intracapsular. The patellar tendon is associated with the quadriceps tendon to secure the patellar. The sides of the patellar are attached to the capsule, allowing its articulating surface to be intracapsular but the non-articulating face of the patellar to be extracapsular. The patellar tendon is attached to the extracapsular non-articulating face of the patella. Extracapsular ligaments include the medial and lateral collateral ligaments and the oblique and arcuate popliteal ligaments. There are a number of bursae associated with the knee joint, these fluid sacks and synovial pockets surround and communicate with the joint cavity, cushioning impact between bones and tendons and/or muscles, and they also act to further reduce friction (Gray, 2000; Sinnatamby, 2006).

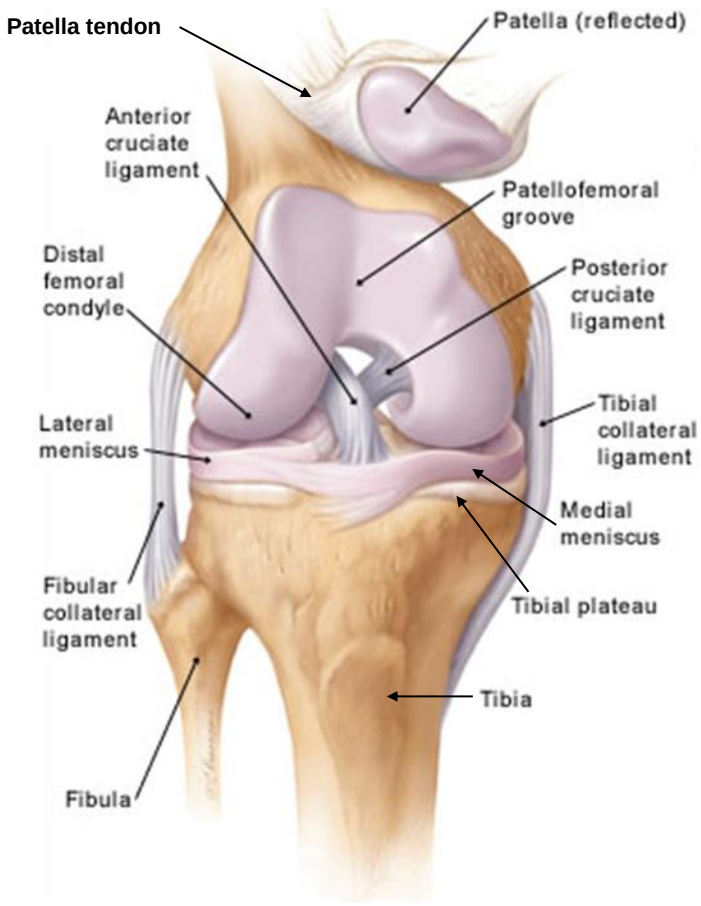

Figure 1.2 The knee joint. Articulation between the femur, patella and tibia. Figure adapted from http://www.digital-doc.com/images/knee.jpg.

1.3 Cartilage

There are three forms of cartilage; elastic cartilage (for example the ear), fibrocartilage (menisci) and hyaline cartilage (synovial joints; Roughley, 2006). Hyaline cartilage covers the articulating surfaces of bones at joints, the function of which is to reduce friction between articulating surfaces during load bearing and movement. Hyaline cartilage is a tough tissue formed predominantly of extracellular matrix (ECM) composed of interwoven collagen fibres, proteoglycans and interstitial water. These components are secreted by chondrocytes which reside dispersed within the ECM. Cartilage is avascular and aneural, qualities which result in limited repair capacity of the tissue.

1.3.1 Cartilage composition

Cartilage is a highly specialised tissue, able to effectively lubricate articular joints throughout a lifetime of movements without experiencing any significant wear. This is possibly due to its ideal composition and structure. The key components of cartilage are collagen, proteoglycans, interstitial water, chondrocytes and lubrication by synovial fluid.

1.3.1.1 Collagen

Collagen comprises ~15% of cartilage ECM and it is present as a network of interwoven fibres. Each procollagen molecule is composed of three α-chains which contain a repeated Gly-X-Y sequence where X is most commonly a proline residue and Y a hydroxyproline residue This repeat region is flanked by short linear telometric regions and globular N- and C-terminal pro-peptides. The stoichiometry of these amino acids results in the chain being a left-handed α-helix. The three chains interact with one another to form a superhelix. These chains can form hetero- or homotrimers, the composition of which, determine the type of collagen fibre produced (Cremer *et al.*, 1998). Cleavage of the procollagen terminal peptides by specific proteases (metalloproteases and disintegrin) allows the spontaneous formation of collagen fibrils (Steplewski *et al*., 2007).

The most dominant form of collagen in cartilage ECM is type II collagen, a homotrimer of α_1(II) chains, it constitutes ~80-85% of the total collagen content. Collagen IX and XI are the second most common comprising ~3-10% each. Both are heterotrimeric, collagen type IX has a large N-terminal globular domain from an α_1(IX) chain, it also has a 'kink' mid chain from which a chondroitin sulphate rich glycosaminoglycan (GAG) chain extends. It runs antiparallel to the fibre and is situated at points of regular D-periodicity (alternating gap and overlap regions along the fibre exterior (Steplewski *et al*., 2007)). Type XI collagen resembles type II in that it is also a straight chain, however some molecules have an α_3(XI) chain propeptide at the N-terminus which projects from the fibril, this molecule is covalently cross-linked to collagen type II molecules in the fibre backbone at hydroxylysine residues. Collagen X is a straight chained cartilage specific homotrimer, although shorter than collagens II or XI, these form a multimeric collagen fibril (Figure 1.3). Type VI collagen is also found sparsely in cartilage (Cremer *et al.*, 1998).

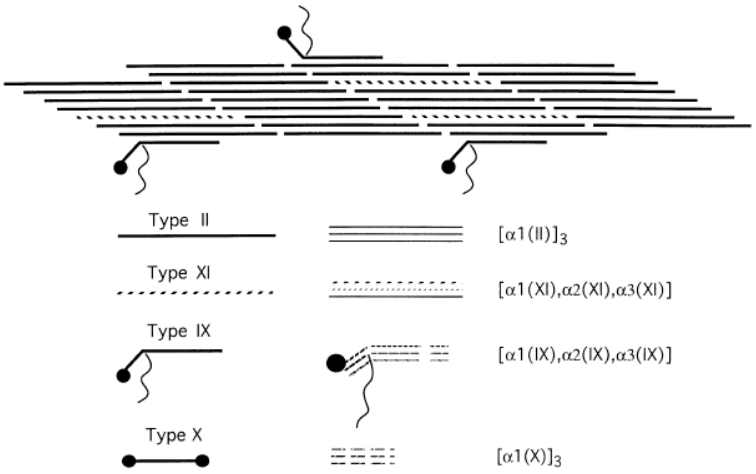

Figure 1.3 Collagen fibril composition. A diagrammatical representation of cartilage fibril composition and the collagen molecules which are specific to articular cartilage. Fibril composition is mainly type II collagen (solid line) with internal type XI collagen (dotted line) molecules and surface type IX molecules (bent line with globular domain). Type X is not intrinsic to the fibril formation and is found elsewhere in the collagenous matrix of cartilage. Figure cited from Cremer *et al.* (1998).

The backbone of heteropolymeric cartilaginous fibrils is mainly formed from type II collagen, type IX is thought to play a role in facilitating the interaction of fibrils with proteoglycans along with acting as a ‘spacer’ between fibrils and a ‘glue’ to bind the type II lattice. Collagen type XI regulates fibril length (Mendler *et al*., 1989; Cremer *et al.*, 1998). Type VI collagen forms independent microfibrils in the ECM around lacunae (Cremer *et al.*, 1998) and plays a role in chondrocyte attachment to the ECM (Poole, 1997) Type X is most abundant in areas where hypertrophic chondrocytes are found (Cremer *et al.*, 1998) and is thought to play a role in the organisation and distribution of cartilage matrix components (Shen, 2005).

Collagen fibres are organised with a specific orientation in the cartilage matrix, known as the arcade concept (Figure 1.4). In the deep calcified zone of cartilage, collagen fibres are anchored to the bony component and run vertically toward the surface in the radial zone, these then turn obliquely in the transitional zone and run parallel to the surface in the tangential zone (Jeffery *et al,*, 1991). The anchorage of collagen fibres into the subchondral bone ensures the soft cartilage tissue and solid bone are firmly fixed together. The specific organisation of collagen fibres in the cartilage structure has a major impact on the mechanical properties of the tissue, as will be discussed later. This inhomogeneity of collagen fibre distribution within cartilage results in differing values of permeability throughout the layers of the tissue with the middle zone being relatively permeable compared to the superficial and deep zones. There are dense collagen fibres at the superficial zone, but a high charge density in the deep zone (Mow *et al*., 1984).

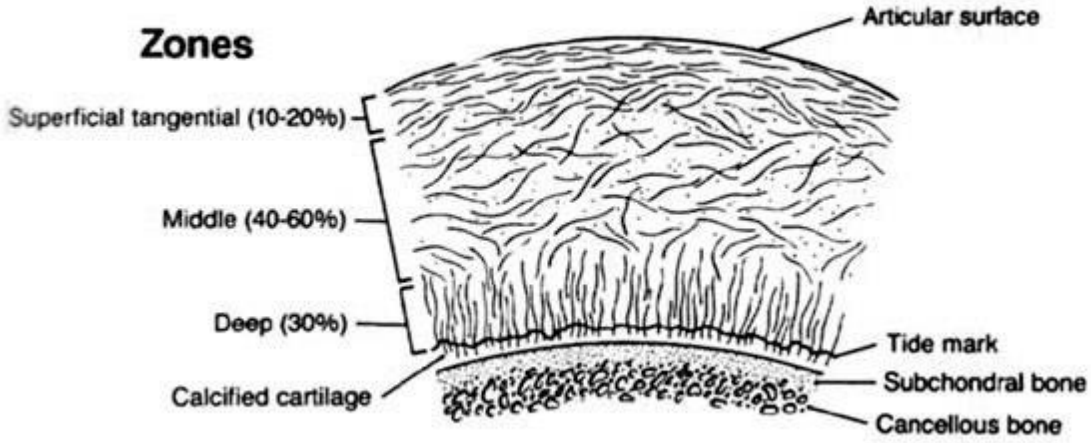

Figure 1.4 Arcade concept of collagen organisation. Collagen fibre orientation is altered though the different layers of the cartilage tissue.

1.3.1.2 Proteoglycans

Proteoglycans are highly glycosylated proteins comprised of a core protein covalently linked to one or more glycosaminoglycan (GAG) chains. A GAG is a disaccharide unit which is repeated to form a long unbranched chain. Aggrecan (Figure 1.5) is a highly abundant, key proteoglycan in cartilage; it exists in the form of large aggregates with hyaluronan (HA) and link protein (LP). Aggrecan is a modular protein with three globular domains (G1, G2 and G3) which contain cystine residues for the formation of disulphide bonds. There is a short interglobular domain between G1 and G2, and between G2 and G3 there is a long GAG attachment region rich in keratan sulphate (KS) and chondroitin sulphate (CS). The N-terminal G1 domain is responsible for attachment to HA, the function of G2 is currently unknown, G3 is key for normal post-translational modification of aggrecan, ensuring correct secretion from the cell (Roughley, 2006). The GAG attachment region is divided into 3 sections, the keratan sulphate attachment region, which is closest to G2, and the adjacent chondroitin sulphate attachment region is comprised of two sections.

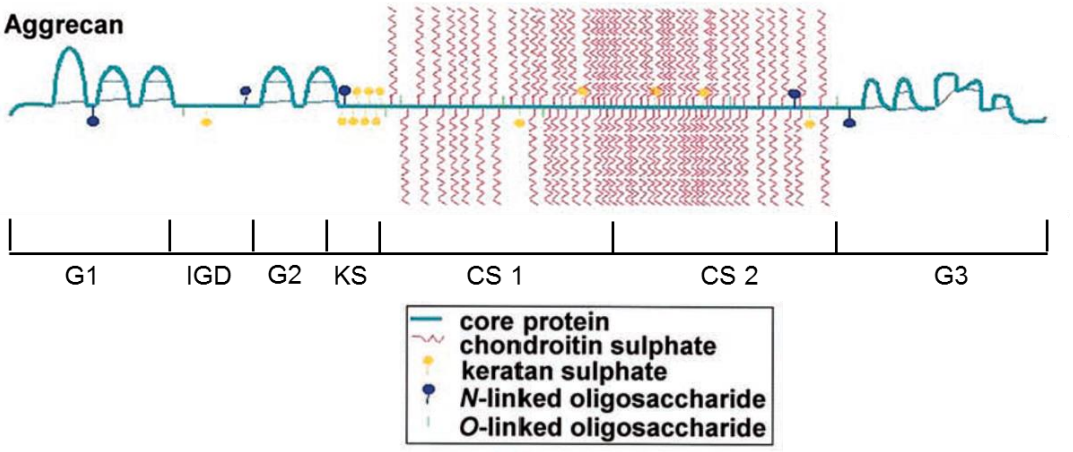

Figure 1.5 Aggrecan. Aggrecan molecule showing all three globular regions (G1, G2 and G3), the interglobular domain (IGD) and the GAG attachment region comprised of one keratan sulphate binding region (KS) and two chondroitin sulphate binding regions (CS1 and CS2). Figure adapted from Dudhia (2005).

Aggrecan exists as large aggregates in cartilage (Figure 1.6) entrapped within the collagenous network. These aggregates are composed of one long HA molecule attached to up to 100 aggrecan molecules stabilised by a link protein (Roughley, 2006). The link protein is similar in structure to the aggrecan G1 region. Through its ability to bind both HA and aggrecan G1 regions, the presence of link protein stabilises the attachment of aggrecan to HA, retaining association of the aggregate under physiological conditions. It also facilitates association of newly secreted aggrecan molecules with HA and finally along with the G1 region of aggrecan forms a protein coat surrounding the HA molecule to protect it from degradation by enzymes or free radicals (Roughley, 2006).

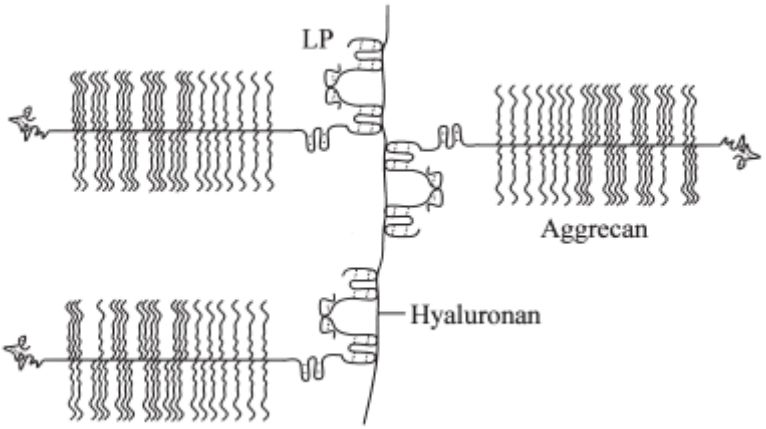

Figure 1.6 Proteoglycan aggregate. Proteoglycan aggregate of aggrecan molecules attached to a single hyaluronan chain stabilised by link protein (LP). Three aggrecan molecules are shown here, but up to 100 can be attached to a single hyaluronan molecule. Figure cited from Dudhia (2005).

HA is a unique GAG of notably large molecular weight, it is unsulphated. The HA polysaccharide chain is composed of a repeated disaccharide unit of glucuronate (GlcUA) and N-acetylgalactosamine (GlcNAc; Figure 1.7), the size of the chain decreases as HA abundance increases with age, which may be relevant to osteoarthritis onset later in life. The decrease in size is thought to be related to degradation of the GAG post synthesis (Roughley, 2006). HA molecules have carboxyl groups along their length which are fully ionised at physiological pH, resulting in the molecule having high osmotic activity allowing it to affect the distribution and movement of water (Fraser *et al*., 1997). Formation of secondary hydrogen bonds along the chain produces twists resulting in some stiffness of the molecule and hydrophobic patches which assist the molecule in interacting with other HA chains to form a network and allow association with lipid structures such as cell membranes (Scott, 1992). HA is synthesised at the chondrocyte plasma membrane by hyaluronan synthase (HAS) of which there are three types. The HAS's produce the same composition, however vary in the length of HA chain they synthesise, which may have implications of the overall matrix composition (Roughley, 2006).

The GAG side chains are the key to aggrecan function; they have a fixed negative charge which allows hydrophilic interactions between the proteoglycan molecules of the cartilage ECM and interstitial water, controlling the movement of water through the collagen network. Chondroitin sulphate and keratan sulphate (Figure 1.7) are the GAGs associated with aggrecan (Roughley, 2006), they attach at serine residues located along the core protein chain within the GAG attachment region of aggrecan.

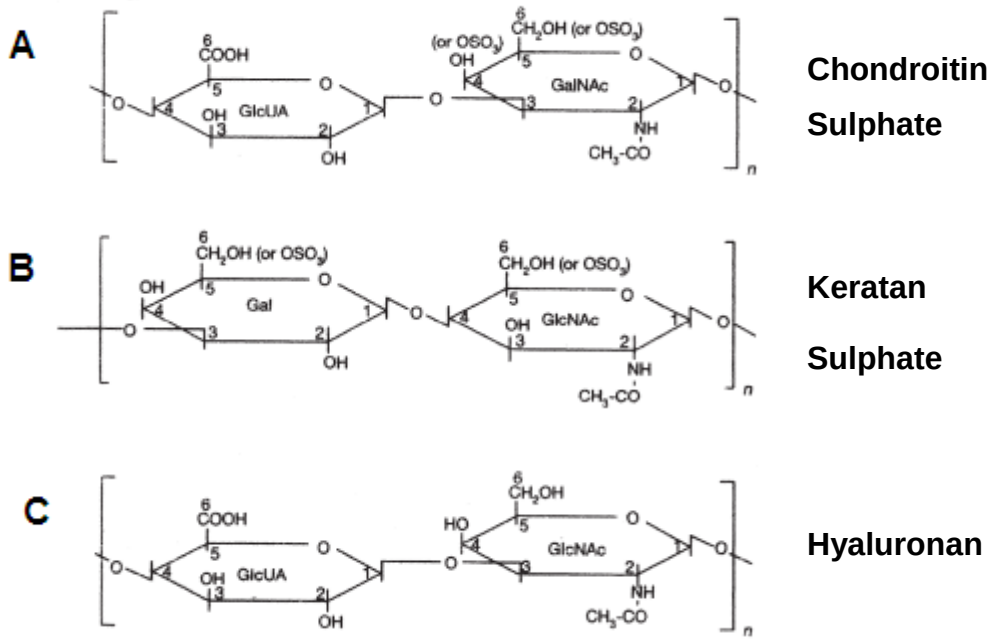

Figure 1.7 Glycosaminoglycan molecular structures. A - Chondroitin sulphate disaccharide unit, showing specific sites where the sugar can be sulphated, unit is repeated many times to form a GAG chain. B – keratan sulphate disaccharide unit, also showing possible sulphated regions, unit is repeated many times. C – Hyaluronan disaccharide unit, characteristically unsulphated, repeated to form a long polysaccharide chain. Figure adapted from Dudhia (2005).

GAGs are polysaccharides composed of repeating disaccharide units of one of two modified sugars: GalNAc or N-acetylglucosamine, and a uronic acid: GlcUA, iduronate or galactose (Gal). The sulphate and acidic substitutions on the chains of KS and CS result in the molecule being polyanionic. CS is post translationally modified with sulphate ester

substitutions at carbon-4-*O*-hydroxyl or carbon-6-*O*-hydroxyl positions of many of the GalNAc residues, which can be unsulphated, monosulphated or disulphated. These negatively charged groups within the GAG are fixed to the aggrecan protein and provide the proteoglycan with its hydrophilic properties (Dudhia, 2005).

KS GAG chains associate with the aggrecan protein in the KS region, where there is a repeated residue motif of Glu-Glu/Lys-Pro-Phe-Pro-Ser (Antonsson, 1989), KS molecules attach at the serine residue. There are also KS chains in the G1 domain attached by N- and O-linked substitutions. A few KS chains are also found in the CS rich regions of aggrecan attached via O-linked substitutions on threonine residues (Barry *et al*., 1992). The proline-rich repeats of the KS attachment region have a moderate affinity for collagen, allowing interaction with the collagenous network of the cartilage matrix (Hedlund *et al*., 1999). The CS rich region of aggrecan also contains a repeated motif of either Ser-Gly-X-Gly in the CS1 region or (Asp/Glu)-X-Ser-Gly in the CS2 region (Doege *et al*., 1997).

1.3.1.3 Non-collagenous proteins

There are other proteins in the cartilage matrix besides aggrecan aggregates and collagens, these include other proteoglycans, such as members of the small leucine-rich repeat protein (SLRP) family. There are also a number of structural proteins which are of importance in cartilage function. Other proteins found in articular cartilage play a regulatory role in controlling cellular activities; their involvement is not directly relevant to the mechanical function of the cartilage matrix (Roughley, 2001). These proteins play various roles in the cartilage matrix, some of which are listed in Tables 1.1 and 1.2.

Proteoglycan	Function	Reference
Decorin	SLRP associated with collagen fibrils as a decorating proteoglycan, carries a dermatan or chondroitin sulphate chain, thought to play a role in fibril diameter regulation. Decorin knockout mice have shown reduced tensile strength of skin and tendons.	Knudson & Knudson, 2001, Danielson *et al*., 1997
Biglycan	SLRP with two chondroitin or dermatan sulphate chains is found primarily in the pericellular matrix of cartilage. Biglycan interacts with collagen type IX and II regulating fibril formation and stability.	Knudson & Knudson, 2001 Chen *et al*.,2006
Lumican	SLRP with keratan sulphate GAG chains is able to bind collagen fibres to modulate fibril formation and the GAG chain acts to regulate interfibrillar spacing.	Nikitovic *et al*., 2008
Fibromodulin	Another keratan sulphate SLRP acts along with decorin, biglycan and lumican to regulate collagen fibril diameter and stability. It is probable that there is a level of redundancy between these small glycoproteins.	Hedlund *et al.,* 1994 Roughley, 2001
Perlecan	Perlecan is commonly substituted with heparin or chondroitin sulphate GAG chains. Located pericellularly, perlecan is able to stimulate fibrillogenesis when glycosylated with 4-6-disulphated chondroitin sulphate residues.	Melrose *et al*., 2008 Kvist *et al*.; 2006
SZP/Lubricin	A secreted glycoprotein, lubricin is present at the superficial zone of articular cartilage. It functions to lubricate the articular surface, reducing wear, and also to inhibit invasion of the cartilage surface by synoviocytes and prevent protein deposition onto the surface by synovial fluid.	Rhee *et al*., 2005 Roughley, 2001

Table 1.1 Non-collagenous Proteins – Proteoglycans. A list of the less common cartilage structural proteins, detailing their function within the tissue. SZP= Superficial zone protein.

Structural protein	Function	Reference
COMP	A disulphide-bonded pentamer, the carboxy-terminal regions of which interact with collagen fibrils, the correct folding of the molecule is determined by calcium binding. The protein has also been shown to interact with cell surface integrins supporting cellular attachment. COMP is thought to play an important role in matrix assembly.	Chen *et al*., 2005 Hecht *et al*., 2005
Matrilin-1/CMP **& Matrilin-3**	Matrilins are a family of proteins, matrilin-3 is normally associated with matrilin-1, however matrilin-1 is only expressed at low/negligible levels in articular cartilage whereas matrilin-3 is more abundant. It is thought that matrilins are able to interact with aggrecan, COMP and decorin molecules as well as collagen fibrils, acting in a structural capacity.	Wagener *et al*., 2005 Segat *et al*., 2001
CILP	Found in the intermediate zone of articular cartilage, this protein is thought to play a role in modulating the architecture of the cartilage matrix, but has also shown to be an IGF-1 antagonist.	Johnson *et al*., 2003
Fibronectin	There is a unique splice variant of fibronectin produced by chondrocytes. This protein is involved in cell-matrix interactions.	Roughley, 2001 Burton-Wurster *et al*., 1998

Table 1.2 Non-collagenous Proteins – Structural Proteins. A list of the less common cartilage structural proteins, detailing their function within the tissue. COMP= Cartilage oligomeric matrix protein (thrombospondin-5), CMP= Cartilage matrix protein (matrilin -1), CILP= Cartilage intermediate layer protein.

1.3.1.4 Interstitial water

The interstitial water of the ECM plays an integral role in cartilage function through interactions with GAG molecules, it forms 60-85% wet weight of cartilage. Water is composed of two hydrogen atoms covalently bound to an oxygen atom. The molecule is not linear, and oxygen has a higher electronegativity than hydrogen, resulting in a dipole. The slight positive charge on the hydrogen atoms allows for interaction with charged molecules.

Water within the cartilage tissue contains small proteins, metabolites and a high concentration of cations (Buckwalter & Mankin, 1998). The immobilised sulphate and carboxyl groups on CS and KS of aggrecan become charged in solution and produce a net negative charge in the tissue relative to the surrounding fluid. These negative fixed charges are situated close together in the collagen network and repel one another, this unbalanced charge density is neutralised by increased positive sodium ion concentration, and repulsion of negative chloride ions in the fluid. The overall increase in total inorganic ion concentration results in increased osmolarity of the tissue – creates a Donnan effect, causing water to enter the tissue and swell the cartilage. However, this Donnan osmotic pressure is resisted by the tensile strength of the collagen network, allowing the tissue to resist deformation (Mow *et al*., 1984; Buckwalter & Mankin, 1998).

1.3.1.5 Chondrocytes

Articular cartilage is exclusively populated by one cell type, chondrocytes. The cells are sparsely dispersed and exist in the cartilage matrix as chondrons, a unit comprising one cell linked at its surface to a pericellular glycocalyx which is encased in a fibrillar pericellular capsule. The morphology of chondrons differs throughout the different layers of the cartilage tissue (Figure 1.8), in the superficial zone the chondrocytes are flattened disc-shape, these become rounded and spherical in the middle layers. In the deep layer, chondrocytes are rounded and arranged in linear columns. In the calcified layer, chondrocytes are also rounded and surrounded by uncalcified lacunae (Poole, 1997).

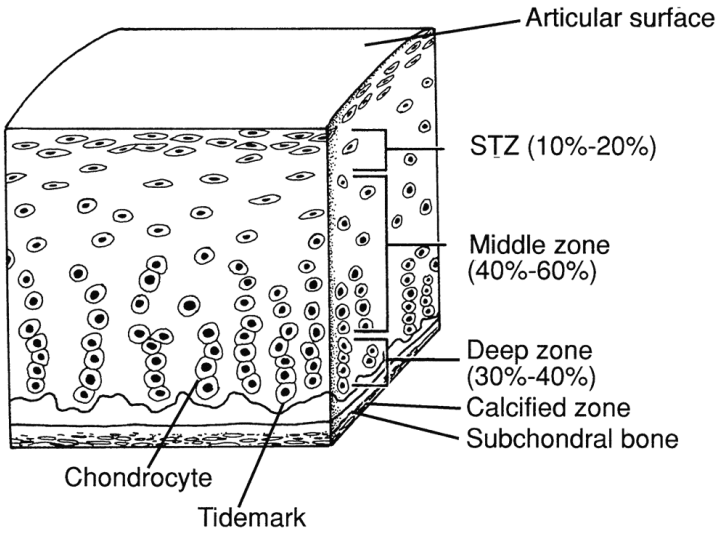

Figure 1.8 Chondrocyte distribution and morphology. The distribution and morphology of chondrocyte chondrons within the cartilage layers.

There is a degree of polarity, with the chondron pole facing the articular surface being more dense than the basal pole (Figure 1.9). A loosely woven ‘tail’ can be seen at the basal pole and in columns of multiple chondrons these ‘tails’ form interconnecting segments between chondrons, ensuring that adjacent chondrons are aligned linearly (Poole, 1997).

The composition of cartilage matrix has already been defined in terms of horizontal matrix subdivisions, however many studies have highlighted a circumferential differentiation of matrix composition, based on pericellular, territorial and interterritorial matrices surrounding each chondrocyte. The pericellular matrix is in direct contact with the chondrocyte, and contains high concentrations of HA, sulphated proteoglycans, biglycan and a number of glycopoteins including link protein, fibronectin and laminin. Collagen composition also differs in these concentric subdivisions, with thinner fibrils being tightly interwoven to encase the cell in the pericellular region. In the territorial region, the collagen fibrils are larger and form radial bundles; this region is dense in chondroitin sulphate, whereas keratan sulphate is most concentrated in the interterritorial regions where the collagen fibres are largest and can form the classical ‘collagen arcade’ structural organisation. As described previously, there are different types of collagen, these are not uniformly distributed in the matrix, with type VI

being exclusively pericellular. Type IX is also more concentrated in the pericellular region (Poole, 1997).

The pericellular matrix of the chondron is thought to be highly specialised, providing hydrodynamic protection for the chondrocyte during physiological loading due to high pericellular concentrations of HA and aggrecan in combination with differential organisation of specific collagen molecules. The pericellular matrix also plays a metabolic role in retention, temporal assembly and spatial migration of synthesised macromolecules in the different chondron territories (Poole, 1997).

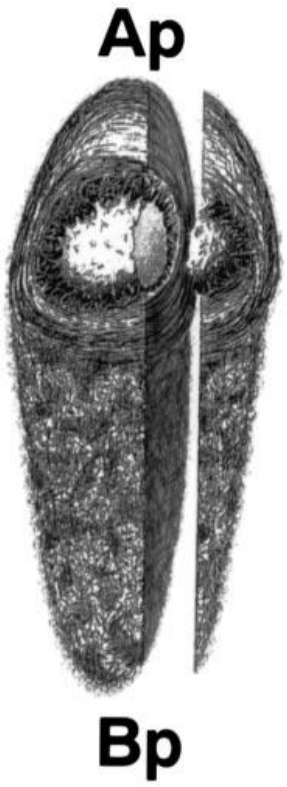

Figure 1.9 Chondron composition and morphology. Three-dimensional cutaway representation of a single chondron showing the central chondrocyte, dense collagen organisation at the articular pole (Ap) and more loosely packed collagen tail at the basal pole (Bp). Figure from Poole (1997).

The role of chondrocytes is to secrete and maintain components of the ECM, these processes are tightly controlled by a number of regulatory factors (Goldring, 1999). Chondrocytes are cells of the mesenchymal lineage (Pettenger *et al.,* 1999) and differentiate from mesenchymal stem

cells to initially produce an osteochondral precursor cell, which further differentiates down a chondrogenic route to produce chondrocytes, thought to be the default differentiation state of the precursors (Hartmann, 2006). Sox9 is the key transcription factor responsible for ensuring differentiation of an osteochondral progenitor cell towards a chondrogenic rather than osteogenic lineage, it recruits further chondrocyte specific transcription factors Sox5 and Sox6 (Lefebvre *et al*., 2001; Hartmann, 2006).

1.3.1.6 Synovial fluid

The synovial intima is the thin cellular layer which lines the luminal surface of the synovial membrane in the joint capsule. This layer is populated by synoviocytes, which can be two to three cells deep. There are two different types of synoviocytes, type A are resident macrophages which phagocytose debris and waste from the joint cavity, and the more abundant type B are fibroblast-like cells which are involved in secretion of matrix constituents such as HA. Type B cells have a characteristically high endoplasmic reticulum content, suggesting that they are active in protein synthesis. These cells secrete HA, collagens, fibronectin and other glycosaminoglycans into the intimal interstitium and joint cavity. Type B cells have long membranous processes that extend into the joint cavity allowing a larger surface area for delivery of secreted products (Iwanaga *et al*., 2000).

The composition of synovial fluid is almost identical to that of blood plasma, with the exception of larger globulins which are filtered out as plasma passes through synovial capillary walls. There are additional molecules secreted into the synovial fluid by synoviocytes. The level of glucose in synovial fluid is lower than that of plasma, as it is metabolised by chondrocytes (Gerwin *et al*., 2006).

HA and lubricin have been reported to determine the viscosity of synovial fluid, allowing its primary function as a lubricant, they cause the fluid to be a thixotropic non-newtonian fluid which decreases in viscosity as the shear strain rate increases. The fluid forms a thin film over the synovial membranes and joint surfaces to provide effective hydrodynamic

lubrication at low shear rates. The viscoelasticity of HA allows it to behave as a viscous lubricant at low impact movements, and as an elastic shock absorber under high impact movement, maintaining joint homeostasis. Under high load, lubricin is thought to play a role by interacting with surface-active phospholipids (Gerwin *et al*., 2006).

1.3.2 Cartilage function

The role of cartilage in the synovial joint is to effectively transmit loads and articulate with low levels of friction. During normal walking conditions, articular cartilage in the lower joints often has to withstand very high loads of up to 4 times body weight, the mechanical properties of hyaline cartilage allow it to perform this function throughout a person's life. Cartilage distributes the load across the joint, over a wide area to minimise stress and allow movement with minimal friction. A number of different lubrication regimes operate in cartilage to allow minimal friction under a vast range of different loading conditions. These many different lubrication mechanisms can be categorised under three main types occurring in synovial joints: fluid film, boundary and biphasic lubrication.

1.3.2.1 Fluid film lubrication

Fluid film lubrication (Figure 1.10 A) works well under many physiological conditions, however cannot alone completely account for low friction in joints, as it is unsuccessful in certain conditions, such as start-up after a period of standing. Fluid film lubrication is based on two solid bearing surfaces being separated by a thin film of lubricant, so that the load bearing and friction capacity is governed by the laws of hydrodynamics, rather than the behaviour of rubbing solid surfaces (Dowson, 1995). This film must be thick enough to prevent any isolated asperity on one surface from touching a similar peak on the opposing surface. Fluid film lubrication encompasses hydrodynamic, elastohydrodynamic and squeeze film lubrication (Walker *et al*., 1968). Entraining action is the mechanism by which lubricant is dragged back into the contact area, this is due to the motion of two opposing surfaces sliding across one another.

Hydrodynamic lubrication (Figure 1.10 B) occurs when two rigid surfaces are separated by a thin film of viscous lubricant, but they oppose each other at an angle, so the fluid is in a ‘wedge’ shape. When the surfaces move tangentially, fluid is moved into the diminishing gap by viscous forces. The pressure in the fluid is sufficient to support the transverse load (Walker *et al*., 1968).

If the pressure in the fluid becomes too great, it may result in deformation of the solid surfaces and if the geometric alteration is great enough then elastohydrodynamic lubrication (Figure 1.10 C) operates. Here, the softer, more elastic surfaces allow a larger volume of fluid to be drawn into the converging gap. With increased relative radius of curvature of the solid, viscosity of the lubricant, sliding speed and increased softness of the material, the subsequent lubricant layer is thicker (Dowson *et al*., 1995).

Squeeze film lubrication (Figure 1.10 D) occurs when the surfaces produce force on one another in a normal direction not necessarily with transverse movement. Increased load results in increased pressure and lubricant viscosity. The approaching surfaces attempt to squeeze out the intervening fluid; this is, however, resisted by viscous forces and the film thickness is maintained, preventing solid-to-solid contact (Walker *et al*., 1968).

Unsworth (1991) believed fluid film lubrication to be of great importance in diarthroidial joints. However, the activity of such lubrication mechanisms within synovial joints has been disputed by Ateshian (2009).

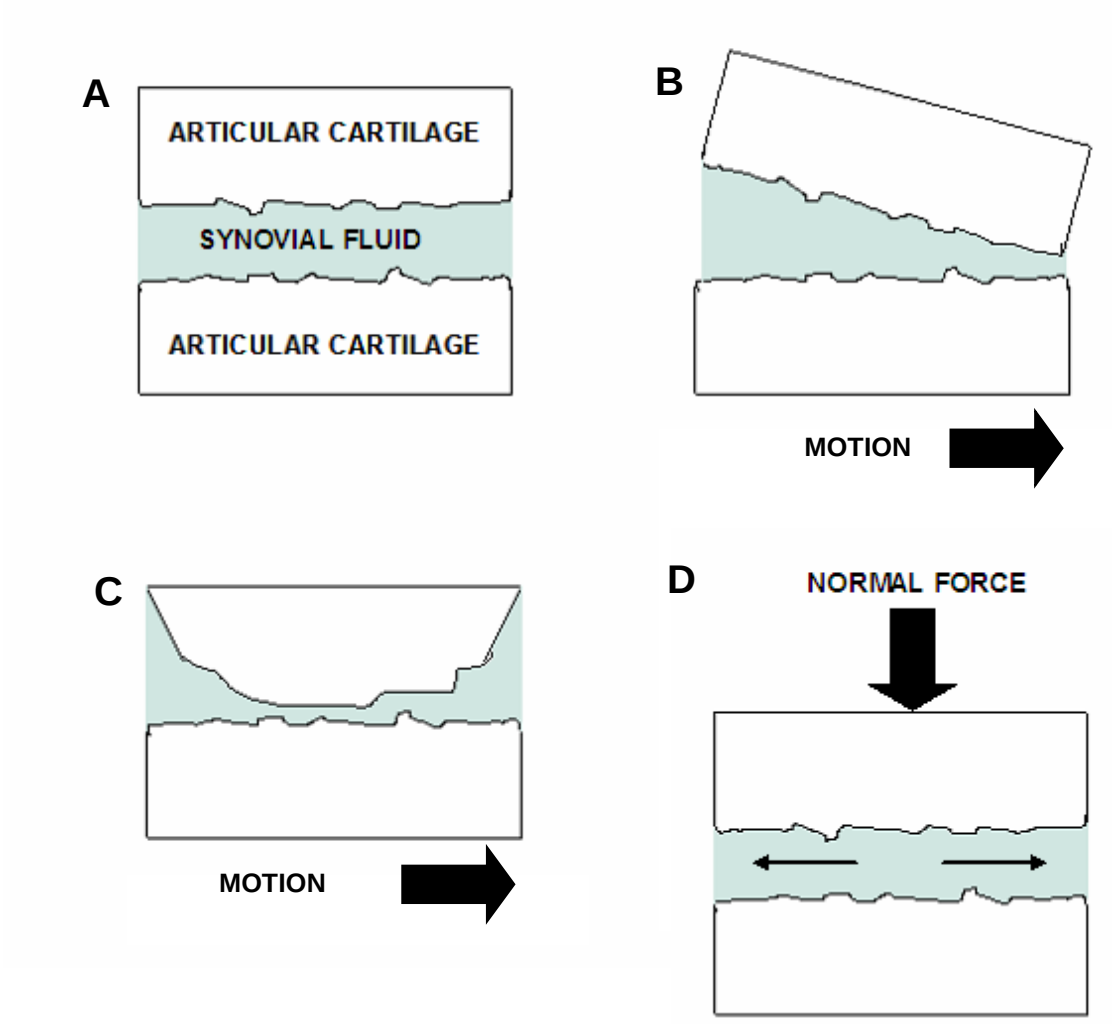

Figure 1.10 Fluid film lubrication. Schematic representations of fluid film lubrication mechanisms. A: Fluid film lubrication showing two surfaces or articular cartilage separated by a thin film of viscous synovial fluid lubricant. B: Hydrodynamic lubrication, fluid is forced into wedge-shaped gap by viscous forces during motion. C: Elastohydrodynamic lubrication, where deformation of the surface occurs and film is maintained due to viscous forces. D: Squeeze film lubrication force in the normal direction causes opposing surfaces to come together and pressurise fluid which is maintained by viscous forces.

1.3.2.2 Boundary lubrication

Boundary lubrication occurs when the fluid film thickness becomes very reduced resulting in increased asperity contact between two solid surfaces (Walker *et al*., 1968). This encompasses boosted lubrication, mixed lubrication, and boundary lubrication.

Boosted lubrication was first proposed by Walker *et al.* (1968) whereby pressure from load causes water and other small molecules from synovial fluid to enter the porous cartilage tissue. High molecular weight glycoproteins such as HA, for instance, are too large to be forced into the tissue so become highly concentrated at the surface, thus the resulting lubricating film is highly viscous (Walker *et al*., 1968).

Prior to the full use of boundary lubrication there is a stage of mixed lubrication (Figure 1.11 A), during which the majority of the surface is lubricated by fluid film mechanisms, however some points of contact between asperities on the surface use boundary lubrication.

During boundary lubrication (Figure 1.11 B) the fluid film is negligible so the surfaces touch; however, they are protected by boundary lubricants, which in the synovial joint are GAGs such as HA and, to a lesser extent, phospholipids. These molecules bind to the surface and prevent direct contact between the surfaces, instead sliding occurs between GAG molecules within the boundary lubricant layers. These GAG layers are replenished by the synovial fluid, ensuring they remain (Walker *et al*., 1968).

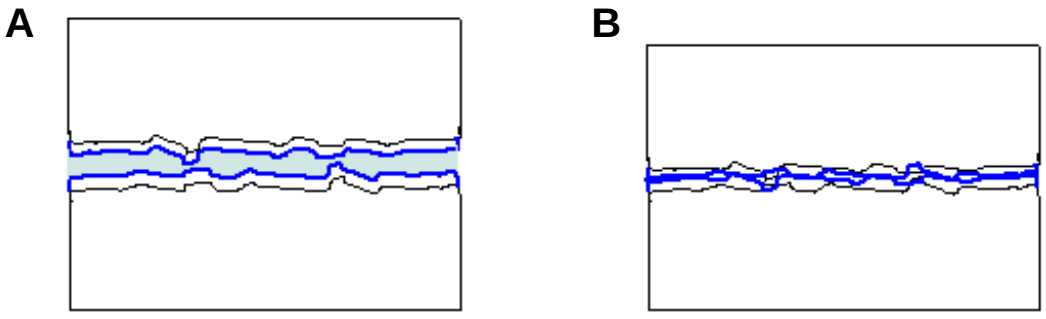

Figure 1.11 Boundary lubrication. Schematic representation of boundary lubrication regimes. Articular cartilage lined with a layer of boundary lubricants (blue line). A: Mixed lubrication where the fluid film is discontinuous, and boundary lubrication occurs at asperities which touch. B: Boundary lubrication where all the load is carried on the solid surface which is protected by a layer of boundary lubricants.

1.3.2.3 Biphasic lubrication

The biphasic mechanism of lubrication is possibly the most important in articular cartilage, it describes how initial load is supported by the interstitial water or fluid phase of the cartilage tissue, then load is gradually passed to the solid phase as water content of the tissue depletes. This lubricating mechanism can maintain low friction under extreme loading conditions in the absence of surface lubricant (Forster & Fisher, 1996).

The solid phase of cartilage denotes the collagen matrix and associated proteoglycans. The collagenous network has great tensile stiffness, however, poor compressive stiffness due to its fibrillar morphology, it has negligible charge. The proteoglycan component of the ECM, conversely, has many fixed negatively charged groups, which allow repulsion between molecules and therefore, considerable expansion of the volume which they occupy. However, proteoglycans are entrapped within the collagen network, which prevents them expanding to their full potential, also, the high concentration of free counterions within the interstitial fluid phase results in high Donnan osmotic pressure, slight external mechanic or ionic environment alterations lead to the loss or gain of water (Mow *et al*., 1984).

The architecture of the collagen matrix and the hydrophilic nature of the proteoglycans results in a micro-porous tissue. With increased compression, the tissue becomes less permeable based on its physiochemical composition. The permeability of the tissue to fluid movement and the equilibrium of swelling force from ionic interactions with collagen network tensile strength are directly affected by the volume of interstitial water (and the hyaluronic acid content). This pressurised interstitial water is capable of supporting the load (Katta *et al*., 2008; Mow *et al*., 1984).

Under compression, the forced flow of water from the tissue results in higher organic material concentration, and increased charge density. When charge density, collagen tension and applied load are balanced, a new equilibrium compressive stiffness is reached. Proteoglycan molecules interact with the collagen network to provide the tissue with shear strength.

So, in the solid phase, flow independent behaviours arise, where cross-linking between collagen fibres in the network and also interactions with this network and proteoglycan aggregates provide strength to resist deformation (Mow *et al*., 1984).

With significant fluid flow (under load) the frictional drag causes flow-dependant viscoelastic effects such as creep and stress relaxation. The collagen network provides resistance to tensile stress while the proteoglycans provide compressive stress resistance; there is also diffuse resistance as fluid flows through the ECM (Mow *et al*., 1984).

Under compression, fixed charge density increases which leads to reduced permeability. Compaction of the solid matrix under compression results in increased drag forces against the fluid flowing through, therefore a further reduction in permeability. Permeability is also dependent on the viscosity of the fluid (Mow *et al*., 1984).

The coefficient of friction is lower when load is carried by the fluid phase as compared to the solid phase. The biphasic lubrication mechanism is successful over long periods of load bearing. When movement occurs, the water content of the previously loaded tissue is replenished as the load is transferred to a different contact area of the cartilage surface. Continued movement of the load allows for the fluid phase to continue bearing the load at a lower coefficient of friction than if the solid phase was allowed to bear the load (Forster & Fisher, 1999; Forster & Fisher, 1996).

It has been noted that alterations of the counterion concentrations within the interstitial fluid can have major effects on the interaction of proteoglycans, which would have severe effects on the compressive resistance of the tissue, it has therefore been suggested that this ionic phase may be highly crucial in cartilage mechanics, so a triphasic model has been proposed by Lai *et al.* (1991).

Above the superficial tangential zone of articular cartilage there is a surface amorphous layer (SAL) comprised of sulphated sugars, glycoproteins and lipids. This layer is suggested to also be biphasic in nature and play a role

in friction reduction during shock loads, to prevent damage to the underlying bulk of cartilage (Katta *et al.,* 2008).

1.4 Osteoarthritis

Osteoarthritis is the most common disorder affecting joints (Herrero-Beaumont *et al*., 2009). The progressive, degenerative disease causes degradation of articular cartilage which becomes more severe over time, as cartilage is unable to repair itself. More recently OA has been highlighted as a disease of the whole joint, not merely the cartilage and underlying bone (Felson, 2009). OA can result in great pain and morbidity for sufferers and can be debilitating at later stages, when the whole joint fails (Felson, 2009).

1.4.1 Epidemiology

OA has a major impact globally, with an estimated 26.9 million adults aged 25 or over in the USA presenting with the disease in some joint (Lawrence *et al*., 2008). In the United Kingdom 8.5 million people are estimated to be living with osteoarthritis, and this number is predicted to double by 2030 (OANation2012). There is also a gender difference in OA prevalence, with more cases reported in women than men (Gabriel & Michaud, 2009). Arthritis Research UK report statistics that 1.8 % of males and 3.0 % of females consulting with their general practitioner per year are presenting with OA of any body part. Extrapolated, this would total 435,500 males and 769,000 females presenting with OA each year (www.arthritisresearchuk.org). Although it is possible to detect OA in x-rays by observing joint space narrowing, it is unethical to x-ray patients who do not present with symptoms, so estimates are restricted to those with symptomatic painful OA, and the percentage of the population with unsymptomatic OA is unknown. Along with increasing age and female sex, obesity is a major risk factor associated with OA (Gabriel & Michaud, 2009) so it would appear that with the increasing life expectancy of the

population, and increased incidence of obesity, OA can only become more prevalent unless effective treatments can be found, Felson & Zhang (1998) have proposed a doubling in prevalence from 2000 to 2020.

OA is a major economic burden, the most recent figures report around 58,952 primary hip replacements and 62,150 primary knee replacements were performed in the UK in 2006/2007, at a cost of around £430 million and £460 million respectively (www.arthritisresearchuk.org). In the USA, musculoskeletal procedures (predominantly knee arthroplasty and hip replacements) cost $31.5 billion in 2005. More recently it has been suggested that OA in the USA has a direct cost of $81 billion per year (Lützner *et al*., 2009). However, it is not just costs from hospital procedures and care, but loss of wages through inability of sufferers to work; estimated as indirect costs of $47 billion in the USA (Lützner *et al*., 2009). Clearly OA poses a major economic burden to the population as well as causing great morbidity in the many sufferers, therefore reduction in the incidence of OA is imperative (Gabriel & Michaud, 2009).

1.4.2 Pathogenesis

There are classically thought to be two forms of OA, primary and secondary. Secondary OA is caused by well-recognised predisposing conditions such as anatomic abnormalities, trauma, metabolic and inflammatory disorders. Conversely, primary OA has no apparent triggering event and occurs in previously undamaged joints (Herrero-Beaumont *et al*., 2009). There are many different factors which can lead to the onset of OA, these are outlined in Figure 1.12. Any combination of factors can lead to OA onset, it is likely that systemic factors predispose a person to OA, and the application of local biomechanical factors triggers the process of cartilage disruption (Felson & Zhang, 1998).

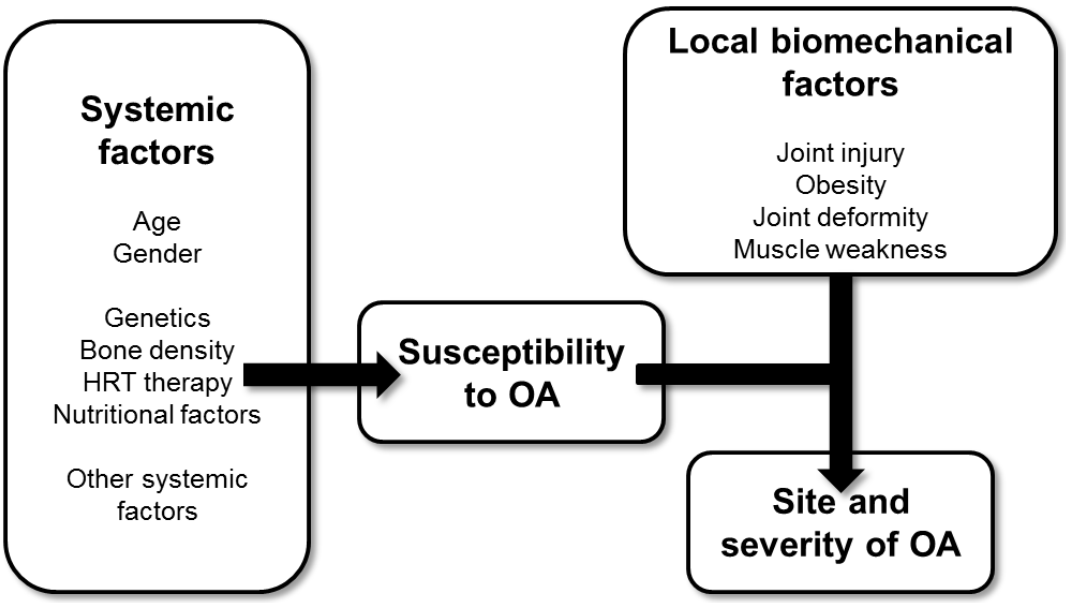

Figure 1.12 Osteoarthritis pathogenesis. A schematic representation of the pathogenesis of osteoarthritis detailing the different types of risk factors involved. HRT= hormone replacement therapy. Figure adapted from Felson & Zhang (1998).

Osteoarthritic cartilage is altered from a normally silvery/white, firm tissue to become yellow, pitted, soft, uneven and fissured. This condition progressively spreads across an articular surface. Degradation of articular cartilage can occur through mechanical wear processes; however there can also be a molecular basis to cartilage degeneration (Martel-Pelletier *et al*., 2008).

The subchondral bone undergoes areas of necrosis and resorption, which appear as cysts. The tissue undergoes sclerosis where new bone is laid down in areas under stress. Marginal osteophytes arise at the joint periphery, composed of a centre of new bone with a surface layer of cartilage containing a mixture of hyaline and fibrocartilage (Altman, 1987). At the clinical stage of OA there is also inflammation of the synovial membrane. Failure results from an inability of chondrocytes to balance this progressive degradation with the synthesis of new matrix. When synovial inflammation occurs the production of inflammatory mediators regulates chondrocyte homeostasis, favouring catabolic activities resulting in matrix loss (Martel-Pelletier *et al*., 2008).

Cartilage matrix is turned over throughout life and many cellular factors regulate cartilage homeostasis, balancing anabolic and catabolic activities, however disruption of this balance can lead to increased catabolism and therefore degradation of the tissue (Martel-Pelletier *et al*., 2008).

One of the key anabolic factors in cartilage homeostasis is transforming growth factor β (TGF-β) which is thought to play a proactive role in regulating cell proliferation and ECM synthesis. The growth factor functions to increase proteoglycan synthesis and to inhibit interleukin 1β (IL-1β) mediated proteoglycan synthesis suppression. It also acts to inhibit production of matrix metalloproteinase 9 (MMP-9) and MMP-1, molecules which are involved in ECM destruction. TGF-β is also able to induce MMP-13 and the aggrecanase ADAMTS-4 (a disintegrin and a metalloprotease with thrombospondin motifs-4) allowing macromolecular turnover in normal cartilage. (Martel-Pelletier *et al*., 2008). TGF- β is usually present at low levels in healthy joints, but levels are increased in OA cartilage. Other anabolic factors include bone morphogenic proteins (BMPs), cartilage-derived morphogenic proteins (CDMPs), insulin-like growth factors (IGFs) connective tissue growth factor (CTGF), hepatocyte growth factor (HGF) and fibroblast growth factor (FGF). These factors, combined, work to stimulate matrix deposition, cell proliferation and inhibit catabolic activity (Martel-Pelletier *et al*., 2008).

Of greater interest are the catabolic factors, many of which appear to have increased production or function in OA cartilage, which may act as catalysts or amplifiers of OA development. These include proteases, in particular matrix metalloproteinases (MMPs). MMPs are classified into groups: collagenases (MMP-1, -8 and -13 which degrade specific collagen molecules), stromelysins (MMP-3 and -11 which degrade proteoglycans, fibronectin, elastin and laminins), gelatinases (MMP-9 and -2 which degrade collagen types IV and V along with denatured collagen and gelatine), and adamalysin (ADAMTS-5 which has aggrecanase activity). These MMPs have all been shown to be uniquely expressed or upregulated in OA cartilage. Other proteases involved in OA development include certain serine and thiol proteases (Martel-Pelletier *et al*., 2008).

Inflammatory factors also play a key role in the catabolism of cartilage, the proinflammatory cytokine IL-1β is thought to be the most important factor responsible for the catabolic processes in OA. It forms a positive amplification loop in chondrocytes leading to increased production of itself, proteases, cytokines and other inflammatory factors. It is also able to inhibit antagonists of such enzymes and inhibit synthesis of ECM constituents (Daheshia & Yao, 2008). Other proinflammatory factors involved in OA development include tumour necrosis factor alpha (TNF-α) (Goldring, 1999), oncostatin M (OSM) (Hui *et al*., 2003), leukaemia inhibitory factor (LIF) (Lotz *et al*., 1992), IL-17, IL-18 (Martel-Pelletier *et al*., 2008), nitric oxide (NO) (Vuolteenaho *et al*., 2007), eicostanoids (prostaglandins and leukotrines) and also protease-activated receptors (PARs) (Martel-Pelletier *et al*., 2008).

There are a number of factors other than proteases and inflammatory molecules which have catabolic activity in cartilage which are upregulated in OA including fibronectin fragments (Homandberg *et al*., 1998), leptin (Teichtahl *et al*., 2005) and neuropeptides (Martel-Pelletier *et al*., 2008).

OA was historically thought to be a disease of the cartilage, but more recent evidence indicates that it is a disease of the whole joint. The initiating lesion resulting in osteoarthritis may arise in many different tissues of the joint. McGonagle *et al.* (2010) discuss a site specific pathogenic classification of OA in which the disease can arise from cartilage, ligaments, meniscus, synovium, bone or a combination of many of these tissues (Halstead *et al*., 2010). They suggest that injury or disregulation of these tissues could progress to whole joint effects resulting in OA, and with improved magnetic resonance imaging (MRI) technology, these initial tissue lesions can be detected earlier, before clinical onset of OA.

1.4.3 Articular cartilage defects

Many cases of OA stem from an initially minor cartilage defect; these can be caused by acute injury to the joint, or from osteochondral pathology, such as osteonecrosis or osteochondritis dissecans. Due to the poor ability

of cartilage to heal, these small defects progressively deteriorate under regular joint loading and articulation, and advance to clinical OA (Chaing & Jiang, 2009). Not only do these lesions pose a risk of deterioration to OA, but are troublesome in themselves, often causing pain, swelling and mechanical symptoms such as locking of the joint, reducing the quality of life for patients (Minas & Nehrer, 1997). An estimated 10,000 patients in the UK each year suffer knee cartilage damage warranting repair (NICE TA89, 2008).

To prevent onset of OA and reduce symptoms, it is possible to repair these defects. There are various approaches, although these depend on the severity and position of the defect (Schindler, 2011). Cartilage defects can be graded by severity, highlighting cartilage properties, as well as the size, shape and depth of lesions. There are many systems for categorising cartilage defects; two different approaches were developed by Outerbridge (1961) and Bauer & Jackson (1988). The latter is useful in a more descriptive sense, allowing for association with recent trauma (grades I-IV) or lesions undergoing a degenerative process (grades V & VI), as it defines fracture pattern. However, the Outerbridge system is most useful to delineate a symptomatic focal area suitable for repair as it is concerned with depth of the lesion (Minas & Nehrer, 1997). More recently, the ICRS grading system has been widely used (Figure 1.13).

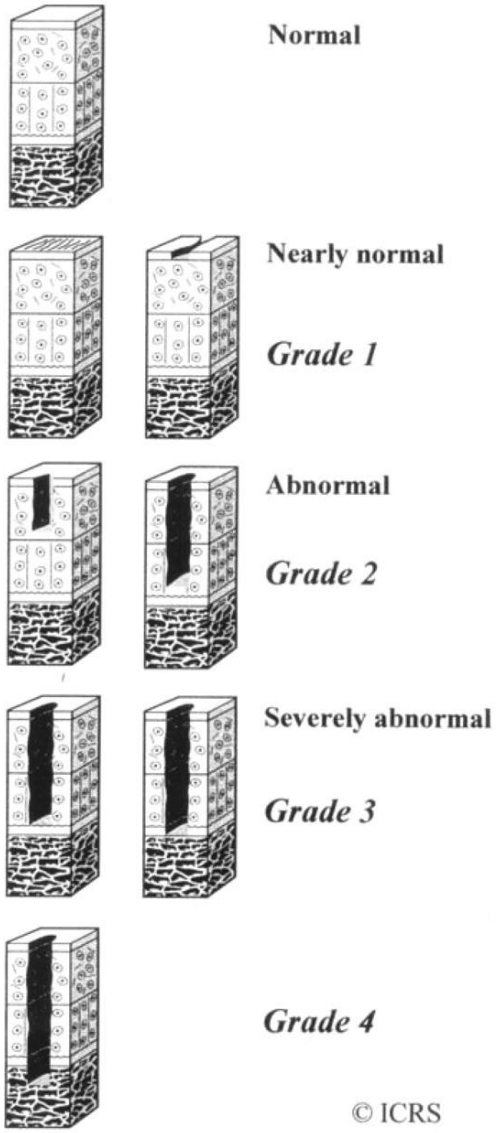

Figure 1.13 ICRS cartilage grading system. Normal (grade 0): healthy cartilage, grade 1: the cartilage has a soft spot or blisters, grade 2: minor tears visible in the cartilage, grade 3: lesions have deep crevices (more than 50% of cartilage layer), grade 4: the cartilage tear exposes the underlying (subchronal) bone.

It has been suggested that cartilage defects can result in increased cartilage breakdown, leading to a decrease in cartilage volume resulting in decreased joint space, and breakdown of collagen type II fibres (Ding *et al*., 2005). Due to the link between cartilage defects and development of early OA, it is proposed that repair of these defects can prevent further cartilage degradation and progression to OA.

1.5 Current approaches to defect repair

Current treatments aim to restore the integrity of the joint surface and allow a full range of motion with the absence of pain. These treatments include; lavage and debridement, marrow stimulation techniques, perichondral/periosteal grafts, mosaicplasty and autologous chondrocyte implantation (Minas *&* Nehrer, 1997). When determining which of these procedures to use, it is important to take into account the location and severity of cartilage damage, the patient's characteristics and risk factors (Figure 1.14; Lützner *et al*., 2009; Schindler, 2011). Many of these techniques can be performed in the knee, but are inappropriate in the hip due to difficulties in accessing the joint, although arthroscopy is becoming more advanced, usually, end stage total joint replacement is the only option for hip arthritis.

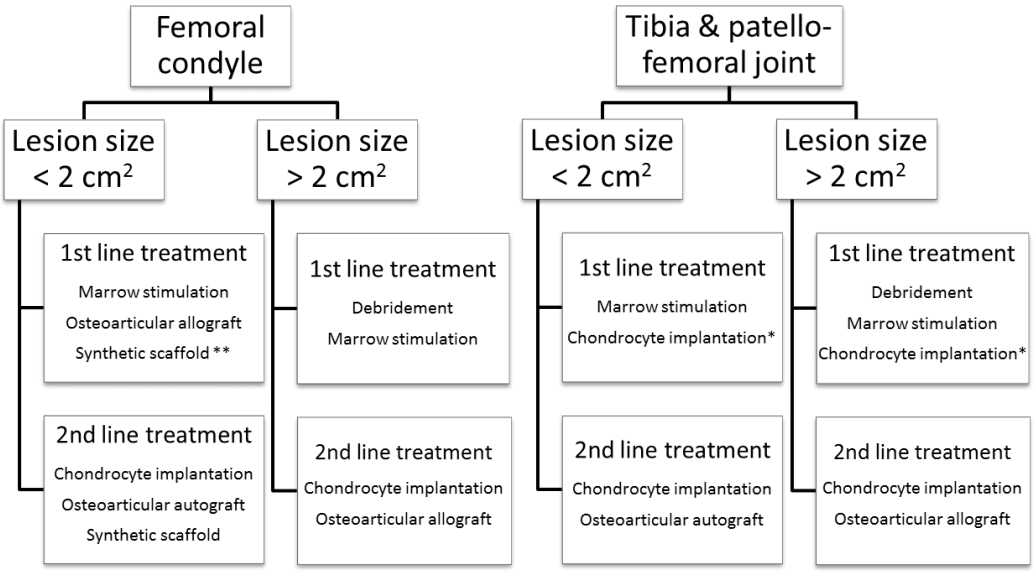

Figure 1.14 Treatments for focal cartilage defects in the knee. The selection of a cartilage repair procedure based on location, lesion size and whether it is a first or second line treatment. * = treatment for young/high demand patient, ** = treatment with no medium-long term clinical results available to date. Figure from Schindler (2011).

1.5.1 Lavage & debridement

The aim of lavage is to remove loose articular debris and inflammatory mediators from the joint space through arthroscopy, therefore reducing inflammatory synovitis and pain and improving function (Minas *&* Nehrer, 1997, Lützner *et al*., 2009). Debridement is often performed alongside lavage to provide advanced benefit, with the intention of improving mechanical conditions by removing loose bodies, hypertrophied synovium and, in the knee, torn meniscal fragments, and often removing flaps and shaving fibrillated cartilage (Lützner *et al*., 2009).

Following a randomised six month controlled trial, lavage and tidal irrigation of the knee were found have an equal effect on pain relief to corticosteroid injection into the joint space. The effect was more prolonged with lavage and tidal irrigation, lasting up to 6 months in 64 % patients compared to only 29 % of patients receiving corticosteroid injection (Arden *et al*., 2008). Hubbard (1996) compared the effects of lavage alone to the use of combined debridement and lavage, and found more effective pain relief and sustained results when both techniques were used (Hubbard, 1996). Beneficially, lavage and debridement are cheap procedures which are relatively simple to perform.

However, many studies have suggested that the pain relief from debridement is no greater than that from lavage alone (Chang *et al*., 1993) and no greater than can be achieved with a placebo (Moseley *et al*., 2002). Kirkley *et al.* (2008) found no significant benefit of arthroscopic surgery over optimised physical and medical therapy alone. This view however is still controversial, and the treatment may be beneficial in a small number of patients with specific lesion types. Furthermore, the application of this treatment does not replace lost tissue and has not been shown to defer progression into OA (Lützner *et al*., 2009).

1.5.2 Marrow stimulation techniques

The aim of bone marrow stimulation is to cause bleeding into the joint space from the subchondral bone resulting in fibrin clot formation in the

defect. This is followed by migration of undifferentiated mesenchymal stem cells to the lesion where they form fibrocartillagenous tissue to fill the full thickness cartilage defect (Minas *&* Nehrer, 1997; Lützner *et al*., 2009, Schindler, 2011). Techniques used to penetrate the subchondral bone are drilling, microfracturing and abrasion arthroplasty. Of these microfracturing is most commonly used as it is easiest to perform (Figure 1.15). Firstly debridement is used to remove unstable cartilage from the rim of the lesion, and then holes are made 2-4 mm deep and 3-4 mm apart in the centre of the defect. Rehabilitation involves passive motion and partial weight bearing for 6-8 weeks (Minas *&* Nehrer, 1997; Lützner *et al*., 2009).

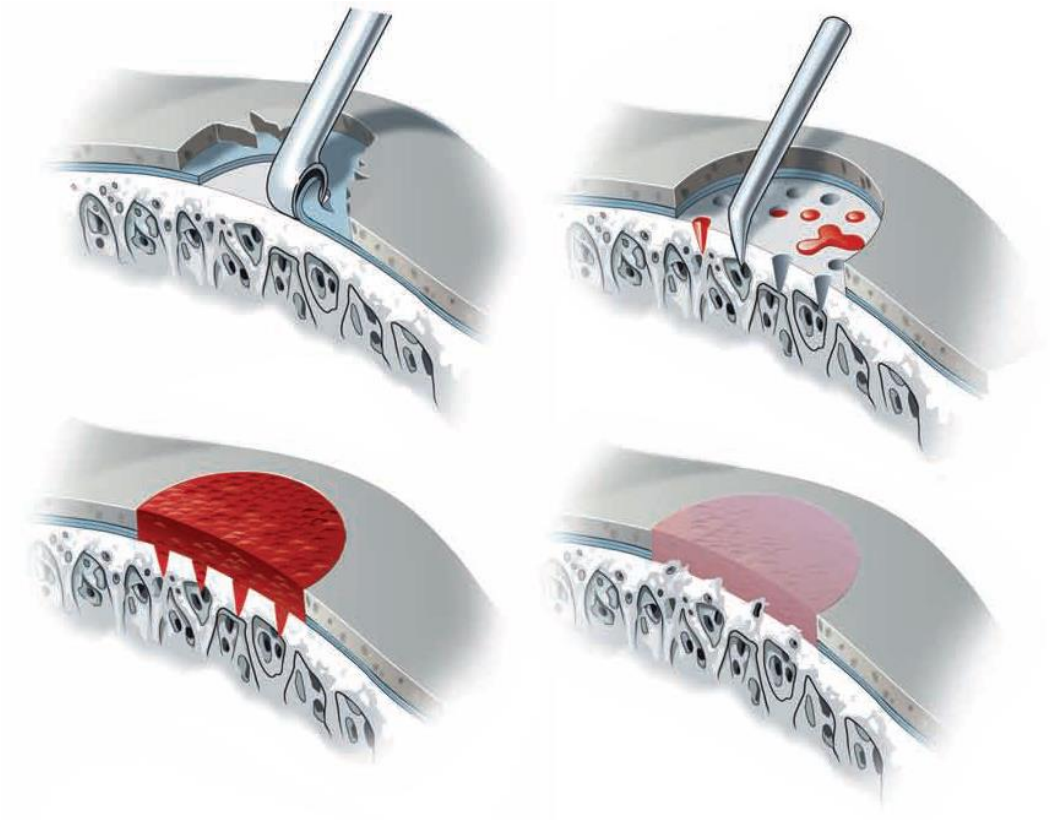

Figure 1.15 Microfracture procedure. Firstly debridement is used to define the edge of the defect, holes are made in the bone to stimulate bleeding, a fibrin clot forms in the defect which overtime forms repair fibrocartilage. Figure from Schindler (2011).

Steadman *et al.* (2003) found that microfracture marrow stimulation greatly reduced pain and improved knee function for a minimum of 7 years in patients under the age of 45 (Steadman *et al*., 2003). Bae *et al*. (2013)

reported that 67.9 % of patients who underwent microfracture surgery did not require further treatment for cartilage pathologies at 10 year follow up. However, this repair technique produces fibrocartilage which has inferior biomechanical properties and durability compared to the original hyaline cartilage (Steinwachs *et al*., 2008; Lützner *et al*., 2009). It is unlikely, therefore, to be a curative measure or prevent disease progression (Lützner *et al*., 2009)

Autologous matrix induced chondrogenesis (AMCI® Geistlich Pharma) has been developed to produce more consistent results from microfracture procedures. A cell free collagen matrix is secured into the defect to provide an environment for mesenchymal stem cells and aid chondrogenesis. The success of AMIC® has been reported for the repair of osteochondral lesions of the knee in a two year follow up study (Gille *et* al., 2013) Furthermore, the technique (alongside the use of autologous bone grafting) has been reported to be successful at 24 month follow up for the repair of osteochondral lesions of the ankle joint (Valderrabano *et al*., 2013). The long term clinical benefits of this procedure are currently unknown.

1.5.3 Perichondrial/periosteal grafting

The key problem with marrow stimulation techniques is that they produce an inferior fibrocartilaginous repair tissue. It has been shown that autogenous rib perichondrium, when grafted onto a cartilage defect which had undergone debridement, produced a repair tissue which resembled hyaline cartilage. Autogenous periosteal grafts have also been performed and produce hyaline-like repair cartilage (O'Driscoll *et al*., 1988). Therefore perichondrial/periosteal grafting is possibly a superior alternative to microfacture (Minas *&* Nehrer, 1997). A study conducted by Homminga *et al*. (1990) in 25 patients under the age of 45 with 30 chondral lesions used periostium grafts from the rib and anchored them to cartilage lesions of the knee using fibrin glue. They found a mean increase in knee function when questioning patients on the Ranawat knee scoring system, and 14 people

maintained that score after two years. In 28 cases, the defect was completely filled with hyaline cartilage (Homminga *et al*., 1990).

Bouwmeester *et al*. (2002) performed a retrospective analysis of two studies comparing patients receiving perichondrial grafting and those receiving subchondral drilling. The success rate of perichondrial grafting was 78% (three grafts failed) compared to a surprisingly high 100% success rate of subchondral drilling. No long term advantage of having a hyaline-like repair tissue compared to fibrocartillage was found within the 10 year scope of the study. Grafting has to be performed via an 'open' procedure, whereas microfracture techniques are performed arthroscopically, which is preferable. Furthermore there was a degree of calcification of the grafts (Bouwmeester *et al*., 2002). Perichondral grafting is now more commonly performed as part of autologous chondrocyte implantation procedures (Section 1.5.5; Chaing & Jiang*, 2009*).

1.5.4 Osteochondral autografts/allografts (mosaicplasty)

During autologous osteochondral transplantation (Figure 1.16), pins of cartilage attached to subchondral bone, which contain metabolically active chondrocytes, are taken from non-load-bearing areas of the affected joint and like periosteal/chondrial grafting are fixed to the site of chondral defects. Osteochondral grafts are thought to have greater stability along with the benefit of producing hyaline cartilage repair tissue (Minas *&* Nehrer, 1997). Koulalis *et al.* (2004) performed osteochondral autografts in knee joints of 18 patients with a follow-up time of 27 months. All showed defect coverage 12 months postoperatively and all cases had osseous integration, although there was some indication of donor site morbidity in 11 patients which decreased over time. This is a good approach to defect repair; however the factor of donor site morbidity is a disadvantage (Koulalis *et al*., 2004).

Solheim *et al.* (2010 and 2013) performed mosaicplasty surgeries on 69 patients (mean age 33) and recorded Lysholm score and visual analogue scale (VAS; 0=no pain; 100=worst possible pain) of pain. At 12 month

follow up the mean Lysholm score and VAS of pain improved from 48 and 62, respectively, at the time of surgery to 81 and 24, respectively. However, at mid-term (5-9 years) follow up pain levels were observed to have increased and mean scores of 68 and 32 were reported, respectively (Solheim *et al.*, 2010). At long-term (10-14 years) follow up, mean pain scores were still improved from baseline, at 72 and 27 respectively. However an unsatisfactory Lysholm score of < 64 was reported in 40 % of patients. Although, the outcome was found to be improved in a specific demographic of patients (males under 40 years old) with small (< 3 cm^2) initial defects (Solnheim *et al*., 2013). It is therefore necessary to accurately select recipients for mosaicplasty to improve long term clinical success.

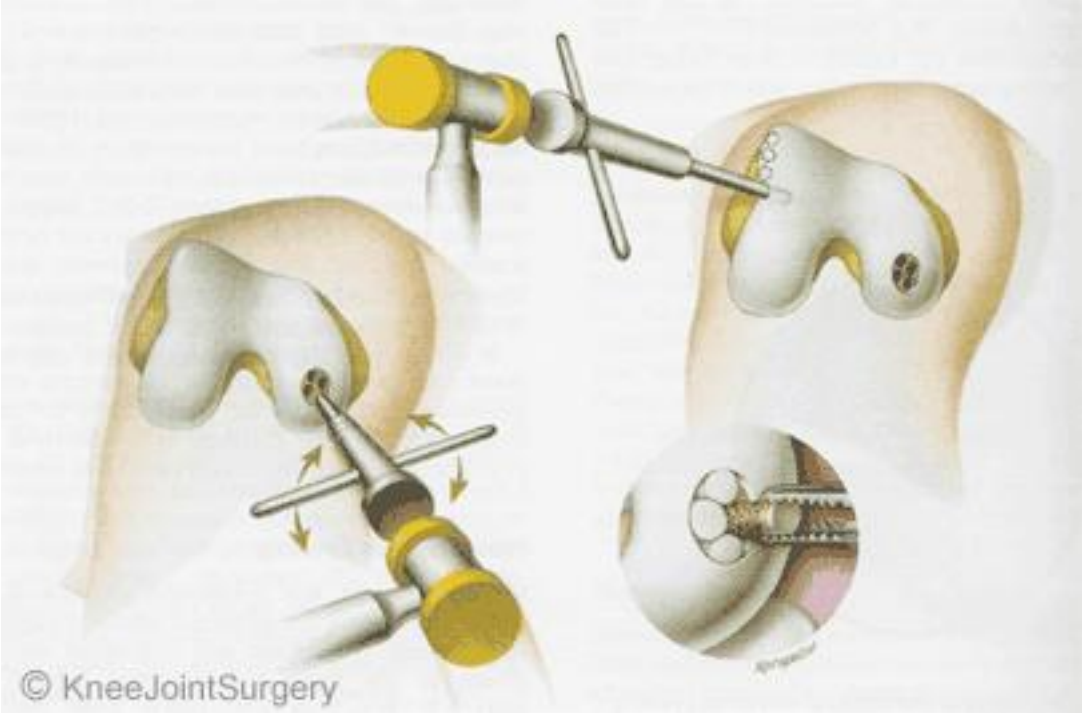

Figure 1.16 Mosaicplasty procedure. The use of autologous osteochondral pins taken from non-load-bearing joint surfaces to repair lesions in load bearing regions. Figure from www.kneejointsurgery.com.

To overcome the issues with donor site morbidity, osteochondral allografts, which still contain metabolically active chondrocytes, have been used. As they are allogeneic, rather than taken from donor sites, grafts of a much larger size are able to be produced. The grafts are anueral and avascular and so were thought to be immuneprivileged, making them ideal for

allogenic transplantation, however, immune reactions can be evoked from the immersing synovial fluid (Chaing & Jiang, 2009). There are concerns about possible transmission of infection for allograft recipients, so further steps are required to sterilise grafts (LaPrade *et al.,* 2009). Storage and preparation of allografts, if not used fresh, is troublesome, as chondrocytes die during the process (Chaing & Jiang, 2009).

1.5.5 Autologous chondrocyte implantation (ACI)

ACI is a technique developed in the late 1900s whereby articular cartilage is harvested from a patient and the chondrocytes from which are expanded in vitro. These expanded, autologous chondrocytes are then reimplanted into chondral defects of the same patient, beneath a perichondrial patch (Chaing & Jiang, 2009). Grande (1989) initially performed this procedure on rabbits and found improved defect healing and decreased synovitis in joints in which chondrocytes had been implanted compared to controls where just the perichondrial flap had been attached. The repair cartilage was hyaline-like, and cell labelling revealed that the implanted cells were present in and responsible for production of the repair cartilage. A follow-up study by Minas (2001) looked at the capacity of ACI to repair cartilage defects in the human knee. In a sample of 169 patients a 87% success rate was found. Moradi *et al.* (2012) found a substantial improvement in all clinical outcome parameters at up to 14 years post-operatively, with complete defect filling in 52 % of patients as observed by MRI.

Despite having a relatively high success rate and producing a mechanically and biologically superior hyaline-like repair tissue with a non-immunogenic graft, there are disadvantages to this procedure. The treatment involves an open technique, as opposed to arthroscopic which results in a more prolonged recovery period for patients (Minas, 2001). Also, the procedure is technically demanding, with multiple stages, so differences in surgical skill may well correlate to altered outcomes of the treatment (Grande *et al*., 1989).

A variation of ACI, matrix assisted chondrocyte Implantation (MACI®; Genzyme, Cambrige, MA), has been in clinical use for a number of years. Similarly to AMCI®, this procedure uses a collagen matrix onto which the autologous chondrocytes are cultured prior to implantation into the defect. Beneficially, use of MACI enables the procedure to be performed arthroscopically, as harvest of periosteum is not required (Getgood *et al*., 2009). Good clinical mid-term results have been reported with this approach (Kon *et al*., 2009).

1.6 Current tissue engineering approaches

As current surgical interventions for osteochondral defect repair have shown variable outcomes, there is need for the development of a biologically and biomechanically superior repair biomaterial which will avoid the use of autologous tissue and circumvent donor site morbidity. Tissue engineered approaches are currently undergoing research and development to fulfil this clinical niche.

There are three key components in tissue engineering, cells which characterise the tissue type, biomaterial scaffolds which provide a habitat for the cells and chemical, mechanical or biological environmental factors which determine cell behaviour (Chaing & Jiang, 2009).

Cells can be can be used in regenerative medicine associated with a scaffold, or injected directly, without a scaffold. Often these cells are extracted from donor tissue and either expanded or implanted directly into the host. These cells can be allogeneic (from another human) but most preferably autologous, from the individual themselves, as these will be immunocompatible. Enough cells may not be available from a tissue biopsy, or cells extracted may not be easily expanded, in these circumstances, stem cells are an alternative source. Stem cells can be embryonic, foetal-related tissue (amniotic fluid or placenta) or adult stem cells derived from bone marrow, skin etc. (Atala, 2007). The growth of research in the field of stem cell biology has opened up new possible cell

sources including pluripotent stem cell lines created by somatic cell nuclear transfer (Wakayama *et al*., 2001), and induced pluripotent stem cells (Takahashi *et al*., 2007), which may be of use in the future. Often scaffolds can be implanted without cells, to allow native cell in growth in vivo (Atala, 2007).

Biomaterials used to form a scaffold need to be tailored to the tissue being engineered, to mimic the biological and mechanical characteristics of the natural ECM. The scaffold should ideally be biodegradable and bioresorbable. These materials can be natural decellularised ECM, naturally derived materials formed in vitro or synthetic polymers. Beneficially, natural materials can be recognised biologically and thus avoid rejection, however polymers have the ability to be reproduced on a large scale, and the properties of strength, degradation and the microstructure can be easily controlled (Atala, 2007).

Cartilage is a complex tissue and as such there have been a number of different approaches taken to engineer the tissue for use in articular cartilage defect repair. These approaches include synthetic polymer and natural biomaterial scaffolds.

1.6.1 Synthetic scaffolds

Synthetic polymers are used in research to engineer many different tissue types as they are easy to manufacture and their specific properties can be accurately controlled to mimic the natural ECM. However, the biomechanical properties of such materials are inferior to natural cartilage (Atala, 2007). Some examples of polymers which have been used as cartilage scaffolds are shown in Table 1.3. A single material can be used, but more commonly they are used in combination to provide better physical characteristics.

Problems encountered with synthetic polymers include low GAG content of repair tissue and inconsistent subchondral bone reformation (Chu *et al*., 1996). van Susante *et al.* (1998) found that the repair cartilage formed with hydroxyapatite scaffolds was inferior fibrocartilage. Scaffolds are designed

to biodegrade, so if cell seeding, retention or metabolism is not sufficient, the ECM will not be replicated by resident cells before the scaffold degrades and the implant will fail. The use of copolymers allows control of degradation rate (Frenkel & DiCesare, 2004). Other problems have been found with integration of successful polymer hydrogels with the existing cartilage, composites of polyvinyl alcohol (PVA) gels with nano-hydroxyapatite allowed for better integration with host tissues (Pan & Xiong, 2009).

Recently, nanofabrication technology has been used to produce an anisotropic cartilage repair biomaterial. The electrospinning of poly (ε-caprolactone) (PCL) fibres enabled tangential surface alignement and random orientation in the rest of the material, increased fibre diameter was included in the base of the material to mimic natural cartilage zonal microstructure with promising *in vitro* results (McCullen *et al*., 2012).

Some synthetic scaffolds have begun to undergo testing in clinical trials such as Trufit® plug (Smith&Nephew, Andover, USA) and BioMatrix® Cartilage Repair Device (Arthrex, Karlsfeld Germany).

Synthetic biomaterial	Reference
Polylactic acid (PLA)	Chu *et al*., 1996 Giurea *et al*., 2003
Polyglycolic acid (PGA)	Liu *et al*., 2002 Schaefer *et al*., 2002
PLA-PGA copolymer	Cohen *et al*., 2003
Poly(ethylene glycol) diacrylate (PEGDA)	Kim *et al*., 2003
Hydroxyapetite	van Susante *et al.*, 1998 Pan & Xiong., 2009
Polycaprolactone (PCL)	McCullen *et al*., 2013
Polyvinyl alchohol (PVA)	Pan & Xiong, 2009

Table 1.3 Synthetic biomaterials. Synthetic biomaterials used as scaffolds in cartilage tissue engineering for repair of osteochondral defects.

1.6.2 Natural scaffolds

Natural biomaterials have the advantage of biological recognition, however, they are more difficult to use than synthetic polymers, resulting in scaffolds which are less reproducible (Atala, 2007). Collagen for example, has great advantages as a biomaterial for cartilage production, as it is the main ECM component of the natural tissue, and has specific RGD sequences which allow cell adhesion and phenotype retention (Atala, 2007). Fibrin is also a logical candidate, as the clots which form during the natural cartilage repair process are fibrin based (Frenkel & DiCesare, 2004). Some of the natural biomaterials which have been used in the production of cartilage scaffolds are shown in Table 1.4. As with synthetic polymers, these materials can be used in isolation, or in combination with a number or other materials to produce the optimum properties to function as a scaffold.

Natural biomaterial	Reference
Collagen	Wakitani *et al*., 1994 Frenkel *et al*., 1997
Collagen-GAG-calcium phosphate	Getgood *et al*., 2012
Fibrin	Hendrickson *et al*., 1994 Kreuz *et al*., 2009
Gelatin	Chang *et al., 2004*
Hyaluronan	Butnariu-Ephrat *et al*., 1996 Grigolo *et al*., 2001 Dausse *et al*., 2003
Agarose and alginate	Marijnissen *et al*., 2002 Dausse *et al*., 2003
Bacterial cellulose	Müller *et al*., 2006
Chitosan	Hoemann *et al*., 2005
Gellan Gum	Oliveira *et al*., 2010

Table 1.4 Natural biomaterials. Natural biomaterials which have been used as scaffolds for cartilage tissue engineering.

Good results have been seen in terms of hyaline-like cartilage repair tissue formation in animal studies, however as with synthetic materials, there were problems with scaffold integration into the existing tissue, and also

with the thickness of the resulting tissue, being thinner than the surrounding cartilage. In many cases repair tissues were biologically and mechanically inferior to natural cartilage. It is however, suggested that despite the promising functionality of some biological scaffold materials, there are still concerns with batch variation, and the potential for pathogen transfer, especially bovine spongiform encephalopathy from prions within bovine collagen sources (Frenkel & DiCesare, 2004).

1.6.3 Natural acellular scaffolds

As discussed previously, the architecture of the cartilage ECM is essential for its load bearing and lubrication functions. Therefore, using a simplistic homogenous scaffold may not be sufficient to recreate the biological and mechanical properties of natural cartilage (Chaing & Jiang, 2009). An approach taken in the engineering of other tissues has been to use natural acellular ECM scaffolds. These collagen rich matrices are produced by chemical, enzymatic and mechanical manipulation of natural tissues resulting in the removal of resident cells. These scaffolds slowly degrade once implanted and ingrowing or transplanted cells secrete ECM proteins to slowly replace and remodel the scaffold (Atala, 2007). Acellular scaffolds also have the benefit of being biocompatible, biodegradable and bioresorbable as they are natural materials. Additionally, acellular tissue matrices can be bioactive, retaining cell attachment motifs, growth factors and other biological cues (Hofmann & Garcia-Fuentes, 2011).

Work is currently underway in developing acellular porcine bladder for use in tissue engineering (Bolland *et al*., 2007), along with meniscus (Stapleton *et al*., 2008), other acellular matrices have been developed for tendon (Lee, 2008), heart valves (Korossis *et al*., 2002), blood vessels (Cronklin *et al*., 2002), skin (Chen *et al*., 2004), nerves (Kim *et al*., 2004) and small intestinal submucosa (Badylak *et al*., 1999) amongst others.

Decellularised small intestinal submucosa (SIS) has been used clinically for over a decade to repair tissues such as skin, muscle and tendon (eg. Restore™, DePuy Orthopaedics; Surgisis®, Cook Biotech Inc). Although

the application of decellularised SIS for osteochondral repair has not been reported .

1.6.3.1 Immunogenicity of tissue transplants

If allogeneic or xenogeneic tissue engineered biomaterials are to be of use clinically, it is necessary to understand the immunological response to such materials upon implantation, to avoid the rejection of tissue engineered implants.

1.6.3.1.1 Immunological response to allografts

The extracellular matrix components of biological tissues such as collagens and proteoglycans are conserved between individuals and across species, so are not recognised as foreign upon transplantation. However, human leukocyte-associated (HLA) proteins are present on the cell membrane of every nucleated cell and are encoded for by highly polymorphic set of major histocompatibility complex (MHC) genes. Each individual has six sets of MHC I and six sets of MHC II genes, three from each parent, which are expressed co-dominantly. The histocompatibility proteins expressed are therefore unique to each individual (excluding monozygotic twins, who share the same genetic material). It is the presence of these histocompatibility proteins on the surface of cells which enables identification and distinction between “self” and “non-self”, and therefore poses a barrier in transplantation of allogeneic and xenogeneic tissues.

The role of the MHC molecules is to present foreign antigens, such as epitopes from cytoplasmic or internalised pathogens. The presentation of a foreign antigen elicits a cell mediated immune response, however, as the MHC molecules are specific to each individual, allogeneic “non-self” MHC molecules will also be recognised as foreign, without presenting an antigen. Initial acute rejection of transplants can occur through direct recognition of allogeneic MHC Class II proteins presented on the surface of antigen presenting cells (APC’s) by CD4+ Helper T- cells (Figure 1.17). The binding of T-cell receptor to allogeneic MHC Class II, followed by binding of co-stimulatory cell surface molecules results in the formation of an immunological synapse which activates the CD4+ T-cell. Once

activated, the CD4+ T-cell produces interluken-2 (IL-2) which is able to stimulate CD8+ T-cells. CD8+ T-cells have a receptor which binds MHC Class I on all nucleated cells. Once CD4+ and CD8+ T-cells are activated they undergo clonal expansion, to rapidly produce many more T-cells reactive against the specific MHC molecule shape recognised as “non-self”. Clonal expansion produces both memory and effector cells. Effector CD4+ T-cells release cytokines which stimulate APC’s to kill foreign cells, for example Interferon-γ (IFN-γ) release stimulates macrophages to destroy foreign cells via the production of oxygen radicals and enzymes. Effector CD8+ T-cells are themselves able to kill the cell presenting allogeneic MHC Class I which they have bound. Destruction of transplanted cells results in the tissue becoming necrotic and dying. Memory T-cells are long lived cells which reside in the body to rapidly expand if the same foreign MHC molecules are presented again in the future, resulting in a much more rapid response (Janeway, *et al*., 2005, Knight & Ingham, 2006).

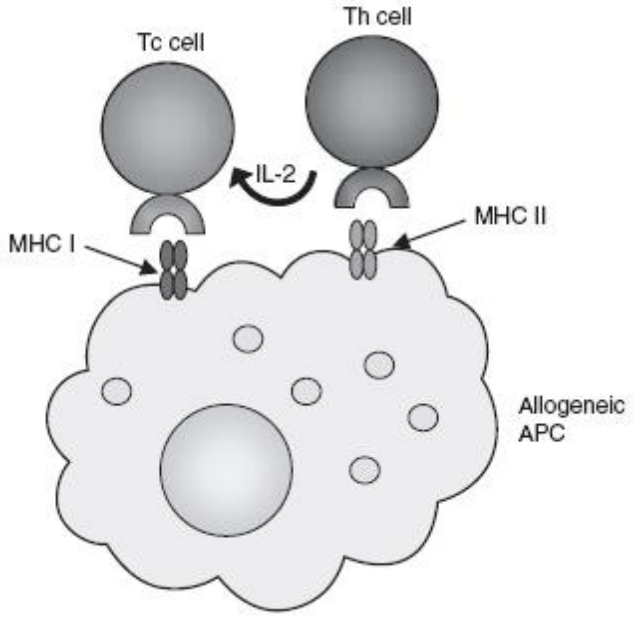

Figure 1.17 Direct antigen recognition. Helper T-cells recognise allogeneic MHC Class II on allogeneic antigen APC and release IL-2 to stimulate cytotoxic T-cells which then recognise allogeneic MHC Class I. Th cell = CD4+ Helper T-cell, Tc = CD8+ Cytotoxic T-cell. Figure adapted from Knight and Ingham (2006).

In addition to the mechanism of recognising allogeneic MHC molecules described above, MHC molecules shed by cells of the transplant tissue can be picked up by antigen presenting cells, and epitopes derived from the MHC molecule presented, leading to a cell mediated immune response. Cytotoxic CD8+ T-cells can then respond to MHC Class I molecules presented on all allogeneic cells (Figure 1.18; Janeway, *et al*., 2005, Knight & Ingham, 2006).

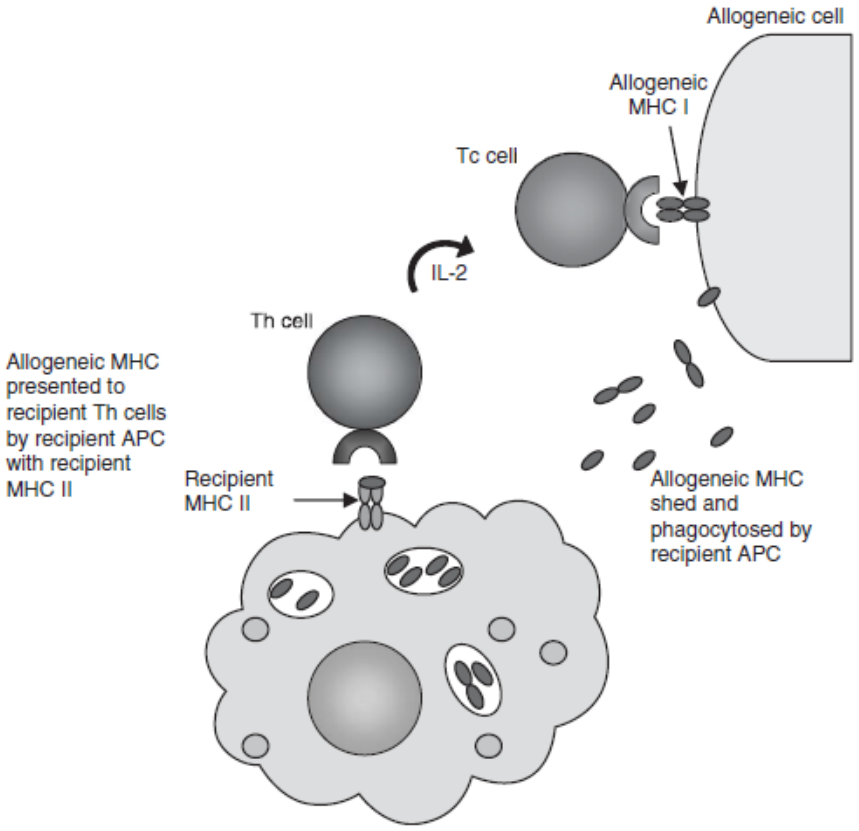

Figure 1.18 Indirect antigen recognition. MHC fragments are shed by allogeneic cells, these are then taken up and epitopes presented on MHC Class II by APCs. Helper T-cells recognise allogeneic MHC epitopes release IL-2 to stimulate cytotoxic T-cells which then recognise allogeneic MHC Class I. Th cell = CD4+ Helper T-cell, Tc = CD8+ Cytotoxic T-cell. Figure adapted from Knight and Ingham (2006).

1.6.3.1.2 Immunological response to xenografts

Although xenogeneic cells will elicit immune rejection via the response described for allogeneic cells, they primarily induce hyper-acute rejection. Cells of xenogenic tissues possess a cell surface sugar, galactose α1-3

galactose (α-gal), which is present in all mammals except for humans and old world monkeys (Galili *et al*., 1987). Humans have a high titre of antibodies against a sugar epitope present on bacteria in the human gut which is similar in shape to α-gal. Upon transplantation of xenogeneic cells expressing α-gal, antibodies rapidly bind to the epitope on endothelial cells of blood vessels, activating the complement cascade leading to inflammation and blood clotting, the vessels become blocked which results in hypoxia and death of the transplant tissue (Janeway, *et al*., 2005, Knight & Ingham, 2006).

By removing whole cells, membranes and cytoplasmic proteins from allogeneic or xenogeneic tissues, only the nonimmunogenic ECM proteins will remain. The tissue will retain its biological/biochemical structure and function yet will not elicit an immune response upon implantation.

1.6.3.1.3 Macrophage response to decellularised tissues

Macrophages are large mononuclear cells of the immune system which have been reported to be “classically activated” or “alternatively activated”. More recently macrophage phenotype has been shown to be a continuum between the two forms (Mills *et al.*, 2000). Classically activated or M1 macrophages are aligned with the Th1 CD4+ T-cell response. The secretion of IFN- γ by T-cells or the presence of TNFα or bacterial lipopolysaccharide (LPS) activate macrophages with enhanced microbicidal capacity and increased proinflammatory cytokine secretion. Alternatively activated, M2 macrophages are aligned with the Th2 CD4+ T-cell response. The secretion of IL-4 and IL-13 by T-cells activate macrophages with a role in the immune response to parasites, but also in allergy, wound healing, and tissue remodelling (Cassetta *et al*., 2011).

Brown *et al.* (2009) identified a change in macrophage polarisation in response to transplanted tissues with or without a cellular component. *In vivo*, cellular xenografts were infiltrated by M1 type macrophages which resulted in a proinflammatory response and scar tissue formation, whereas acellular xenografts and allografts were infiltrated with M2 polarised macrophages which resulted in constructive tissue remodelling.

Furthermore, Kean *et al*. (2012) have reported an association between decellularisation efficacy and macrophage polarisation, with ineffective removal of cell debris (despite histological confirmation of whole cell removal) resulting in a higher M1:M2 ratio.

It is therefore, not only important to ensure the full removal of cells to avoid eliciting an immune response and graft rejection, but it is necessary to ensure effective removal of cellular debris, to tailor the tissue remodelling response from macrophages.

1.6.3.2 Natural acellular (osteo)chondral scaffolds

With the success of natural acellular scaffold materials for the repair of other tissues, it is possible that the most optimal treatment for articular cartilage repair is to use decellularised xenogeneic or allogeneic (osteo)chondral tissues. These constructs would ideally be structurally, biologically and mechanically relevant to natural articular cartilage. Acellular natural materials would also be biocompatible, biodegradable and bioresorbable. Removal of the existing allogeneic/xenogeneic cells would allow the construct to be immunocompatible. A limited number of approaches for natural cartilage tissue decellularisation are currently undergoing research and development (Benders *et al*., 2013).

1.6.3.2.1 Decellularisation of homogenised cartilage matrix

Yang *et al*. (2008) developed a method whereby human cadaveric cartilage was physically shattered in PBS containing protease inhibitors and then centrifuged to produce microfilaments. Treatment with triton X-100 (1 % v/v in hypotonic tris-HCl) and hypotonic solution, nucleases and extensive phosphate buffered saline (PBS) washes resulted in decellularised cartilage microfilaments.

Yang *et al.* (2010) developed a method whereby bovine cartilage was lyophilised and ground to a powder prior to decellularisation with trypsin, nucleases, hypotonic buffer and triton X-100 (1 % v/v in PBS) in the presence of protease inhibitors and antimicrobial agents, again followed by extensive PBS washes.

In both instances, the acellular cartilage matrix was then freeze dried into moulds and cross linked to produce a biomaterial. Scaffolds produced from decellularised homogenised cartilage have the benefit of retaining bioactive cues for cell growth and are also more customisable; however, they lack the 3D architecture and structure of native cartilage and therefore have reduced biomechanical function

1.6.3.2.2 Decellularisation of cell derived matrix

Elder *et al*. (2009) cultured week old calf chondrocytes in agarose to produce a 3D disc shaped cell-derived cartilage ECM. They then investigated the efficacy of different detergents to remove the cells from the construct. Discs were treated with a PBS decellularisation solution containing nucleases, protease inhibitors and antibiotics and either sodium dodecyl sulphate (SDS; 1% and 2% w/v), tributyl phosphate (TnBP; 2% w/v) or triton X-100 2% (v/v) then washed in PBS.

Although decellularised cell-derived-ECM scaffolds have no issues regarding biocompatibility, the need to culture cells renders the process time consuming and this approach requires cell harvesting from the patient, increasing the number of invasive procedures performed and potentially causing donor site morbidity. The 3D structure and composition of the cell derived matrix is currently not comparable to natural cartilage tissues.

1.6.3.2.3 Decellularisation of native cartilage

Elder *et al.* (2010) developed a decellularisation protocol (based on earlier work; Elder *et al*., 2009) for 4 week old calf distal femur articular cartilage with the intention of producing a facet joint cartilage repair biomaterial. The short protocol included one freeze/thaw cycle followed by the use of 2 % SDS (w/v) in PBS with deoxyribonuclease (DNase), ribonuclease (RNase), ethylenediaminetetraacetic acid (EDTA) and penicillin/ streptomycin/ fungizone, then a final wash step in PBS. Different durations of SDS incubation were investigated. Incubation for 2 hours had no detrimental effects on cartilage GAG content or biomechanics, however no significant reduction in DNA content was seen and whole cell nuclei were still present, although the number was reduced. Incubation of cartilage for 8 hours in

SDS enabled the removal of all whole cell nuclei, however the DNA content was still 3861 ng.mg^{-1}, only a 40 % reduction from fresh. In addition, increased duration of SDS wash incubations led to loss of GAGs and a reduction in biomechanical properties. With > 50 ng.mg^{-1} DNA remaining, the treated cartilage did not meet the criteria set by Crapo *et al*. (2011) to be defined as a decellularised matrix. The poor DNA reduction with this protocol was likely due to the initial high cellularity seen in the immature source tissue and also potential inhibition of nucleases through inappropriate application conditions. Nucleases require the presence of magnesium to perform nucleotide cleavage and would be denatured by SDS within the buffer.

Schwarz *et al*. (2012) aimed to develop a porous collagen matrix from natural cartilage tissues, including meniscus and nasal septum cartilage from porcine and human source tissue. As such they did not make an attempt to retain the natural proteoglycan structure and biomechanical properties of the tissues. Cartilages were successfully decellularised using a protocol involving osmotic cell lysis with distilled water, following which sodium hydroxide (> pH 12) was used to inactivate pathogens, denature DNA/RNA and remove cellular debris. Samples were defatted in 70 % (v/v) ethanol and GAGs and other non-collagenous proteins were denatured and removed using a guanidine hydrochloride (1 M) solution containing sodium acetate (0.05N). Cartilages were finally sterilised using hydrogen peroxide (5% v/v). This produced a highly porous collagen scaffold, devoid of GAGs, which would encourage rapid cell infiltration. This protocol was not intended for articular cartilage decellularisation, and the produced matrix would not provide an acceptable repair material.

The decellularisation of intact native cartilage tissues has the potential to produce an ECM with bioactive cues, the natural biological, biochemical and biomechanical composition and structure. However, the clinical relevance/success of such products may be limited, as such approaches do not provide a subchondral bone component for integration and stability of a cartilage repair biomaterial upon implantation.

1.6.3.2.4 Decellularisation of osteochondral tissues

Here it is proposed that the decellularisation of osteochondral xenogeneic tissues may provide the best osteochondral lesion repair graft material. The addition of a bony component to the overlying cartilage layer may improve integration of the graft to the natural joint to avoid problems associated with graft loosening. Using a xenogeneic donor allows for a larger range of graft sizes, as many treatments such as mosicplasty are limited by available graft sizes and donor site morbidity. Another benefit of the proposed biomaterial would be the 'off the shelf' availability, with no reliance on donor human tissue, allowing greater ease of use and convenience during surgery. Acellular osteochondral pins could easily be adopted into current surgical procedure for mosaicplasty.

Preliminary work has been performed to determine the capacity for decellularising natural xenogeneic tissues to use as an osteochondral graft. Kheir *et al.* (2011) investigated the use of a decellularisation protocol developed by Booth *et al* (2002) to develop an acellular porcine scaffold. Osteochondral tissues were subject to four cycles of freeze thaw (the final two in hypotonic solution) and then incubated through 6 cycles of 24 h in hypotonic solution followed by 24 h in 0.1 % (w/v) SDS in hypotonic solution, both containing aprotinin and EDTA at 45 °C with agitation. Blocks were than treated with nuclease and sterilised using 0.1 % Peracetic acid (PAA; v/v). The process was completed by 2 x 30 min PBS washes and a short 24 h final PBS wash. This technique enabled complete decellularisation with no detectable remnants of cellular debris or the α-gal epitope, but still with retention of original collagen content. However there were severely depleted levels of GAGs within the tissue and the collagen fibres seemed to be disrupted, appearing more loosely packed. The decellularisation process had the effect of massively decreasing the compressive stiffness of the tissue in mechanical studies, with the resulting matrix being inappropriate as a graft material.

This previous work has outlined the possibility of using acellular xenogenic scaffolds, however it highlighted various issues which need to be addressed. The loss of GAGs and collagen disruption seen when full

decellularisation was achieved, led to the loss of the biomechanical properties of cartilage. The initial starting material for decellularisation may not have been optimal, Kheir *et al*. (2011) used porcine osteochondral tissues extracted from 4 month old pigs. Characterisation of osteochondral pins from various species of different ages may determine which material has properties most similar to that of human cartilage and may indicate more robust materials which will be least affected by harsh decellularisation protocols. Materials with higher levels of GAGs and more defined structure initially may show less disruption.

The decellularisation protocol used previously employed EDTA as a proteinase inhibitor, however, this also acts to decalcify the bony component of osteochondral pins. Removal of EDTA from the process may retain the structural stability of decellularised pins. Previous studies have highlighted problems with detergents removing GAGs from the tissue. Altering the concentration of detergents may reduce the effect of decellularisation protocols on GAG content. Fewer wash cycles or reduced cycle times may also act to retain GAGs, but adversely may not adequately remove cellular components. Taking into account these possible alterations, a more effective protocol for osteochondral decellularisation may be developed.

1.7 Aim & Objectives

Hypothesis

It is hypothesised that a biocompatible xenogeneic osteochondral matrix can be developed with the structure and function of native tissue ECM for use in osteochondral lesion repair.

Aim

The aim of this project is to develop a natural decellularised xenogeneic osteochondral biomaterial with similar biological, biochemical and biomechanical properties to natural articular cartilage for use in articular cartilage defect repair.

Objectives

- To determine the optimal starting material for decellulartisation by assessing the biological, biochemical and biomechanical characteristics of osteochondral tissues taken from hips and knees of bovine, porcine and ovine animals.
- To optimise the protocol for decellularisation xenogeneic osteochondral tissues.
- To determine the biological and biochemical and biomechanical characteristics of the acellular osteochondral tissues by histological, immunohistochemical and quantitative methods
- To investigate the regenerative capacity of the biomaterial in terms of cytotoxicity and biocompatibility.

Chapter 2
Materials and Methods

2.1 Materials

2.1.1 Equipment

The equipment used and equipment suppliers are listed in appendix A Table 1.

2.1.2 Chemicals

The chemicals/reagents used and chemical suppliers are listed in appendix A Table 2

2.1.3 Consumables

The consumables and plastic ware used and suppliers are listed in appendix A Table 3 and appendix A Table 4 respectively.

2.1.4 Cells

The cells used in this study and suppliers are listed in Table 2.1.

Cells	Type	Species	Supplier
3T3 Cells	Fibroblasts	Murine	European collection of cell cultures
BHK	Fibroblasts	Hamster	Health Protection Agency

Table 2.1 Cells used throughout the study.

2.1.5 Glassware

Glassware (beakers and bottles [100 ml, 1,000 ml and 2,000 ml]) were cleaned by immersion in a 1% (v/v) solution of phosphate-free detergent (Neutracon®, Decon Laboratories Ltd) overnight. Following this, glassware

was rinsed in tap water, and a final rinse in distilled water to remove any residual detergent. Glassware was then dried and sterilised (180 °C for 4 h, as required) by dry heat.

2.1.6 General stock solutions

2.1.6.1 Phosphate buffered saline (PBS)

One PBS tablet was dissolved in 100 ml distilled water. The pH was adjusted to pH 7.2 -7.4.

2.1.6.2 Baby hamster kidney (BHK) cell culture medium

Glasgow's minimal essential media (GMEM) was used with 5 % (v/v) foetal bovine serum (FBS), 2.5 % (v/v) tryptone phosphate broth (TPB), 1 mM L-glutamine, 100 $U.ml^{-1}$ penicillin and 100 $U.ml^{-1}$ streptomycin.

2.1.6.3 3T3 cell line culture medium

Dulbecco's modified Eagle's medium (DMEM) was used with 10 % (v/v) FBS, 2 mM L-glutamine, 100 $U.ml^{-1}$ penicillin and 100 $U.ml^{-1}$ streptomycin.

2.2 Methods

2.2.1 General methods

2.2.1.1 Measurement of pH

The pH of solutions was measured using a Jenway 3020 pH meter. The pH meter was firstly calibrated using solutions of pH 4, 7 and 10 made from buffer tablets dissolved in deionised water. The pH of solutions was measured using temperature compensation. For pH adjustment of solutions, 1M hydrochloric acid or 1M sodium hydroxide was added drop-wise with stirring.

2.2.1.2 Microscopy

Bright-field microscopy was carried out using an Olympus BX40 microscope. In order to use polarized-light microscopy, a polarizer and analyser were incorporated in the usual bright-field set up. Fluorescence microscopy was carried out with the fluorescent vertical illuminator (BX51-RFA) and appropriate filters using the same microscope. Cells in tissue culture plates were viewed using an inverted microscope (Olympus IX71) set up for phase contrast microscopy. Images were captured using an attached Olympus digital camera controlled through Cell^B software (image capture and digitalisation).

2.2.1.3 Sterilisation

Solutions and equipment were sterilised using one of three procedures

- Dry heat sterilisation – Items suitable for dry heat sterilisation were placed in a hot air oven for 4 h at 180 °C.
- Moist heat sterilisation – Items which were not suitable for dry heat sterilisation were sterilised in an autoclave for 20 min at 121 °C at a pressure of 103 kPa.
- Filter sterilisation – Solutions which were not suitable for heat sterilisation were filtered using 0.2 µm pore sized filters using a disposable syringe in a class II safety cabinet.

2.2.2 Tissue acquisition

2.2.2.1 Dissection equipment

The dissection equipment used and suppliers are listed in Table 2.2 and shown in Figure 2.1.

Equipment	Size/model	Supplier
Bench top Clamp	-	Irwin
Corer (serrated drill attachment)	9 mm diameter	University of Leeds
Corer (serrated)	9 mm diameter	University of Leeds
Corer (smooth)	9 mm diameter	University of Leeds
Hand drill	-	Bosch
Hand saw	-	-
Rat toothed forceps	125 mm length	Fisher Scientific Ltd
Scalpel handle	Size 4	Scientific Laboratory Supplies Ltd
Straight fine point forceps	115 mm length	Fisher Scientific Ltd
Straight scissors with fine point	125 mm length	Fisher Scientific Ltd

Table 2.2 Dissection equipment used throughout the study.

Figure 2.1 Dissection equipment. A – Hand held power drill. B – Metal File. C – Smooth corer. D – Serrated corer. E – Serrated corer drill attachment. F – Scalpel. G – Hack saw. H – Clamping apparatus to hold large limbs in place. I – Bench top vice for holding smaller limbs in place.

2.2.2.2 Dissection

Porcine, ovine and bovine legs were supplied by local abattoirs, usually within 24 h of slaughter (bovine legs within 96 h). Pigs were aged ~ 6 months, sheep 8-12 months and > 4 yr and cows ~ 18 months. Joints were used fresh, or stored at 4 °C overnight for dissection the following day.

Porcine and ovine legs were dissected as shown in Figure 2.2. Excess flesh was removed from the skeletal structures to allow easier access and maneuverability. Joints were exposed by cutting the surrounding tissue and extracapsular ligaments, then the joint capsule was excised. All ligaments were severed and the menisci removed from the knee so that all joint surfaces were exposed. Any exposed cartilage surfaces were kept hydrated throughout by covering in PBS soaked tissue. Bovine legs were supplied without the acetabulum and with the meat already removed, so only excision of the patella and menisci was required.

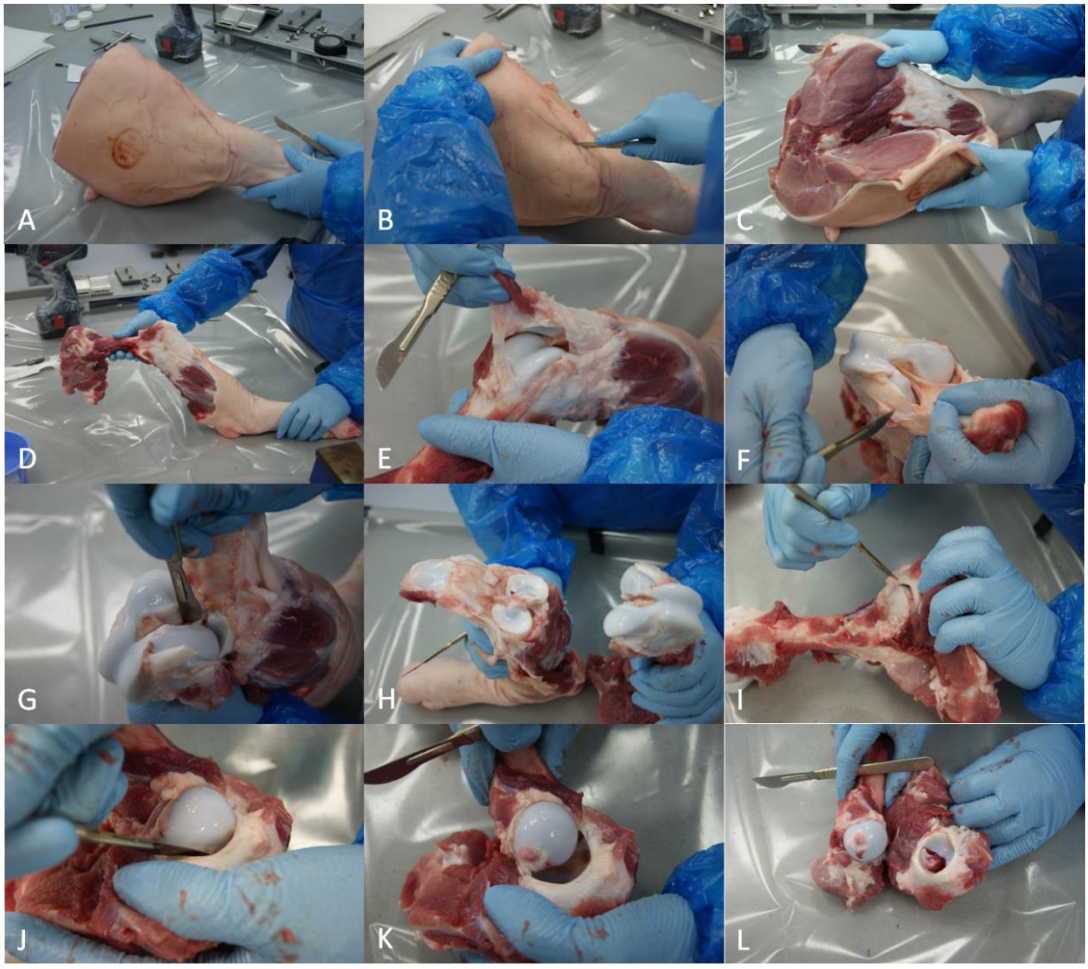

Figure 2.2 Dissection of porcine legs. A – Whole porcine Leg. B – Incision made laterally to the knee. C – Enlargement of incision site, parallel to femur. D – Full removal of flesh. E – Incision made into joint cavity between patella and grove on the lateral side. F – Collateral ligaments severed. G – Severing of cruciate ligaments. H – All knee surfaces exposed. I – Incision made to medial side of the hip joint capsule. J – Teres ligament severed. K – Incision to joint capsule extended following the labrum. L – Femoral head and acetabulum fully exposed.

2.2.2.3 Pin extraction

Osteochondral pins 9 mm in diameter and ~12 mm deep were extracted from cartilage surfaces of the acetabulum, femoral head, femoral groove, medial and lateral condyles and the medial and lateral tibial plateau. The side of each joint was removed with a hacksaw to ease pin extraction. The pins were initially marked out then a power drill with a specialist corer drill bit was used to cut into the subchondral bone. A handheld corer was then used to loosen the pin and extract it from the joint. Images showing the procedure for the bovine femoral groove are shown in Figure 2.3.

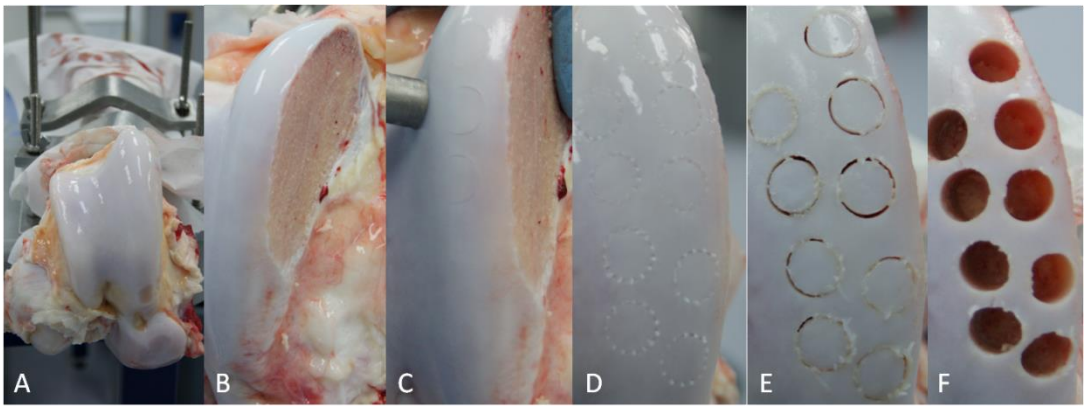

Figure 2.3 Extraction of osteochondral pins. A – Intact bovine femoral groove. B – Edge of groove removed for ease of extraction. C – Position of extraction marked out with smooth corer. D – indentations made with serrated corer to allow drill attachment to grip. E – Cores drilled out. F – Pins fully extracted.

2.2.2.4 Storage

Pins were rinsed in PBS before being placed in plastic storage pots on PBS moistened filter paper and kept at -20 °C for up to 3 months.

2.2.3 Basic histological techniques

2.2.3.1 Fixation

Osteochondral pins were placed in a universal with 15 ml 10 % (v/v) neutral buffered formalin (NBF) for 48 hours to achieve complete fixation prior to decalcification.

2.2.3.2 Decalcification

2.2.3.2.1 Decalcification solution (12.5 % (w/v) EDTA)

Ethylenediaminetetraacetic acid (EDTA; 250 g) and NaOH (25 g) were dissolved in 1.75 L distilled water. The pH was adjusted to 7.0 using 6 M HCl or 6 M NaOH if necessary.

2.2.3.2.2 Decalcification procedure

Bone was decalcified using 25 ml 12.5 % (w/v) EDTA for 2 weeks (or until bone was soft enough to be sectioned) at 45 °C with agitation. Decalcification solution was changed every 2-3 days.

2.2.3.3 Paraffin wax embedding

Osteochondral pins were bisected as described in Figure 2.4 before being placed in plastic cassettes (Histocette®) and cycled in the Leica TP 120 automated tissue processor. Tissues were processed by immersion in 70 % (v/v) ethanol for 1 h followed by 1 h in 90 % (v/v) ethanol. Tissues were then immersed in absolute ethanol for 2 h 20 min, 3 h 20 min then 4 h 20 min. Immersion in xylene followed for cycles of 1 h, 1 h 30 min and 2 h. Tissues were then embedded with molten paraffin wax for 1 h 30 min then 2 h. Tissue cassettes were taken from the automated processor, tissues removed and orientated cut-surface-down in moulds. Samples were covered in molten wax, left to set overnight at room temperature, after which, excess wax was trimmed away.

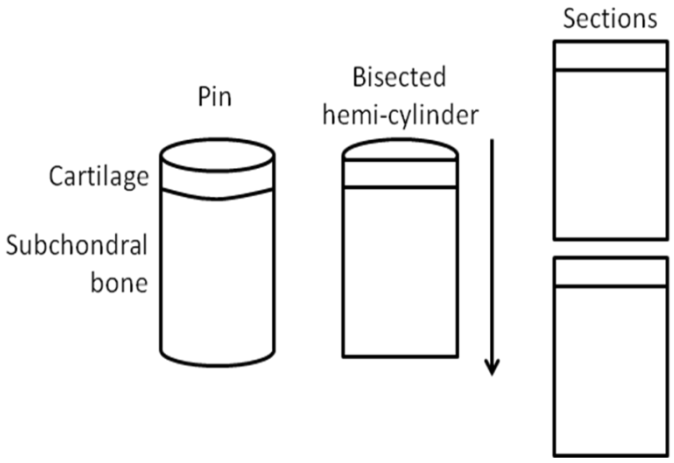

Figure 2.4 Orientation of osteochondral pins for histology. Pins were bisected before being placed in histology cassettes, then the cut surface was laid face down when moulded in wax, so that sections could be cut from the cartilage surface through the osteochondral face.

2.2.3.4 Sectioning and slide preparation

Wax embedded tissues were sectioned on a microtome (Leica RM2125RTF) to a thickness of 6 µm, sections were taken from the cartilage surface through the bone as shown in Figure 2.4, to avoid dragging of bone fragments through the cartilage. Using forceps and a brush, sections were carefully placed in a water bath at 40 °C. The wax sections were then transferred onto Superfrost Plus slides and placed directly onto a hotplate at 45 °C to bake on and dry.

2.2.3.5 Dewaxing and rehydration

Sections were dewaxed in xylene for 10 min, then in fresh xylene for another 10 min. Sections were then dehydrated in 3 successive immersions in 100% (v/v) ethanol for 3 min, 2 min then 2 min followed by immersion in 70% (v/v) ethanol for 2 min. Slides were then placed under running tap water for 3 min to rehydrate the sections.

2.2.3.6 Dehydration and mounting

Stained sections were dehydrated by immersion in 70% (v/v) ethanol for 5 sec, followed by successive washes in 100% ethanol for 1 min, 2 min and 3 min. Sections were then immersed twice in xylene for 10 min each time. Cover slips were mounted to slides using a drop of DPX mountant, avoiding

bubbles. Slides were left to dry in a fume hood for a minimum of 4 h before visualizing using microscopy.

2.2.4 Histological staining methods

2.2.4.1 Haematoxylin and eosin staining

Haematoxylin and eosin (H&E) was used to stain cell nuclei and general tissue architecture. Once paraffin embedded tissue sections had been dewaxed and rehydrated (Section 2.2.3.5) slides were immersed in pre-made haematoxylin (Mayer's) for 1 min, rinsed under running tap water until the water ran clear then immersed in eosin for 3 min. Slides were then dehydrated and mounted (Section 2.2.3.6).

2.2.4.2 Sirius red/ Miller's staining

Reagents:

- *5 % (w/v) potassium permanganate* — 15 g potassium permanganate; 300 ml distilled water
- *1 % (w/v) oxalic acid* — 1 g oxalic acid; 100 ml distilled water
- *Weigert's haematoxylin* — 1 part solution A; 1 part solution B
- *0.1 % (w/v)Sirius Red* — 0.1 g Sirius red; 100 ml saturated piric acid solution

Sirius red stains collagen fibers, while Miller's stains for elastin fibers. Following dewaxing and rehydration sections were immersed in potassium permanganate for 5 min then rinsed using distilled water. Sections were immersed in oxalic acid for 2 min then distilled water for 1 min then 4 min. Sections were then dehydrated in 70 % (v/v) ethanol for one min then 95 % (v/v) ethanol for one minute before being immersed in Millers stain for 1 h. Sections were rinsed in 70 % (v/v) ethanol until clear, immersed in 95 % (v/v) ethanol for 1 minute then rinsed in running tap water for 2 min. Sections were immersed in Weigert's haematoxylin for 10 min then rinsed in

running tap water for 1 min then distilled water for 30 sec. Sections were immersed in Sirius red for 1 h, rinsed in distilled water and blotted dry before being dehydrated and mounted (Section 2.2.3.6). Sections were viewed using polarized light microscopy.

2.2.4.3 Alcian blue staining

Alcian blue was used to stain cartilage proteoglycans, a counter stain of periodic acid and Schiff's reagent (PAS) was used to stain other structures and nuclei were stained with haematoxylin (Gills III). Following dewaxing and rehydration sections were immersed in pre-made 1 % (w/v) alcian blue for 15 min. Sections were rinsed in distilled water then immersed in pre-made periodic acid for 5 min. Sections were again rinsed (three times) in distilled water before immersion in Schiff's reagent for 15 min. Sections were cleared in running tap water for 5 min before being immersed in haematoxylin for 90 sec. Sections were returned to running tap water to clear before being dehydrated and mounted (Section 2.2.3.6).

2.2.4.4 Van Gieson staining

Reagents:

- *1.0 % (v/v) Acid alcohol* — 2 ml hydrochloric acid (37 %, v/v)
  200 ml 70 % (v/v) ethanol

Van Gieson stains for collagen fibres, nuclei are stained with haematoxylin. Following dewaxing and rehydration sections were immersed in Weigert's haematoxylin for 15 min, then running tap water for 15 min. Sections were then differentiated in acid alcohol for 2 min and cleared in running tap water for 3 min before being immersed in van Gieson stain for 3 min. Each section was blotted dry before being dehydrated and mounted.

2.2.4.5 Safranin O/ fast green staining

Reagents:

- *0.1 % (w/v) Safranin O* — 0.1 g safranin O
  100 ml distilled water
- *0.02 % (w/v) Fast green* — 0.02 g fast green

100 ml distilled water

- *1.0 % (v/v) acetic acid* — 3 ml glacial acetic acid; 300 ml distilled water

Safranin O stains proteoglycans while fast green stains collagen, nuclei are stained with Weigert's haematoxylin. Following dewaxing and rehydration, sections were immersed in Weigert's haematoxylin for 3 min then running tap water for 10 min. Sections were differentiated in 1 % (v/v) acid alcohol for 1 min then rinsed for 3 min in running tap water. Sections were immersed in fast green for 5 min before being rinsed in acetic acid for 10-15 sec. sections are immersed in safranin O for 4 min before being dehydrated and mounted.

2.2.4.6 DAPI staining

Reagents:

- *Sodium hydrogen carbonate buffer (1 M, pH 9.0)* — 4.2 g sodium hydrogen carbonate; 500 ml distilled water
- *2.5 % (w/v) DABCO (pH 9.0)* — 2.5 g 1,4-diazobicyclo-(2, 2, 2)-octane (DABCO); 100 ml 1 M sodium hydrogen carbonate buffer
- *DABCO:glycerol mountant* — 10 ml 2.5 % (w/v) DABCO; 90 ml glycerol
- *Dye Buffer (pH 7.4)* — 1.211 g Trizma base; 0.3724 g EDTA; 0.0058 g sodium chloride; 1 L distilled water
- *DAPI dye solution* — 10 mg DAPI; 10 ml nuclease free water
- *DAPI working solution (pH 7.4)* — 20 µl DAPI dye solution

200 ml dye buffer

4',6-diamidino-2-phenylindole (DAPI) binds DNA which enables cell nuclei and DNA remnants to be visualised. Following dewaxing and rehydration, sections were immersed in DAPI working solution for 10 min in the dark. Sections were then washed 3 times for 10 min each in PBS in the dark before being mounted in DABCO:glycerol. Sections were kept in the dark until visualised using an upright fluorescent microscope and a DAPI filter.

2.2.5 Tissue culture

Cells were cultured in cell culture medium (Section 2.1.6). All cell culture work was performed aseptically in a class II safety cabinet. Cultures were incubated at 37 °C in 5 % CO_2 (v/v) in air. Before use, all culture medias and additives were equilibrated to 37 °C.

2.2.5.1 Resurrection and maintenance of cells

Following removal from liquid nitrogen storage, cells were thawed in a 37 °C water bath. Thawed cell stock (2 ml) was added to a T75 cell culture flask containing 13 ml of the appropriate, pre-warmed cell culture medium. Flasks were incubated for at least 18 h at 37 °C in 5 % CO_2 (v/v) in air to allow cells to attach to the culture plastic. Culture medium was changed every 2-3 days until cells were confluent and could be passaged.

2.2.5.2 Cell passaging

Cell culture medium was aspirated and the monolayer gently washed two times with 10 ml PBS without calcium or magnesium. Trypsin/EDTA (1.5 ml) was added to the flask and incubated for 5 min at 37 °C in 5 % CO_2 (v/v) in air. Flasks were gently tapped to detach cells and 10 ml culture medium was added to suspend cells and inhibit trypsin activity. The cell suspension was then centrifuged for 10 min at 150 g. The supernatant was carefully aspirated from the cell pellet, which was then resuspended in 5 ml culture medium. Following a count of viable cells (Section 2.2.5.3), the appropriate cell density was seeded into a fresh flask with culture medium and the medium replaced every 2-3 days until confluent and ready for passage again.

2.2.5.3 Cell viability

In order to test the viability of cells, trypan blue was added to cell suspensions before counting. Trypan blue is able to enter dead cells due to a loss of membrane potential, so live cells microscopically appeared transparent while dead cells appeared blue and could therefore be excluded from cell counts.

To perform a cell count, 20 µl cell suspension was added to 20 µl trypan blue and added to an Improved Neubauer counting chamber. Viable cells were counted in n number of grids which resulted in a cell count of between 100-300 cells. The total number of cells per ml suspension was calculated as follows:

$$Number\ of\ cells.ml^{-1} = \frac{Number\ of\ viable\ cells}{n} \times 10^4 \times Dilution\ factor$$

Where n = number of grids used in count and

And $Dilution\ factor$ = correction required due to dilution of cell suspension in trypan blue (in this case $Dilution\ factor = 2$)

2.2.5.4 Cell cryopreservation

Cells were harvested from flasks and a cell count performed as detailed previously (Section 2.2.5.2 and 2.2.5.3). Cells were resuspended at 10^6.ml^{-1} in cryopreservation medium (DMEM containing 20 % (v/v) FBS and 10 % (v/v) filter sterilised dimethyl sulphoxide (DMSO)). Cell aliquots (1 ml) were put in cryovials and placed into cryofreezing pots containing isopropanol. Pots were frozen at -80 °C for 12 – 24 h following which vials were transferred to liquid nitrogen for long term storage.

2.2.6 Statistical analysis

2.2.6.1 Confidence limits

Numerical data was analysed using Microsoft Excel (version 2007, Microsoft) and presented as the mean (n≥3) ± 95 % confidence level (CL). The 95% confidence intervals (α = 0.05) were calculated using the descriptive statistics part of the data analysis package in Microsoft Excel.

x = Individual value

n = Sample number

∑ = Sum of

$$mean = \frac{\Sigma x}{n}$$

$$StDev = \sqrt{\frac{\Sigma x^2}{n-1}}$$

$$SE\ mean = \frac{StDev}{\sqrt{n}}$$

$$95\ \%\ CL = mean\ \pm t \times SE$$

2.2.6.2 Statistical analysis

The student's t-test was used to compare groups of two means or a one-way analysis of variance (ANOVA) was used when comparing the means of more than two groups. Individual differences between group means were identified by calculating the minimum significant difference (MSD) at p = 0.05 using the T-method, or T'-method when comparing groups of unequal sample size (Sokal & Rohlf, 1995).

Q = Critical value

α = p = 0.05

k = number of groups

v = degrees of freedom (n-1)

$$MSD = Q(_{\alpha[k,v]}) \times SE$$

2.2.6.3 Arcsin transformation

Where data is presented as a percentage or proportion, values were transformed to arcsin to allow accurate calculation of 95 % CL and statistical analysis. Following analysis, values were transformed back for presentation.

2.2.6.4 Linear regression analysis

When interpolation of results was required, a linear regression analysis was performed on standard curves.

$$unknown\ x = \frac{mean\ measured\ y\ variables}{y\ value\ of\ linear\ regression\ line\ equation}$$

Chapter 3
Characterisation of porcine, bovine and ovine osteochondral tissues

3.1 Introduction

To provide successful long-term cartilage lesion repair, a biomaterial should closely mimic the function of natural articular cartilage. As discussed in Chapter 1, the composition and structure of cartilage is essential for the load bearing, low friction function of the tissue. The glycosaminoglycans (GAGs) within the cartilage matrix create a Donan osmotic pressure, reducing fluid flow within the tissue under loading, providing the compressive strength of cartilage, and reducing friction between solid phase components of the matrix. The collagen fibres provide tensile strength for the tissue (Mow *et al.,* 2005, Roughly, 2006). Variations in the biochemical composition and biological structure alter the function of articular cartilage.

Here, it is proposed that the use of an acellular osteochondral biomaterial will enable successful repair of osteochondral lesions. Procedures to decellularise tissues are performed with the aim of producing an immunocompatible scaffold which retains the original tissue function, so the properties of any source material should be retained in the final scaffold. Cartilage biology, biochemical composition and biomechanical function (Athanasiou *et al.*, 1991) varies between species and joint regions (Rogers *et al.*, 2006). Before developing a decellularisation protocol it was sensible to assess the potential tissue sources currently available and to identify which species/joint region has properties most similar to that of human cartilage. Furthermore, assessment of composition will allow any cartilages with high GAG content to be identified, as sulphated proteoglycan concentration is known to be diminished following decellularisation using SDS (Stapleton *et al.*, 2008; Elder *et al.*, 2010; Kier *et al.*, 2011; Crapo *et al.*, 2011; Benders *et al*., 2013).

To achieve good clinical outcomes in osteochondral repair with an acellular xenogeneic scaffold it was therefore necessary to characterise and understand the biochemical composition, biological structure and biomechanical function of any potential source materials and chose a tissue with properties desirable in the decellularised scaffold.

3.2 Aims and objectives

Aims:

The aim of the study presented in this chapter was to characterise osteochondral tissues from various joint regions and species. The intention was to determine the most suitable material for use in the development of a decellularisation process.

Objectives:

- To qualitatively assess the osteochondral tissues using histology, looking at the general histoarchitecture, GAG distribution and to measure cellularity and cartilage thickness.
- To quantify biochemical components of the cartilage, including sulphated proteoglycan, collagen and water content.
- To characterise biomechanical properties of cartilage, measuring the percentage deformation and cartilage thickness, then to determine cartilage permeability and equilibrium elastic modulus using a finite element method.

3.3 Biological methods

Osteochondral pins were collected from the acetabulum, femoral head, femoral groove, medial and lateral condyles and medial and lateral tibial plateau as described in Section 2.2.2. Porcine (~6 month old), bovine (~18 month), ovine (~1 yr and >4 yr) and human cadaveric tissues were characterised. Acetabular tissues were not available from cows, so were not characterised in this study.

3.3.1 Histological evaluation of osteochondral tissues

The general histological methods used in this study can be found in Section 2.2.3.

3.3.2 Cell count

Sections were stained with H&E and the resulting images were analysed using Image-Pro Plus software (Media Cybernetics). For each image n=6, 500 μm^2 regions were manually selected to sample cells from all three cartilage zones (two regions of superficial cartilage, two of middle zone cartilage and two of deep zone cartilage). All cells which fell in that defined region were counted manually. The mean number of cells was calculated for each image. Images from n=5 animals were counted for each joint region. The mean number of cells for each species and joint region and the 95 % CL were calculated.

3.3.3 Thickness measurement

Image-Pro Plus software (Media Cybernetics) was used to measure the thickness of cartilage from all animals, using images of sections stained with alcian blue. Measurements (n=6) were made through the depth of the cartilage at even intervals across the image, the cartilage-bone interface was defined as when the blue stain colour finished and became red/pink staining. Again, the mean thickness of each image was calculated, then the mean of n=5 animals determined plus 95 % CL for that species/ joint region.

3.4 Biochemical methods

3.4.1 Sample preparation

3.4.1.1 Lyophilisation

Cartilage tissue was cut away from the subchondral bone and macerated. Samples were weighed three times and a mean wet weight calculated. Samples were placed in a freeze dryer (Thermo, Savant ModulyoD) at -50 °C, 0.15 – 0.2 mbar, and the weight measured every 24 h until constant (48 - 72 h).

3.4.1.2 Papain digestion

For sulphated proteoglycan quantification, macerated, freeze-dried tissues were digested using papain.

- *Digestion buffer (pH 6.0)* 0.788 g L-cystine hydrochloride
  1.8612 g EDTA
  1 L PBS
- *Digestion solution* 1250 U papain
  25 ml digestion buffer

Papain digestion solution (5 ml) was added to 10 – 20 mg (dry weight) lyophilised cartilage in a bijou and incubated in a water bath at 60 °C for 36 – 48 h, until fully digested.

3.4.1.3 Acid hydrolysis

For quantification of hydroxyproline residues, cartilage was macerated, lyophilised and hydrolysed in hydrochloric acid. Tissues (15 mg) were placed in polypropylene universals and 5 ml 6 M hydrochloric was added. Samples were incubated in a block heater at 120 °C for 8 - 16 h as verified in Figure 3.1, before being neutralised with 6 M sodium hydroxide.

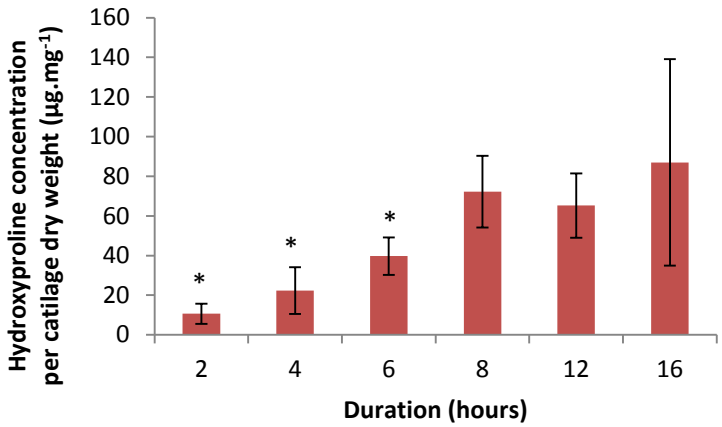

Figure 3.1 Hydroxyproline concentration after varying durations of acid hydrolysis. Data is displayed as the mean (n=3) ± 95 % CL. * Represents a significant difference from 16 h, one-way ANOVA ($p < 0.05$).

3.4.2 Water content

The percentage water content of tissue was determined by weighing before and after lyophilisation (Section 3.4.1.1). The water weight was calculated from the dry and wet weights and was then presented as percentage of tissue wet weight.

3.4.3 GAG quantification

Quantification of GAGs (sulphated/carboxylated proteoglycans) in tissues is possible by colorimetric analysis, using a method first developed by Farndale *et al.* (1982). Under acidic conditions the cationic dye 1,9-dimethylemethylene blue (DMB) undergoes metachromatic changes upon binding with carboxyl or sulphate groups of GAG chains, this can then be measured spectrophotometrically.

Reagents:

- *Phosphate buffer (pH 6.8)* 137 ml sodium di-hydrogen orthophosphate (0.1M)
  63 ml di-sodium hydrogen orthophosphate (0.1M)

- *DMB dye (pH 3.0)* 16 mg DMB
  5 ml ethanol
  2 ml formic acid
  2 g sodium formate
  Make up to 1 L with distilled water

Method:

Tissues were lyophilised and papain digested (Sections 3.4.11 & 3.4.1.2). Standard calibration solutions of dermatan sulphate were made up in phosphate buffer at 0, 3.125, 6.25, 12.5, 25, 50, 100, 150 and 200 $\mu g.ml^{-1}$. Test samples were neat, or diluted 1:10, 1:25, 1:50, 1:100, 1:250, 1:500, 1:1000 in phosphate buffer, a dilution of 1:50 was found to be optimal. Each standard and sample (40 µl) were added to a clear, 96 well flat bottomed plate in triplicate, to which 250 µl DMB dye was added. Plates were gently shaken for 2 min on a plate shaker before the optical density of each well was read at 525 nm using a micro plate spectrophotometer. A standard curve was plotted of the absorbance of the dermatan sulphate standards vs concentration, linear regression analysis was performed (Section 2.2.6.4) to interpolate the GAG concentration of test samples based on their absorbance. Dilution factors were then accounted for, and the concentration of GAG was determined for tissue dry weight.

3.4.4 Hydroxyproline quantification

Hydroxyproline residues are a major constituent of collagen, and are unique to this protein in articular cartilage. Hydroxyproline residues can be oxidised to pyrroles which produce a red chromophore with p-dimethylaminobenzaldehyde, this can then be measured colorimetrically. This method is based on that of Edwards & O'Brien (1980). The hydroxyproline levels can then be used to calculate collagen content.

Reagents:

- *Hydroxyproline buffer (pH 6.2)* 13.3 g citric acid
  3.2 ml glacial acetic acid

32 g sodium acetate 3 hydrate

9.1 g sodium hydroxide

80 ml propan-1-ol

Made up to 400 ml with distilled water

- *Chloramine T* — 1.41 g Chloramine T

  100 ml distilled water

- *Ehrlich's reagent* — 7.5 g p-dimethylbenzaldehyde

  30 ml propan-1-ol

  13 ml 62 % (v/v) perchloric acid

  Made up to 50 ml with distilled water

Method:

Samples were lyophilised and acid hydrolysed (Section 3.4.1.1 & 3.4.1.3). Standard concentrations of trans-4-hydroxy-L-proline were made up in hydroxyproline buffer at 0, 2, 4, 6, 8, 10, 15, 20, 25 & 30 $\mu g.ml^{-1}$. Test solutions were neat and diluted 1:5, 1:10, 1:25, 1:50, 1:100 in assay buffer, a dilution of 1:10 was found to be optimal. Standard and test solutions (50 µl) were added to a clear, flat bottomed 96 well plate in triplicate. Chloramine T (100 µl) was added to each well and the plate shaken gently for 5 min to oxidise the hydroxyproline residues. Ehrlich's reagent (100 µl) was then added to each well and the plate incubated in a water bath at 60 °C for 45 min. The optical density of each well was then measured at 570 nm using a micro plate spectrophotometer. A standard curve was produced of absorbance vs. concentration, from which the hydroxyproline concentration of test samples could be interpolated. Neutralisation and dilution factors were accounted for and the hydroxyproline concentration was determined for cartilage dry weight.

3.5 Biomechanical methods

3.5.1 Creep indentation

In order to assess the time dependent biomechanical behaviour of articular cartilage, osteochondral pins underwent creep indentation. The equipment used is shown in Figure 3.2. Pins were secured in a collet, mounted in a sample holder and submerged in PBS to maintain cartilage hydration (Figure 3.3). An impermeable, stainless steel, hemispherical indenter (3 mm diameter) was used to indent the cartilage with a load of 0.82 N over 1 h. The indenter was positioned ~ 1 mm above the cartilage surface and the lowering of the indenter shaft was controlled via a silicone oil filled dashpot, to reduce the speed of impact, the full load was applied within 0.2 sec. The displacement of the indenter was measured using a linear variable differential transducer (LVDT; RDP D5-200H, Electrosence, PA, USA) and the resistance force measured using a piezo-electric force transformer (Part No. 060-1896-02, Electrosence, PA, USA). LabView 8 software (National Instruments, TX, USA) was used to collect and store data produced by the force transducer and LVDT.

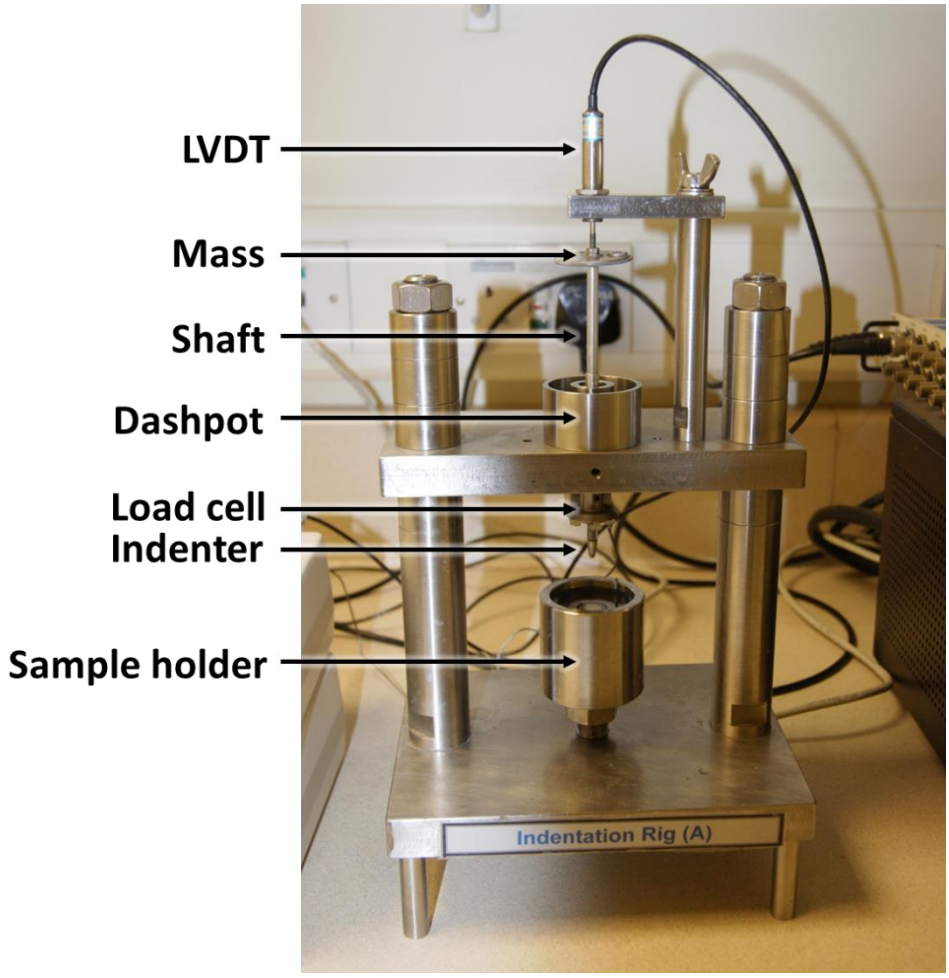

Figure 3.2 Indentation apparatus. The equipment used to perform creep indentation testing to determine deformation of osteochondral pins.

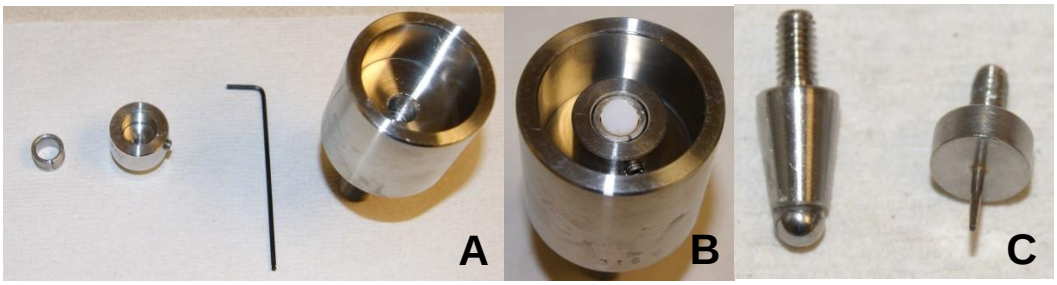

Figure 3.3 Sample holder and indenters. A – collet, collet holder and sample bath, B – Pin held in place, C – hemispherical and needle indenters used during testing.

3.5.1.1 Calibration†

Calibration was required to convert the voltage outputs of the LVDT and force transducer into millimetres and Newtons respectively. Standard steel slip gauges were used to calibrate the LVDT, the voltage was recorded for each height increase following the addition of slip gauges. Voltage was plotted against slip gauge height and the linear trend line calculated, the equation of which was used as a calibration factor (Figure 3.4).

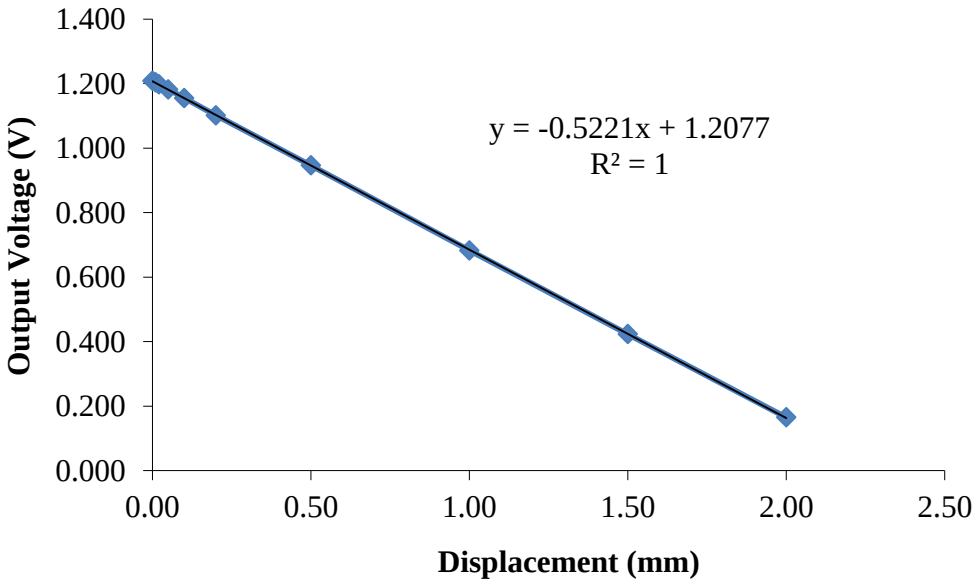

Figure 3.4 LVDT calibration. Calibration of LVDT from the indentation apparatus using standard height slip gauges to determine factor to convert output voltage to displacement.

To calibrate the force transducer, the voltage was recorded over incremental increases of known mass. This again, was plotted as a graph and the equation of the trend line used to convert voltage to Newtons (Figure 3.5).

† Work performed by Abdellatif Abdelgaied

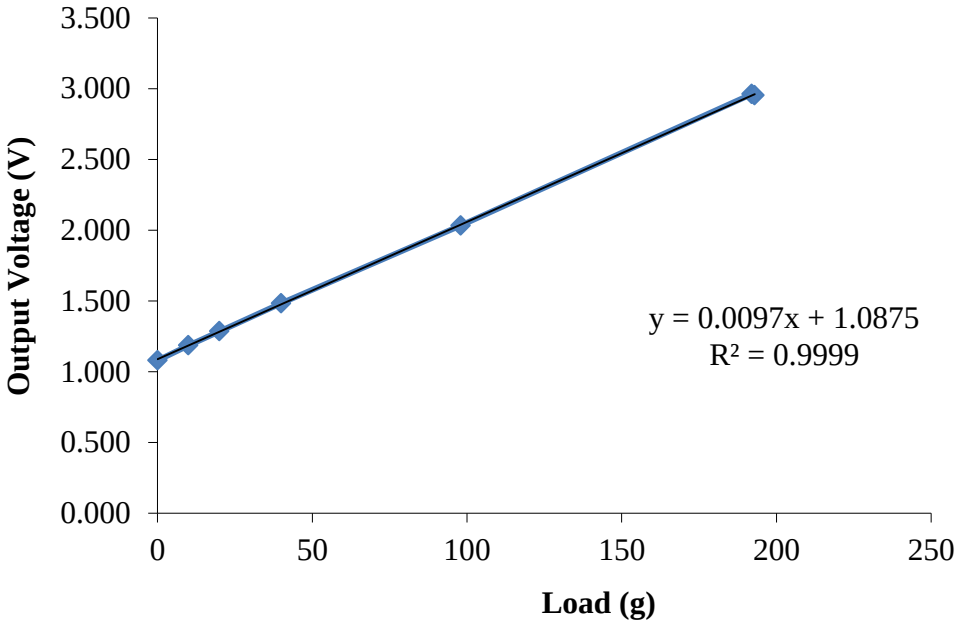

Figure 3.5 Load cell calibration. Calibration of the load cell from the indentation apparatus using standard known masses to determine the factor to convert output voltage to load.

3.5.2 Needle indentation

The thickness of cartilage was measured in order to normalise deformation data for each osteochondral pin so that the percentage deformation could be presented and the material properties could be derived. Cartilage thickness was assessed using needle indentation. An Instron material testing machine (Instron 3365, Bucks, UK) was used for this purpose (Figure 3.6). Osteochondral pins were secured in a PBS bath as described in Section 3.5.1, a needle attached to the instron arm was manually positioned ~1 mm above the cartilage surface. During testing the arm was controlled via a PC graphic user interface and lowered at a rate of 4.5 $mm.min^{-1}$. The resistance to motion was measured using a 500 N load cell.

Cartilage thickness was defined as the distance between the increase in resistance from initial needle contact with the surface and the steep increase in resistance from needle contacting the much stiffer bone (Figure 3.7). Each pin was indented 6 times and the mean thickness calculated.

Figure 3.6 Instron material testing machine. Equipment used to indent osteochondral pins with a needle indenter to determine cartilage thickness.

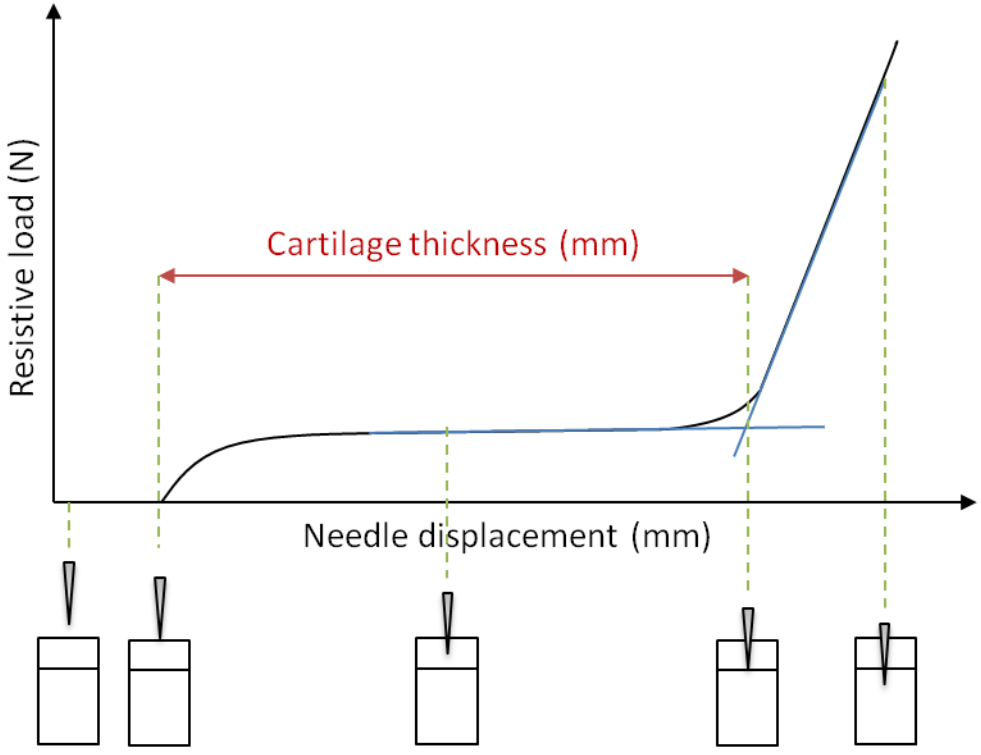

Figure 3.7 Needle indentation graph interpretation. This schematic shows how cartilage thickness was determined from needle indentation.

3.5.3 Finite element method for derivation of material properties

Cartilage deformation curves generated in Section 3.5.1 along with cartilage thicknesses measured in Section 3.5.2 were used to derive the permeability and equilibrium elastic modulus of cartilage. An axisymmetric biphasic poroelastic finite element (FE) model (ABAQUS, version 6.9-1 Dassault Systemes, Suresnes Cedex, France) created and published by Pawaskar *et al.* (2010, 2011) was used for the derivation of these properties (Figure 3.8).

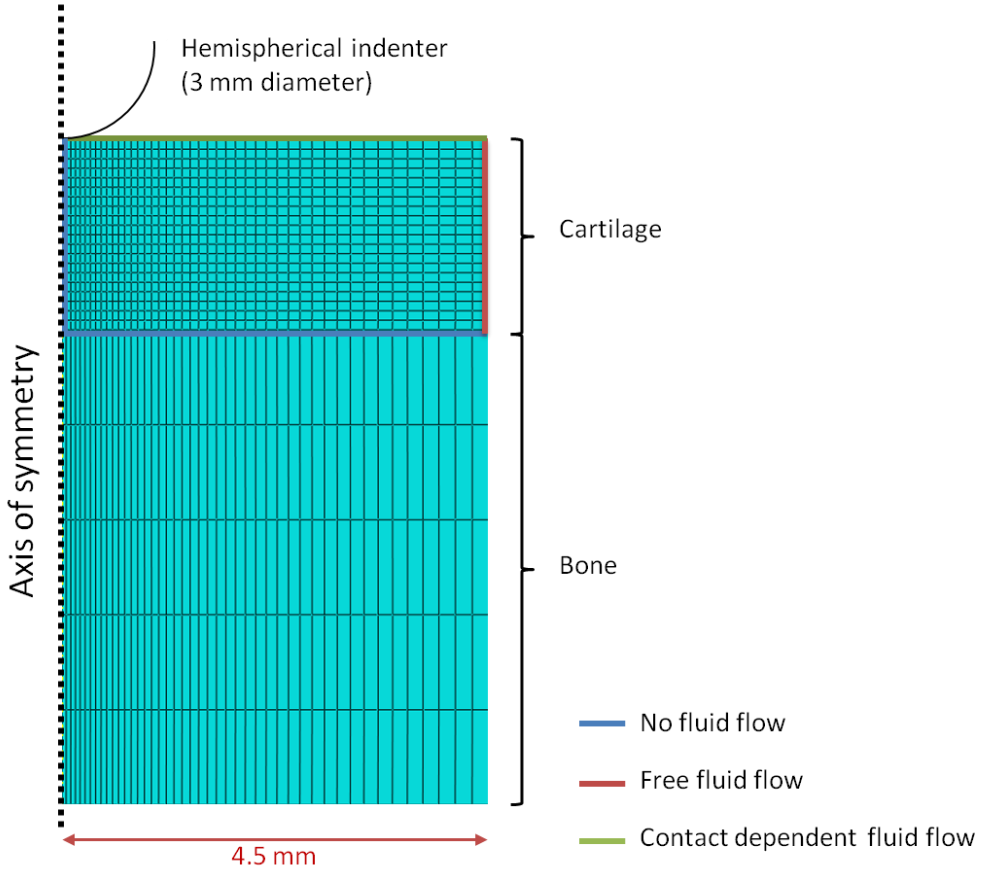

Figure 3.8 Finite element model of an osteochondral pin. This schematic shows the axis of symmetry, and the imposed fluid flow restrictions.

Cartilage was modelled as a poroelastic material and meshed using four-node bilinear displacement and pore pressure axisymmetric elements (CAX4P), cartilage was assigned the water content value calculated in section 3.4.2 and a Poisson's ratio of zero was assumed. Bone was meshed using four-node bilinear elastic axisymmetric elements (CAX4), A Poisson's ratio of zero and was assigned and elastic modulus of 17 GPa (Pawaskar, 2010).

The FE model mimicked the method for collecting experimental data (Section 3.5.1), the load was increased from 0 – 0.82 N over 2 sec through the indenter and was applied for 3600 sec in total. A deformation/time graph was produced by the FE model based on the material properties (equilibrium elastic modulus and permeability) set. The closeness of fit between the final 30 % of the FE generated and experimental curves was assessed using MATLAB (version 7.4, MathWorks Inc, Boston, MA, USA; Figure 3.9). The input material properties were incrementally changed to minimise squared error, an R^2 value greater than 0.6 was accepted as significant for biological tissues. The material properties input into the FE model which gave the highest R^2 were taken as the equilibrium elastic modulus and permeability for that cartilage.

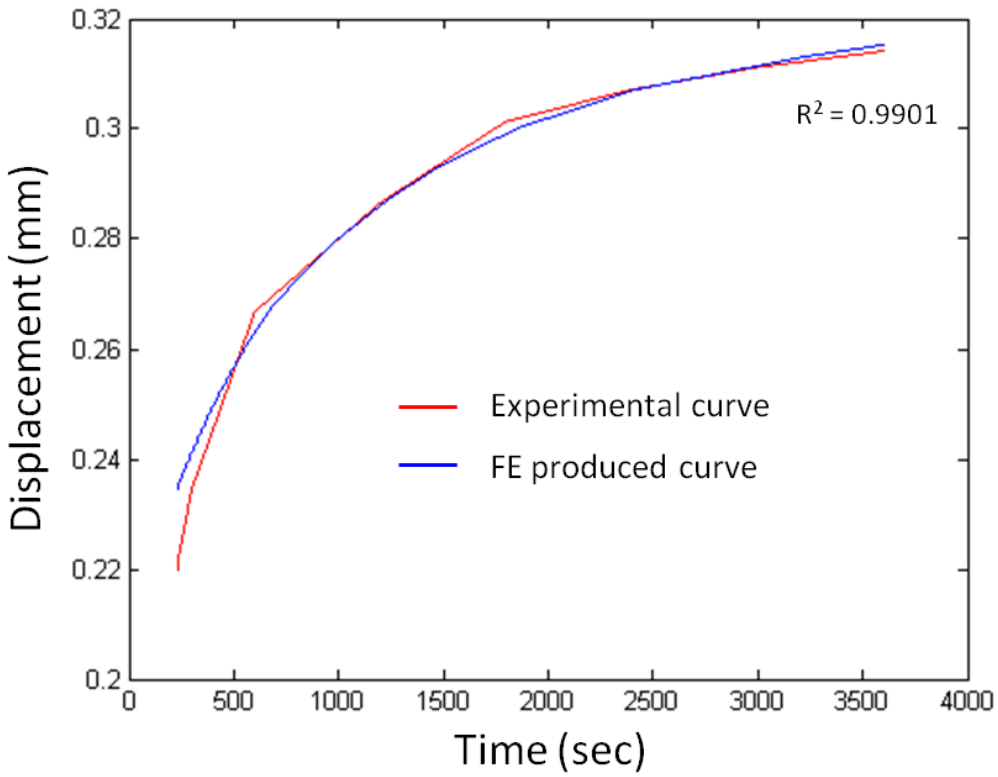

Figure 3.9 Experimental and modelled cartilage displacement curves. The FE modelled curve was fitted to the deformation curve produced by experimental data to reach the highest possible agreement by altering the input material properties.

3.6 Results

3.6.1 Macro scale observations

Upon dissection, physical differences were observed between species. The length of the femurs from femoral head to the front of the condyles was ~ 20 cm in both pigs and sheep; however this was double in cows, ~ 40 cm (Figure 3.7). This size difference was reflected in the size of the joints; the bovine femoral head measured ~ 8 cm from the terres ligament to femoral neck, while the porcine was ~ 4 cm and ovine only ~ 2 cm. This pattern in joint size was seen for both the hip and knee. Cartilage generally appeared white, glossy and healthy with exception of ovine (> 4 yr) cartilage which had a yellowed appearance in most cases. Upon drilling, the bone of porcine and young ovine was notably softer than that of bovine and older ovine samples. Old ovine bone, despite being hard, was also found to be quite brittle when cores were extracted from the joints.

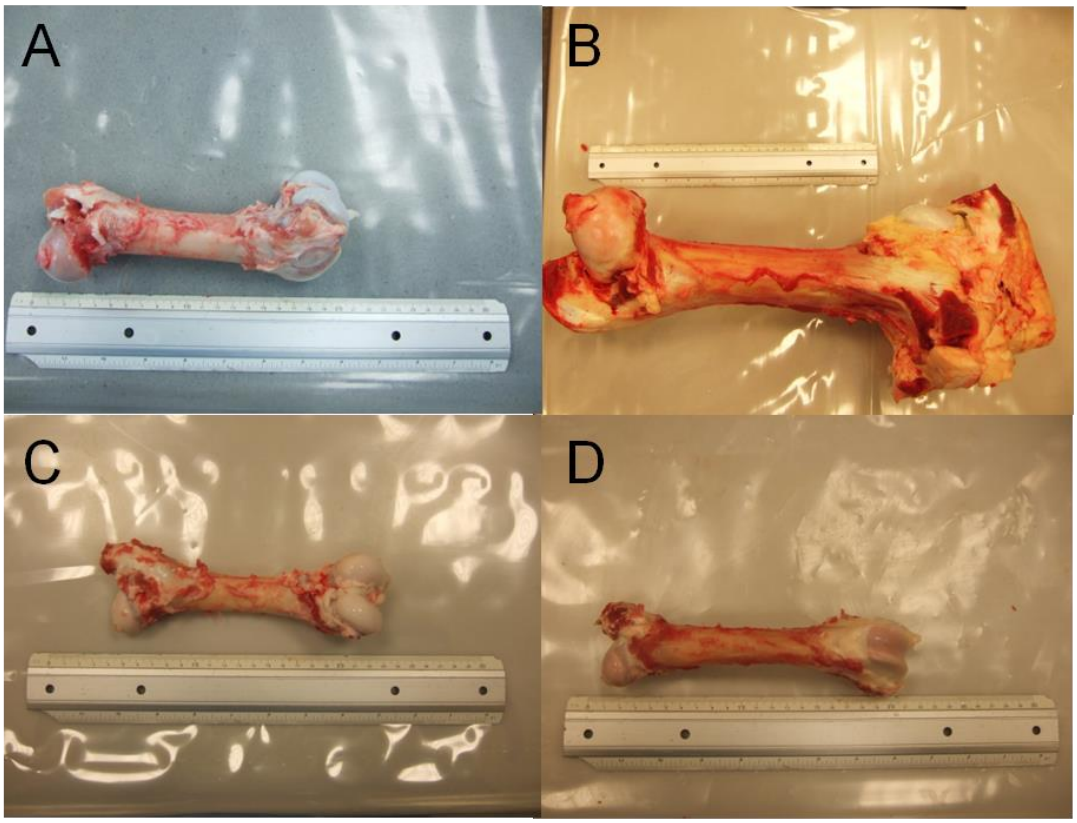

Figure 3.10 Dissected femurs. a) porcine, b) bovine, c) ovine ~ 1 yr and d) ovine > 4 yr.

3.6.2 Histological evaluation of cartilage

3.6.2.1 H&E

H&E staining of osteochondral sections from each species showed characteristic cell orientation (Figure 3.11), with smaller flattened cells at the superficial zone becoming rounder and more randomly distributed in the middle zone and then forming linear columns perpendicular to the cartilage surface in the deep zone. This characteristic cell organisation was less pronounced in porcine (a) and young ovine (c) cartilage and cells in the deep zone showed a more hypertrophic appearance.

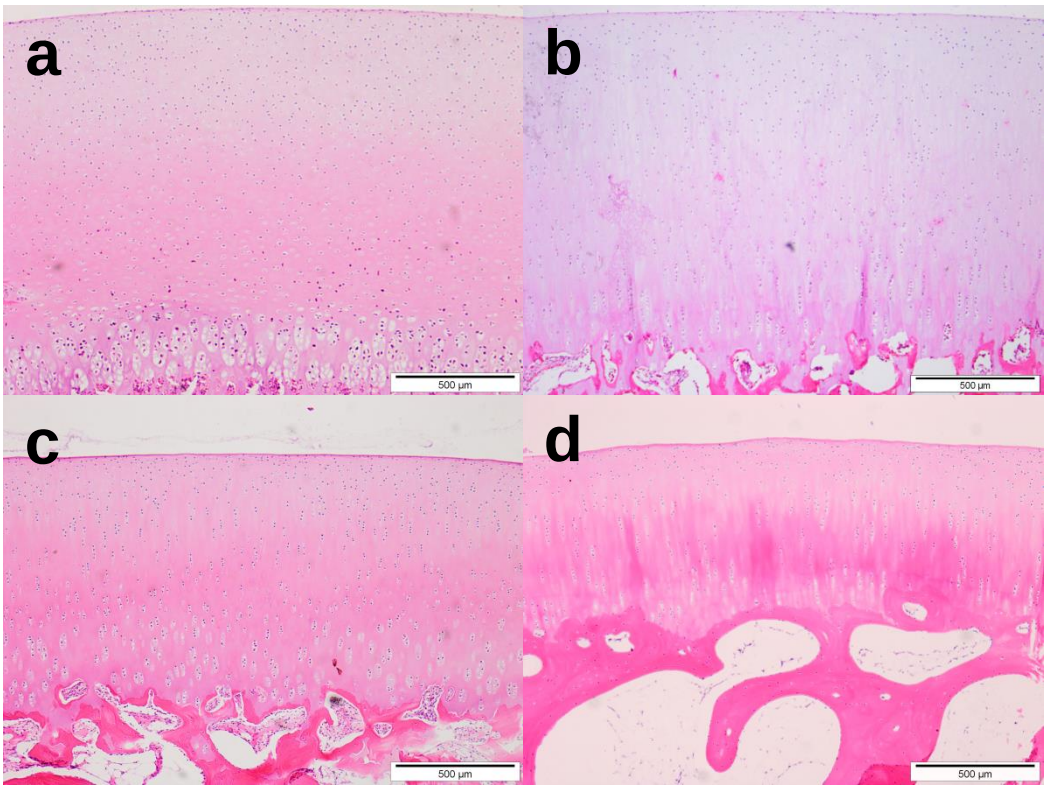

Figure 3.11 H&E staining of cartilage from the medial condyle. a) porcine, b) bovine, c) ovine ~1 yr, d) ovine > 4 years. Size bars are 500 µm.

3.6.2.2 Alcian blue

Alcian blue staining of osteochondral sections from each species showed characteristic proteoglycan distribution (Figure 3.12). All cartilage tissues showed strong alcian blue staining in the middle and deep zones, while the superficial zones and deep calcified cartilage and bone showed reduced

alcian blue staining, highlighted by the presence of pink periodic acid-Schiff counterstaining.

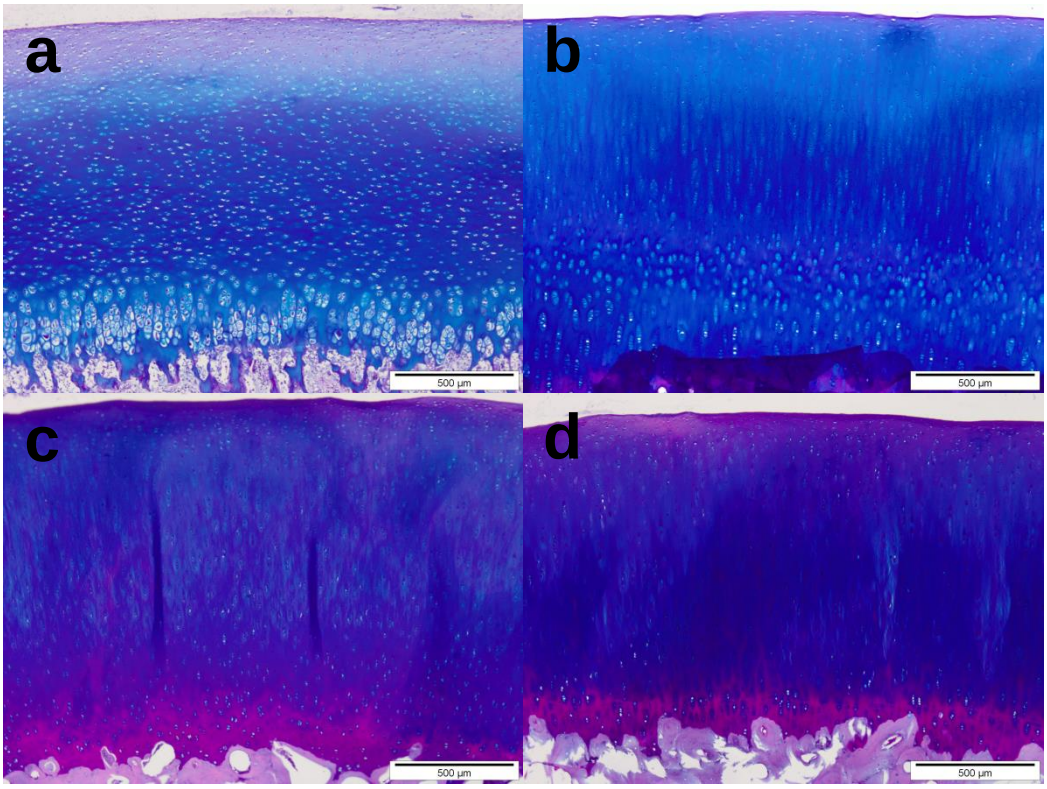

Figure 3.12 Alcian blue and periodic acid-Schiff staining of cartilage from the medial condyle. a) porcine, b) bovine, c) ovine ~1 yr, d) ovine > 4 years. Size bars are 500 µm.

3.6.3 Cell count

From the images of H&E stained sections a cell count was performed to identify cell density of cartilage from the different species and joint areas. Cartilage from the younger animals (pig and young sheep) tended to have the highest concentration of cells and cartilage from old sheep was least cellular, this trend was significant in a number of joint regions (Figure 3.13). Within species, cartilage from the porcine tibial plateau had a significantly higher cell concentration that cartilage from the femoral groove, unlike bovine tibial plateau cartilage, which was significantly less cellular than all other joint regions except for the femoral head. Old ovine cartilage from the acetabulum and medial tibia had significantly fewer cells than other joint regions. No significant difference was seen in young ovine cartilage cellularity across joint regions ($p<0.05$ ANOVA).

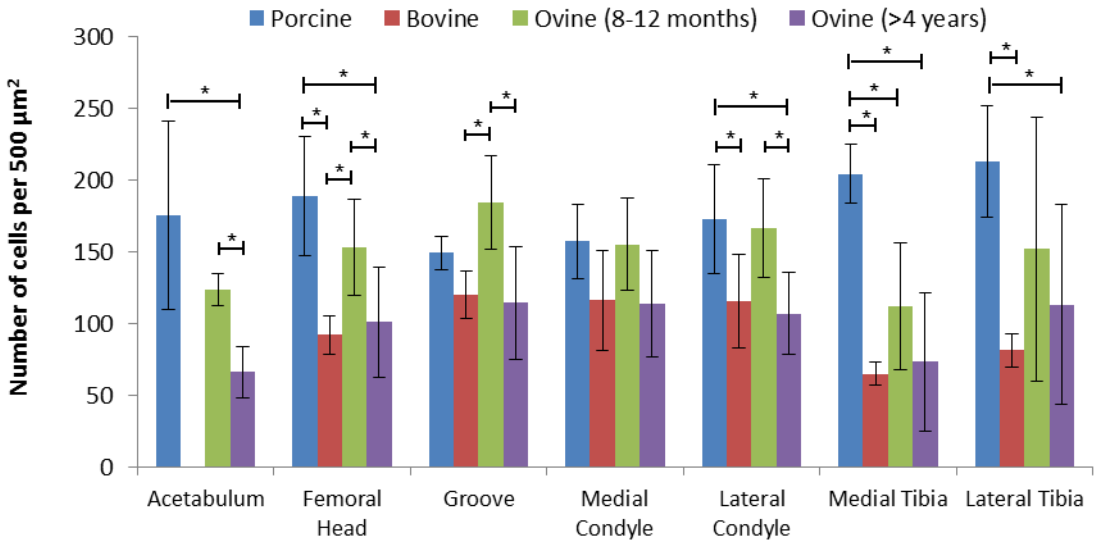

Figure 3.13 Cellularity of cartilage from various joint regions of the pig, cow and sheep. Data is expressed as the mean (n=5) ± 95 % confidence limits. Data for a given tissue site was analysed by one-way analysis of variance and individual means compared by the T-method. * indicates $p<0.05$.

3.6.4 Cartilage thickness measurement

Thickness of cartilage for each species was measured from digital images of the stained sections (Figure 3.14). Ovine cartilage tended to be thinner than porcine and bovine cartilage, significantly so in a number of joint regions. Porcine tibial cartilage was significantly thinner than that of the groove and medial condyle, young ovine femoral head cartilage was significantly thinner than that of the medial tibia, no significant difference between joint areas was seen in bovine or old ovine ($p<0.05$ ANOVA). There was a trend toward cartilage of the condyles and femoral groove being thicker than other joint regions.

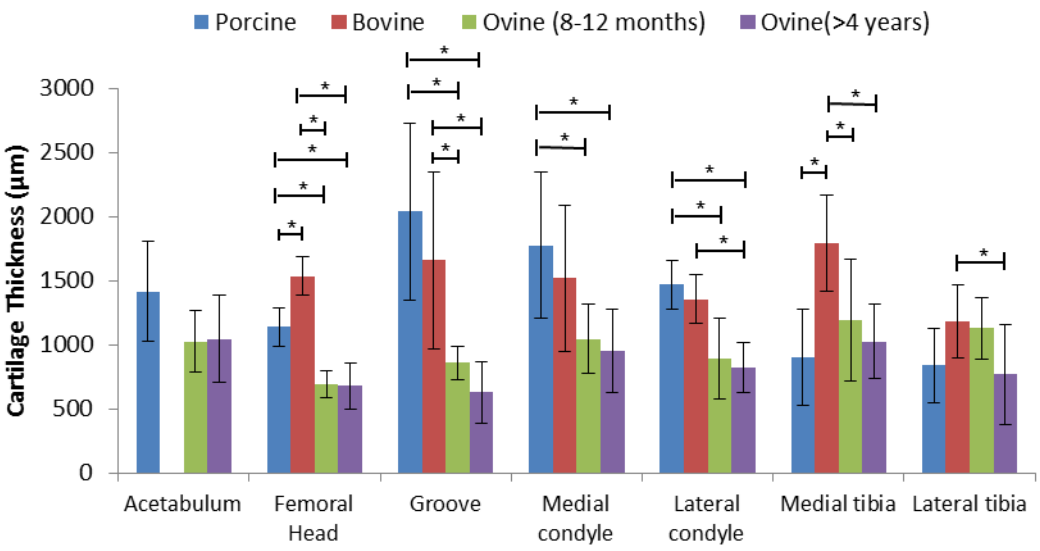

Figure 3.14 Thickness of cartilage from various joint regions of the pig cow and sheep. Data is expressed as the mean (n=5) ± 95 % confidence limits. Data for a given tissue site was analysed by one-way analysis of variance and individual means compared by the T-method . * indicates $p<0.05$.

3.6.5 Water content

The water content of cartilage did not vary significantly between any species except for bovine lateral tibial cartilage which had a significantly higher water content than cartilage from the lateral tibia of older sheep (Figure 3.15). Significant intra-species water content variation was only seen in bovine cartilage, with that from both sides of the tibia having a significantly higher water content than bovine femoral head and medial groove cartilage, cartilage from the lateral tibia also had significantly higher water content than from the bovine femoral head ($p<0.05$ ANOVA). All cartilages had a water content between 70 - 82 %.

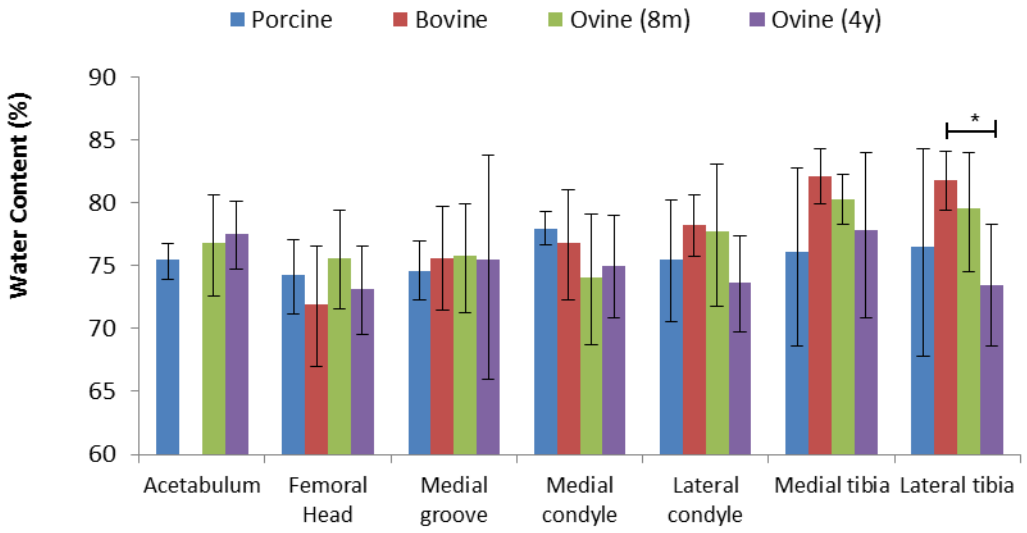

Figure 3.15 Water content of cartilage from various joint regions of the pig cow and sheep. Data was subject to arcsin transformation prior to calculation of the 95% confidence limits and analysis of variance. Data is expressed as the back transformed mean (n=5) ± 95 % confidence limits. Data for a given tissue site was arcsine transformed then analysed by one-way analysis of variance and individual means compared by the T-method . * indicates $p<0.05$.

3.6.6 GAG quantification

The GAG content of porcine cartilage was significantly higher than that of other species in a number of joint regions (Figure 3.16), cartilage from old sheep tended to have the lowest GAG concentration. There was a trend seen across the joint regions, similar to that seen for cartilage thickness, with femoral knee (groove & condylar) cartilage having higher concentrations of GAGs compared to other joint regions. In the pig, cartilage of the groove and both condyles had a significantly higher GAG content than that of the medial side of the tibial plateau, only the medial condyle and groove showed higher concentration than the lateral side. Cartilage from the medial condyle of the older sheep had a significantly higher GAG content than that of the acetabulum, groove and tibia. Cartilage of the bovine lateral condyle had significantly fewer GAGs than the medial tibia ($p<0.05$ ANOVA).

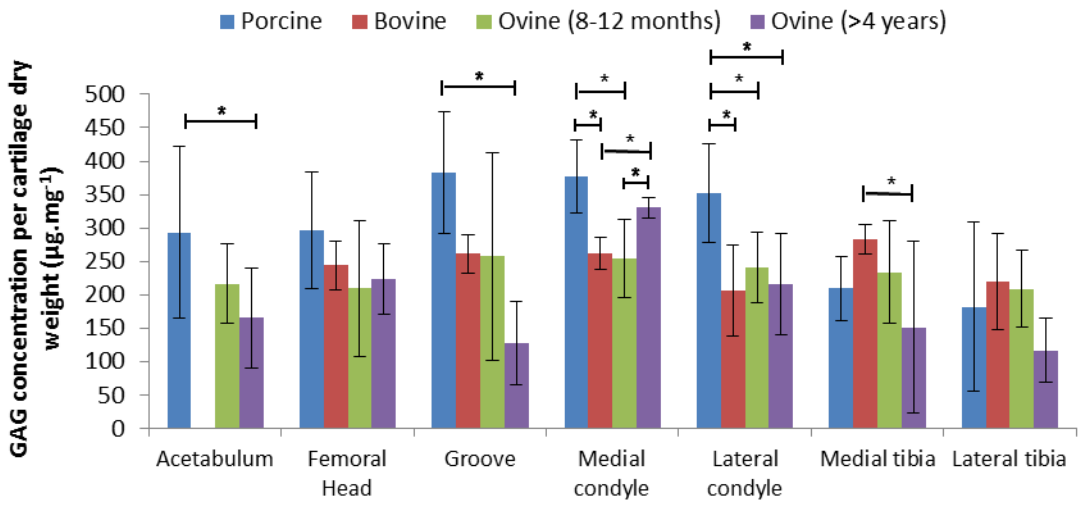

Figure 3.16 GAG content of cartilage from various joint regions of the pig cow and sheep. Data is expressed as the mean (n=5) ± 95 % confidence limits. Data for a given tissue site was analysed by one-way analysis of variance and individual means compared by the T-method . * indicates $p<0.05$.

3.6.7 Hydroxyproline quantification

Quantification of hydroxyproline content (relative to collagen content) showed there was an inverse relationship to GAG content (Figure 3.17). Porcine cartilage had the highest GAG content in most regions, and had the lowest hydroxyproline content, whereas old ovine cartilage had low GAG content, but had highest hydroxyproline content. Cartilage of the porcine lateral condyle had significantly lower hydroxyproline content than that of the medial condyle, there were no other significant differences within species ($p<0.05$ ANOVA).

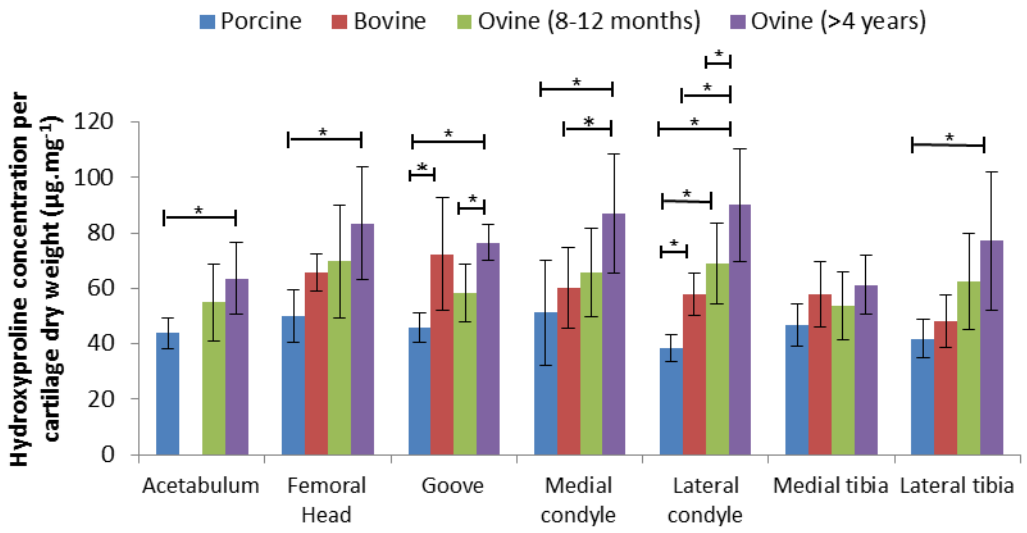

Figure 3.17 Hydroxyproline content of cartilage from various joint regions of the pig cow and sheep. Data is expressed as the mean (n=5) ± 95 % confidence limits. Data for a given tissue site was analysed by one-way analysis of variance and individual means compared by the T-method . * indicates $p<0.05$.

3.6.8 Percentage deformation

The mechanical properties of cartilage from the different species and joint regions are shown in Figure 3.18 and Table 3.1, detailing the percentage deformation of cartilage after one hour, the permeability, elastic equilibrium modulus and thickness of each tissue. Properties could not be determined for ovine groove cartilage as the joints were too small to collect suitable pins.

Cartilage of the hip (femoral head and acetabulum) tended to have a lower percentage deformation than that of the tibial plateau and lateral condyles. Porcine tibial cartilage showed significantly greater percentage deformation than all other joint areas. Bovine lateral condyle and lateral tibial cartilage had significantly higher percentage deformation than that of the femoral head and medial condyle and tibia. Cartilage from the young ovine acetabulum deformed significantly less than that of the femoral head. Acetabular cartilage from the older sheep had a significantly lower percentage deformation than cartilage from the lateral condyle and tibial plateau, and acetabular cartilage from young sheep and pigs.

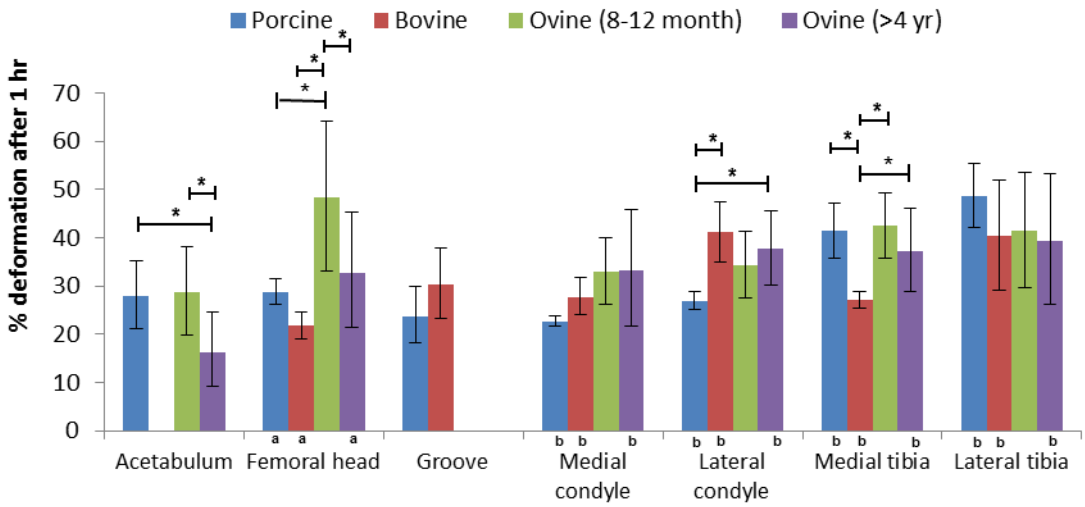

Figure 3.18 Percentage deformation of cartilage from various joint regions of the pig cow and sheep. Data was subject to arcsin transformation prior to calculation of the 95% confidence limits and analysis of variance. Data is expressed as the back transformed mean (ovine 8-12 months, acetabulum and groove n=5; all other n=6) ± 95 % confidence limits. Data for a given tissue site was arcsine transformed then analysed by one-way analysis of variance and individual means compared by the T-method . * indicates $p<0.05$. a) From Taylor *et al.* (2011), b) from McLure *et al.* (2012), all other data from the present study.

3.6.9 Equilibrium elastic modulus, permeability and thickness

The equilibrium elastic modulus was generally lowest for porcine cartilage, increasing in bovine then young ovine cartilage, with old ovine having a much higher equilibrium elastic modulus than the other species. A trend was seen across the joint regions in all species, with cartilage of the tibial plateau having a lower elastic modulus than the femoral knee and hip.

Permeability showed an inverse relationship with equilibrium elastic modulus. Old ovine cartilage was the least permeable tissue and porcine tended to be most permeable. Permeability was highest in the tibial plateau and cartilage of the hip had the lowest permeability.

Equilibrium elastic modulus	Porcine		Bovine		Ovine (8-12 month)		Ovine (> 4 years)	
(MPa)	Mean	R^2	Mean	R^2	Mean	R^2	Mean	R^2
Acetabulum	1.30	*0.99*	-	-	1.69	*0.98*	4.32	*0.91*
Femoral head	[a]1.13	*0.97*	[a]1.59	*0.91*	1.22	*0.94*	[a]2.52	*0.95*
Groove	1.04	*0.93*	0.86	*0.94*	-	-	-	-
Medial condyle	[b]0.74	*0.63*	[b]1.17	*0.80*	1.31	*0.99*	[b]2.04	*0.89*
Lateral condyle	[b]0.66	*0.67*	[b]0.81	*0.81*	1.42	*0.98*	[b]2.02	*0.86*
Medial tibia	[b]0.88	*0.86*	[b]0.85	*0.73*	0.95	*0.99*	[b]2.02	*0.87*
Lateral tibia	[b]0.70	*0.86*	[b]0.81	*0.85*	1.19	*1.00*	[b]1.96	*0.82*

Permeability, *k*	Porcine		Bovine		Ovine (8-12 month)		Ovine (> 4 years)	
x10^{-16} (m4/Ns)	Mean	R^2	Mean	R^2	Mean	R^2	Mean	R^2
Acetabulum	3.04	*0.99*	-	-	1.12	*0.98*	0.37	*0.91*
Femoral head	5.70	*0.97*	1.78	*0.91*	2.99	*0.94*	0.76	*0.95*
Groove	4.49	*0.93*	6.33	*0.94*	-	-	-	-
Medial condyle	7.18	*0.63*	4.49	*0.80*	2.91	*0.99*	1.64	*0.89*
Lateral condyle	6.77	*0.67*	5.45	*0.81*	2.73	*0.98*	1.59	*0.86*
Medial tibia	8.09	*0.86*	4.52	*0.73*	3.67	*0.99*	1.30	*0.87*
Lateral tibia	10.29	*0.86*	5.75	*0.85*	2.87	*1.00*	1.37	*0.82*

Table 3.1a Material properties of cartilage from various joint regions of the pig, cow and sheep.

Thickness	Porcine		Bovine		Ovine (8-12 month)		Ovine (> 4 years)	
(mm)	Mean	95% CL	Mean	95% CL	Mean	95% CL	Mean	95% CL
Acetabulum	1.12	*0.15*	-	-	0.85	*0.12*	1.06	*0.45*
Femoral head	1.22	*0.05*	1.32	0.13	0.48	*0.07*	0.52	*0.10*
Groove	1.70	*0.53*	1.36	*0.10*	-	-	-	-
Medial condyle	2.23	*0.20*	1.28	*0.17*	0.87	*0.12*	0.71	*0.24*
Lateral condyle	2.08	*0.23*	0.93	*0.15*	0.80	*0.22*	0.55	*0.18*
Medial tibia	0.87	*0.15*	1.70	*0.36*	0.76	*0.23*	0.61	*0.24*
Lateral tibia	0.82	*0.08*	1.02	*0.21*	0.70	*0.28*	0.59	*0.27*

Table 3.1b Material properties of cartilage from various joint regions of the pig, cow and sheep.

Thickness data is expressed as the mean (ovine 8-12 months, acetabulum and groove n=5; all other n=6) ± 95 % confidence limits, Elastic equilibrium modulus and permeability data was modelled on mean deformation data and R2 values for modelled and experimental deformation curve agreement are presented. a) from Taylor *et al*. (2011), b) from McLure *et al*. (2012), all other data from the present study.

3.7 Discussion

A xenogeneic source material for decellularisation should have properties as similar as possible to those of human osteochondral tissues to improve the chances of clinical success. Additionally a higher GAG content in source materials compared to that of human cartilage may be beneficial, as GAGs are depleted following decellularisation with SDS which can result in diminished mechanical properties (Stapleton *et al.*, 2008; Elder *et al.*, 2010; Kier *et al.*, 2011; Crapo *et al.*, 2011; Benders *et al*., 2013). The work in this chapter looked at the biological, biochemical and biomechanical properties of different osteochondral tissues. Porcine, bovine and ovine osteochondral tissues from various regions of the hip and knee were assessed to determine the most suitable source material for the development of a decellularisation protocol.

Initial macroscopic observations of cartilage from the different species showed that old ovine cartilage (>4 years) had a yellowed appearance seen in older cartilage tissues (Altman, 1987), usually attributed to the presence of advanced glycation end products (Bank *et al.*, 1998). These non-enzymatic crosslinks affect the mechanical properties of tissues, increasing the stiffness (Bank *et al.*, 1998; Verzijl *et al.*, 2002). Yellowed, aged ovine cartilage would make and inferior substitute for healthy young cartilage *in vivo*. Joint size may impact on the usefulness of species as donors of osteochondral tissues, as a greater number of osteochondral samples can be harvested from a bovine joint compared to a porcine joint, and even more so than a small ovine joint. When drilling, the apparent softness of porcine and to some extent younger ovine bone highlighted the skeletal immaturity of these tissues.

H&E staining of cartilage tissues showed varying extents of cell organisation, the highly ordered cell orientation seen in bovine and old ovine cartilage was indicative of mature tissues, while the lack of organisation and the increased presence of hypertrophic chondrocytes showed the relative immaturity of porcine and young ovine cartilages. As in humans, the cellularity of animal cartilage decreased with age (Stockwell, 1976), with older sheep (>4 years)

having fewest cells and pigs (6 months) having the most. Porcine cartilage cellularity varied according the thickness of the cartilage from the different joint regions, so cartilage from the groove, which was significantly thicker than that from the tibia, also had significantly fewer cells. Thicker cartilage has been reported to have lower cell density than thin cartilage (Stockwell 1971). A source material with fewer cells would be preferable for decellularisation.

Cartilage thickness has been reported to increase as body weight increases (Stockwell, 1971). This was not necessarily supported by the work in the current chapter. Sheep, with a lower body mass than pigs or cows did have thinner cartilage, however, bovine cartilage was thinner than porcine, despite cows having greater body mass. Julkunen *et al*. (2009) showed that cartilage thickness varies with skeletal maturity, that immature animals have thick cartilage and that cartilage thickness decreases with maturity. This was supported here by the comparison of two age groups of sheep, with the mature ovine cartilage tending to be thinner than that of sheep around 1 year of age. In all species, cartilage of the groove and condyles tended to be thicker than that of the hip and tibia, this trend was also seen when comparing the thickness of cartilage from the same joint regions in humans (Athanasiou *et al.*, 1991; Shepherd & Seedhom, 1999a; Thambya *et al*., 2006). Simon *et al*. (1973) identified a relationship between cartilage thickness and joint congruity, with more congruent joints such as the hip having thinner cartilage than that of less congruent joints such as the knee. Human cartilage, on average, tended to be thicker than that of any of the species studied for a given joint region. Shepherd & Seedhom (1999a) report the thickness of human femoral head cartilage to range between 1.08-2.40 mm whereas ovine cartilage was only ~ 0.68 mm in this area, porcine 1.14 mm and bovine 1.53 mm. Cartilage from the human femoral groove ranged between 1.76-2.59 mm, ovine cartilage was again much thinner; 0.86 mm in young sheep and 0.63 mm in old sheep. Cartilage from the porcine groove was 2.04 mm and bovine 1.52 mm, within or approaching the range of human cartilage thickness. The relative thickness of human cartilage probably reflects the increased loads placed on human knee cartilage due to the bipedal posture, as discussed by Stockwell (1971). For an acellular

xenogenic osteochondral graft to integrate and function well when implanted in a human joint, it is likely that a graft with similar thickness to the surrounding host cartilage would be best, therefore porcine and bovine tissues have preferred cartilage thickness for this purpose.

The GAG content of cartilage from each species was assessed qualitatively with alcian blue staining of tissue sections and quantitatively using a colourimetric assay with DMB dye. Qualitatively, all species showed characteristic zonal distribution of sulphated proteoglycans. Only staining of old ovine cartilage showed a distinct tidemark below which acidic mucins were not found, suggesting that this tissue was fully mature. Quantitatively, porcine cartilage had the highest GAG concentration, likely due to the young age of the tissue, as the concentration of proteoglycans is reportedly higher in immature cartilage, and decreases with age (Roughley & White, 1980). It has been suggested that age related reductions in cartilage GAG concentration are due to changes in chondrocyte activity; aggrecan and link protein synthesis decreases with maturity (Bolton *et al*., 1999). Except for cartilage of the medial condyle, there was no significant difference in the GAG content of bovine and ovine cartilage. A continuing trend showed cartilage of the groove and condyles having higher GAG content than other joint regions. The relationship in these joint areas of increased GAG content alongside increased thickness has been observed when tissues undergo increased loading or activity (Kiviranta *et al.*, 1987). However, forces acting on the healthy knee are reportedly lower than those of the hip (Paul, 1976). This trend across the joint regions may again be due to the congruence of the joints, affecting the contact area and therefore stresses. Increased load on a very local scale may cause specific remodelling at that site, to increase thickness and GAG concentration so to decrease contact pressure. Information on human cartilage GAG content is limited in the literature. Various figures have been quoted for the GAG concentration of cartilage from the femoral head, Vilim & Krajickova (1991) quote 54.7 and 38.6 $mg.g^{-1}$ GAG per wet weight cartilage from two donors, while Hollander *et al*. (1991) reported values ranging between 25 – 40 $\mu g.mg^{-1}$ wet weight. In the current study, porcine femoral head cartilage was 78 ± 30 $\mu g.mg^{-1}$, bovine was 68 ± 8 $\mu g.mg^{-1}$, young ovine was 45 ± 18 $\mu g.mg^{-1}$ and old ovine was 62 ± 16

$\mu g.mg^{-1}$, all higher than values reported for human cartilage. GAG content was reported to be between 5-10 % total cartilage mass, as described for human cartilage by Mow *et al*. (2005). All species have a relatively high GAG content compared to human cartilage, however, as loss of GAGs is a limitation in decellularisation processes with SDS (Stapleton *et al.*, 2008; Elder *et al.*, 2010; Kier *et al.*, 2011; Crapo *et al.*, 2011; Benders *et al*., 2013), porcine cartilage, with the highest GAG content would be preferred.

The hydroxyproline content of cartilage from different species showed an inverse relationship with GAG content. Porcine cartilage had highest GAG content, but also had lowest hydroxyproline content. Muir *et al*. (1970) found great variation in human cartilage collagen content between individuals and joint regions, no correlation between collagen content and age was seen. The present study only quantitatively assessed collagen content of articular cartilage and did not investigate collagen fibre alignment or the ratios of different collagens present within the cartilage. Although collagen content appeared constant across species and joint regions there may be qualitative differences which have not been identified here.

Water content of the cartilages from different species and joint areas did not vary significantly on the whole, only significant differences were seen with bovine tibial cartilage. The water content of human cartilage varies between 68-85 % (Mow *et al*., 2005), the water content of cartilage from all joint regions and species lies within this range. Any species would therefore make an acceptable starting material, in terms of cartilage water content, however this parameter may differ once the tissue has undergone decellularisation.

Percentage deformation of cartilage appeared to vary with joint region, cartilage of the tibia tended to have higher deformation than the hip, this was reflected in the equilibrium elastic modulus derived for each type of tissue, with tibial cartilage showing a lower modulus. Tibial cartilage, with low GAG content, had higher permeability. As proteoglycans are responsible for restriction of fluid flow through the tissue, increased fluid flow results in reduced load supported by the fluid phase so tissues showed greater deformation. The relationship between material properties and

biological/biochemical composition was most pronounced in the bovine knee; cartilage of the medial condyle and medial tibia was thicker and had higher GAG content than its lateral counterpart, cartilage of the medial side of each joint also showed lower permeability, and stiffer equilibrium elastic modulus (lower percentage deformation).

Porcine cartilage was least stiff, and cartilage from old sheep was most stiff. Despite young ovine cartilage having higher GAG content, old ovine cartilage was stiffer, bovine cartilage was also stiffer than porcine cartilage, again despite the GAG content of porcine cartilage being higher. This is possibly due to the quality of the GAGs within these younger tissues. Cartilages from these more skeletally mature animals may have more effective proteoglycan structures which are more adequately immobilized within the cartilage matrix resulting in lower permeability and stiffer cartilage. As mentioned previously, old ovine cartilage had a yellowed appearance indicative of the presence of advanced glycation end products, the increased crosslinking of the collagen matrix results in a stiffer cartilage , which may explain the reduced deformation and increased equilibrium elastic modulus of old ovine cartilage (Bank *et al.*, 1998; Verzijl *et al.*, 2002). Old ovine cartilage being stiffer than bovine may be an effect of yet further maturity in GAG structures or an effect of ovine cartilage being much thinner than bovine. In this study, thinner cartilage tended to have a stiffer equilibrium elastic modulus. The equilibrium elastic modulus of bovine lateral condyle cartilage was similar to the equilibrium aggregate modulus quoted for human (0.70 MPa) and bovine (0.89 MPa) previously (Athanasiou *et al*., 1991; Mow *et al*., 2005). Porcine cartilage also had a similar elastic modulus, but was lower; this was possibly as a result of having softer subchondral bone. Old ovine cartilage had a much higher elastic modulus, so may be too stiff to replace human cartilage. Cartilage from all species was less permeable than values reported for human cartilage (Mow *et al*., 2005; Athanasiou *et al*., 1991).

Many of the differences seen in cartilage properties in the current chapter appear to be as a result of animal age and therefore skeletal maturity. The age of the species considered in this study was restricted by the availability of animals bred from the food chain for human consumption. Not only should

the specific parameters of each cartilage be considered here, but the potential pros and cons of using a skeletally mature versus a more biologically active immature tissue as a osteochondral scaffold as the regenerative capacity may differ.

The characterisation of cartilage from different species and joint areas was carried out with the aim of identifying a source material for decellularisation with properties as similar as possible to those of human cartilage. Porcine cartilage from 6 month old animals was the thickest of all cartilages studied, however was not as thick as human. The GAG content of porcine cartilage was high, however cartilage was highly cellular and did not have a fully defined structure due to the immaturity of the tissue. Bovine cartilage from 18 month old animals, conversely, was mature. The GAG content of bovine cartilage was lower than that found for porcine cartilage, but still within the range of human tissues. Bovine cartilage was also relatively thick. Both porcine and bovine cartilages had an equilibrium elastic moduli similar to the equilibrium aggregate modulus reported for human cartilage. Ovine cartilage from both age ranges was very thin, young ovine cartilage was not fully mature with high cell density and less well defined structural organisation. Ovine cartilages had lower GAG content than porcine.

Based on the parameters characterised in this chapter, osteochondral tissues from the porcine medial condyle and bovine medial groove were identified as the most suitable source materials for development of an osteochondral decellularisation protocol.

Chapter 4
Development of a protocol for the decellularisation of bovine osteochondral tissues

4.1 Introduction

Surgical repair techniques for osteochondral lesions have shown varying degrees of efficacy, producing fibrocartilaginous repair tissue in the case of microfracture (Steinwachs *et al*., 2008; Lützner *et al*., 2009), or in the case of procedures such as autologous chondrocyte implantation (ACI) or mosaicplasty producing more hyaline-like repair materials but with varying degrees of donor site morbidity (Chaing & Xiong, 2009; Minas *et al*., 2001; Koulalis *et al*., 2004). Tissue engineering approaches have focused upon production of synthetic or natural scaffold materials, which avoid issues with donor site morbidity, but are unable to produce a hyaline-like repair tissue with the same composition, structure and function of natural articular cartilage (Frenkel & di Cesare, 2004).

Decellularisation of xenogeneic tissues has the potential to produce a natural extracellular matrix (ECM) scaffold, with the same biological, biochemical and biomechanical characteristics of natural tissue, and does not require tissue harvesting from a host donor site. Ideally, the decellularisation process will remove all immunogenic proteins and avoid issues of immunological rejection upon implantation (Crapo *et al*., 2011).

As discussed in Chapter 1, the ECM plays a key role in the function of articular cartilage as a low friction, load distributing tissue. In addition, it is understood that the molecularly diverse natural ECM is biologically active, having involvement in chemotaxis, cell mitogenesis (Bornstein & Sage, 2002) and differentiation and promoting tissue homeostasis. These attributes are thought to stem from the specific microarchitecture, surface

topology and composition of the ECM (Crapo *et al*., 2011). This interactivity with cells may facilitate the recellularisation and regeneration of acellular ECM more effectively than synthetic or artificially arranged natural material scaffolds, potentially resulting in improved clinical outcomes.

4.2 Decellularisation of natural tissues

There are many different methods which can be employed to decellularise tissues including chemical, enzymatic and physical techniques which can be used to varying extents depending on the type of tissue being treated. An acellular tissue, as defined by Crapo *et al.* (2011), should meet the following criteria:

- <50 dsDNA per ECM dry weight
- <200 bp DNA fragment length
- Lack of visible nuclear material in tissue sections stained with DAPI or H&E

Most decellularisation processes use a combination of chemical, enzymatic and physical methods to achieve adequate decellularisation of natural tissues. Each of these approaches is discussed below.

4.2.1 Chemical methods

4.2.1.1 Acids and bases

Acids and bases can hydrolyse biomolecules, this enables solubilisation of cellular membranes and removal of nucleic acids. Peracetic acid (PAA) has been successfully used at low concentrations (0.1 % v/v in 4% v/v ethanol) as a decellularisation agent for a number of thin tissues, including porcine small intestinal submucosa (SIS) and layers of the urinary bladder with minimal effect on the ECM structure (Freytes *et al.*, 2004; Gilbert *et al.*, 2008). Higher concentrations of PAA (5 % v/v) have, however, been shown to greatly alter the ECM structure (Wu *et al*., 2011). Concomitantly with decellularisation, PAA is a sterilant since it can penetrate microorganisms and generate oxygen free radicals which oxidise microbial proteins (Pruss *et al*., 1999). Other acids such as hydrochloric acid and sulphuric acid and bases such as NaOH (Schwartz *et al*., 2012) are also able to disrupt cellular membranes and decellularise matrices, but have been shown to dissociate GAGs from the tissue. Applying lime (a mixture of calcium hydroxide, soda

ash and sodium sulphate) to porcine dermis lea to severely reduced biomechanical and structural properties (Reing *et al*., 2010).

4.2.1.2 Hypotonic and hypertonic solutions

Hypertonic saline solutions have been shown to dissociate DNA from proteins (Cox & Emili, 2006) while hypotonic solutions induce cell swelling and bursting by osmosis. These solutions are also used to aid washout of cellular debris, however further chemical or enzymatic treatments are likely required to fully remove DNA and cellular debris.

4.2.1.3 Detergents

Detergents are amphipathic molecules comprising of a hydrophilic head group and a hydrophobic tail. In aqueous solution, these molecules spontaneously form micelles (Seddon *et al.*, 2004). Detergents disrupt cellular membranes by inserting into lipid bi-layers. At concentrations above the critical micelle concentration detergents form micelles containing native lipids and encapsulating membrane proteins which can then be washed from the tissue.

4.2.1.3.1 Ionic detergents

Ionic detergents have a hydrophilic head with either a negative or positive net charge. Ionic detergents are extremely effective in the solubilisation of membrane proteins but are almost always denaturing to some extent through the disruption of protein-protein interactions (Seddon *et al*., 2004). SDS (Figure 4.1) is an anionic detergent commonly used in decellularisation processes (Booth *et al*., 2002, Stapleton *et al*., 2008, Kheir *et al*., 2011)

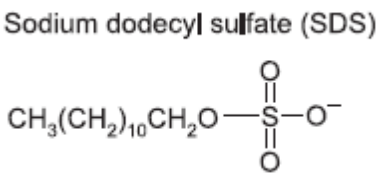

Figure 4.1 Molecular structure of sodium dodecyl sulphate (SDS). Adapted from Seddon (2004).

The use of ionic detergents such as SDS and sodium deoxycholate (SDC) has been shown to be more effective than the use of non-ionic or zwitterionic detergents for tissue decellularisation (Booth *et al*., 2002). However, ionic detergents have been shown to disrupt matrix proteins, with tissues showing a loss of GAGs and collagen damage when ionic detergents, such as SDS have been used at high concentrations (1.0 – 2.0 % w/v; Samouillan *et al*., 2000; Elder *et al.*, 2010). These effects may, in part, have been the result of matrix metalloproteinase activity following release of cellular proteases during cell membrane disruption and cell lysis. These deleterious effects have been minimised by using low detergent concentrations (SDS, 0.1 % w/v; SDC 0.5 % w/v) and protease inhibitors (Booth *et al*., 2002).

4.2.1.3.2 Non-ionic detergents

Non-ionic detergents have uncharged hydrophilic head groups and have minimal effects on protein-protein interactions, so do not have a deleterious effect on the protein components of the ECM (Seddon *et al.*, 2004). Triton X-100 is one of the most widely used non-ionic detergents for decellularisation treatments (Courtman *et al*., 1995; Vavken *et al*., 2009).

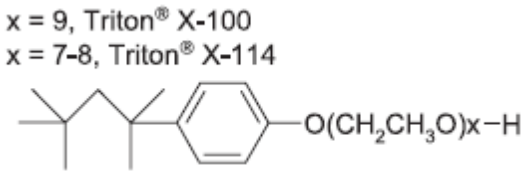

Figure 4.2 Molecular structure of triton X-100. Adapted from Seddon (2004).

The effects of Triton X-100 as a decellularisation agent have been shown to be variable and dependent on exposure time and tissue type. Decellularisation of porcine heart valves with Triton X-100 (1 % v/v) with 0.2 $mg.ml^{-1}$ DNase and 20 $\mu g.ml^{-1}$ RNase for 24 h at 37 ºC was successful, however this lead to a near complete loss of GAG as well as reduction of laminin and fibronetin (Grauss *et al*., 2005). Conversely, Woods & Gratzer (2005) did not see deleterious effects upon GAG or collagen content of ACL-bone tissues following decellularisation with 1% (v/v) Triton X-100 in

combination with hypotonic and nuclease treatment, however full cell removal was not achieved.

4.2.1.3.3 Zwitterionic detergents

Zwitterionic detergents possess both a negative and positive charge at different regions of the molecule. As such, they display properties of both ionic and non-ionic detergents, having greater effect on disrupting protein-protein interactions than non-ionic detergents.

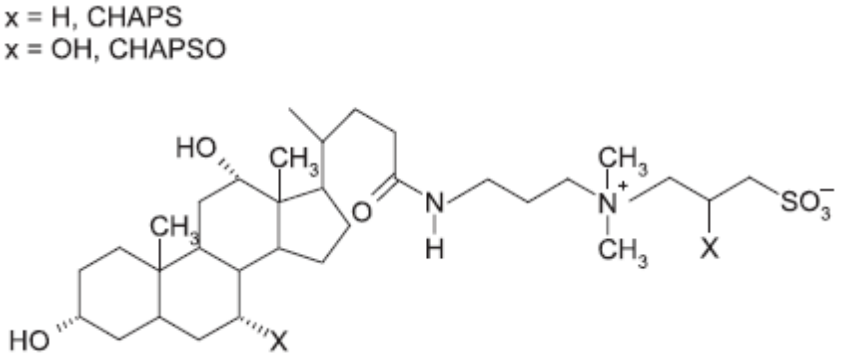

Figure 4.3 Molecular structure of CHAPS. Figure adapted from Seddon (2004).

One of the most commonly used zwitterionic detergents for the decellularisation of tissues is 3-[(3-cholamidopropyl)dimethylammonio]-1-propanesulfonate (CHAPS). Du *et al.* (2010) found that decellularisation of porcine corneas with 0.5 % and 1.0 % (w/v) CHAPS for 36 h histologically had little effect in removing cells and cellular debris, and destroyed tissue histoarchitecture. Booth *et al.* (2002) found no histological differences in the biochemical components of porcine aortic tissue following 72 h incubation with CHAPS (0.5 % w/v), however decellularisation was not achieved with this detergent.

4.2.2 Enzymatic methods

Enzymes such as nucleases, collagenase, lipase and α-galactosidase have been used as part of decellularisation procedures alongside other agents to provide higher specificity for removal of undesirable constituents (Gilbert *et al*., 2006; Crapo *et al*., 2011). Only trypsin has been used on its own as a

successful decellularisation technique. Cebotari *et al.* (2002) treated human aortic and pulmonary heart valves with a solution of trypsin/EDTA (containing 0.5 % w/v trypsin and 0.2 % w/v EDTA) in PBS (1:10 ratio) for 48 h at 37 °C. Complete decellularisation was reported with preservation of ECM. Conversely, Grauss *et al.* (2005) used 0.5 % (w/v) trypsin and 0.05 % (w/v) EDTA in the presence of DNase, RNase and gentamycin for 17 h at 37 °C to decellularise porcine aortic valves and found that pyknotic cell nuclei remained and that significant damage to the elastin and collagen fibres had been sustained, along with a moderate reduction in GAG content seen histologically.

Nucleases are commonly used to cleave nucleic acids and enable the more effective wash out of nuclear material from tissues. The successful use of nucleases to reduce tissue DNA content following detergent treatment has been reported for a number of tissues, including heart valves, tendon, meniscus and osteochondral tissues without adverse effect on tissue ECM (Booth *et al.*, 2002; Ingram *et al*., 2007; Stapleton *et al.*, 2008; Kheir *et al*., 2011).

Treatment of xenogeneic tissues with α-galactosidase can be required as part of a decellularisation bioprocess to specifically remove galactose α1-3 galactose (α-gal), a xenogeneic cell membrane protein which leads to hyperacute rejection of xenografts (Stapleton *et al*., 2011).

4.2.3 Physical methods

A number of physical methods can be employed in combination with chemical and enzymatic methods to decellularise tissues. These include freezing, the application of direct pressure, agitation and sonication (Gilbert *et al*., 2006, Crapo *et al*., 2011). Freezing is commonly used and has been included in processes for cartilage (Kheir *et al*., 2011) and meniscus (Stapleton *et al*., 2008) decellularisation, amongst other tissues. Freezing produces ice crystals within the cells, which disrupt membranes, resulting in cell lysis. The formation of crystals within the ECM also acts to increase tissue permeability, improving perfusion of subsequent solutions through tissues and enhancing the wash out of cellular debris. Freeze-thawing has,

however, been linked to the denaturation of proteins (Cao *et al*., 2003), which may result in adverse effects on the biomechanical performance of the tissues. As ice crystal size is affected by freezing rate, it is important to select the correct temperature at which to freeze tissues so as to balance damage to the matrix against cell lysis (Gilbert *et al*., 2006).

Funamoto *et al*. (2010) have reported successful decellularisation of porcine aortic blood vessels using high-hydrostatic pressure. Vessels were sealed in a bag containing PBS and placed in a cold isostatic pressurization machine. An atmospheric pressure of 980 MPa was gradually applied (at a rate at which the starting temperature was maintained) then sustained for 10 min, following which vessels were washed in PBS for 14 days. At high pressures, the temperature at which water freezes is increased, so temperature and magnitude of pressure needs to be carefully optimised. The rate of pressure increase/decrease should also be monitored, as drastic changes in pressure alter the temperature. The temperature of the pressurisation chamber was maintained above 30 °C at 980 MPa, to prevent ice crystal formation and avoid deleterious effects on the tissue ECM. No histological damage was seen in tissues pressurised at 30 °C, however those decellularised using a starting temperature of 10 °C showed damage to the collagen fibre network following formation of ice crystals as a result of high pressure. Both conditions resulted in reduction of the mechanical properties of the tissue compared to native vessels.

In combination with chemical or enzymatic treatment, mechanical scraping has been employed to remove epithelial layers from basement membranes such as the amniotic membrane. However, results have been inconsistent and often lead to damage of the basement membrane (Hopkinson *et al.*, 2008).

Agitation and sonication can be employed to increase the penetration of enzymatic and chemical decellularisation solutions and therefore improve cell lysis and wash out of cell debris. Orbital shakers, magnetic stirrers and low profile rollers have been used to agitate solutions and the tissues within them (Gilbert *et al*., 2006). The rate of agitation can affect the wash out of DNA from a tissue, and can vary depending on the size and density of the

tissue to be decellularised. Increasing agitation rate has been reported to increase DNA wash out, but adversely can also increase the wash out of ECM components, so needs to be optimised for each tissue type (Crapo *et al.*, 2011). Sonication has been employed in decellularisation bioprocesses to increase the permeability of dense tissues and improve recellularisation (Ingram *et al.*, 2007). However, optimisation of sonication frequency and duration is necessary to avoid excess structural damage to the tissue.

4.3 Aims and objectives

Aims:

The aim of the research described in this chapter was to develop a process using low concentration SDS plus proteinase inhibitors to decellularise bovine osteochondral pins obtained from the medial femoral groove.

Objectives:

- To develop a protocol to remove cells and cellular debris from bovine osteochondral pins while retaining the natural histoarchitecture, biochemical composition and biomechanical function of the native osteochondral tissues.
- To characterise the resultant decellularised ECM and compare to native tissue using:
    - Histological characterisation to identify the presence/lack of cells and to observe any changes in the histoarchitecture of the tissue.
    - DNA quantification to determine the reduction in DNA compared to native tissue following decellularisation
    - Determination of the GAG and collagen content of decellularised scaffolds
    - Determination of the mechanical properties of cartilage following decellularisation.
- To characterise immunohistochemically the distribution of collagen type VI and COMP in the native and decellularised bovine osteochondral matrix.

4.4 Methods

4.4.1 Decellularisation solutions

4.4.1.1 PBS

A solution of PBS was produced as described in Section 2.1.7.1. When required, PBS was solution was sterilised by moist heat, as described in Section 2.2.1.3. Solution was stored at room temperature for up to 1 month.

4.4.1.2 PBS with aprotinin (10 KIU.ml^{-1} aprotinin)

A solution of PBS was produced as described in Section 2.1.7.1. When required, the solution was sterilised by moist heat, as described in Section 2.2.1.3. Solution was stored at room temperature and used within 1 month. Just prior to use, 1 ml aprotinin (10,000 KIU.ml^{-1}) was added to 1 L PBS.

4.4.1.3 Hypotonic buffer (10 mM Tris, 10 KIU.ml^{-1} aprotonin)

Trisma base (1.21 g) was dissolved in 990 ml distilled water. The pH was adjusted to 8.0 – 8.2 using 6 M HCl and the volume made up to 1 L. When necessary, the solution was sterilised by moist heat, as described in Section 2.2.1.3. Solution was stored at room temperature for up to 1 month. Just prior to use, 1 ml aprotinin (10,000 KIU.ml^{-1}) was added.

4.4.1.4 SDS in hypotonic buffer (0.1 % w/v SDS, 10 mM Tris, 10 KIU.ml^{-1} aprotonin)

SDS (10 g) was dissolved in 100 ml distilled water to produce an SDS solution. SDS solution (10 ml) was added to 990 ml hypotonic solution. When necessary, the solution was sterilised by moist heat, as described in section 2.2.1.3. Solution was stored at 4 °C and used within 1 week. Just prior to use, 1 ml aprotinin (10,000 KIU.ml^{-1}) was added.

4.4.1.5 Nuclease solution (50 mM Tris, 10 mM $MgCl_2$, 50 U.ml^{-1} DNAase, 1U.ml^{-1} RNAase)

Trisma base (6.1 g) and magnesium chloride ($MgCl_2$; 2 g) were dissolved in 80 ml distilled water. The pH was adjusted to 7.5 – 7.7 using 6 M HCl. The volume was then made up to 990 ml using distilled water. At this stage, when required, the solution was sterilised by moist heat, as described in

Section 2.2.1.3. Just prior to use, 5 ml DNase (10,000 $U.ml^{-1}$) and 10 ml RNase (100 $U.ml^{-1}$) were added. Solution was used within 10 min of preparation.

4.4.1.6 Peracetic acid solution (0.1 % v/v)

Peracetic acid (PAA; 1.57 ml) was added to 500 ml distilled water and adjusted to pH 7.2 – 7.5 using 6 M NaOH. Solution was used within 1 h of preparation.

4.4.1.7 EDTA solution (12.5 % w/v)

EDTA solution was produced as described in Section 2.2.3.2.1, and if necessary was sterilised by moist heat as described in Section 2.2.1.3. Solution was stored at room temperature and used within 6 months of preparation. Just prior to use 1 ml aprotinin (10,000 $KIU.ml^{-1}$) was added to 1 L EDTA solution.

4.4.2 Decellularisation processes

Decellularisation methods using low concentration 0.1 % (w/v) SDS plus proteinase inhibitors were developed based on the initial process described by Booth *et al.* (2002) and adapted following methods developed by Stapleton *et al.* (2008) and Kheir *et al.* (2011). Osteochondral pins (9 mm diameter, 10 – 12 mm deep) were placed 4 – 5 per 150 ml pot into which 125 ml of each solution was added. All incubations were carried out at 42 ± 2 °C except the nuclease treatment which was performed at 37 ± 1 °C and the PAA treatment which was performed at 27 ± 1 °C. All solutions were pre-warmed to the appropriate temperature. Agitation on an orbital shaker at 240 rpm was carried out during each incubation excluding the nuclease step, which was agitated at 80 rpm, pots were laid horizontally on the shaker.

4.4.2.1 dCELL 1 (basic decellularisation)

Osteochondral pins were harvested from the bovine medial femoral groove, as described in Section 2.2.2 and stored at – 20 °C on PBS moistened filter paper. Pins (3 – 5 pins per pot from n=3 animals) were thawed at room temperature (RT) for 1 - 2 h or until fully defrosted and then re-frozen on

PBS moistened filter paper at -20 °C for 3 h. Pins were again thawed at RT for 1 – 2 h or until fully defrosted before hypotonic buffer was added and pins were frozen at -80 °C. Pins were thawed at 45 °C in a water bath for 1 - 2 h or until fully defrosted before 1 further cycle of freeze/ thaw in hypotonic solution was completed. Pins were washed for 3 x 10 min in PBS with aprotinin before being incubated in hypotonic buffer for 16 h. An incubation in SDS in hypotonic solution then followed for 24 h. Pins were washed for 3 x 10 min in PBS with aprotinin and incubated in nuclease solution for 3 h. Pins were then washed for 3 x 10 min in PBS without aprotinin and incubated in PAA solution for 3 h. A final set of 3 x 10 min PBS without aprotinin washes were performed and the pins were stored frozen at -20 °C or used immediately for analysis.

4.4.2.2 dCELL 2 (extended PBS wash)

This process was exactly the same as that described in Section 4.4.2.1 with the addition of a 48 - 60 h extended final PBS wash.

4.4.2.3 dCELL 2 (hypotonic)

This process differed from dCELL 2 described in Section 4.4.2.2 only in that all four freeze/thaw cycles were conducted in hypotonic buffer containing 10 $KUI.ml^{-1}$ aprotinin.

4.4.2.4 dCELL 2 (distilled water)

This process differed from dCELL 2 described in Section 4.4.2.2 only in that all freeze/thaw cycles were conducted in distilled water containing 10 $KUI.ml^{-1}$ aprotinin.

4.4.2.5 dCELL 2 (+ ultrasonication)

This processed followed the same method outlined in Section 4.4.2.2 however, prior to the initial freezing, pins were ultrasonicated. The technique was based on work by Ingram *et al.* (2007) and Stapleton (2008b). Each osteochondral pin was placed in a custom wire mesh holder and positioned under an ultrasonic probe in a bath of ice cold PBS. Each sample was sonicated at 70 watts for 15 min with 6 second pulses.

4.4.2.6 dCELL 3 (water pik)

Water pik treatment of the subchondral bone was added to the dCELL 2 method described in Section 4.4.2.2. Following the first thaw, blood clots and marrow from the subchondral bone were removed using a water pik (Figure 4.4). A thin jet of PBS (200 - 400 ml per pin) was applied directly to the bone to force out marrow components.

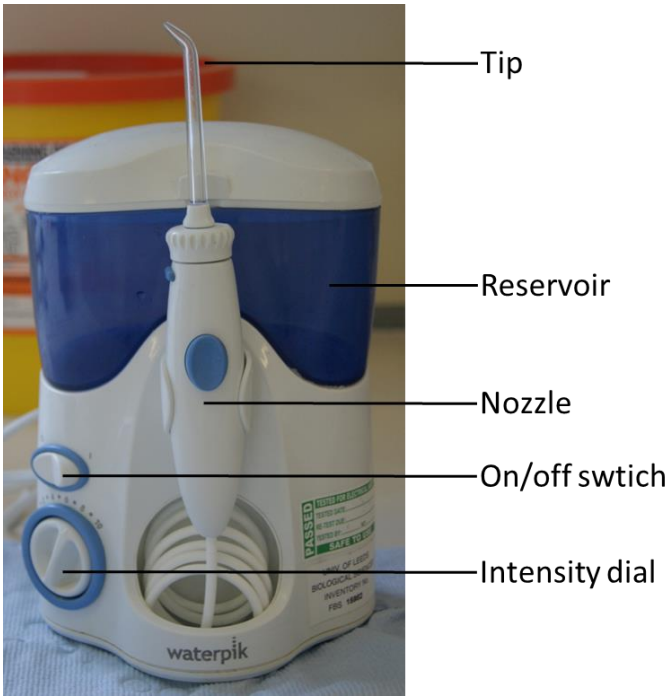

Figure 4.4 Water pik. PBS (stored in the reservoir) was pumped through the nozzle and forced into a thin jet when directed through the tip. The intensity of the jet can be controlled using the dial.

4.4.2.7 dCELL 3 (hirudin)

A 16 h incubation in the anticoagulant enzyme hirudin (1 $U.ml^{-1}$ in PBS with 10 $KUI.ml^{-1}$ aprotinin) at RT was added to the process described in Section 4.4.2.6 before treatment with the water pik.

4.4.2.8 dCELL 3 (hirudin applied to the bone only)

Rather than incubating the entire osteochondral pins in hirudin solution (1 $U.ml^{-1}$ in PBS with 10 $KUI.ml^{-1}$ aprotinin), as described in Section 4.4.2.7, pins were placed in 6 well plates and 8 ml hirudin solution was added to each well (Figure 4.5). The lid of each plate was lined with PBS moistened

tissue paper to maintain a moist environment for the exposed cartilage. Plates were incubated at 37 °C on an orbital shaker at 80 rpm for 18 h.

Figure 4.5 Anticoagulant application to bony region of osteochondral pins. Pins were placed in a 6 well plate with the bony component submerged in an anticoagulant solution.

4.4.2.9 dCELL 3 (monosodium citrate applied to the bone only)

As an alternative to the hirudin used in Section 4.4.2.8, the bone component was incubated in a 0.4 % (w/v) solution of monosodium citrate. Sodium hydrogen carbonate ($NaHCO_3$; 1.98 g) and citric acid ($C_6H_8O_7$; 3.92 g) were dissolved in 1 L distilled water and pH adjusted to 7.0. Plates were incubated at 37 °C on an orbital shaker at 80 rpm for 18 h.

4.4.2.10 dCELL 3 (PBS)

The same method was followed as in Section 4.4.2.7, however the hirudin solution was substituted for PBS and the incubation was completed at RT.

4.4.2.11 dCELL 4 (PBS at 45 °C)

This followed the method outlined in Section 4.4.2.10 however the incubation in PBS prior to the water pik treatment was carried out at 45 °C rather than RT.

4.4.2.12 dCELL 4 (+ extra nuclease)

In this process, an additional nuclease treatment was added to the protocol outlined in Section 4.4.2.11. Following the first 3 h incubation in nuclease solution, pins were washed for 3 x 10 min in PBS without aprotinin before being subject to a second nuclease treatment for a further 3 h incubation.

4.4.2.13 dCELL 4 (+ decalcification)

The process described in Section 4.4.2.11 was adjusted to include a decalcification step. Following water pik treatment, pins were decalcified in 12.5 % (w/v) EDTA for 1, 2, 4, 8 or 12 days with incubation at 45 °C and agitation at 240 rpm. Incubation for 4 days was selected for further process development.

4.4.2.14 dCELL 5 (+ hypotonic/SDS cycle)

The dCELL 4 process described in Section 4.4.2.11 was adapted to include a further cycle of washing with hypotonic buffer and SDS in hypotonic buffer. Following the first 24 h incubation in SDS solution, pins were incubated in hypotonic buffer for 24 h and again in SDS in hypotonic buffer for 24 h before continuing with PBS washes, nuclease and PAA treatments.

4.4.3 Histological characterisation

Histological characterisation of fresh and decellularised osteochondral tissues was carried out as described in Section 2.2.3. H&E, DAPI and alcian blue stains were performed.

4.4.4 DNA quantification

4.4.4.1 Tissue lyophilisation

Tissues were freeze dried prior to digestion as described in Section 3.4.1.1. Cartilage was removed from the bone using a scalpel and macerated prior to freeze drying.

4.4.4.2 Cartilage digestion using proteinase K

Tissues were digested using solutions provided in the QIAGEN DNeasy blood and tissue kit using a method based on the manufactures' instructions. Briefly, lyophilised native cartilage tissue (25 g wet weight) was placed in a sterile 2 ml eppendorf tube. Digestion buffer ATL (180 µl) and proteinase K (20 µl) were pre-mixed then added to the tissue. Digests were vortexed briefly then incubated at 56 °C for 16 h with agitation at 80 rpm.

Lyophilised decellularised cartilage tissue (~250 g wet weight) was digested as above, but using 360 µl buffer ATL with 40 µl proteinase K. If digestion was not complete after 18 h, a further 180 µl ATL and 20 µl proteinase K were added and incubation continued until digestion was complete.

4.4.4.3 Cartilage DNA purification

Once digestions were complete, DNeasy spin columns were used to extract and purify DNA from the digests. The manufacturers' instructions were followed for native tissue. For decellularised tissue digests, the volumes of ethanol and buffer AL were doubled when precipitating DNA, as the digest volume was doubled. Columns were rinsed and then the isolated DNA was eluted from the membrane using 200 µl buffer AE. Elution was repeated a second time into the same eppendorf to ensure that all of the DNA was recovered.

4.4.4.4 DNA quantification

Purified DNA was quantified using a nanodrop nanospectrophotometer. Samples and standards (2 µl) were pipetted onto the pedestal and their absorbance measured at 260 nm. Absorbance was normalised to a blank of AE buffer. A standard curve was produced using known concentrations of calf thymus DNA to calibrate the nanodrop spectrophotometer.

4.4.5 Biochemical characterisation

The GAG, hydroxyproline and water content of fresh and decellularised tissues was determined using methods described in Section 3.4.

4.4.6 Biomechanical characterisation

The percentage deformation of decellularised cartilage was determined using the indentation methods described in Sections 3.5.1 and 3.5.2.

4.4.7 Immunohistochemical labelling

4.4.7.1 Reagents

- *Hydrogen peroxide solution (3 % v/v)*
  20 ml hydrogen peroxide (30 % v/v)
  180 ml PBS
- *Tris buffer (2 M, pH 7.6)*
  242.26 g Trizma base
  758 ml distilled water
- *Sodium chloride solution (3M)*
  175.32 g sodium chloride
  1 L distilled water
- *Tris buffered saline (TBS)*
  25 ml Tris buffer (2 M)
  50 ml sodium chloride solution (3 M)
  925 ml distilled water
- *TBS containing 0.05 % (w/v) Tween 20 (TBS-T)*
  500 µl Tween 20
  1 L TBS
- *Bovine serum albumin (BSA; 5 % w/v)*
  2.5 g BSA
  500 ml PBS
- *Antibody diluent*
  6 ml Sodium azide (1 % w/v)
  300 µl BSA (5 % w/v)
  54 ml TBS
  1 L distilled water

4.4.7.2 Sample preparation

Fresh and decellularised tissues (n=3) were fixed in 10 % (v/v) NBF, decalcified, wax embedded, sectioned and transferred onto slides as

described in Sections 2.2.3.1 – 2.2.3.4, sections were then dewaxed and rehydrated as described in Section 2.2.3.5.

4.4.7.3 Antigen retrieval

As tissues had been NBF fixed, antigen retrieval was performed to re-expose tissue epitopes for antigen binding. Following dewaxing and rehydration, each section was circled using a hydrophobic marker and proteinase K solution applied drop wise until sections were fully covered. Sections were incubated at room temperature for 20 min.

4.4.7.4 Antibodies

All antibodies were diluted to optimised working concentration in antibody diluent.

Antigen	Supplier	Product code	Isotype	Stock concentration	Dilution/ Working concentration
Collagen Type VI	AbD Serotech	AHP2049	IgG	1.0 $mg.ml^{-1}$	1 in 500 2.0 $mg.L^{-1}$
COMP	AbCam	ab74524	IgG	0.4 $mg.ml^{-1}$	1 in 80 5.5 $mg.L^{-1}$
IgG	AbCam	ab27478	-	0.2 $mg.ml^{-1}$	-

Table 4.1 Antibodies. Antibodies and isotype controls used during immunohistochemical analysis of native and decellularised bovine osteochondral tissues

4.4.7.5 Labelling of tissue sections using monoclonal antibodies

Following antigen retrieval (Section 6.3.1.3) sections were immersed in hydrogen peroxide (3 %, v/v) in PBS for 10 min at room temperature to block endogenous peroxidase activity, and then washed for 3 min in running tap water. Sections were briefly washed with TBS on a plate rocker. To block non-specific background staining, dual endogenous enzyme block (25 µl) from the Ultra vision kit was added and sections were incubated for 10 minutes, followed by two ten min washes in TBS on a plate rocker. The primary antibody (Table 6.1) was then applied at working concentration and incubated at room temperature for 1 h. Sections were then washed twice for

10 min in TBS-T, then twice for 10 min in TBS on a plate rocker. Labelled polymer-HRP (20 µl) from the Ultra vision kit was then added to each section and incubated for 30 min in the dark at room temperature. Sections were again washed twice for 10 min in TBS-T, then twice for 10 min in TBS on a plate rocker. Excess buffer was tapped off before substrate chromogen (20 µl liquid 3,3-diaminobenzidine (DAB) chromagen plus 1 ml substrate buffer) was added to each section and incubated at room temperature for 10 min. Sections were rinsed four times in distilled water before being immersed in haematoxylin (Mayer's) for 10 sec. Sections were washed for 3 min in running tap water before being dehydrated and mounted in DPX mountant, as described in Section 2.2.3.6. To verify specific antibody binding, an isotype control was performed on native and decellularised tissue sections using IgG in place of the primary antibody at the same concentration as the primary antibody had been used. An antibody-free negative control was also included, in which sections were incubated in antibody diluent alone in place of the primary and secondary antibody. Once dry, sections were viewed using normal light microscopy.

4.5 Results

Initial attempts to decellularise bovine osteochondral tissues were not successful and this led to numerous alterations to the process which are documented below.

Images of sections of native bovine osteochondral tissue and tissue subject to various decellularisation protocols stained with H&E, DAPI or alcian blue/PAS are presented in Figures 4.6, 4.7 and 4.8 respectively. DNA, GAG and hydroxyproline content of native bovine cartilage and tissues subject to various decellularisation protocols are presented in Figures 4.9, 4.10 and 4.11 respectively. The percentage deformation of native osteochondral tissues and tissues subject to various decellularisation protocols is presented in Figure 4.12.

4.5.1 Native tissue

Native bovine medial groove osteochondral sections stained with H&E (Figure 4.6 a) showed characteristic cartilage architecture and cell organisation, cells were present throughout the depth of the cartilage tissue and were situated in chondrons. At the superficial layer, cells were smaller and more randomly orientated, in the mid and deep zones linear columns of cells aligned perpendicularly to the cartilage-bone interface were seen. There was a darker stained layer at the cartilage surface indicating a healthy, smooth articulating surface. Pink eosin staining become more intense in the bone and the intratrabecular spaces of the bone could be seen, small, round osteocytes were nestled in lacunae within the bone tissue. Bone marrow was also present within the subchondral bone with a high cell density. This organisation of cells and extent of cellularisation could also be seen in DAPI stained sections (Figure 4.7 a). Staining with alcian blue showed more intense blue GAG staining in the middle zone and slightly less staining in the deep and superficial zones. There was an absence of GAGs in the bone (Figure 4.8 a). Native cartilage contained 261.1 ± 29.3 $\mu g.mg^{-1}$ sulphated proteoglycans per cartilage dry weight (Figure 4.10).

Native cartilage had a DNA content of 119 ± 36 ng.mg^{-1} wet weight (Figure 4.9).

4.5.2 dCELL 1

After application of the dCELL 1 basic protocol developed by Stapleton *et al.* (2008), staining of treated tissue sections with H&E revealed that there were still a number of cells present in the cartilage and bone (Figure 4.6 b). In the superficial zone, a number of empty lacunae could be seen, which were slightly enlarged. The general structure of the tissue was maintained, marrow was present in the bone, but did not contain whole cell nuclei. DAPI staining confirmed a reduction in cell nuclei, but showed that a large number of cells remained (Figure 4.7 b). There was no significant reduction in cartilage DNA content compared to native tissue (Figure 4.9). There was a slight loss of intensity of alcian blue staining throughout the cartilage, and PAS staining was slightly present at the very superficial layer (Figure 4.8 b), indicating that loss of GAGs has occurred. The GAG content of cartilage following treatment with the dCELL 1 protocol was not significantly different from native tissue, however a reduction was noted (Figure 4.10).

4.5.3 dCELL 2

Following the introduction of an extended PBS wash to the end of the basic protocol, sections of osteochondral pins decellularised using the dCELL 2 protocol as outlined in Section 4.4.2.2 showed a much greater reduction in cell content (Figure 4.6 c). Empty lacunae, again, appeared slightly enlarged and within the empty lacunae, there was light eosin staining, which may have indicated the collapsed collagen type VI shell, as previously reported by Kheir *et al.* (2011). These stained regions within lacunae did not stain with haematoxylin or DAPI (Figure 4.7 c) so do not contain nuclear material. DNA quantification showed a significant reduction from native tissues (Figure 4.9). However, nucleated cells were still visible in the deep/calcified cartilage regions and in the subchondral bone. There appeared to be an

overall reduction in GAGs in cartilage tissues (Figure 4.8 c), which when quantified, was not significantly different from native tissues (Figure 4.10).

To enhance osmotically induced cell lysis in the deep/calcified regions and improve decellularisation, alterations were made to dCELL 2 protocol to freeze/thaw entirely in hypotonic buffer or distilled water. As seen in Figure 4.6 d & e and Figure 4.7 d & e cells were still present in the dense deep cartilage and bone in similar numbers to those seen following use of the dCELL 2 protocol. The DNA content of cartilage treated with hypotonic freeze/thaw did not differ significantly from native cartilage, however distilled water freeze/thawed tissue did show a significant reduction (Figure 4.9). Both protocols resulted in similar GAG reduction to that of dCELL 2 protocol (Figure 4.8 d & e), which when quantified, was not significantly different from native tissues (Figure 4.10).

Ultrasonication was employed in an attempt to increase the permeability of the matrix and aid perfusion of decellularisation solutions through the deeper cartilage and bone. No histological changes could be seen in cartilage or bone structure following treatment with the sonicating probe (Figure 4.6 f). Similar to the freeze/thaw alterations to the dCELL 2 protocol, ultrasonication did not improve the removal of cells (Figure 4.7 f) nor did it have any additional effects on GAG retention (Figure 4.8 f and Figure 4.10) although DNA content was significantly reduced from that of native tissue (Figure 4.9).

4.5.4 dCELL 3

To increase decellularisation solution access to the bone and deep cartilage layers a water pik was used to remove bone marrow from within the trabecular spaces (dCELL 3 protocol). Visibly, not much marrow was removed following application of the water jet. Histologically, no damage to the cartilage or bone was seen (Figure 4.6 g), there was no additional adverse effects on cartilage GAGs (Figure 4.8 g and Figure 4.10), although cells were still visible in the tissue and within denser areas of bone (Figure 4.7 g). The DNA content of cartilage was significantly reduced compared to native cartilage (Figure 4.9).

As bovine tissues were received 3 – 4 days post-slaughter, blood within the marrow had clotted, potentially making removal using the water pik difficult. To overcome this issue, an anticoagulant, hirudin, was applied to osteochondral pins to increase the efficacy of the water pik treatment. Marrow was more easily removed, and histolgically, there appeared to be a greater extent of cell removal (Figure 4.6 h and Figure 4.7 h) compared to use of the water pik alone. The DNA content of cartilage was significantly reduced compared to native cartilage (Figure 4.9).However, blue staining was less intense, indicating a greater loss of GAGs with use of the enzyme (Figure 4.8 h), however the reduced GAG content was not significantly different to native cartilage (Figure 4.10).

Since application of hirudin to the cartilage had an adverse effect on GAGs, a different method was developed to submerge only the bony component of osteochondral pins into the enzyme (section 4.4.2.8), a non-enzymatic anticoagulant, monosodium citrate, was also used in this novel set up to avoid enzymatic removal/degradation of GAGs. The incubation temperature was increased to 37 °C to increase the rate of diffusion. This method was unsuccessful as there was significant loss of GAGs with hirudin treatment (Figure 4.8 I and Figure 4.10). Monosodium citrate did not cause as great a reduction in cartilage GAGs as hirudin (Figure 4.8 j & Figure 4.10). Cell removal was not as effective following either of these treatments as was seen when pins were completely submerged in hirudin (Figure 4.6 i & j and Figure 4.7 i & j). However, the reduction in DNA was still significant (Figure 4.9).

As a negative control for the anticoagulant activity of hirudin, pins were also incubated in PBS prior to use of the water pik. Water pik treatment was equally effective at removing marrow following incubation of pins in PBS as it was with hirudin incubation (Figure 4.6 k and Figure 4.7 k). The reduction in DNA content was equally acceptable (Figure 4.9). The adverse effects on GAGs were minimised using PBS rather than hirudin (Figure 4.8 k and Figure 4.10).

4.5.5 dCELL 4

As bone marrow has a high lipid content, it was thought that marrow wash out would be more effective at a higher temperature, when marrow fats would be liquid rather than solid. To this end, the temperature of the pre-water pik treatment PBS incubation was increased to 45 °C. This greatly improved ease and extent of marrow removal with the water pik (dCELL 4 protocol). However no improvement in cell presence or DNA reduction in cartilage tissue was seen compared to incubation in PBS at room temperature (Figure 4.6 l, Figure 4.7 l and Figure 4.9), and a significant reduction in GAG content compared to native tissue was observed (Figure 4.8 l, Figure 4.10).

To improve DNA removal, an additional nuclease step was included in the dCELL 4 protocol. No improved cell removal was seen compared to the use of a single nuclease treatment (Figure 4.6 m and Figure 4.7 m) and again, GAG content was significantly lower than that of native cartilage (Figure 4.8 m and 4.10).

As cell retention appeared to occur in dense bony regions and calcified cartilage, it was thought that decalcification of the osteochondral pins might improve access to these regions. Cells were still visible in the deep cartilage regions (Figure 4.5 n and Figure 4.7 n) and cartilage DNA content did not differ from dCELL 4 (Figure 4.9). GAG content of EDTA treated cartilage was significantly lower than native tissues (Figure 4.8 n and Figure 4.10)

4.5.6 dCELL 5

To achieve full decellularisation, other processes have required repeat cycles of SDS and hypotonic washes (Stapleton *et al*., 2008; Kheir *et al*., 2011), however these have resulted in greater GAG loss. Two cycles of SDS were incorporated into the dCELL 5 protocol, so cells were exposed to additional osmotic stress and membranes would be more effectively removed. Following decellularisation with dCELL 5 protocol, cartilage only contained 7 ± 6 $ng.mg^{-1}$ DNA per wet weight (39 $ng.mg^{-1}$ DNA per dry weight), a reduction of 94 % (Figure 4.9). This protocol also led to full

removal of whole cells from both cartilage and bone (Figure 4.6 o and Figure 4.7 o). Empty lacunae were enlarged throughout the cartilage ECM (Figure 4.6 o). However, following the application of the protocol, the presence of GAGs within the cartilage tissue was greatly reduced (Figure 4.8 o). The GAG content of the acellular cartilage was significantly reduced to 2.5 ± 2.8 $\mu g.mg^{-1}$; a 99 % (w/w) reduction from native tissue (Figure 4.10). Previous protocols, despite resulting in reduced cartilage GAG content, did not have adverse effects on the tissue biomechanics. Following application of this protocol however, the severe reduction in GAGs was found to result in a significant increase in the percentage deformation from 30.4 (+ 7.6, - 7.1) % deformation of native cartilage to 48.4 (+ 20.1, - 21.2) % (Figure 4.12). The reduction in GAG content resulted in a significant increase in the cartilage collagen content as a proportion of tissue dry weight from 72.3 ± 26.5 $\mu g.mg^{-1}$ (native) to 146.3 ± 65.1 $\mu g.mg^{-1}$ (dCELL 5; Figure 4.11).

To further characterise the acellular bovine osteochondral matrix produced following the application of the dCELL 5 protocol, immunohistochemical analysis was performed to localise specific matrix proteins in native and decellularised tissues. Tissues were labelled with antibodies for collagen type VI (Figure 4.13). In native tissues, brown staining was seen throughout the superficial and middle zones of the cartilage, with greater intensity in the superficial region, little to no staining was seen in the deep zone. Intense staining was found localised to the cartilage chondrons around chondrocytes. Decellularised tissues showed very little staining, and no increased intensity could be seen at chondrons. Isotype and antibody free controls did not show any brown staining for native tissue, however slight brown staining was seen in the decellularised tissue isotype control.

Images of tissue sections labelled with antibodies against COMP care presented in Figure 4.14. Staining was evenly dispersed across the native cartilage, but was absent in the deep calcified region and was slightly depleted at the cartilage surface. Decellularised tissues also showed similar staining, however there was a more distinct loss of staining it the surface layer and at higher magnification (100 x) a graininess could be seen in the stain, which was not present in the native tissue stains. Again, isotype and antibody-free controls were negative for native tissue, however the isotype

control for decellularised tissue was positive (Figure 4.14 g), although the graininess seen when labelling the decellularised cartilage with antibody against COMP was not present in the isotype.

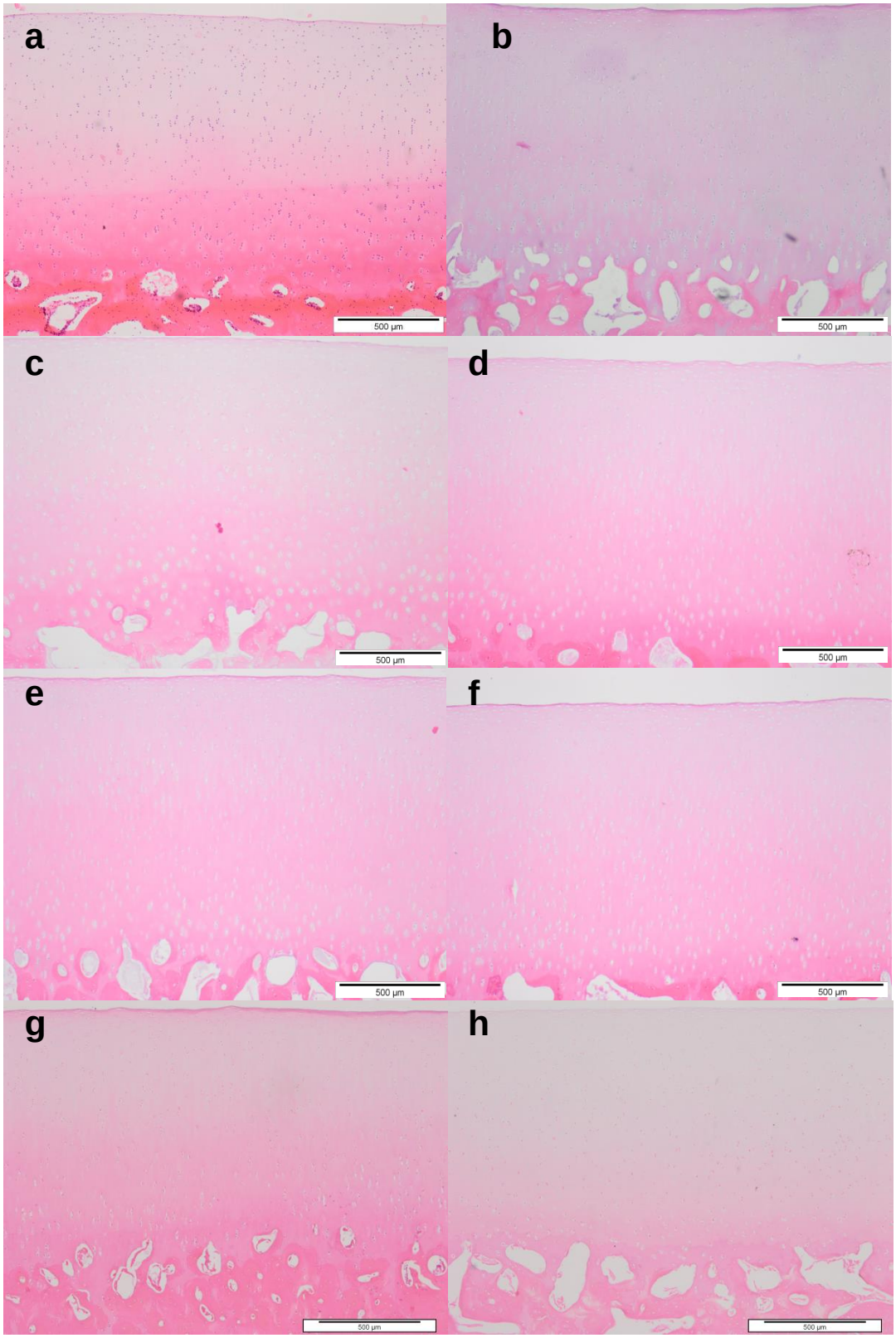

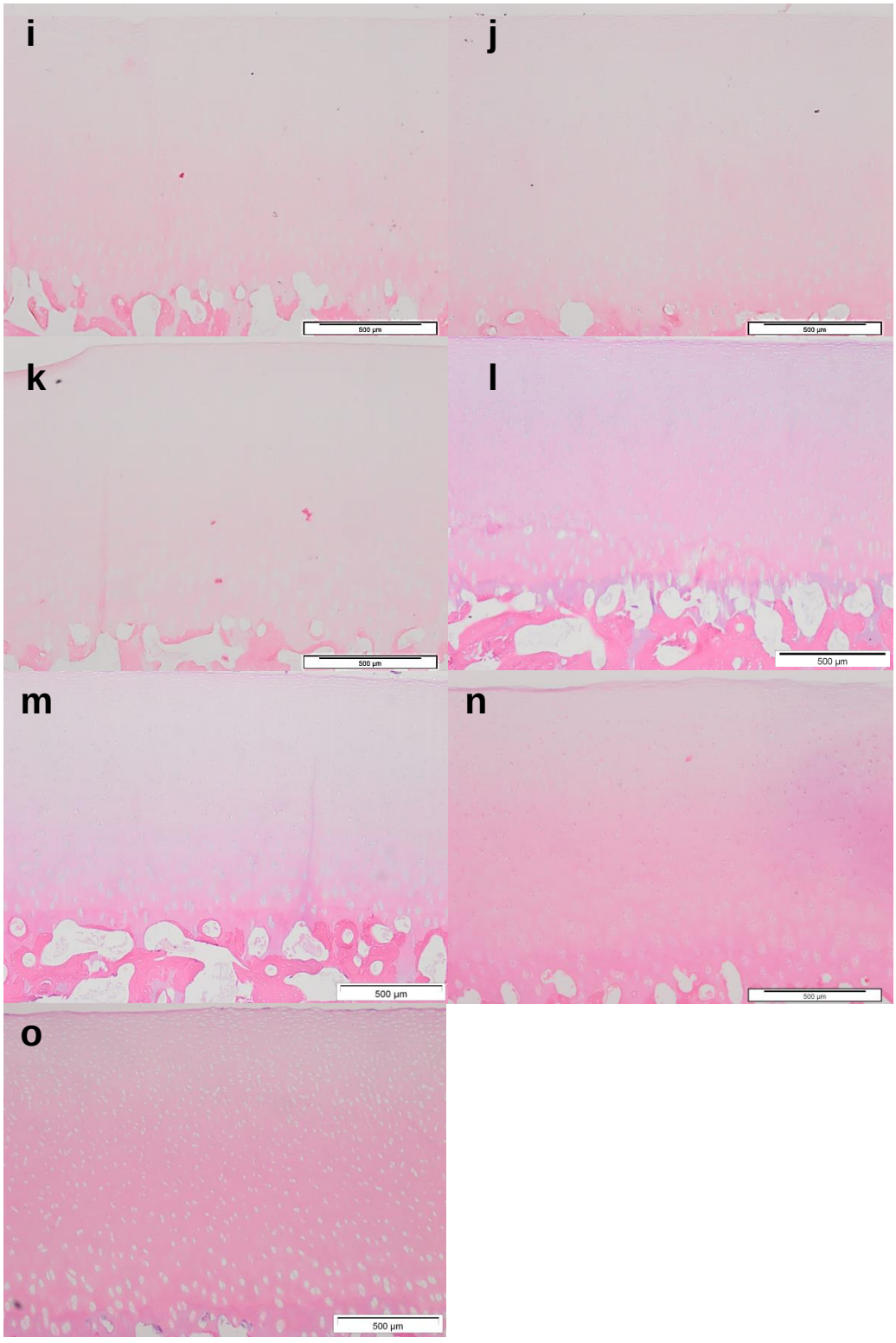

Figure 4.6 H&E stained sections of native and decellularised bovine osteochondral pins. a) fresh, b) dCELL 1, c) dCELL2, d) dCELL 2 with hypotonic freeze/thaw, e) dCELL 2 with distilled water freeze/thaw, f) dCELL 2 with ultrasonication, g) dCELL 3, h) dCELL 3 with hirudin, i) dCELL 3 with hirudin applied to bone only, j) dCELL 3 with monosodium citrate, k) dCELL 3 with PBS, l) dCELL 4, m) dCELL 4 with two nuclease washes, n) dCELL 4 with EDTA pre-treatment, o) dCELL 5. Scale bar = 500 µm.

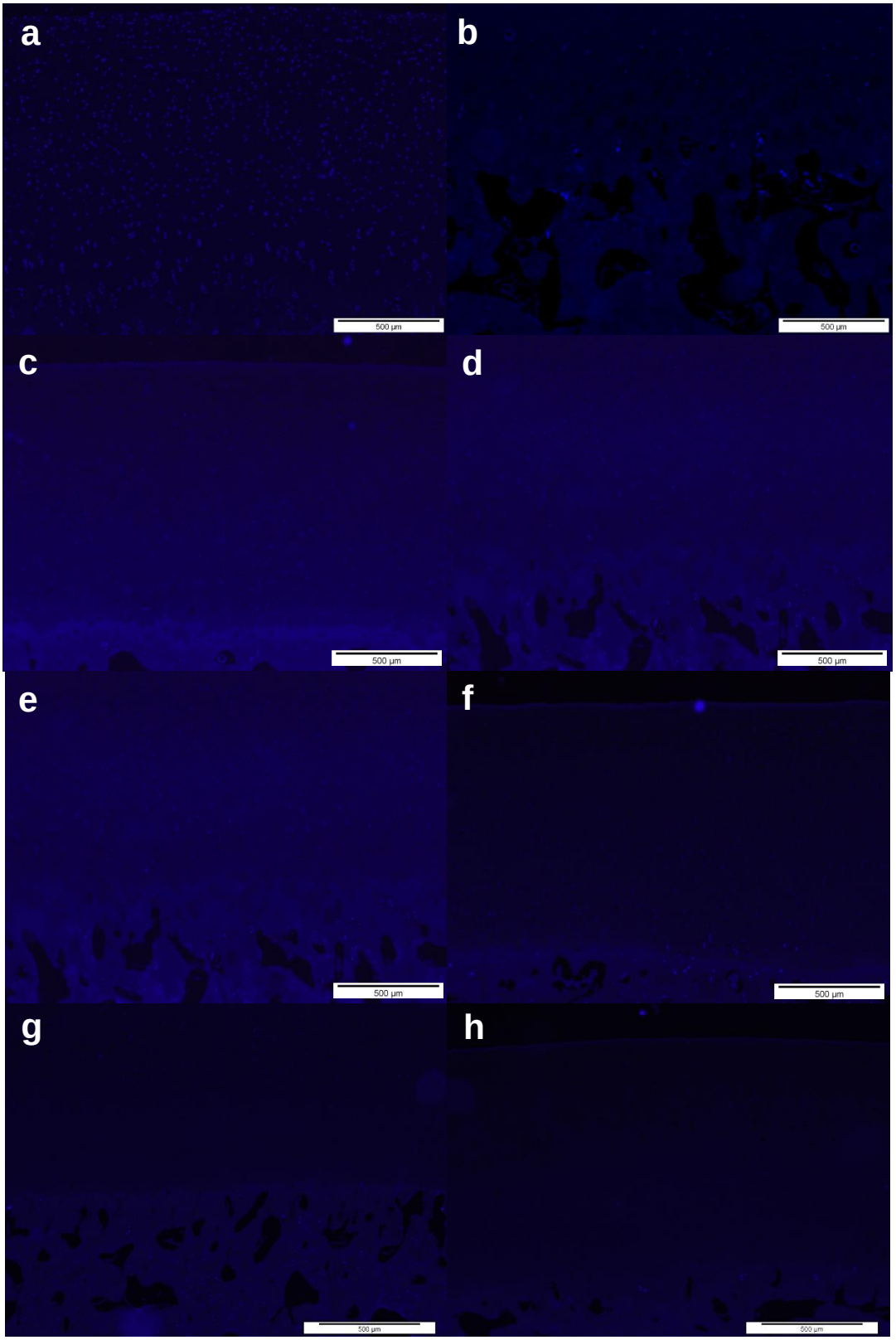
a
500 µm
b
500 µm
c
500 µm
d
500 µm
e
500 µm
f
500 µm
g
500 µm
h
500 µm

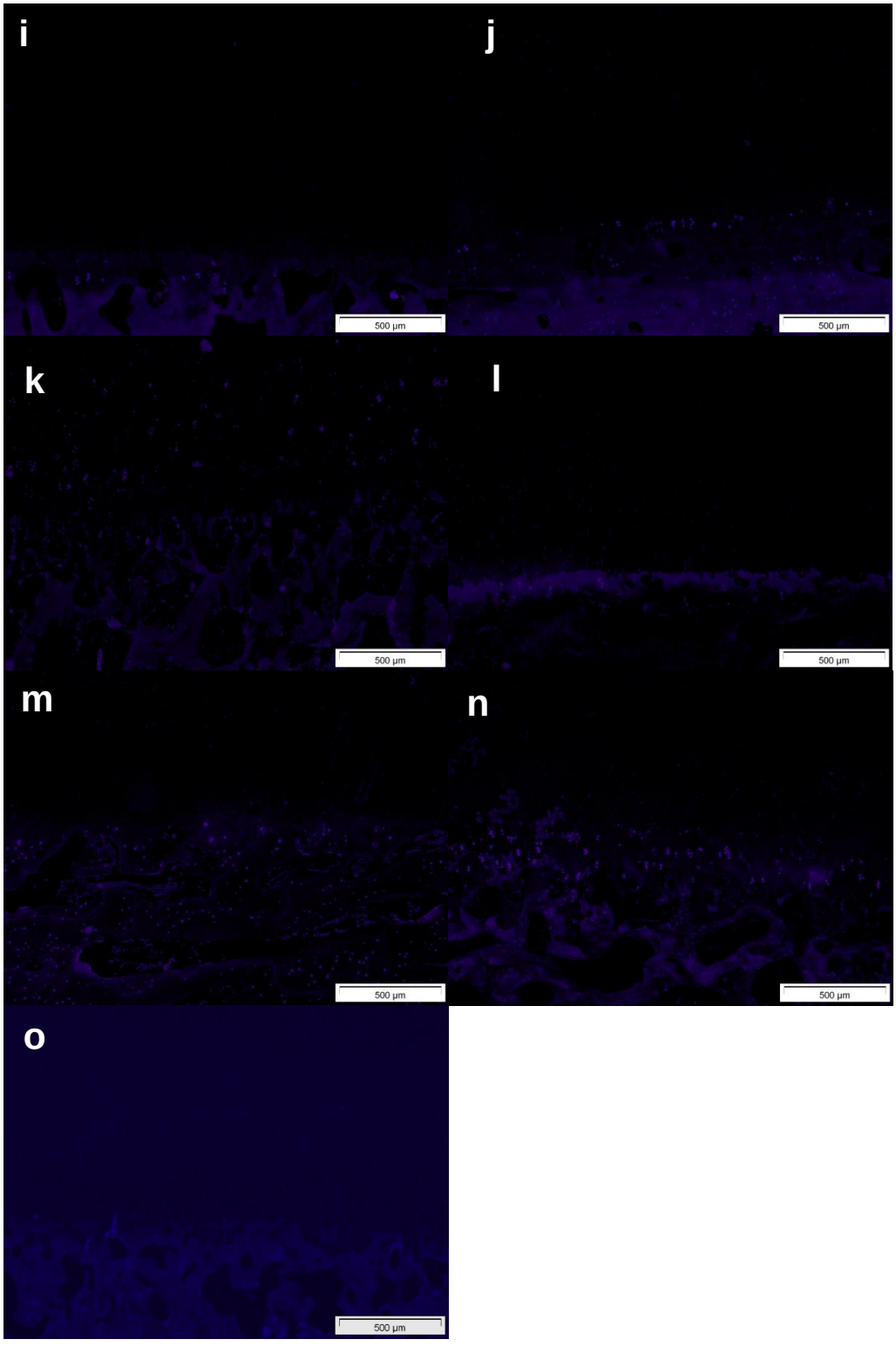

Figure 4.7 DAPI stained sections of native and decellularised bovine osteochondral pins. a) fresh, b) dCELL 1, c) dCELL2, d) dCELL 2 with hypotonic freeze/thaw, e) dCELL 2 with distilled water freeze/thaw, f) dCELL 2 with ultrasonication, g) dCELL 3, h) dCELL 3 with hirudin, i) dCELL 3 with hirudin applied to bone only, j) dCELL 3 with monosodium citrate, k) dCELL 3 with PBS, l) dCELL 4, m) dCELL 4 with two nuclease washes, n) dCELL 4 with EDTA pre-treatment, o) dCELL 5. Scale bar = 500 µm.

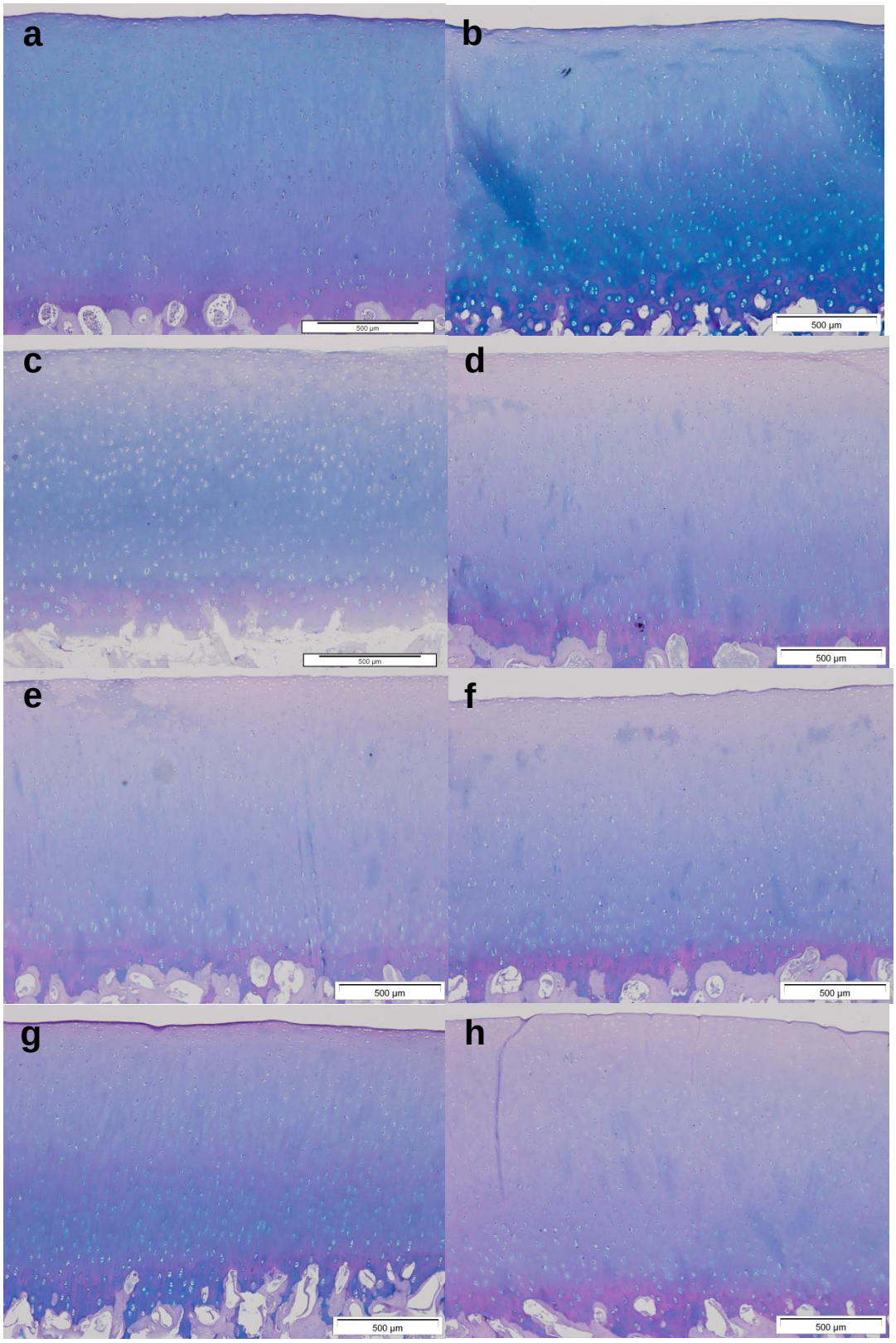
a
500 µm
b
500 µm
c
500 µm
d
500 µm
e
500 µm
f
500 µm
g
500 µm
h
500 µm

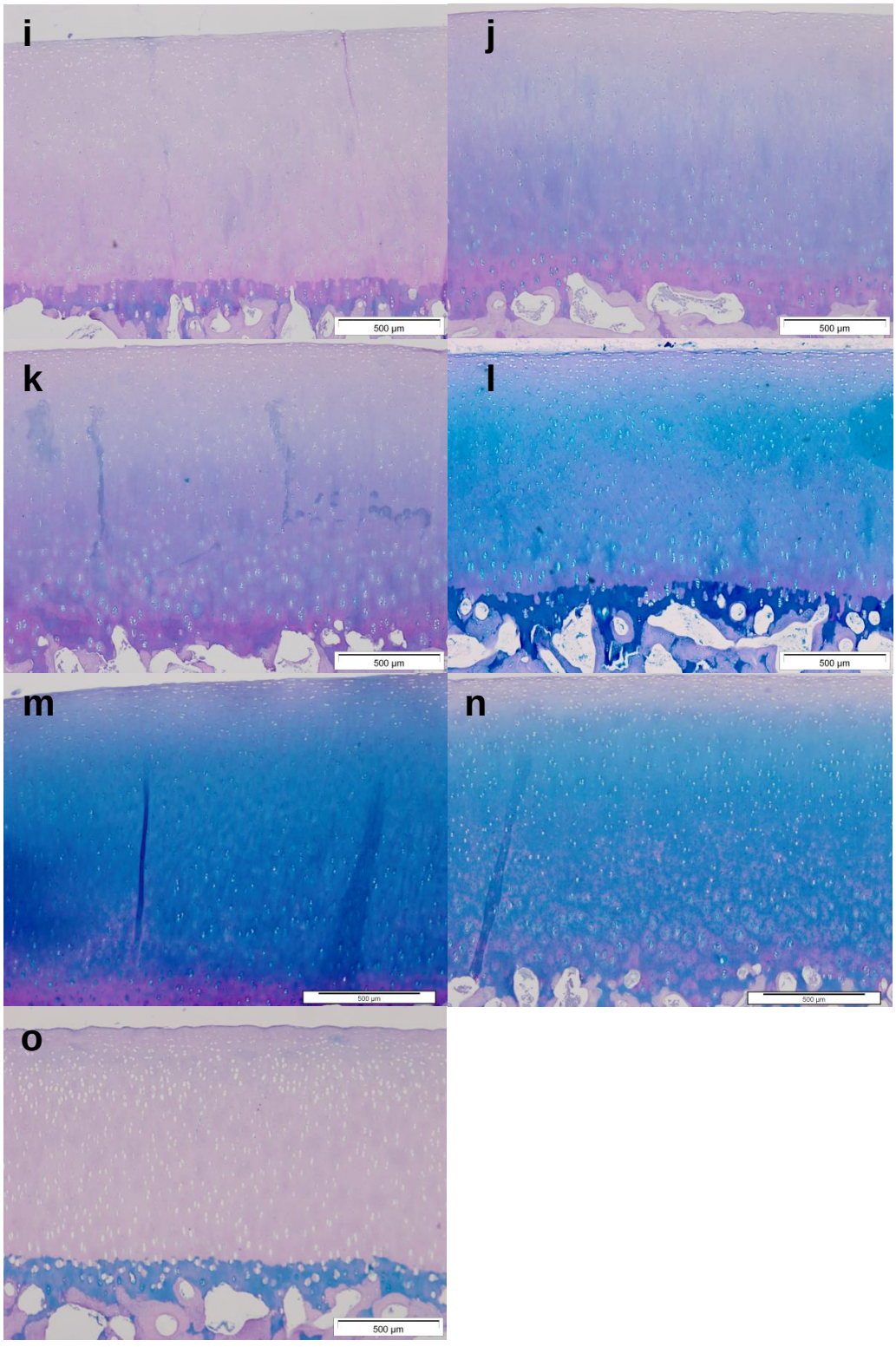

Figure 4.8 Alcian blue stained sections of native and decellularised bovine osteochondral pins. a) fresh, b) dCELL 1, c) dCELL2, d) dCELL 2 with hypotonic freeze/thaw, e) dCELL 2 with distilled water freeze/thaw, f) dCELL 2 with ultrasonication, g) dCELL 3, h) dCELL 3 with hirudin, i) dCELL 3 with hirudin applied to bone only, j) dCELL 3 with monosodium citrate, k) dCELL 3 with PBS, l) dCELL 4, m) dCELL 4 with two nuclease washes, n) dCELL 4 with EDTA pre-treatment, o) dCELL 5. Scale bar = 500 µm.

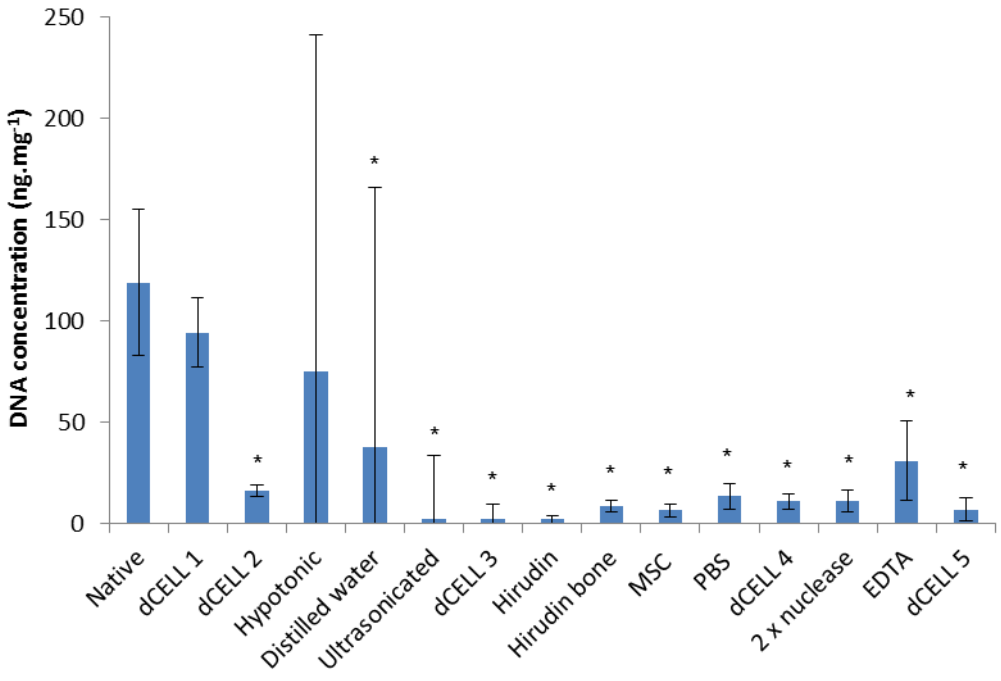

Figure 4.9 Cartilage DNA content. Data is shown as the mean (fresh and dCELL 1 n=5, others n=3) ± 95 % confidence limits. * significant difference compared to native tissue p<0.05 (ANOVA).

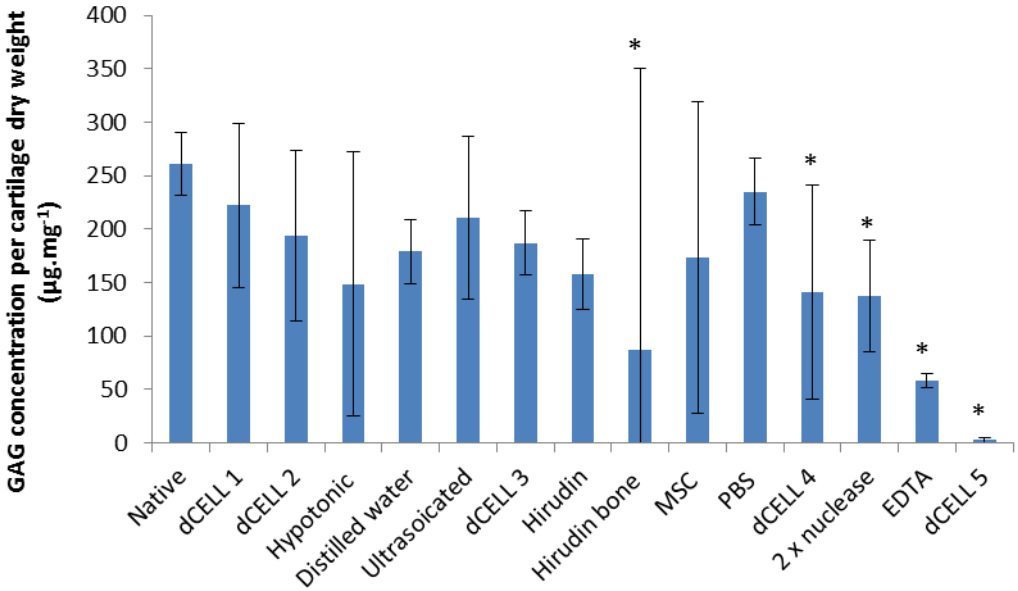

Figure 4.10 Cartilage GAG content. Data is shown as the mean (fresh and dCELL 1 n=5, others n=3) ± 95 % confidence limits. * significant difference compared to native tissue p<0.05 (ANOVA).

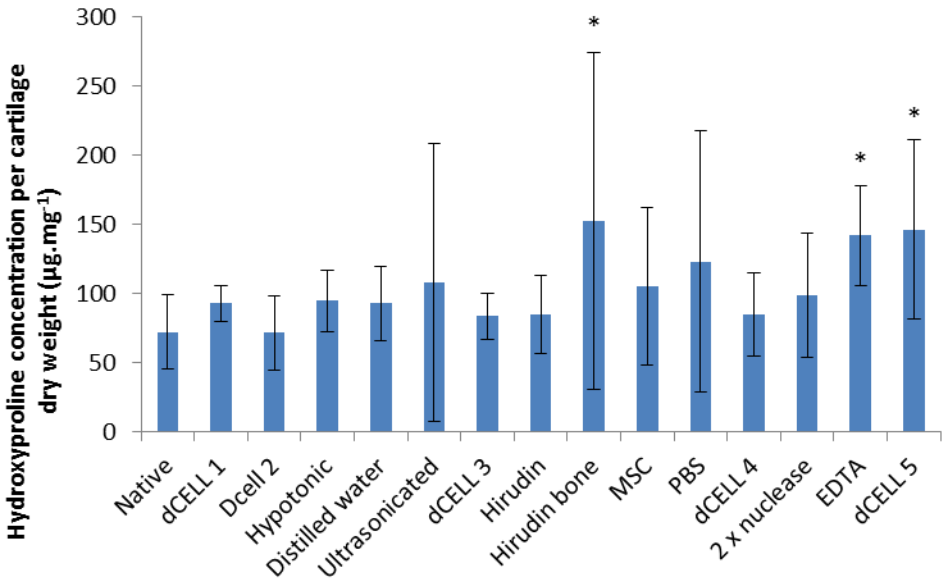

Figure 4.11 Cartilage hydroxyproline content. Data is shown as the mean (fresh and dCELL 1 n=5, others n=3) ± 95 % confidence limits. * significant difference compared to native tissue $p<0.05$ (ANOVA).

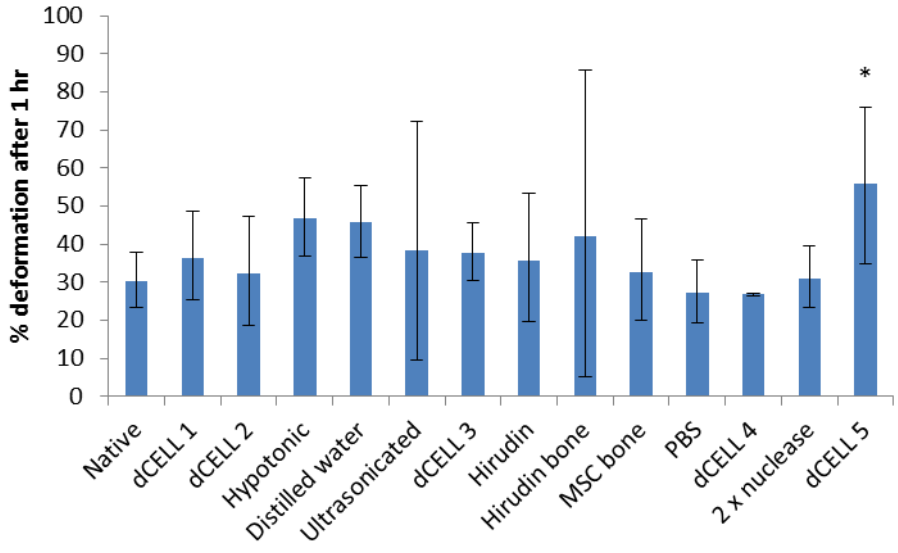

Figure 4.12 Percent deformation of cartilage. Data was subject to arcsin transformation prior to calculation of the 95% confidence limits and analysis of variance. Data is shown as the back transformed mean (fresh and dCELL 1 n=5, others n=3) ± 95 % confidence limits. * significant $p<0.05$ (ANOVA).

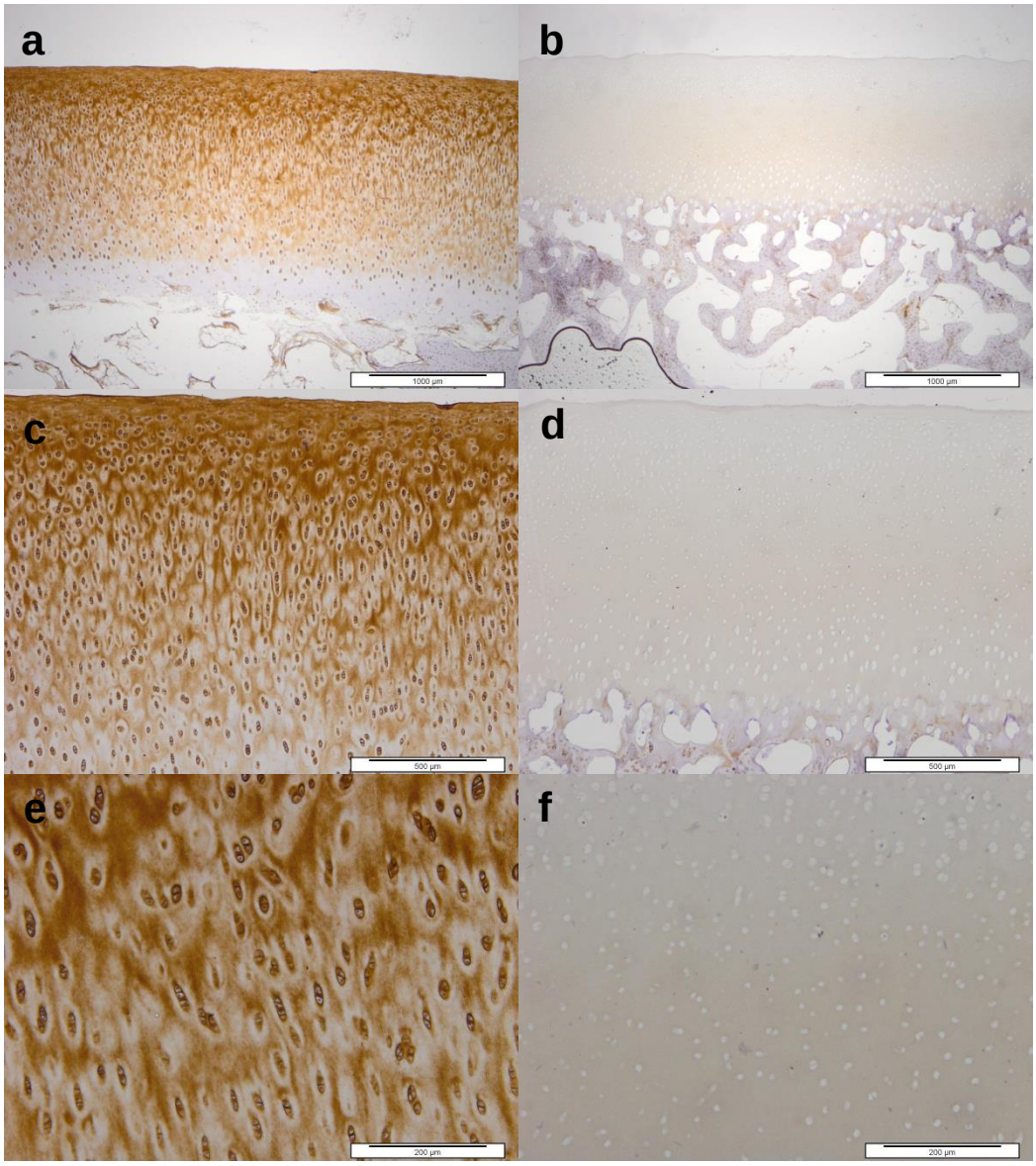

Figure 4.13 Localisation of collagen type VI in native and decellularised bovine osteochondral tissues. a) native tissue (20 x magnification) scale bar = 1000 µm, b) decellularised tissue (20 x mag.) scale bar = 1000 µm, c) native tissue (40 x mag.) scale bar = 500 µm, d) decellularised tissue (40 x mag.) scale bar = 500 µm, e) native tissue (100 x mag.) scale bar = 200 µm, f) decellularised tissue (100 x mag.) scale bar = 200 µm.

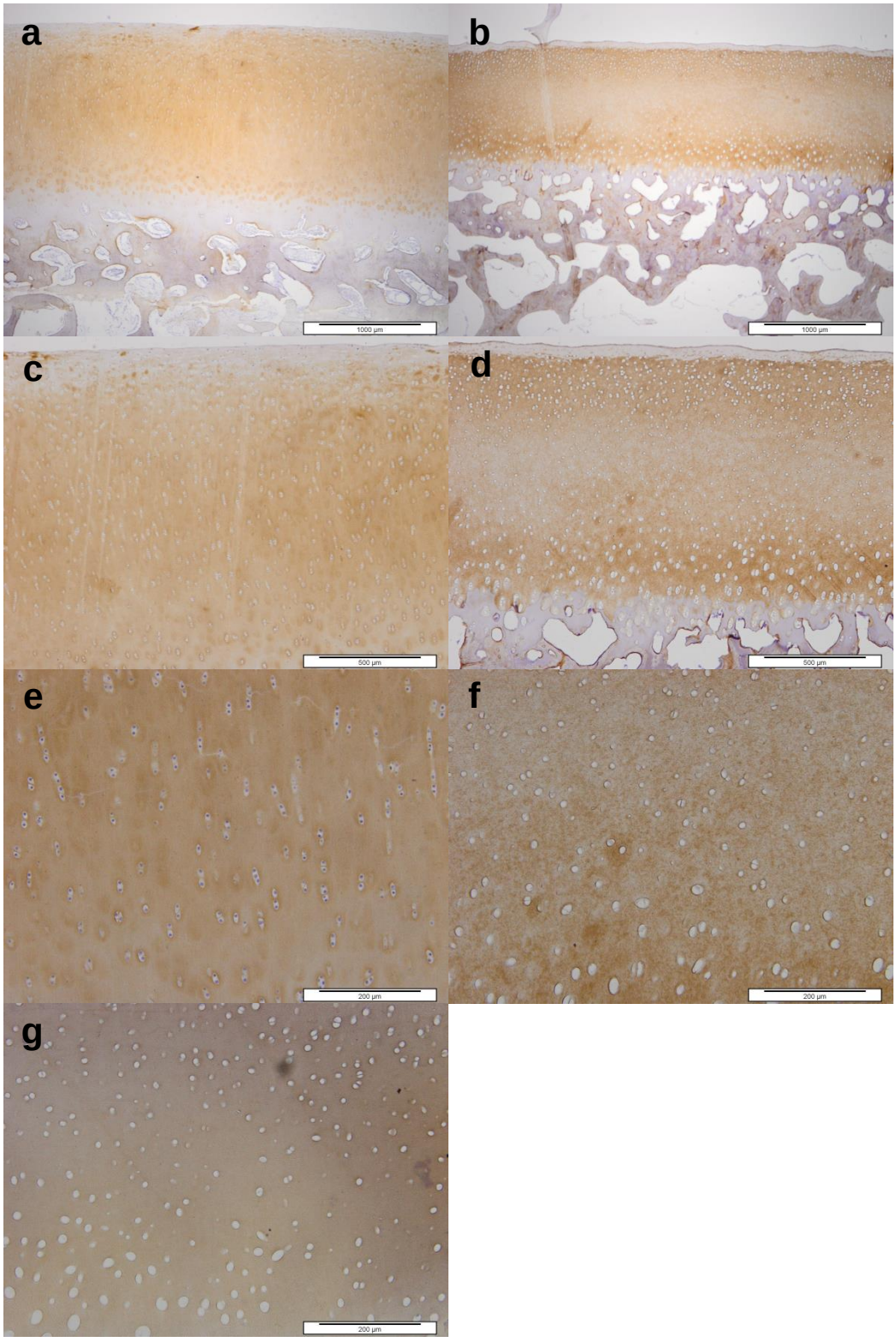

Figure 4.14 Labelling of COMP in native and decellularised bovine osteochondral samples. a) native tissue (20 x magnification) scale bar = 1000 µm, b) decellularised tissue (20 x mag.) scale bar = 1000 µm, c) native tissue (40 x mag.) scale bar = 500 µm, d) decellularised tissue (40 x mag.) scale bar = 500 µm, e) native tissue (100 x mag.) scale bar = 200 µm, f) decellularised tissue (100 x mag.) scale bar = 200 µm, g) decellularised tissue isotype control (100 x mag.) scale bar = 200 µm.

4.6 Discussion

This study aimed to produce an acellular bovine osteochondral pin for use in osteochondral lesion repair. The aim was to achieve complete removal of whole cells and cellular debris from the ECM scaffold to eliminate the immunogenic effects of xenogeneic cellular antigens. As the fundamental macromolecules of the ECM, such as collagens, are conserved throughout mammalian species, these matrix proteins should not evoke an immune response.

A protocol for decellularisation was developed, based on previous work by Booth *et al.* (2002). Increased incubation temperatures (Stapleton *et al*., 2008 and Khier *et al.*, 2011) were required to overcome issues with dense matrix and high GAG concentrations of osteochondral tissues which can inhibit the diffusion of decellularisation solutions. Additionally, EDTA, incorporated as a protease inhibitor in existing protocols was initially removed from the process to avoid decalcification of the bony component of the osteochondral pins.

Histological analysis of osteochondral tissues decellularised using the dCELL 5 protocol showed the full removal of whole cells and large cellular debris, and the DNA content of cartilage was significantly reduced to below 50 $ng.mg^{-1}$. To achieve complete decellularisation, bone marrow first needed to be loosened and removed. This was achieved by incubation in PBS at 45 °C with agitation for 18 h and then use of a water pik. Use of anticoagulants and lower temperatures did not prove as effective at loosening marrow. Removal of bone marrow enabled better diffusion of decellularisation solutions through the bone and up to the subchondral plate. Four cycles of freeze/thaw were required (two of which were in hypotonic solution) to open up the ECM through formation of ice crystals to improve diffusion of solutions through the tissue. The use of hypotonic buffer or distilled water at all stages did not improve the efficacy of freeze/thaw cycles and ultrasonication of tissues prior to decellularisation to increase diffusion was not advantageous. Two applications of hypotonic buffer and low concentration SDS in series were required to fully remove cells from calcified cartilage and the subchondral bone plate, as these areas were most dense.

This number of SDS cycles was fewer than required in the protocol developed by Khier *et al.* (2011) for porcine tissue, likely due to the smaller volume of tissue being decellularised. Extensive washing in PBS following nuclease treatment and PAA sterilisation was required to fully remove cell remnants from the tissue.

Although decellularisation was achieved, there were detrimental effects on the ECM. Histological analysis of the acellular matrix showed an increase in cartilage porosity. A reduction in GAGs was seen with alcian blue staining which was confirmed by sulphated proteoglycan quantification. This loss of GAG had an adverse effect on the mechanical properties of the tissue resulting in a significant increase in cartilage deformation.

The DNA content of the bony section of the osteochondral tissue was not quantified, so the true extent of osteochondral decellularisation is currently unknown. Satisfactory digestion of the mineralised tissue could not be achieved following preliminary alterations to the protocol provided with the Qiagen kit, further work is required to quantify bone DNA. Retention of DNA within the bone is not thought to be problematic, as whole cell nuclei have been shown to be removed following histological analysis. The presence of DNA in the bone will not elicit an immune response, only the presence of cellular membranes and proteins (Knight & Ingham, 2006). Residual DNA is known to result in calcification of decellularised tissues following implantation (Schoen & Levy, 2005), however this would not pose and issue in an already mineralised tissue such as bone.

Immunohistochemical analysis of decellularised tissues showed that most collagen type VI was lost from the tissue. Collagen type VI is a key component of the cartilage ECM and is usually localised to the chondrons (Cremer *et al*., 1998) where it plays a role in chondrocyte attachment to the ECM (Poole *et al*., 1997). As cells were removed from the tissue during the process, it was expected that some damage to the immediate pericellular matrix would occur. Damage to collagen type VI following decellularisation was also seen by Kheir *et al*. (2011), where the collagen shell of the chondron had collapsed in.

COMP is a non-collagenous matrix protein which plays a role in matrix assembly. The protein is uniformly distributed in the interterritorial matrix, with slightly increased density in the deep zone and decreased density around the tidemark and calcified cartilage (DiCesare *et al*., 1995). Depletion of COMP has been seen in osteoarthritic cartilage (DiCesare *et al*., 1996), and is thought to be a good soluble biomarker for the disease (Saxne & Heinegård, 1992). Immunolabelling of tissue sections showed COMP to be uniformly distributed throughout native bovine cartilage, with some reduction in staining at the superficial zone and an absence of staining in the calcified cartilage. Decellularised tissues showed similar stain distribution, however there was a distinct boundary of stain loss at the superficial zone, and throughout the cartilage staining appeared grainy, suggesting some clumping of COMP proteins.

Isotype controls were negative for native tissues but positive for decellularised tissue sections, showing non-specific binding of the secondary antibody. It is likely that residual SDS from the decellularisation process is interacting ionically with the secondary antibody, resulting in positive staining.

Other studies have been conducted to decellularise bovine articular cartilage without the subchondral bone. Elder *et al.* (2010) used 2 % (w/v) SDS over a range of incubation times to decellularise immature calf cartilage. They found that minimal detrimental effects to GAG content and therefore mechanical function occurred at short (2 h) incubation times, however, there were also minimal reductions in cell and DNA content. To achieve decellularisation, longer incubation (8 h) with SDS was required, however this lead to detrimental effects on GAG content and mechanical properties, as also seen in this study.

Yang *et al.* (2012) achieved successful decellularisation of mature bovine cartilage and retained GAGs, however their protocol involved freeze drying and homogenisation of cartilage to a powder before decellularising and re-forming, thus completely removing the structure of the natural ECM.

The regenerative capacity of the acellular bovine osteochondral scaffold developed in this study will need to be determined. The biological and

structural changes which have occurred following decellularisation and the biocompatibility of the resultant matrix need to be investigated further. As a number of alterations to the protocol for the decellularisation of bovine tissues have been explored in the current study, with varying degrees of success, the efficacy of some of these initial protocols will be investigated using porcine tissues. It may be possible to produce a porcine ECM scaffold which retains more of the characteristics of native tissues than was seen for bovine tissues.

Chapter 5
Investigation of methods for the decellularisation of porcine osteochondral tissues

5.1 Introduction

As introduced previously (Chapter 1 and Chapter 4), an acellular xenogeneic osteochondral scaffold may provide a more effective early intervention treatment for osteochondral lesions. An analysis of osteochondral tissues from different species and joint areas in Chapter 3 identified bovine medial groove and porcine medial condyle tissues as appropriate source materials for decellularisation. A protocol was developed for the successful decellularisation of bovine osteochondral tissues using a water pik to remove bone marrow followed by four cycles of freeze-thaw (two of which were in hypotonic buffer solution), two cycles of hypotonic buffer solution followed by incubation in 0.1 % (w/v) SDS, treatment with nucleases and sterilisation with 0.1 % (v/v) peracetic acid. In this chapter, the process required to decellularise porcine osteochondral tissues was investigated.

5.2 Aims and objectives

Aims:

The aim of the research in this chapter was to investigate methods using low concentration SDS plus proteinase inhibitors to decellularise porcine osteochondral pins obtained from the medial condyle.

Objectives:

- To develop a protocol to remove cells and cellular debris from porcine osteochondral pins while retaining the same natural histoarchitecture, biochemical composition and biomechanical function as the native osteochondral tissues.
- To characterise the resultant decellularised ECM and compare to native tissues
    - To characterise the tissue histologically in order to identify the presence/lack of cells and to observe any changes in the histoarchitecture of the tissue.
    - To quantify the total DNA, to identify the reduction in DNA compared to native tissue following decellularisation
    - To characterise the tissue biochemically to assess GAG and collagen content of decellularised scaffolds
    - To determine the biomechanical properties in order to determine any changes in the mechanical properties of cartilage following decellularisation.

5.3 Methods

5.3.1 Decellularisation solutions

Solutions for decellularisation were produced as described in Section 4.4.1. Additional solutions used in this part of the study are described below.

5.3.1.1 0.05 % (w/v) SDS in hypotonic buffer

SDS (10g) was dissolved in 100 ml distilled water to produce a 10 % (w/v) SDS solution. SDS solution (5 ml) was added to 995 ml hypotonic buffer. When required, the solution was sterilised by autoclaving and could be stored at room temperature for up to 3 months. Just prior to use, 1 ml aprotinin (10,000 $KIU.ml^{-1}$) was added to give a final concentration of 10 $KUI.ml^{-1}$.

5.3.1.2 PBS with aprotinin and EDTA (0.1% w/v)

A solution of PBS was produced as described in Section 2.1.7.1. EDTA (1 g) was dissolved in 1 L PBS and the pH adjusted to 7.2 – 7.4. When required, the solution was sterilised by autoclaving and could be stored at room temperature for up to 3 months. Just prior to use 1 ml aprotinin (10,000 $KIU.ml^{-1}$) was added to give a final concentration of 10 $KUI.ml^{-1}$.

5.3.1.3 PBS with mannitol (1 % w/v)

A solution of PBS was produced as described in Section 2.1.7.1. Mannitol (10 g) was dissolved in 1 L PBS and the pH adjusted to 7.2 – 7.4. When required, the solution was sterilised by autoclaving and could be stored at room temperature for up to 3 months. Just prior to use 1 ml aprotinin (10,000 $KIU.ml^{-1}$) was added to give a final concentration of 10 $KUI.ml^{-1}$.

5.3.1.4 PBS with mannitol (2 % w/v)

A solution of PBS was produced as described in Section 2.1.7.1. Mannitol (20 g) was dissolved in 1 L PBS and the pH adjusted to 7.2 – 7.4. When required, the solution was sterilised by autoclaving and could be stored at room temperature for up to 3 months. Just prior to use 1 ml aprotinin (10,000 $KIU.ml^{-1}$) was added to give a final concentration of 10 $KUI.ml^{-1}$.

5.3.2 Development of the decellularisation process

Decellularisation processes developed for bovine cartilage in the previous chapter were used to determine the response of porcine osteochondral tissues to decellularisation. Porcine osteochondral pins (9 mm diameter, 10 – 12 mm deep) were harvested from the porcine medial condyle and stored frozen as described in Section 2.2.2.

5.3.2.1 dCELL 1 (basic decellularisation)

Porcine osteochondral pins were decellularised as described in Section 4.4.2.1.

5.3.2.2 dCELL 3 (water pik)

Porcine osteochondral pins were decellularised as described in Section 4.4.2.6.

5.3.2.3 dCELL 3 (0.05 % w/v SDS)

Porcine osteochondral pins were decellularised as described in Section 4.4.2.6, however a reduced concentration (0.05 % w/v) of SDS in hypotonic buffer was used.

5.3.2.4 dCELL 3 (6 h 0.1 % w/vSDS)

Porcine osteochondral pins were decellularised as described in Section 4.4.2.6, however the 24 h 0.1 % (w/v) SDS in hypotonic buffer wash was replaced with 6 h in 0.1 % (w/v) SDS followed by 18 h in PBS.

5.3.2.5 dCELL 3 (0 % w/v SDS)

Porcine osteochondral pins were decellularised as described in Section 4.4.2.6, however the 24 h 0.1 % (w/v) SDS wash was replaced with 24 h in hypotonic buffer without SDS.

5.3.3 Cartilage characterisation

Following application of the decellularisation process detailed in Section 5.3.2.5, the cartilage was assessed histologically using the methods detailed in Section 2.2.3.

5.3.3.1 Denatured collagen quantification

5.3.3.1.1 Lyophilisation

Cartilage (50 mg) was lyophilised to a constant weight as described in Section 3.4.1.1.

5.3.3.1.2 α-chymotrypsin digestion

To determine the extent of collagen denaturation, macerated, freeze-dried tissues were digested using α-chymotrypsin.

- *Digestion Buffer (pH 7.8)* 1.21 g trizma base
  0.15 g calcium chloride
  100 ml distilled water
- *Digestion solution* 100 mg α-chymotrypsin
  20 ml digestion buffer

α-chymotrypsin digestion solution (5 ml) was added to each sample and incubated at 30 °C for 24 h.

5.3.3.1.3 Acid hydrolysis of α-chymotrypsin digest supernatant

Following digestion, each sample was centrifuged at 600 g for 10 min. The supernatant (4 ml) was collected in a polypropylene universal and hydrolysed with hydrochloric acid (6 M; 4ml) and then neutralised as described in Section 3.4.1.3.

5.3.3.1.4 Hydroxyproline quantification

The hydroxyproline residues from denatured collagen in the hydrolysed supernatant were quantified using the method detailed in Section 3.4.4. The supernatant was not diluted before assaying.

5.3.4 Investigation of the cause of cartilage damage

Osteochondral pins were harvested from the medial condyle of n=3 pigs. Unless otherwise stated, two pins from each individual were placed in one pot and three pots (n=3) were used for each condition. One pin from each pot was analysed.

5.3.4.1 Analysis of incubation temperature

Osteochondral pins (2 pins per pot, n=3) were decellularised as described in Section 5.3.2.4. One group was decellularised at 40 °C and the other group at 45 °C. The solution temperatures were measured with a thermometer at the beginning and end of each wash step and the temperature inside the incubator measured at the end of each wash step.

5.3.4.2 Systematic removal of major steps of the decellularisation process

Osteochondral pins (2 pins per pot, n=3) were decellularised using the dCELL 3 protocol as described in Section 5.3.2.2 at 42 °C. The complete protocol was used as a positive control for cartilage damage. Each major step of the protocol was systematically removed as detailed in Table 5.1 to identify the effect on cartilage. Incubation in PBS with aprotinin for the same duration was performed as a negative control.

Run name	+ve	a	b	c	d	e	f	-ve
Water pik	+	+	+	+	+	+	+	-
dry freeze/thaw (-20°C)	+	-	-	+	+	+	+	-
Hypotonic freeze/thaw (-80°C)	+	+	-	+	+	+	+	-
PBS	+	+	+	+	+	+	+	PBS
Hypotonic	+	+	+	-	+	+	+	PBS
SDS	+	+	+	+	-	+	+	PBS
PBS	+	+	+	+	+	+	+	PBS
Nuclease	+	+	+	+	+	+	+	PBS
PBS	+	+	+	+	+	+	+	PBS
PAA	+	+	+	+	+	-	+	PBS
PBS	+	+	+	+	+	+	+	PBS
PBS end wash	+	+	+	+	+	+	-	PBS

Table 5.1 Protocols with systematic removal of major steps of the process. The wash steps of the decellularisation protocol are listed in order. Variations are labelled a-f and positive (+ve) and negative (-ve) control protocols are also listed. The presence of each individual step is denoted with (+) and if the step was omitted this is indicated with (-).

5.3.4.3 Matrix metalloproteinase Inhibition

Osteochondral pins (2 pins per pot, n=3) were incubated in PBS with aprotinin and EDTA (0.1 % w/v) for 5 days at 42 °C with agitation. Another set of pins (2 pins per pot, n=3) were incubated in PBS without aprotinin or EDTA as a positive control.

5.3.4.4 Analysis of solution tonicity

5.3.4.4.1 Osmolality measurements

The osmolality of synovial fluid (collected from the porcine knee cavity using a 1 ml syringe, n=3) and of PBS containing 1 % and 2 % (w/v) mannitol was measured. Each sample (20 µl, n=3) was measured using a micro-osmometer (Advanced Instruments, 3MO Plus Freezing Point Osmometer).

5.3.4.4.2 Incubation of pins in PBS with mannitol

Osteochondral pins (2 pins per pot, n=3) were incubated in solutions of 1 % and 2 % (w/v) mannitol in PBS for 5 days at 42 °C with agitation.

5.3.4.4.3 Decellularisation of pins using PBS with mannitol

Osteochondral pins (2 pins per pot, n=3) were decellularised following the dCELL 3 process detailed in Section 5.3.2.2 however PBS washes were carried out in 1 % or 2 % (w/v) mannitol in PBS.

5.3.4.5 Analysis of pig skeletal maturity

Osteochondral pins were harvested from the medial condyle of 3 month old (n=3) and ~ 3 year old (n=3) pigs as described in Section 2.2.2. Pins were decellularised (1 pin per pot) following the dCELL 3 process detailed in Section 5.3.2.2.

5.3.4.6 Decellularisation with 1 vs 5 pins per pot

Osteochondral pins were decellularised by dCELL 3 as described in Section 5.3.2.2 with either 1 or 5 pins per pot (n=3).

5.3.5 Histological characterisation

Histological characterisation of native and decellularised osteochondral tissues was carried out as described in Section 2.2.3.

5.3.6 DNA quantification

The DNA content of native and decellularised cartilage and bone was quantified as detailed in Section 4.4.4.

5.3.7 Biochemical characterisation

The GAG, hydroxyproline and water content of native and decellularised tissues was assessed using methods described in Section 3.4.

5.3.8 Biomechanical characterisation

The percentage deformation of decellularised cartilage was determined using the indentation methods described in Sections 3.5.1 and 3.5.2.

5.4 Results

5.4.1 Decellularisation optimisation

5.4.1.1 dCELL 1

Following application of the dCELL 1 basic protocol the general tissue structure was maintained, however, there were still a number of cells present in the cartilage and bone (Figure 5.2 b and 5.3 b). Only a 77.5 % reduction in cartilage DNA was found (Figure 5.5). Native cartilage contained 262.1 ± 72.9 ng.mg^{-1} DNA per cartilage wet weight while cartilage which had been subject to the dCELL 1 protocol had 58.9 ± 9.9 72.9 ng.mg^{-1}. There was some loss of intensity of alcian blue staining (Figure 5.4 b) and PAS staining was stronger in the middle zone, suggesting loss of GAGs in this zone. Native cartilage contained 377.4 ± 54.2 µg.mg^{-1} GAG per cartilage dry weight while cartilage which had been subject to the dCELL 1 protocol had 151.7 ± 105.1 µg.mg^{-1}, a reduction of 59.8 % (Figure 5.6). This reduction in GAGs had a detrimental effect on the biomechanics of the tissue (Figure 5.7), with the percentage deformation of the cartilage increasing from 22.8 (+1.1, -1.0) % (native) to 34.7 (+7.3, -6.9) % (dCELL 1). The hydroxyproline content of cartilage following dCELL 1 was significantly increased from 43.6 ± 14.6 µg.mg^{-1} per dry weight (native) to 115.2 ± 16.4 µg.mg^{-1} (Figure 5.8). The water content of cartilage was not significantly different following the application of dCELL 1 (Figure 5.9).

5.4.1.2 dCELL 3

As application of the dCELL 1 protocol did not result in complete decellularisation of porcine osteochondral tissues, dCELL 3 as developed for bovine tissues in the previous chapter was employed. This again resulted in the general ECM structure being maintained (Figure 5.2 c) and following this protocol no whole cell nuclei could be seen (Figure 5.2 c and 5.3 c). The DNA content of cartilage was reduced by 98 % to 5.3 ± 0.4 ng.mg^{-1} cartilage wet weight (Figure 5.5). Images of alcian blue stained section showed a loss of blue intensity and increased PAS staining in the superficial and middle zones (Figure 5.4). The GAG content of cartilage had reduced by 60.3 % to 149.8 ± 284.6 µg.mg^{-1} cartilage dry weight (Figure 5.6), however variation

between samples was high, with one sample only having 19.2 µg.mg^{-1}. This again resulted in significantly increased percentage deformation (Figure 5.7) to 41.9 (+21.5, -20.0) %. The hydroxyproline content was not significantly different to native cartilage (Figure 5.8), however the water content had increased to 83.5 (+3.6, -4.0) % (Figure 5.9).

5.4.1.3 dCELL 3 (0.05 % SDS)

Upon completion of the dCELL 3 protocol using 0.05 % (w/v) SDS in place of 0.1 % (w/v) SDS, following the extended PBS end wash the solutions containing the osteochondral pins (n=3) were cloudy, and in one of the three pots, cartilage had dissolved away from the bone. Another pot of pins were subject to the process to achieve n=3. The cartilage in the remaining pots appeared gelatinous and had shrivelled away from the edge of the bone (Figure 5.1).

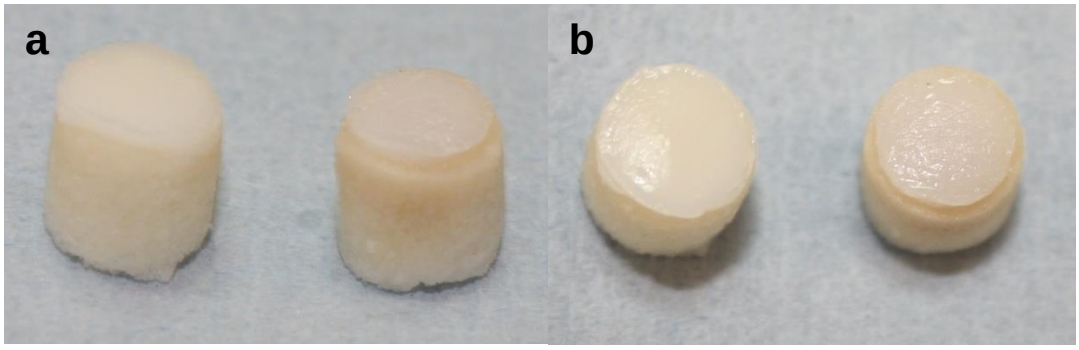

Figure 5.1 macroscopic observation of damaged pins. a) side view and b) top view of dCELL 3 pin (left) and dCELL 3 with 0.05% SDS pin (right).

No cell nuclei were observed in the decellularised tissue (Figure 5.2 d and 5.3 d) however the cartilage structure was highly porous and had reduced alcian blue staining for GAGs (Figure 5.2 d and Figure 5.4 d). The cartilage DNA content of these samples was significantly reduced by 98.2 % (Figure 5.5). The GAG content of cartilage was reduced by 82.1 % to 67.7 ± 161.7 µg.mg^{-1} (Figure 5.6). The hydroxyproline content of the tissue following this protocol was significantly increased compared to native tissue and was 115.2 ± 48.9 µg.mg^{-1} (Figure 5.8). The water content of the tissue was significantly increased to 84.2 ± 0.8 % compared to native tissue (Figure

5.9). Following measurement of deformation using a hemispherical indenter, this damaged cartilage did not recover, so needle indentation could not subsequently be performed to measure cartilage thickness. No percentage deformation data is therefore available for presentation.

5.4.1.4 dCELL 3 (6 h)

Similarly to the previous protocol using 0.05 % SDS, when samples were incubated in 0.1% SDS for only 6 h, cartilage damage was seen again. Cartilage was porous, the surface was wrinkled (Figure 5.2 e) and cartilage GAG content was depleted (Figure 5.4 e). No cell nuclei were present in the tissue (Figure 5.2 e and 5.3 e). The DNA content of this cartilage was significantly reduced by 90.6 % compared to native tissue. No sulphated proteoglycans could be detected using the DMB dye assay, there was no significant difference in the absorbance of the sample to that of the blank (ANOVA). The hydroxyproline content of the tissue was significantly increased compared to native tissue to 137.3 ± 59.1 $\mu g.mg^{-1}$. The cartilage water content was also significantly increased to 93.8 ± 0.3 %. Again, tissue did not recover following indentation, so the percentage deformation of the cartilage could not be determined.

5.4.1.5 dCELL 3 (0.0% SDS)

As seen following the two previous decellularisation protocols, cartilage appeared shrivelled and gelatinous, the tissue volume was greatly reduced. The histological appearance was also as previously reported (Figure 5.2 f, 5.3 f and 5.4 f). Since limited tissue was available, this group of damaged pins were used to investigate the nature of the cartilage damage by performing histological analysis and quantitative analysis of collagen damage (Section 5.4.2).

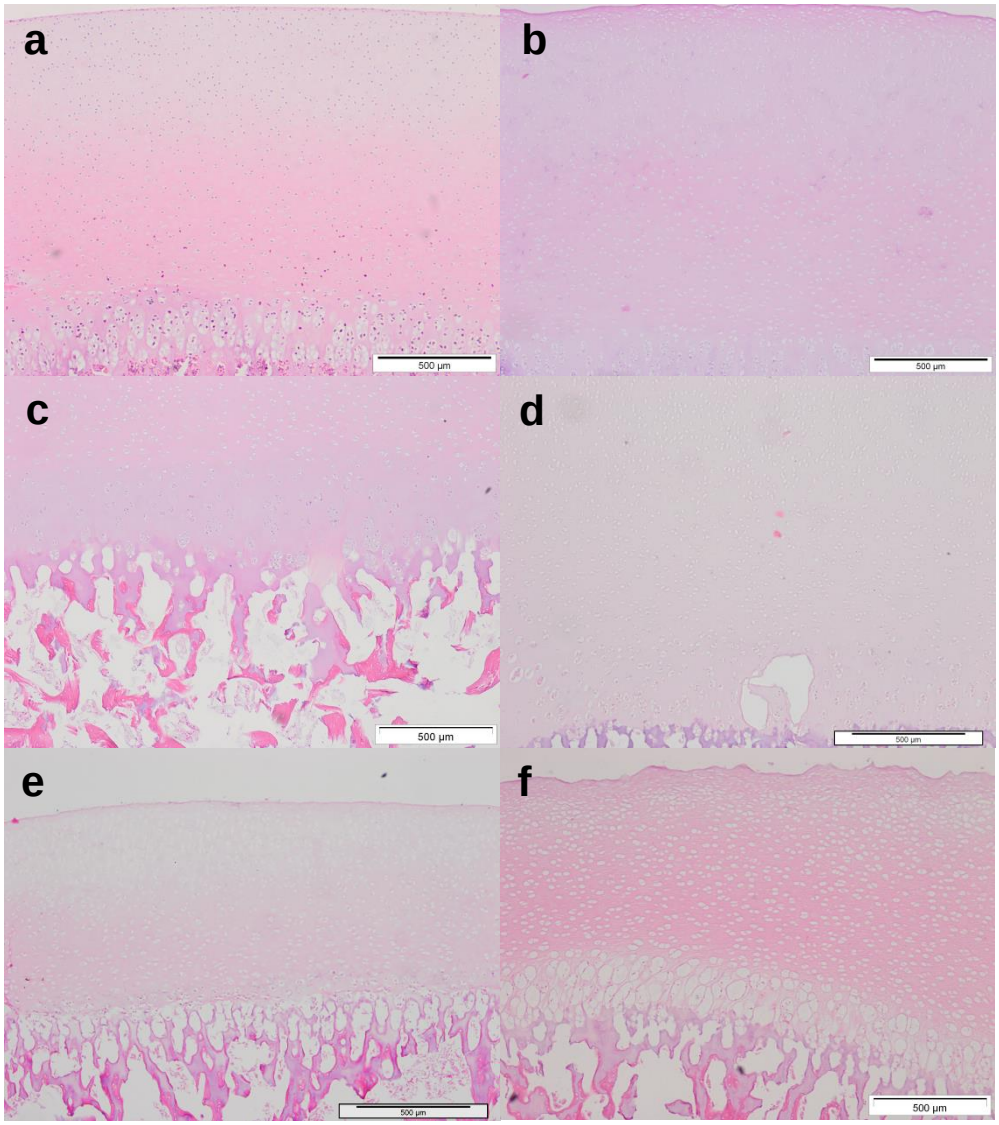

Figure 5.2 H&E stained sections of native and decellularised osteochondral pins. a) native, b) dCELL 1, c) dCELL 3, d) dCELL 3 (0.05 % SDS), e) dCELL3 (6 h SDS) and f) dCELL 3 (0.0 % SDS). Scale bar = 500 µm.

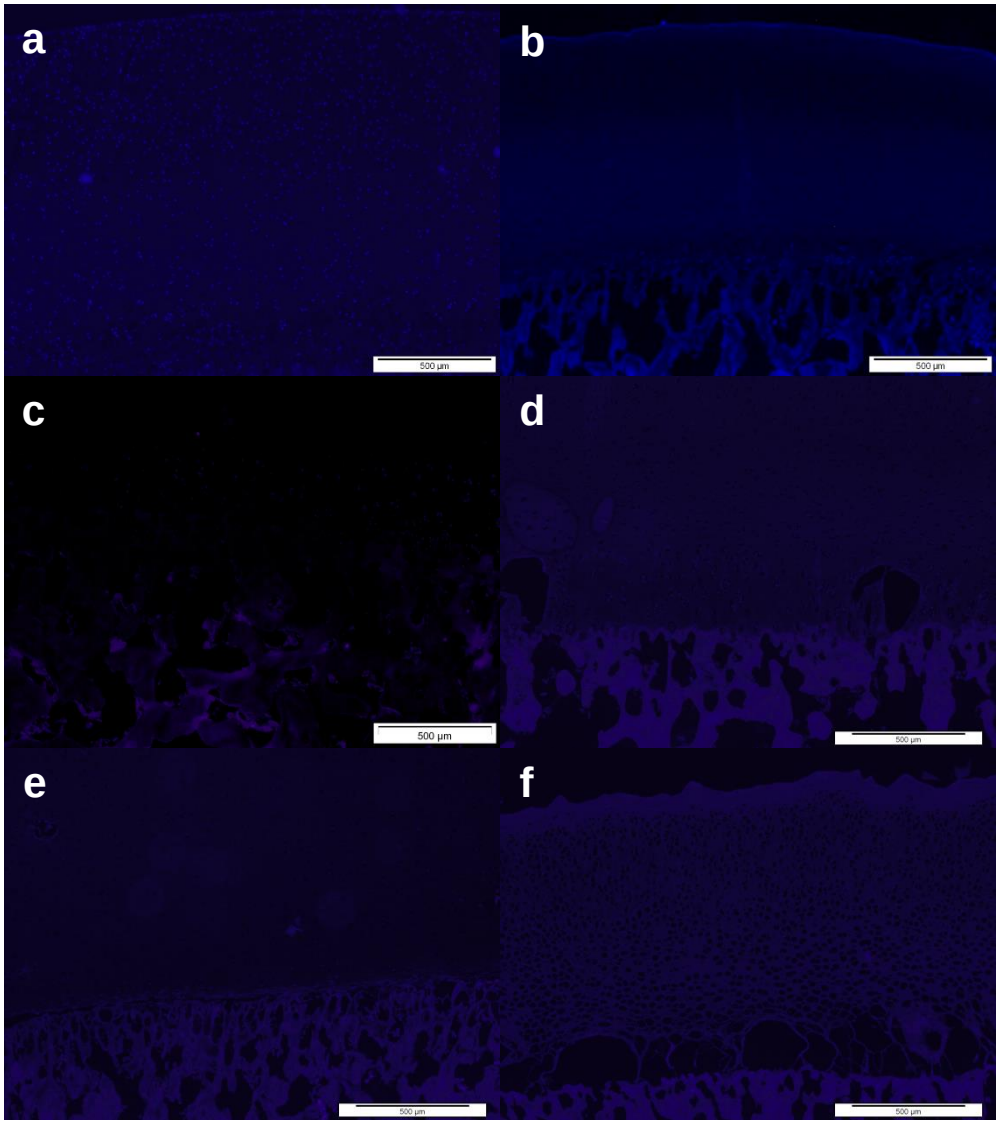

Figure 5.3 DAPI stained sections of native and decellularised osteochondral pins. a) native, b) dCELL 1, c) dCELL 3, d) dCELL 3 (0.05 % SDS), e) dCELL3 (6 h SDS) and f) dCELL 3 (0.0 % SDS). Scale bar = 500 µm.

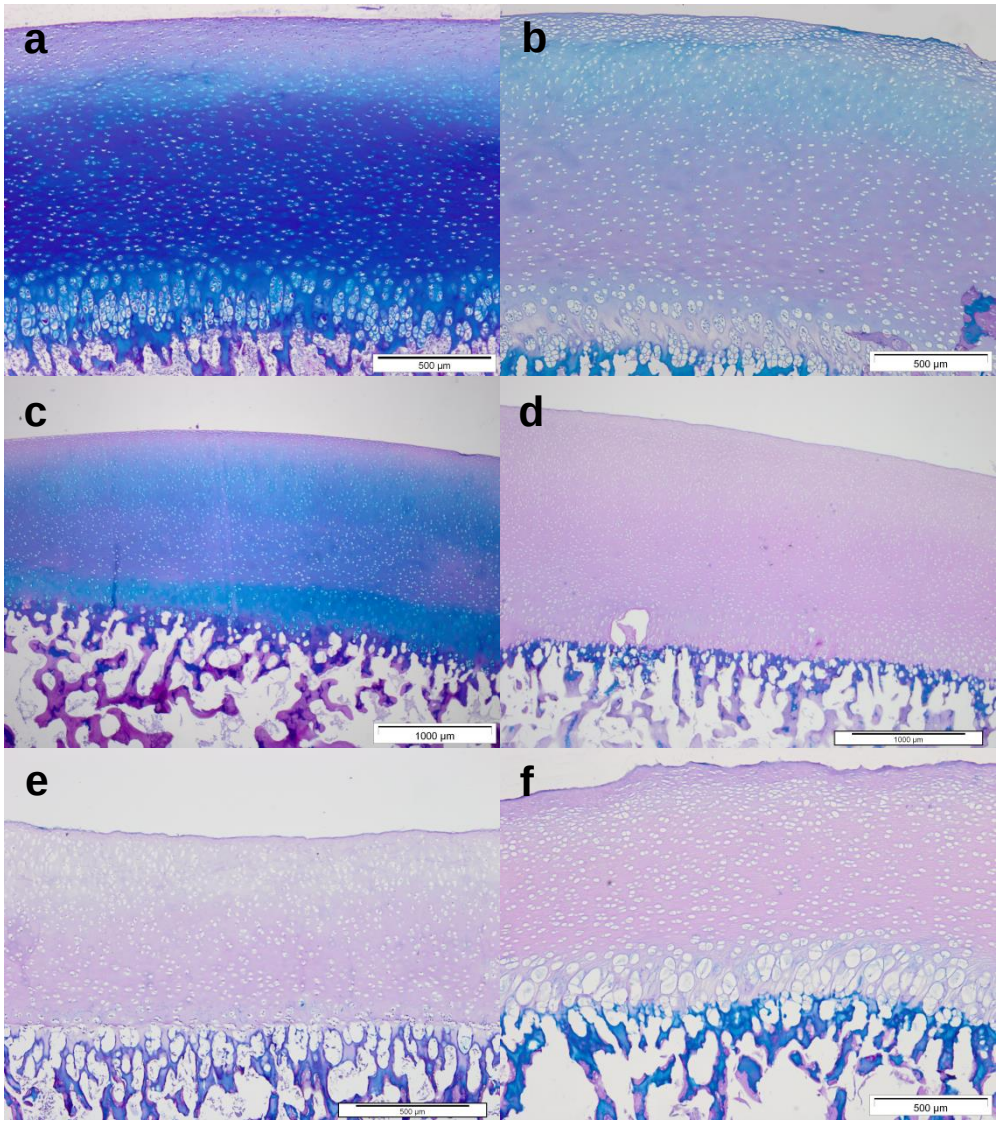

Figure 5.4 Alcian blue/PAS stained sections of native and decellularised osteochondral pins. a) native, b) dCELL 1, c) dCELL 3, d) dCELL 3 (0.05 % SDS), e) dCELL3 (6 h SDS) and f) dCELL 3 (0.0 % SDS). a, b, e and f scale bar = 500 µm, c and d scale bar = 1000 µm.

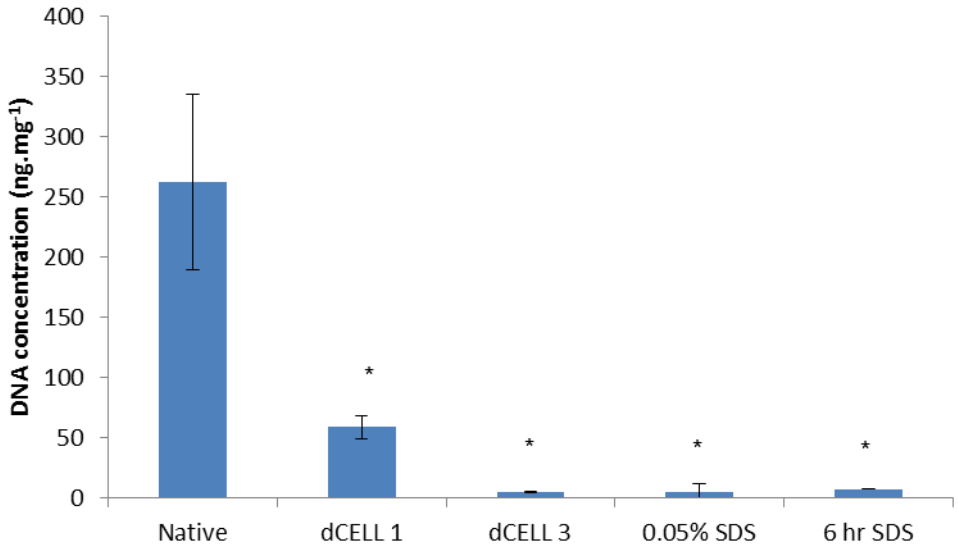

Figure 5.5 Cartilage DNA content. Data is shown as the mean (native and dCELL1 n=5, others n=3) ± 95% confidence limits. * significantly different to native ($p<0.05$ ANOVA).

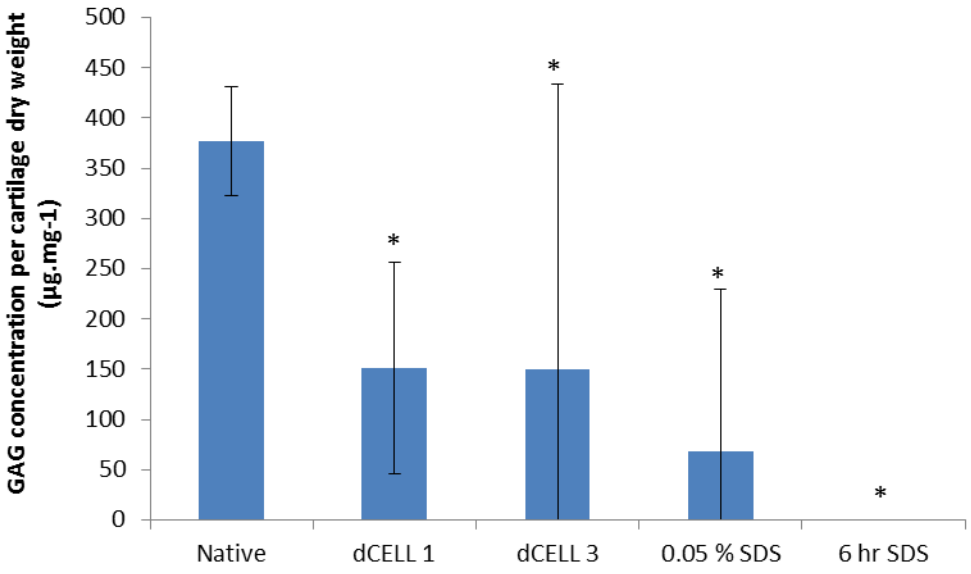

Figure 5.6 Cartilage GAG content. Data is shown as the mean (native and dCELL 1 n=5, others n=3) ± 95% confidence limits. * significantly different to native ($p<0.05$ ANOVA).

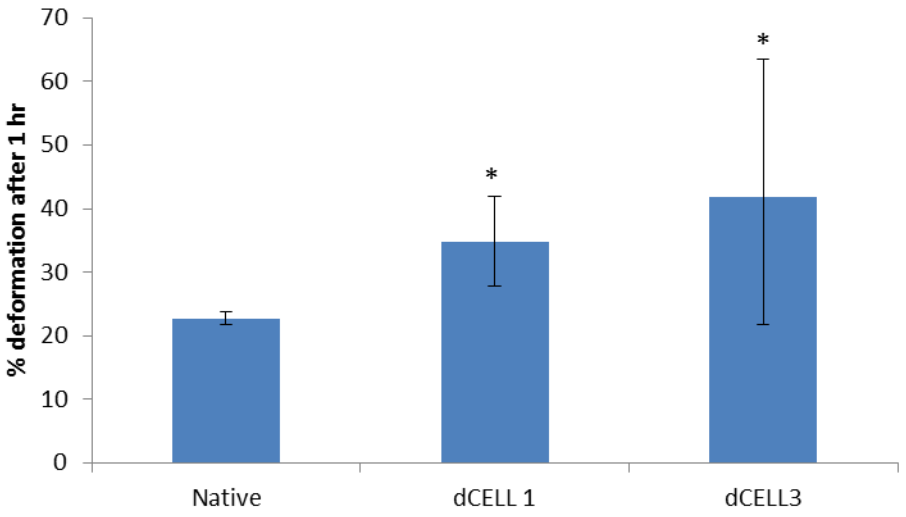

Figure 5.7 Percent deformation of cartilage. Data was subject to arcsin transformation prior to calculation of the 95% confidence limits and analysis of variance. Data is shown as the back transformed mean (native n=6, dCELL 1 and 3 n=3) ± 95% confidence limits. * significantly different to native ($p<0.05$ ANOVA).

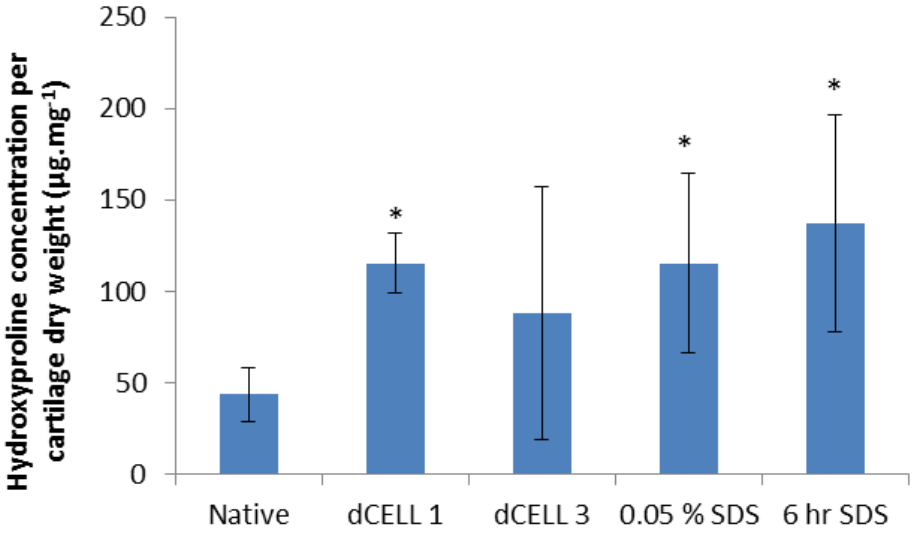

Figure 5.8 Cartilage hydroxyproline content. Data is shown as the mean (native and dCELL 1 n=5, others n=3) ± 95% confidence limits. * significantly different to native ($p<0.05$ ANOVA).

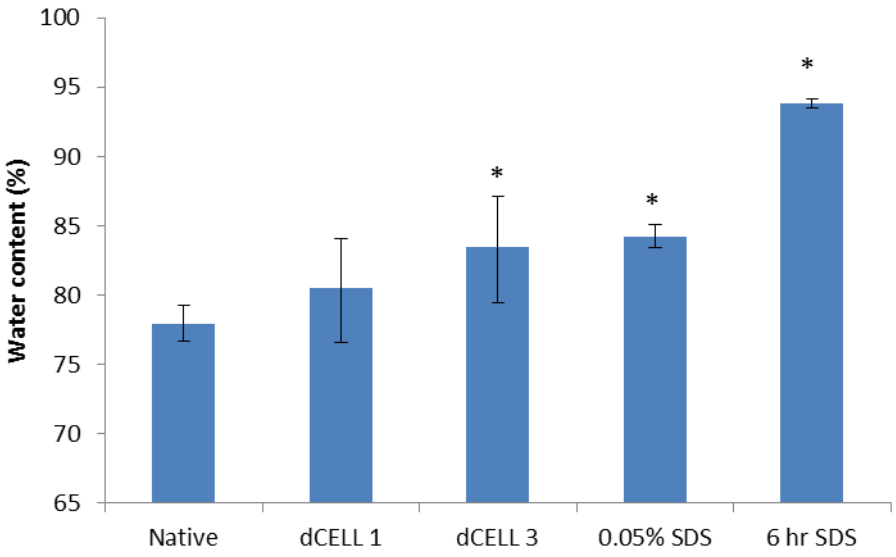

Figure 5.9 Cartilage water content. Data was subject to arcsin transformation prior to calculation of the 95% confidence limits and analysis of variance. Data is shown as the back transformed mean (native and dCELL 1 n=5, others n=3) ± 95% confidence limits. * significantly different to native ($p<0.05$ ANOVA).

5.4.2 Cartilage damage characterisation

5.4.2.1 Histological analysis

Cartilage which was damaged following application of the dCELL 3 (0.0% SDS) protocol was analysed histologically to identify changes to the general structure. H&E stained sections (Figure 5.2 f) showed that the cartilage surface was much rougher than native cartilage, no cell nuclei were visible, and lacunae appeared enlarged. The cartilage also appeared to be generally thinner. The bone appeared histologically normal. Use of alcian blue (Figure 5.4 f) and safranin O staining of cartilage sections (Figure 5.10 a & b) showed a severe loss of GAGs. There was no safranin O staining visible in the damaged cartilage and PAS staining was present throughout all layers of the cartilage in the damaged samples. Staining of sections with van Geison (Figure 5.10 c & d) and Sirius red (Figure 5.10 e & f) was performed to visualise collagen fibres within the cartilage ECM. Both stains showed a clumping of the collagen fibres into a more mesh-like network in the damaged samples as opposed to the evenly dispersed collagen seen in the native tissues. The attachment of cartilage to the underlying bone in the

damaged samples also appeared to be less secure, with long threads of collagen sparsely attaching to the underlying bone.

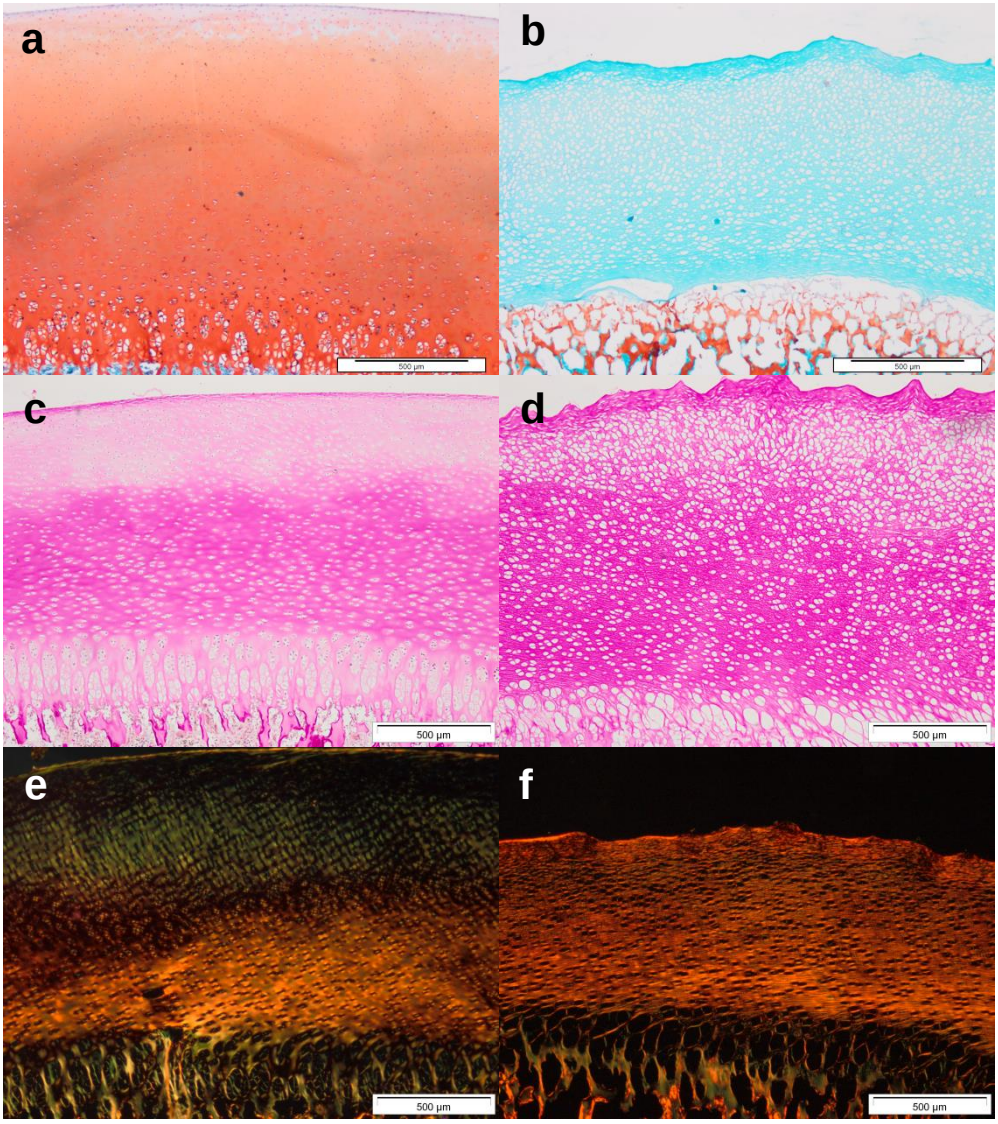

Figure 5.10 Histological characterisation of cartilage damage following application of the dCELL 3 (0.0 % SDS) protocol. Safranin O/Fast green stained sections of a) native and b) damaged cartilage, van Gieson stained sections of c) native and d) damaged cartilage, Sirus red/Millers elastin stained sections of e) native and f) damaged cartilage. Scale bar = 500 µm.

5.4.2.2 Denatured collagen quantification

To determine whether collagen fibres were being denatured during the decellularisation processes, samples of native and treated cartilage (dCELL 3, 0.0 % SDS) were digested with α-chymotrypsin which can only cleave denatured collagen. The digest was hydrolysed and the hydroxyproline

content quantified to determine the amount of denatured collagen in the tissues. There was no significant difference between the levels of denatured collagen in cartilage subject to the dCELL 3 (0.0 % SDS) protocol compared to native tissue (Figure 5.11).

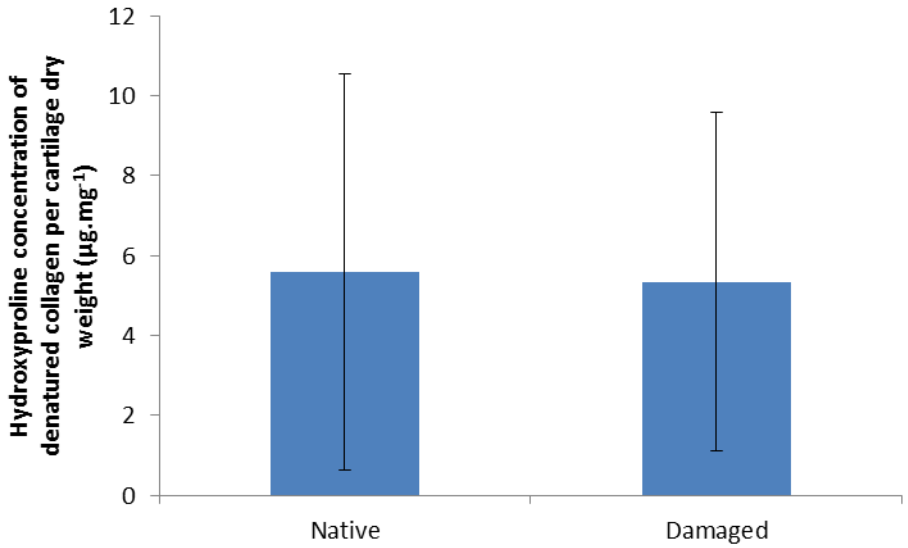

Figure 5.11 Denatured collagen content of native and damaged cartilage (dCELL 3, 0.0% SDS). Data is shown as the mean (n=3) ± 95% confidence limits. * significantly different to native ($p<0.05$ ANOVA).

5.4.3 Investigation into cartilage damage

To determine the cause of the cartilage damage which was occurring during decellularisation, key steps in the process were changed or omitted systematically to determine their effect on cartilage stability.

5.4.3.1 Analysis of incubation temperature

To better understand the temperature changes during the decellularisation process and how temperature could affect cartilage stability, the temperature of all solutions and incubators was measured when set to 45 °C which was used as standard and at a lower temperature of 40 °C. The incubator and solution temperatures recorded during dCELL 3 (6 h 0.1 % SDS) process are shown in Figure 5.12. The highest solution temperature reached during incubation at 40 °C was 43 °C, whereas solutions incubated at 45 °C

reached temperatures of 47.5 °C during the extended PBS end wash. At the end of the decellularisation process the cartilage was still attached to all pins decellularised at 40 °C, however the cartilage on the pins decellularised at 45 °C had all become detached and had begun to completely dissolve in solution. All subsequent decellularisation processes were performed at 42 °C to minimise any detrimental effects of high temperature on the cartilage structure.

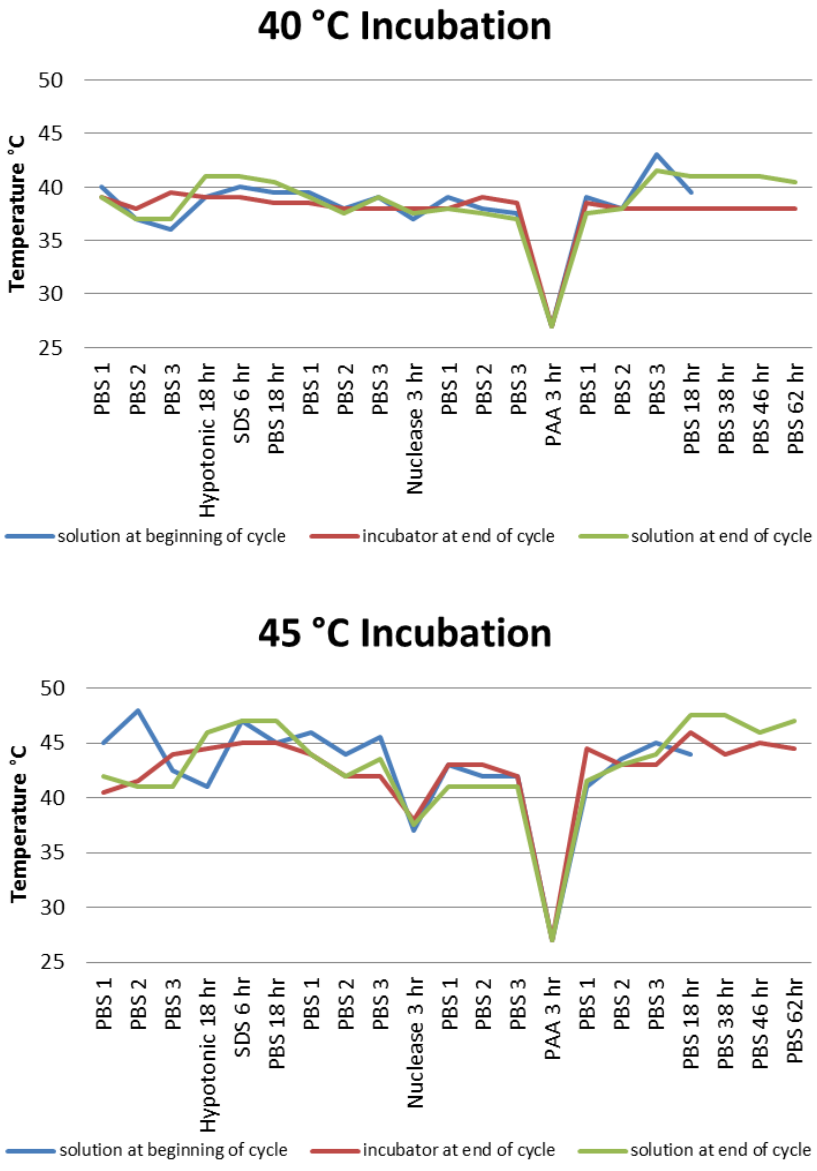

Figure 5.12 Incubator and solution temperatures during decellularisation. The solution temperature before and after incubation (n=1) and the incubator temperature at the end of each incubation are shown for incubators set at 40 °C and 45°C.

5.4.3.2 Systematic removal of key steps of the decellularisation process

Key stages of the decellularisation process were removed to identify how the level of cartilage damage was affected by the presence/absence of that step, as described in Section 5.3.4.2. Histological assessment of tissues following these varied decellularisation procedures are shown in Figure 5.13. 5.14 and 5.15.

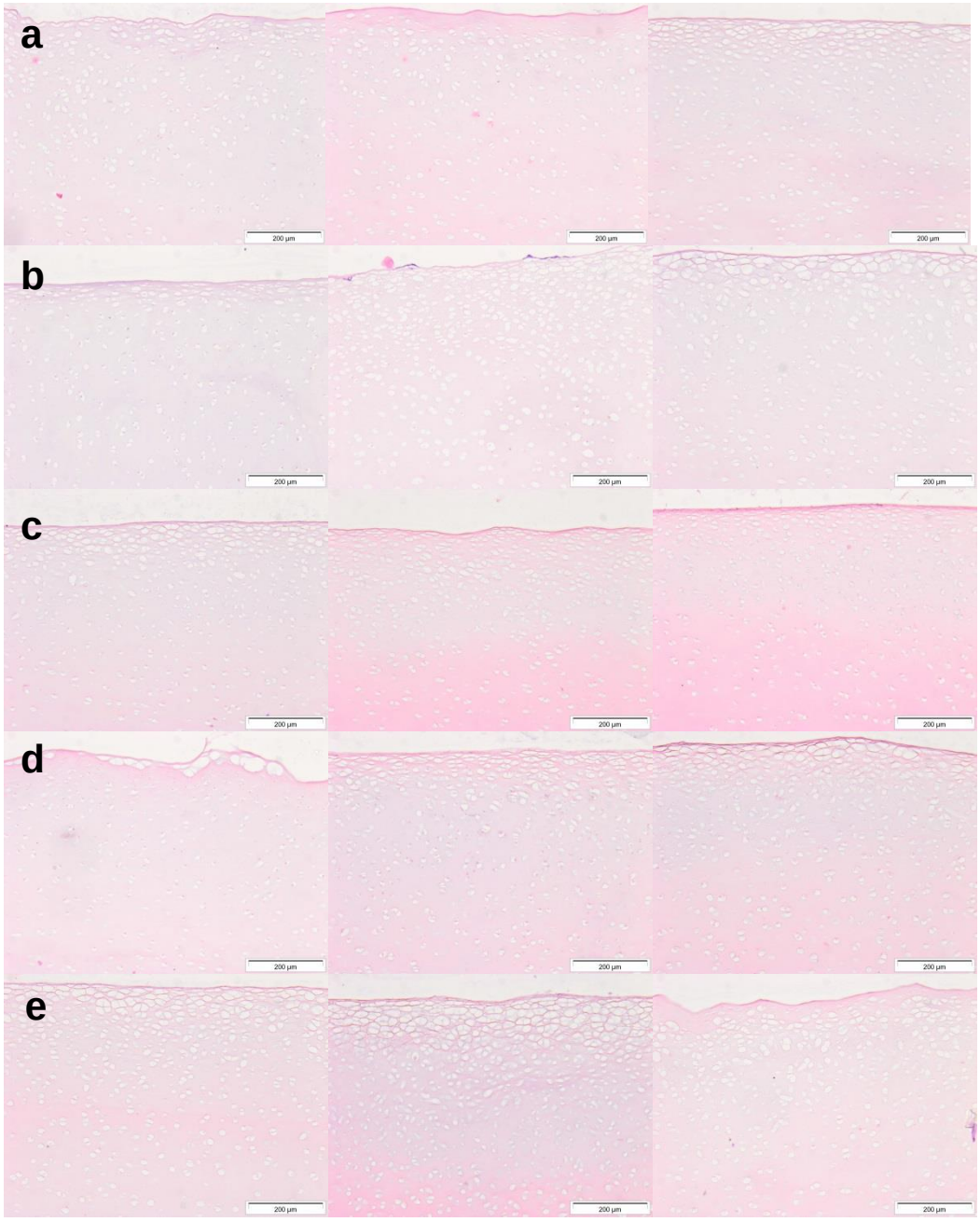

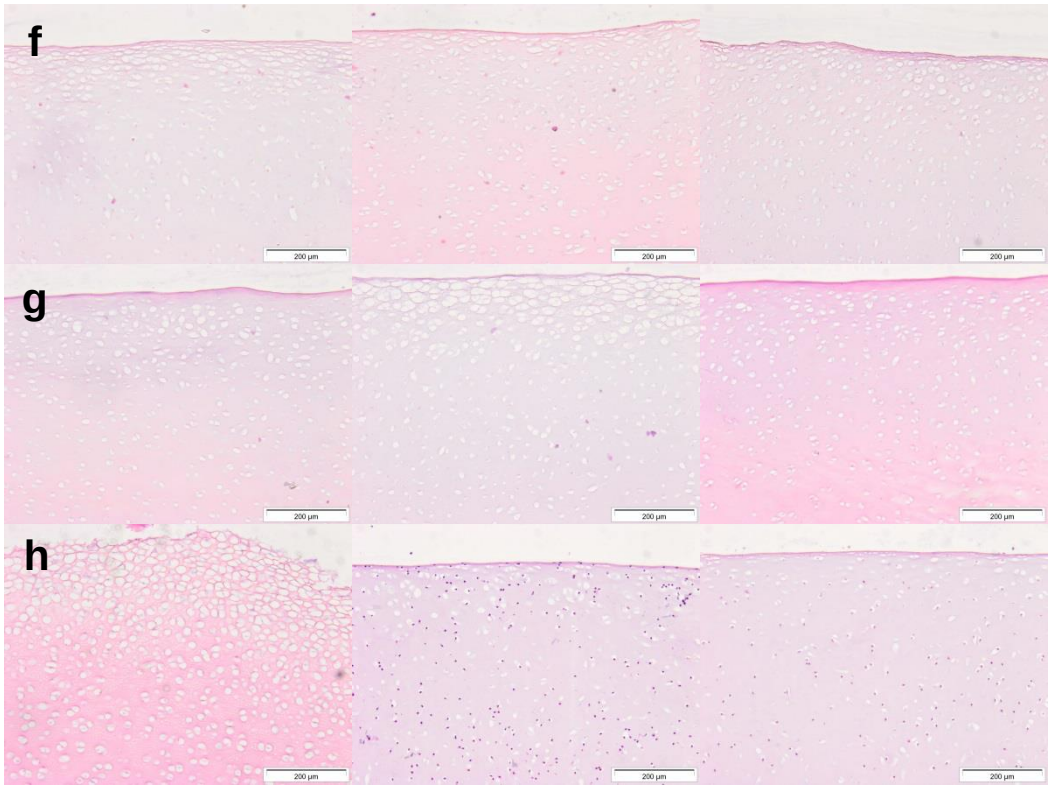

Figure 5.13 H&E stained sections (n=3) of cartilage following decellularisation following protocols with steps systematically removed. Panel a) complete decellularisation dCELL 3 process (positive control), b) dCELL 3 process with the dry freeze/thaw cycle (-20 °C) omitted, c) dCELL 3 process with the all four freeze/thaw cycles omitted, d) dCELL 3 process with the hypotonic wash omitted, e) dCELL 3 process with the SDS wash omitted, f) dCELL 3 process with the PAA sterilisation step omitted, g) dCELL 3 process with the extended PBS end wash omitted, h) PBS only (negative control). Scale bar = 200 µm.

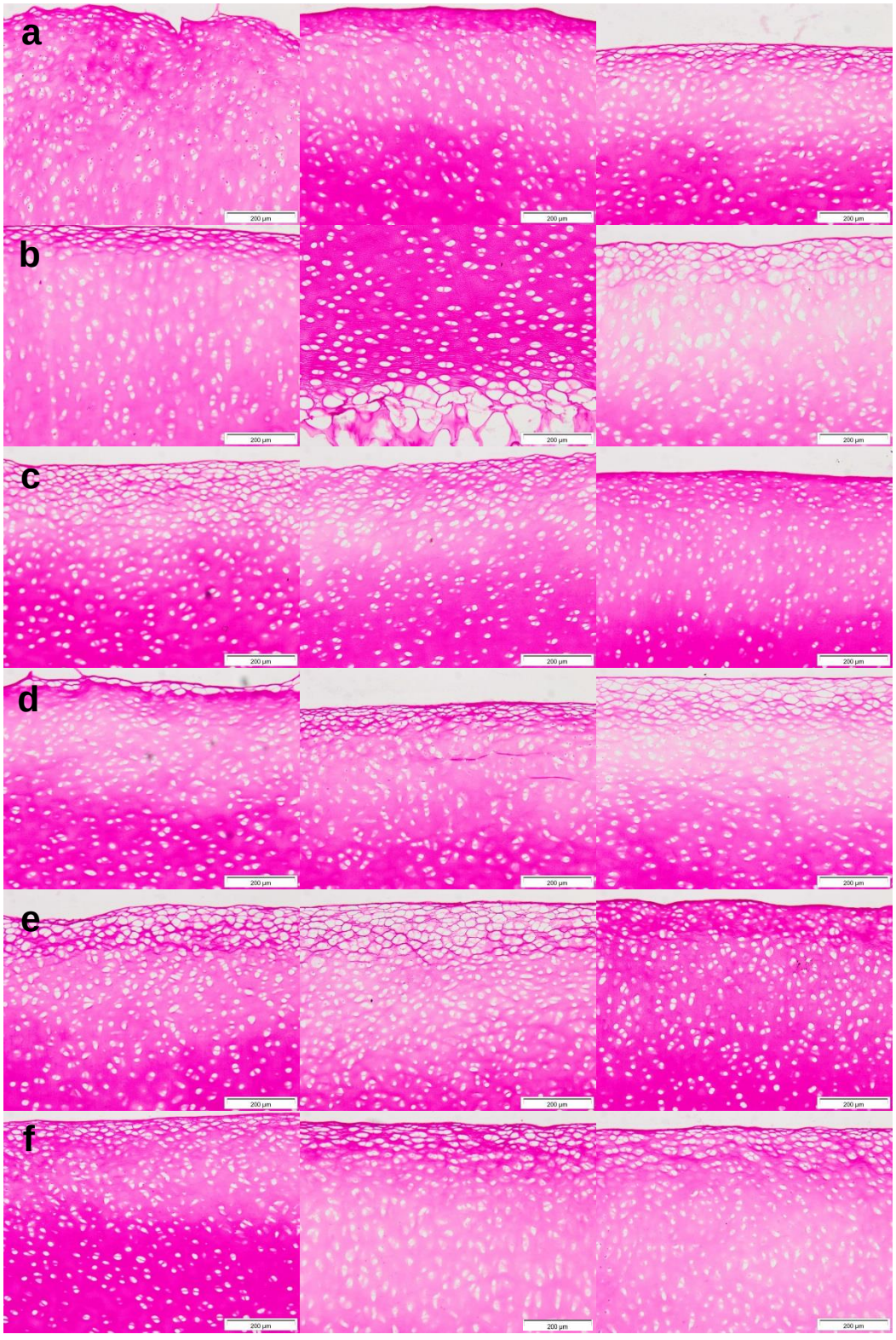
a
b
c
d
e
f

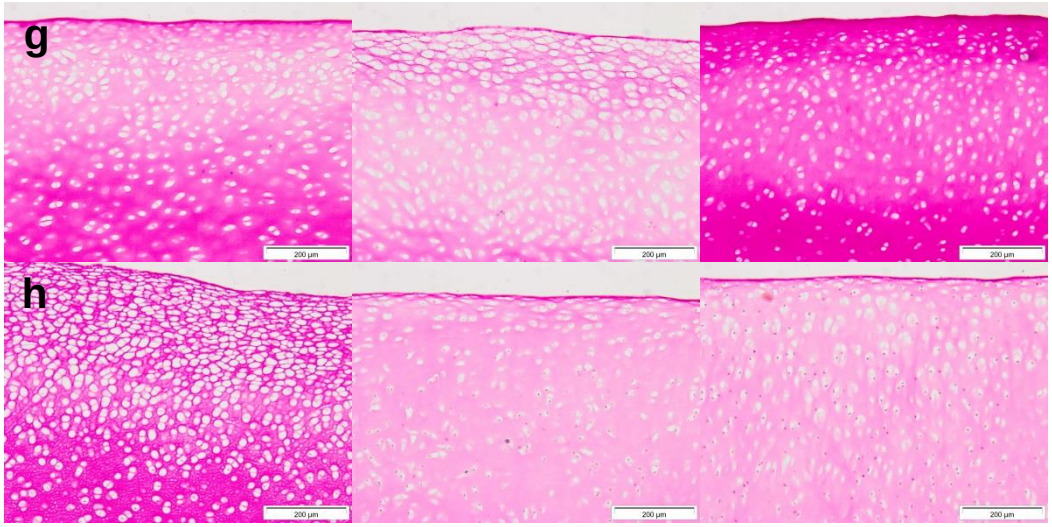

Figure 5.14 van Gieson stained sections (n=3) of cartilage following decellularisation following protocols with steps systematically removed. Panel a) complete decellularisation dCELL 3 process (positive control), b) dCELL 3 process with the dry freeze/thaw cycle (-20 °C) omitted, c) dCELL 3 process with the all four freeze/thaw cycles omitted, d) dCELL 3 process with the hypotonic wash omitted, e) dCELL 3 process with the SDS wash omitted, f) dCELL 3 process with the PAA sterilisation step omitted, g) dCELL 3 process with the extended PBS end wash omitted, h) PBS only (negative control). Scale bar = 200 µm.

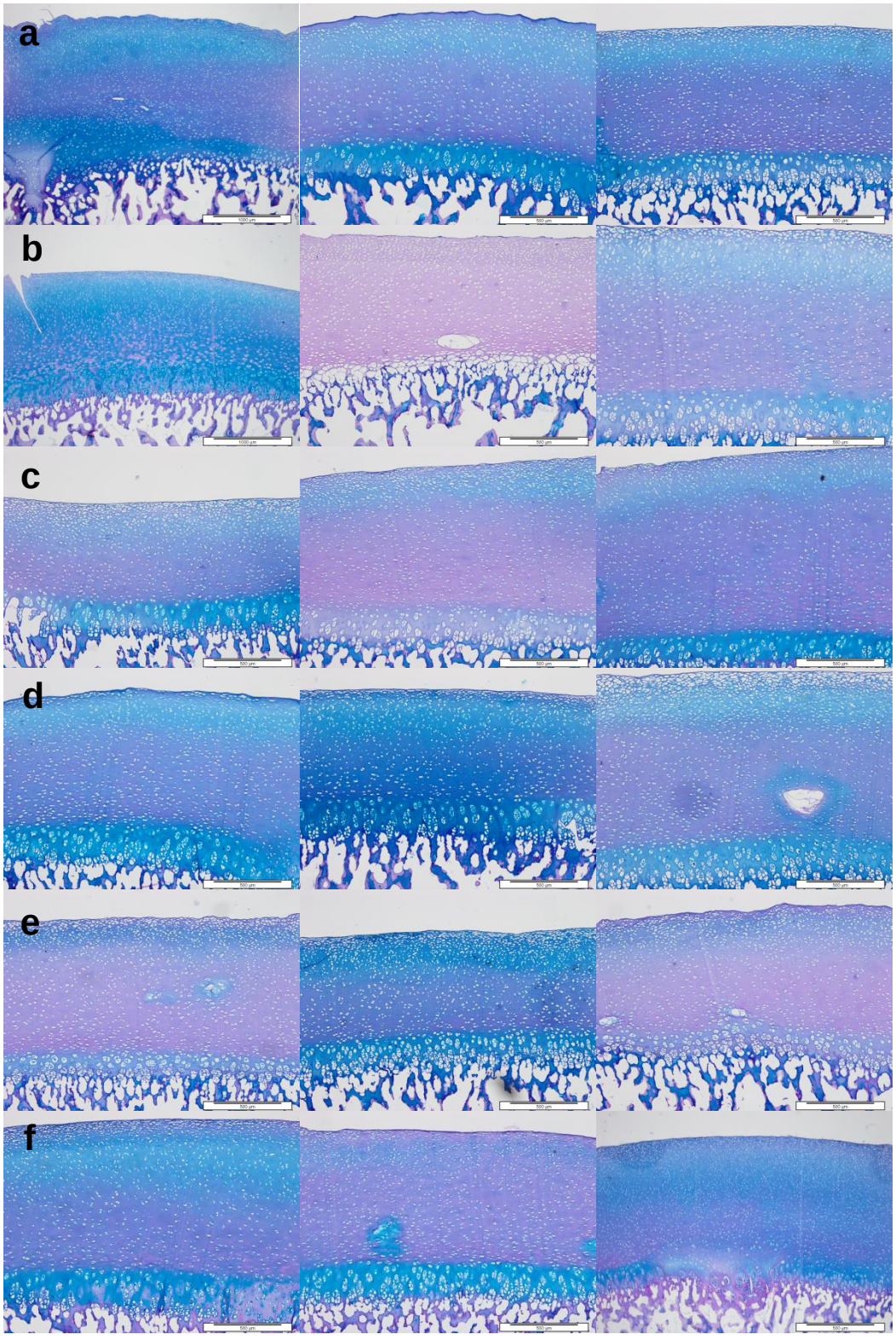
a
b
c
d
e
f

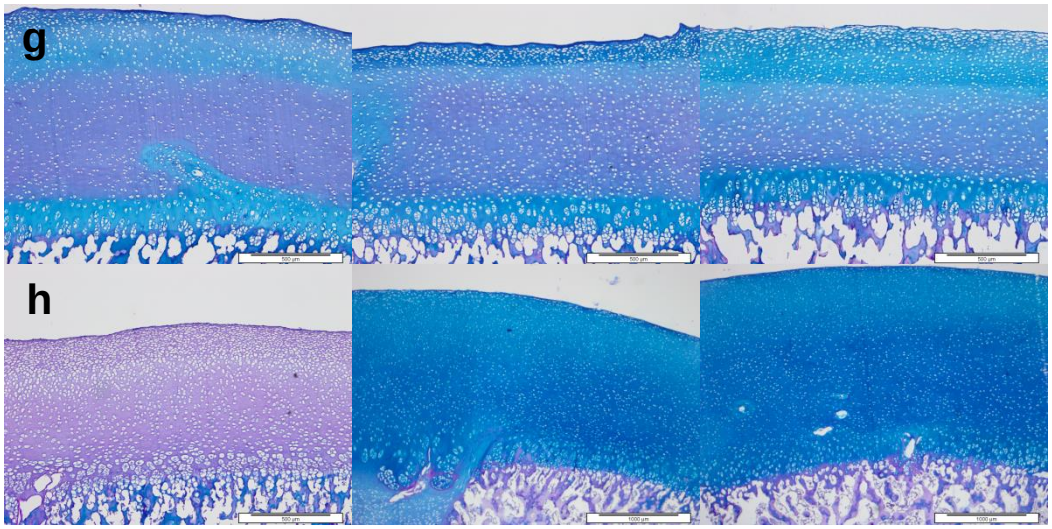

Figure 5.15 Alcian blue stained sections (n=3) of cartilage following decellularisation following protocols with steps systematically removed. Panel a) complete decellularisation dCELL 3 process (positive control), b) dCELL 3 process with the dry freeze/thaw cycle (-20 °C) omitted, c) dCELL 3 process with the all four freeze/thaw cycles omitted, d) dCELL 3 process with the hypotonic wash omitted, e) dCELL 3 process with the SDS wash omitted, f) dCELL 3 process with the PAA sterilisation step omitted, g) dCELL 3 process with the extended PBS end wash omitted, h) PBS only (negative control). Scale bar = 200 µm.

All tissues showed signs of damage, having much larger lacunae than native tissue and showing a rougher cartilage surface. Clumping of the collagen network could be seen at the cartilage surface on most pins. Surprisingly, however, even the PBS negative control also showed cartilage damage.

5.4.3.3 Matrix metalloproteinase inhibition

Since incubation in PBS alone for 5 days at 42 °C resulted in damage to the cartilage, EDTA was added to the PBS plus aprotinin in order to inhibit the activity of matrix metalloproteinases which may have been actively degrading the cartilage ECM. H&E, van Gieson and alcian blue stained sections of pins incubated in PBS with aprotinin and EDTA are shown in Figure 5.16, and pins incubated in just PBS plus aprotinin (as a positive control) can be seen in Figure 5.17.

Damage to cartilage was minimal in both sets, enlarged lacunae and roughened cartilage surface seen previously were less evident in these images, even in the PBS only positive control.

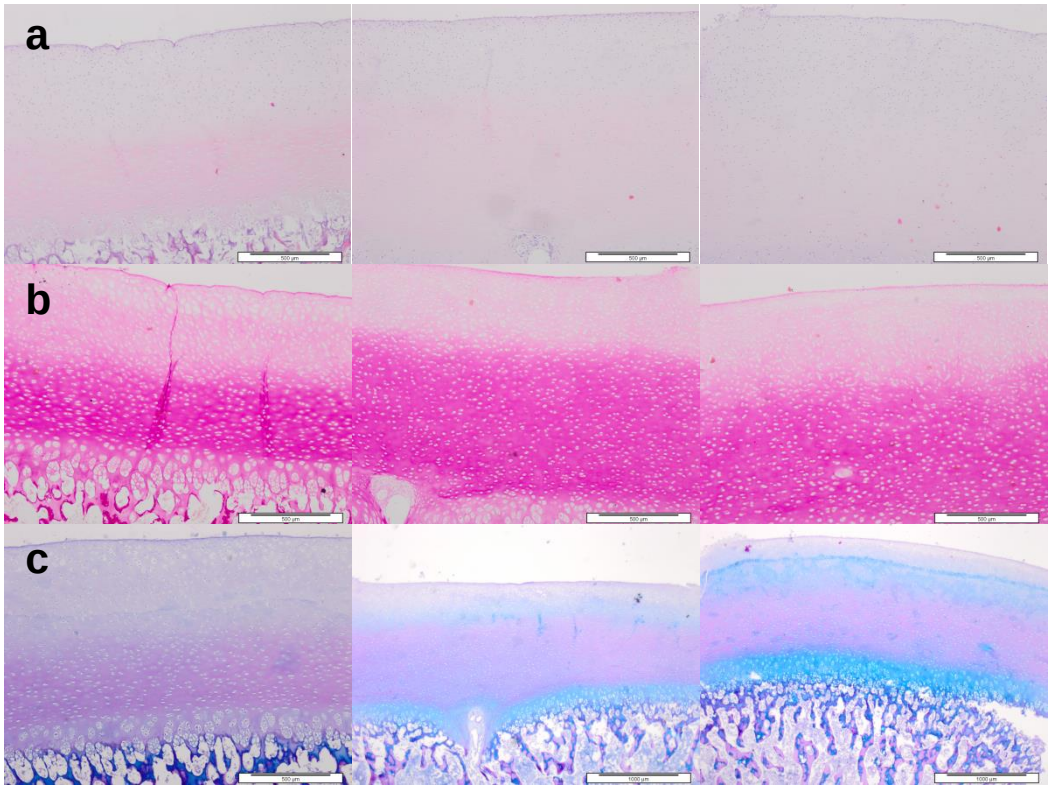

Figure 5.16 Osteochondral pins incubated in PBS with EDTA plus aprotinin for 5 days at 42 °C. Panel a) H&E stained tissue sections, scale bar = 500 µm, b) van Gieson stained tissue sections, scale bar = 500 µm, and panel c) alcian blue stained tissue sections, scale bar = 1000 µm.

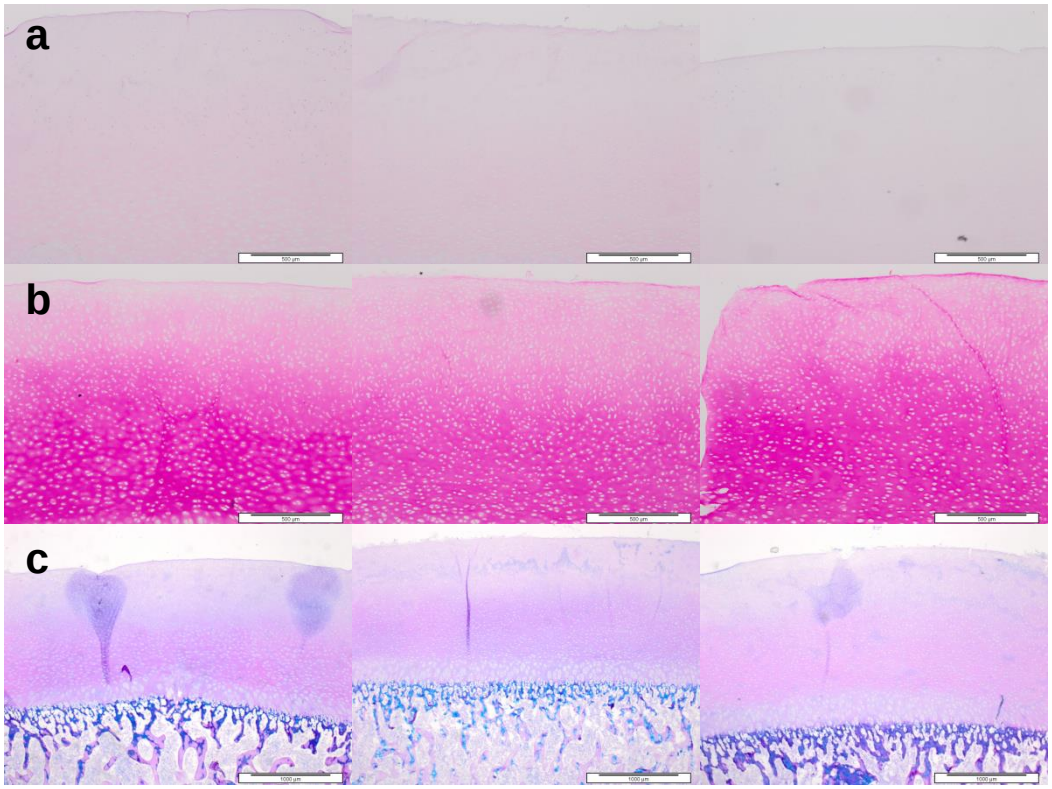

Figure 5.17 Osteochondral pins incubated in PBS plus aprotinin only for 5 days at 42 °C. Panel a) H&E stained tissue sections, scale bar = 500 µm, b) van Gieson stained tissue sections, scale bar = 500 µm, and panel c) alcian blue stained tissue sections, scale bar = 1000 µm.

5.4.3.4 Analysis of solution tonicity

5.4.3.4.1 Osmolality measurements

The osmolality of synovial fluid obtained from porcine knee joints was measured to determine whether PBS was at the correct tonicity for cartilage, as although it is isotonic to the cells, it may not be isotonic to cartilage ECM.

The osmolality of porcine synovial fluid was found to be 329 ± 59 mOsmol.Kg^{-1} and ranged between 302 - 344 mOsmol.Kg^{-1} (Figure 5.18). PBS had a lower osmolality than synovial fluid, but not significantly so. Mannitol was added to PBS at to different concentrations, 1 % (w/v) mannitol in PBS resulted in a solution with an osmolality of 352 ± 6 mOsmol.Kg^{-1}, and 2 % (w/v) mannitol in PBS had significantly higher osmolality than that of synovial fluid at 401 ± 5 mOsmol.Kg^{-1}.

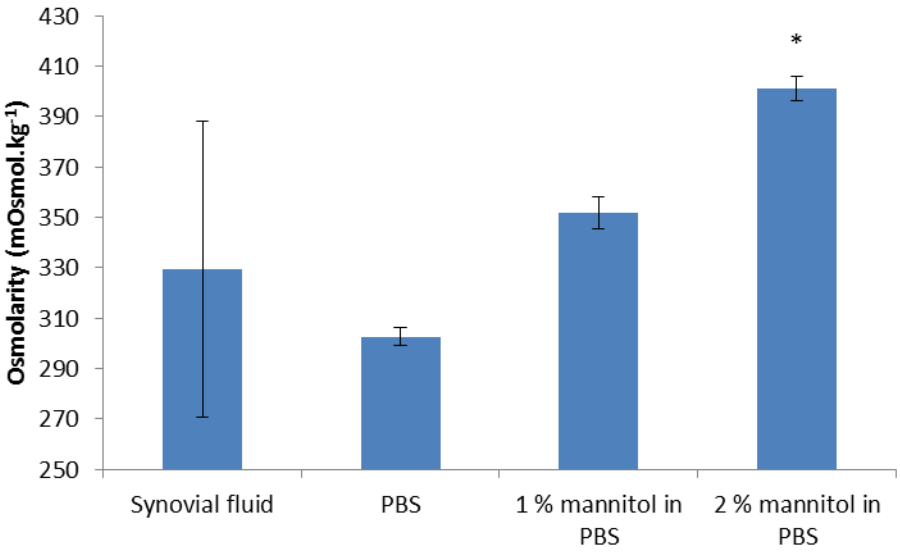

Figure 5.18 Osmolality of porcine synovial fluid, PBS and PBS with mannitol. . Data is shown as the mean (n=3) ± 95% confidence limits. * significantly different to synovial fluid ($p<0.05$ ANOVA).

5.4.3.4.2 Incubation in PBS with mannitol

After incubating osteochondral pins in PBS with 1 % (w/v) and 2 % (w/v) mannitol for 5 days at 42 °C, pins were assessed histologically (Figure 5.19 & 5.20). As previously observed (Section 5.4.3.3), there was no major damage visible. It was hypothesised that in the absence of agents such as SDS to remove the cells, the process was less harsh and occurrence of damage more variable. It was therefore decided to test the hypertonic wash solutions in the complete decellularisation process.

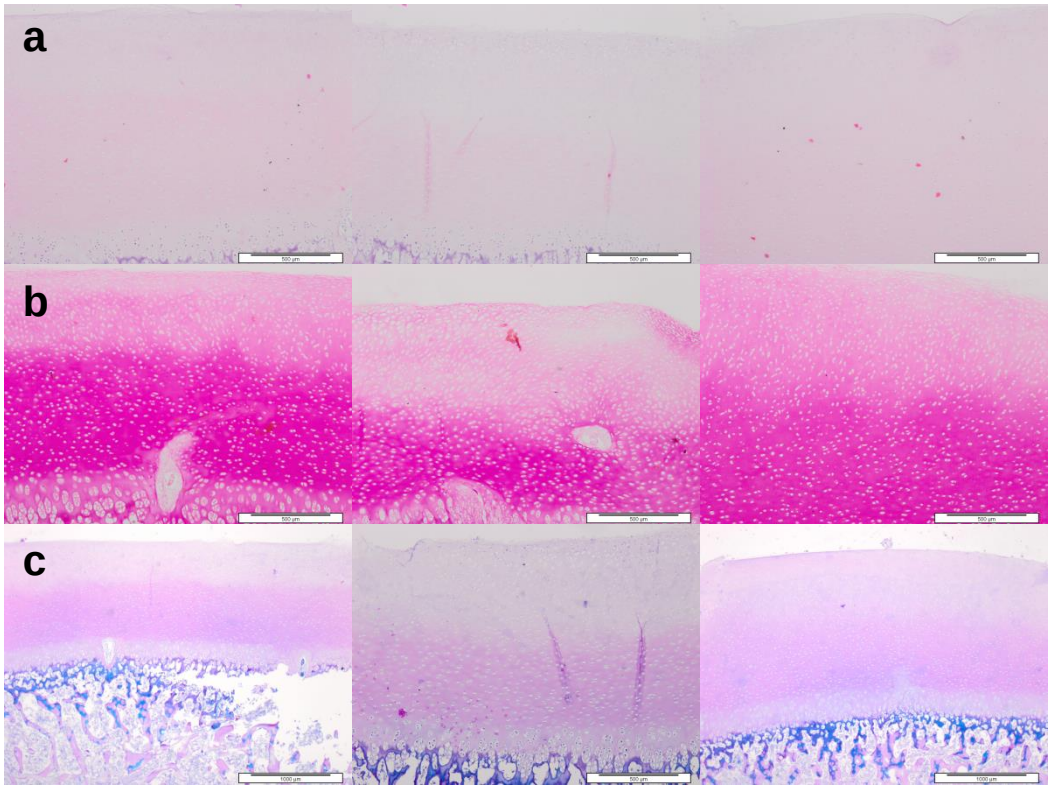

Figure 5.19 Osteochondral pins incubated in 1 % (w/v) mannitol in PBS for 5 days at 42 °C. Panel a) H&E stained tissue sections, scale bar = 500 µm, b) van Gieson stained tissue sections, scale bar = 500 µm, and panel c) alcian blue stained tissue sections, scale bar = 1000 µm.

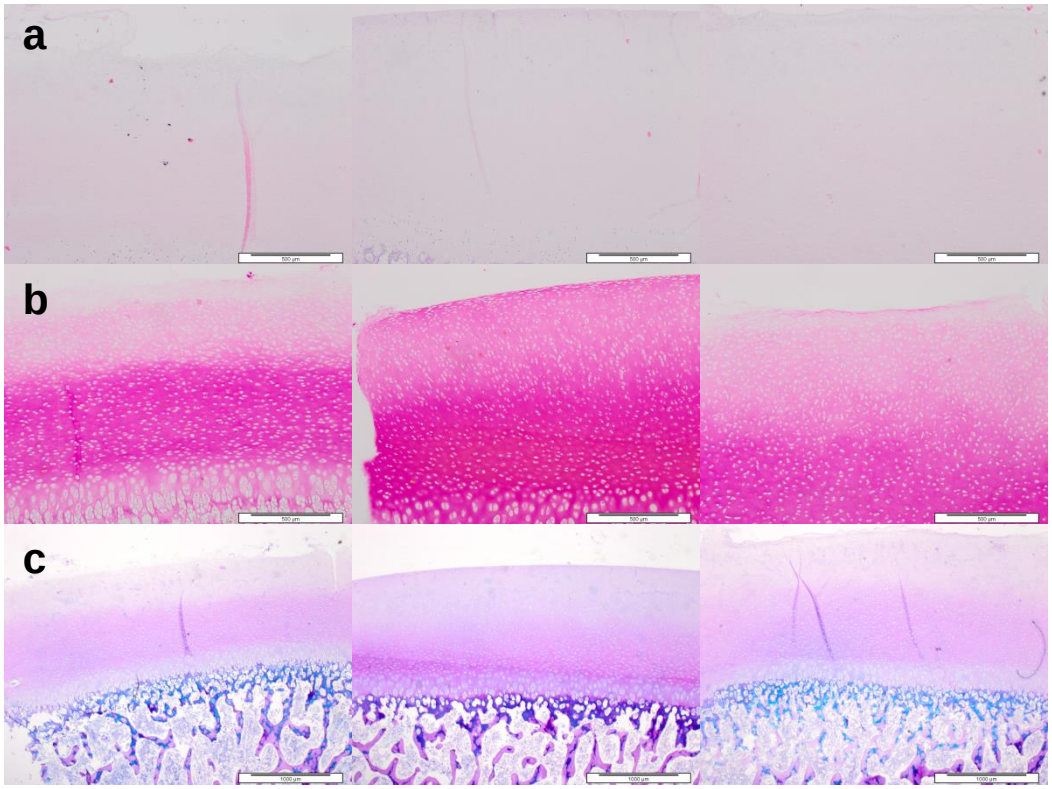

Figure 5.20 Osteochondral pins incubated in 2 % (w/v)mannitol in PBS for 5 days at 42 °C. Panel a) H&E stained tissue sections, scale bar = 500 µm, b) van Gieson stained tissue sections, scale bar = 500 µm, and panel c) alcian blue stained tissue sections, scale bar = 1000 µm.

5.4.3.4.3 Decellularisation of pins using PBS with mannitol

By not incorporating decellularisation steps, the cells remained in the cartilage when washed with PBS alone for five days at 42 °C and the cells may have acted to stabilise the tissue and not allow cartilage damage as seen in Section 5.4.3.4.2. The hypertonic mannitol in PBS solutions were therefore tested in place of standard PBS washes in a decellularisation protocol so that the effect of solution osmolality could be determined.

Histological analysis of pins decellularised using dCELL 3 are shown in Figure 5.21, pins decellularised using dCELL 3 with PBS washes containing 1 % (w/v) and 2 % (w/v) mannitol are shown in Figures 5.22 and 5.23 respectively. All pins showed a severe reduction in GAGs and some signs of damage, including enlarged lacunae, however damage was not as severe as observed previously, and was not improved by the addition of mannitol.

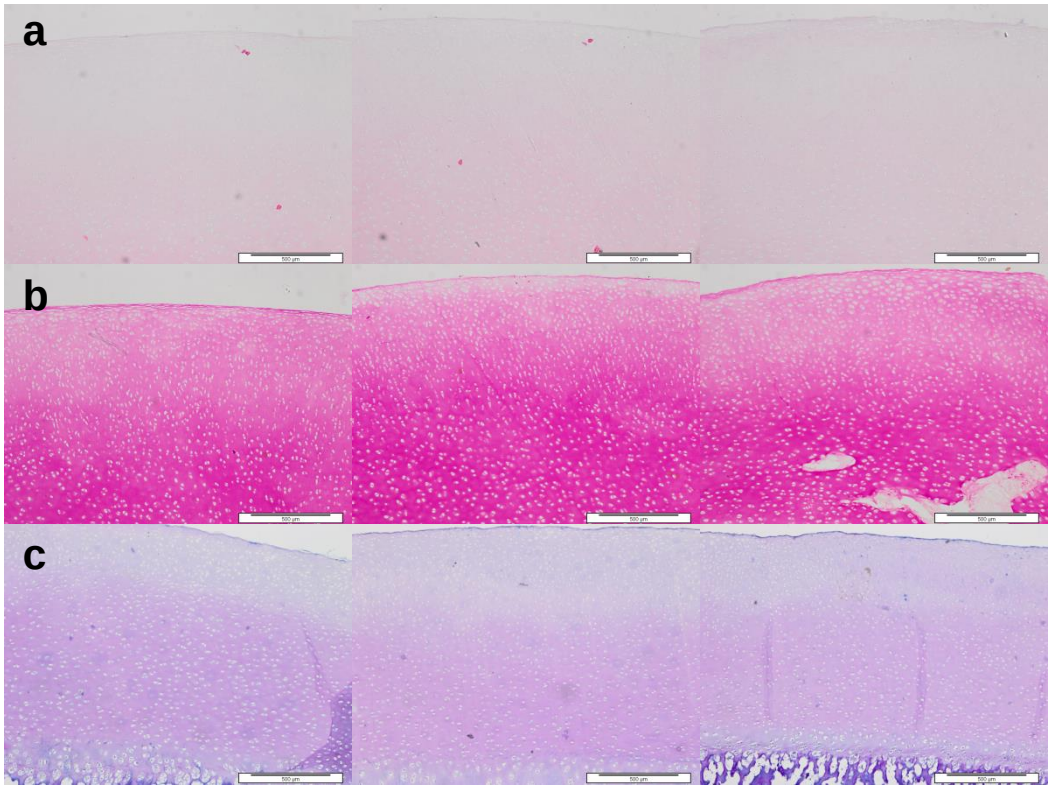

Figure 5.21 Osteochondral pins decellularised with the dCELL 3 protocol at 42 °C. Panel a) H&E stained tissue sections, scale bar = 500 µm, b) van Gieson stained tissue sections, scale bar = 500 µm, and panel c) alcian blue stained tissue sections, scale bar = 1000 µm.

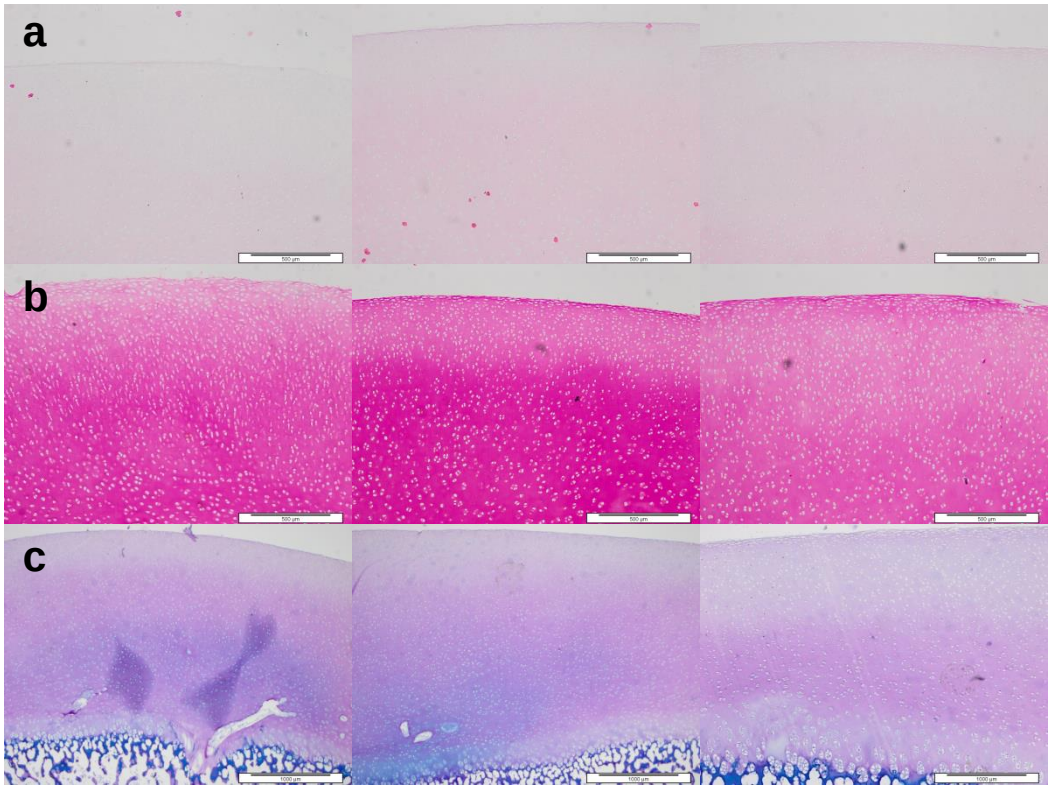

Figure 5.22 Osteochondral pins decellularised with the dCELL 3 protocol using 1 % (w/v) mannitol in PBS at 42 °C. Panel a) H&E stained tissue sections, scale bar = 500 µm, b) van Gieson stained tissue sections, scale bar = 500 µm, and panel c) alcian blue stained tissue sections, scale bar = 1000 µm.

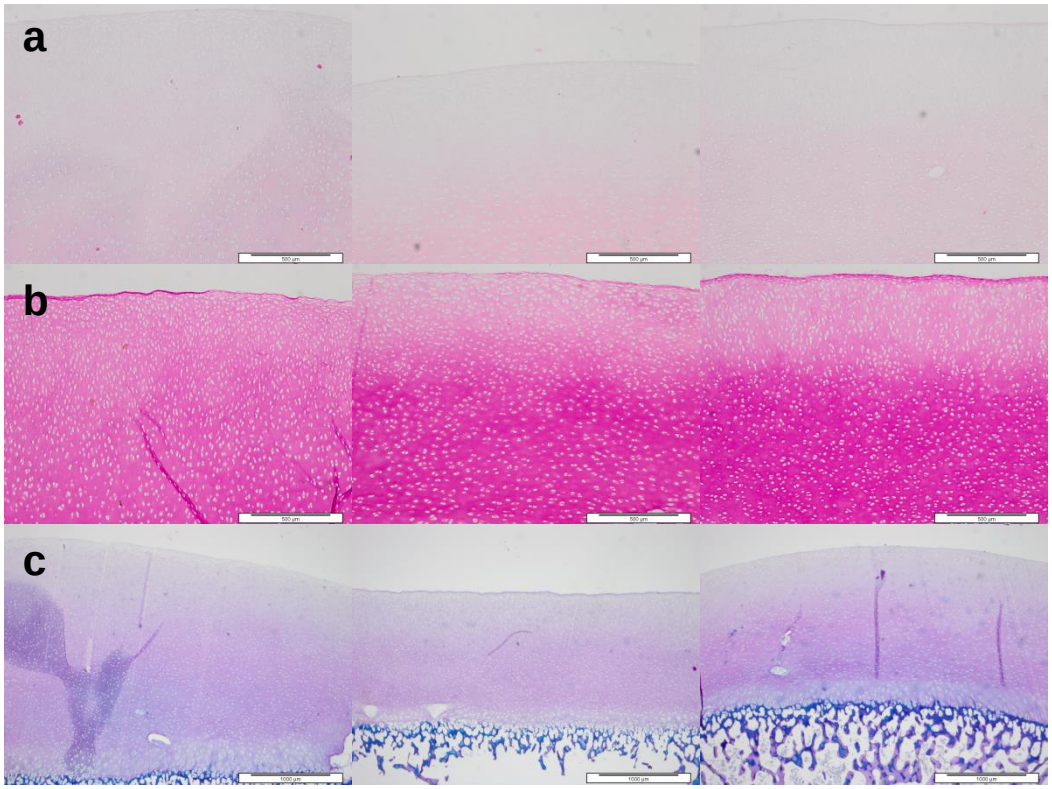

Figure 5.23 Osteochondral pins decellularised with the dCELL 3 protocol using 2 % (w/v) mannitol in PBS at 42 °C. Panel a) H&E stained tissue sections, scale bar = 500 µm, b) van Gieson stained tissue sections, scale bar = 500 µm, and panel c) alcian blue stained tissue sections, scale bar = 1000 µm.

5.4.3.5 Analysis of pig skeletal maturity

Osteochondral pins were taken from skeletally mature pigs (2.4 -3.6 yr) and from immature pigs (3 months). These tissues were analysed by histology in their native form and following decellularisation using the dCELL 3 protocol at 42 °C. H&E stained sections and alcian blue stained sections of native and decellularised mature porcine osteochondral tissues are shown in Figure 5.24 and 5.25 respectively, H&E stained native and decellularised immature porcine osteochondral sections are shown in Figures 5.26 and 5.27, and alcian blue stained sections are shown in Figure 5.28 and 5.29.

Mature cartilage was notably thinner (~ 1.2 mm) than immature cartilage (~ 5.0 mm) and had a lower cell density. The cells of mature cartilage had a much more defined orientation, with linear columns of cells aligning perpendicular to the cartilage-bone interface. The chondrons of immature

cartilage often contained more than one cell, especially in the deep and hypertrophic regions. The subchondral bone plate of mature porcine tissues was well formed, dense and thick, whereas the boundary between cartilage and bone in immature cartilage was much less defined. Trabecular struts of mature bone were much thicker than those of immature bone. Cartilage from immature pigs also appeared to be highly vascularised, vascular tissues could be seen upon dissection and cross sections of vasculature were clearly visible in histological sections, for example Figure 5.28 a and b, where pink PAS stained blood vessels were observed to cross over from bone to cartilage. Vascular tissues have been observed in 6 month old pigs (Figure 5.19 b), however, no vascularisation was present in mature porcine cartilage.

During decellularisation, all osteochondral pins from mature pigs remained intact, cartilage detached from two of the three pins from immature pigs. Upon histological analysis, no damage to the cartilage surface was observed on any of the pins, even those from which the cartilage had detached. Cartilage and bone from immature pigs appeared mostly decellularised, however cells remained in the tissues from mature pigs.

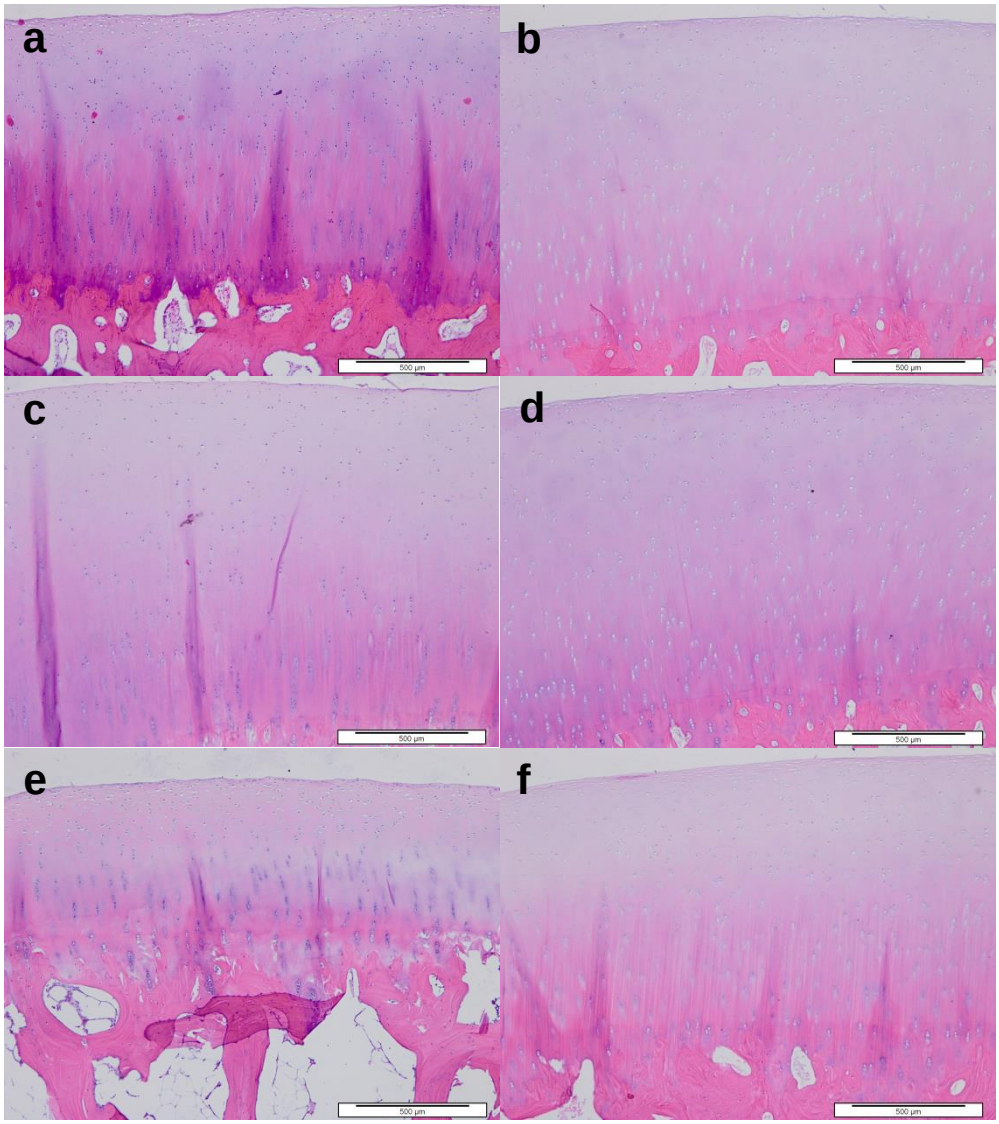

Figure 5.24 H&E stained sections of native and decellularised (dCELL 3 process at 42 °C) mature porcine osteochondral tissues. a) Native (2.4 yr) b) decellularised (2.4 yr), c) native (3.6 yr), d) decellularised (3.6 yr), e) native (3.6 yr), f) decellularised (3.6 yr). Scale bar = 500 µm.

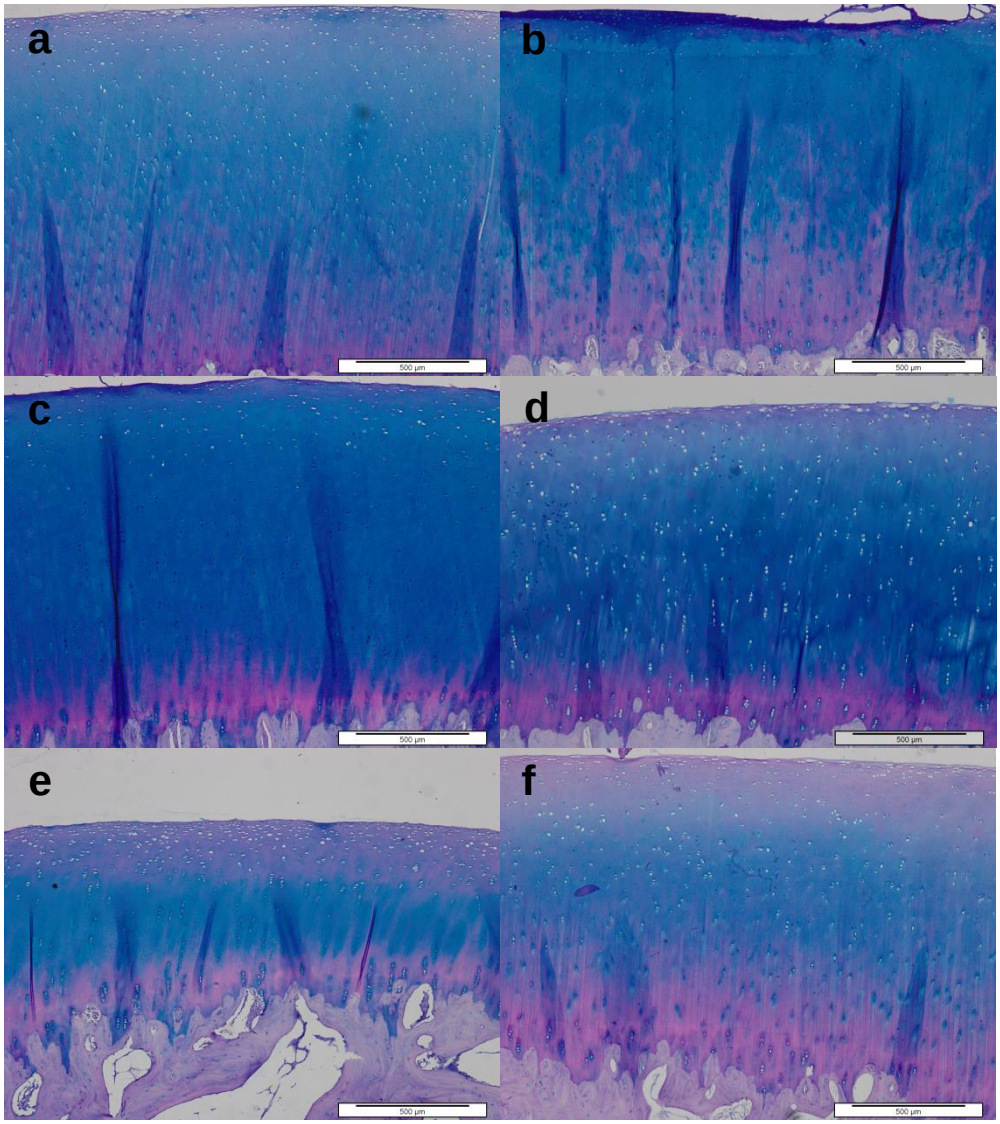

Figure 5.25 Alcian blue stained sections of native and decellularised (dCELL 3 process at 42 °C) mature porcine osteochondral tissues. a) Native (2.4 yr) b) decellularised (2.4 yr), c) native (3.6 yr), d) decellularised (3.6 yr), e) native (3.6 yr), f) decellularised (3.6 yr). Scale bar = 500 µm.

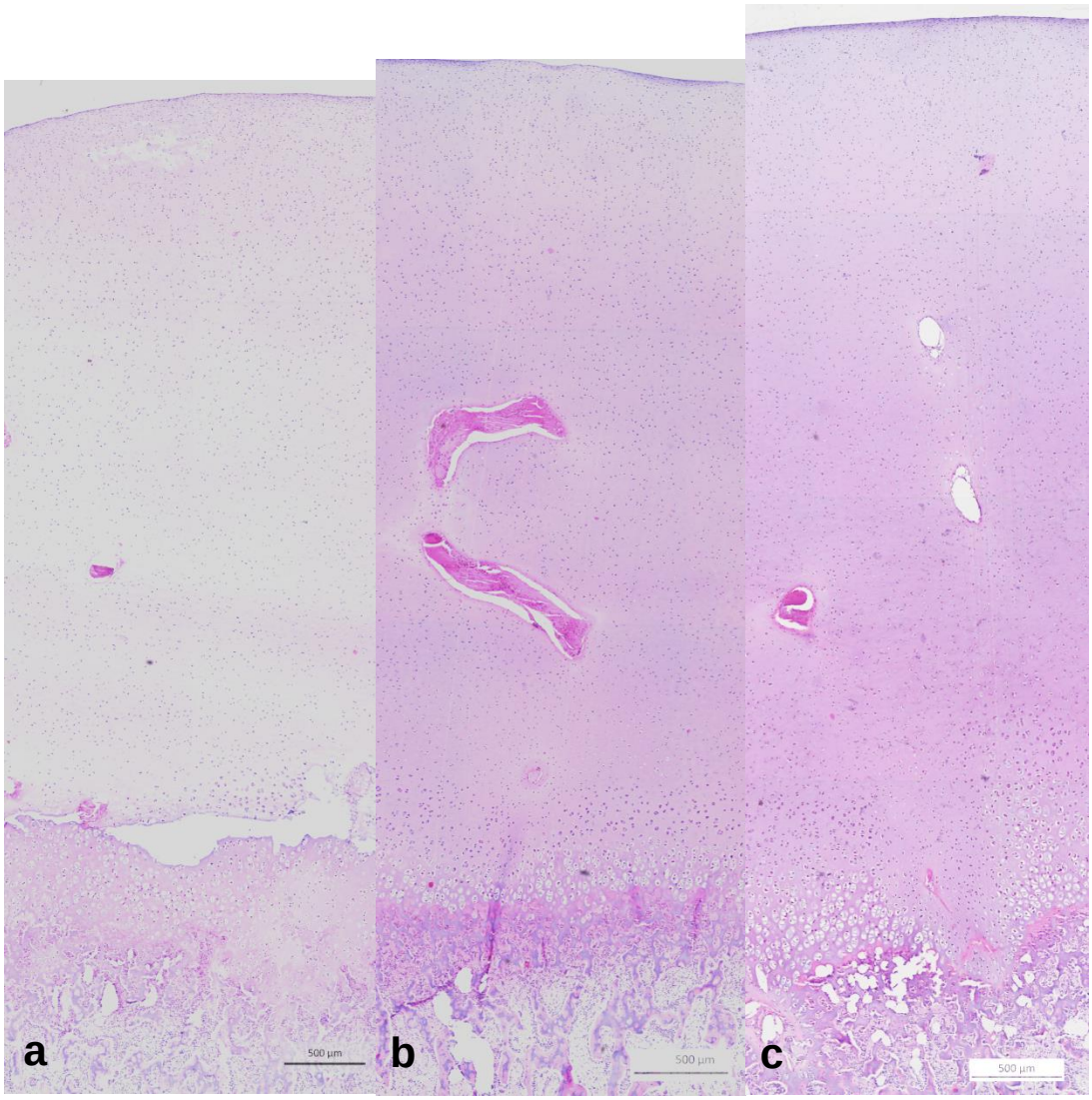

Figure 5.26 H&E stained sections of native immature porcine osteochondral tissues. a) 73 days old, b) 74 days old and c) 77 days old. Scale bars = 500 µm.

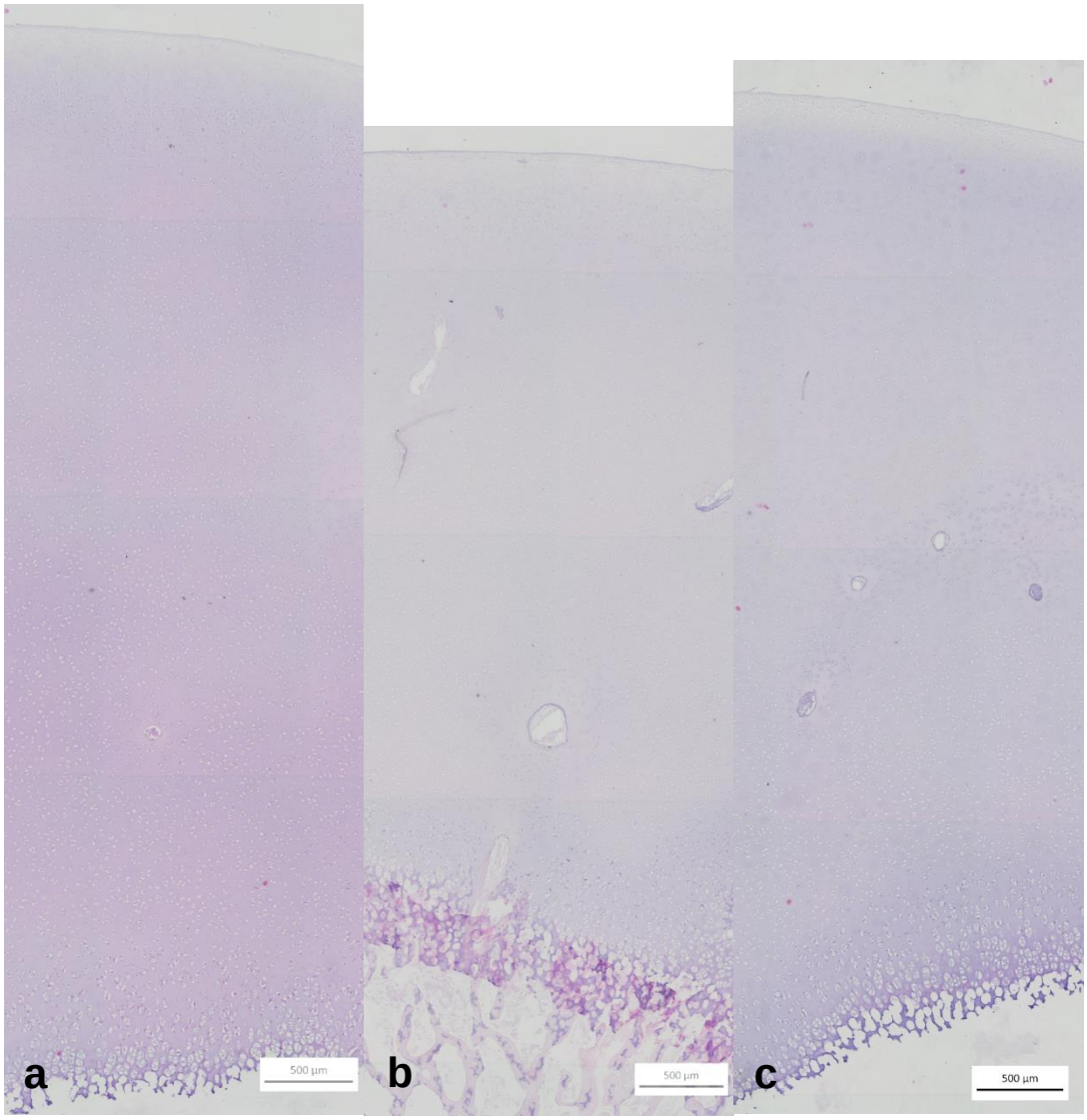

Figure 5.27 H&E stained sections of immature porcine osteochondral tissues following decellularisation with dCELL 3 process at 42 °C. a) 73 days old, b) 74 days old and c) 77 days old. Scale bars = 500 µm.

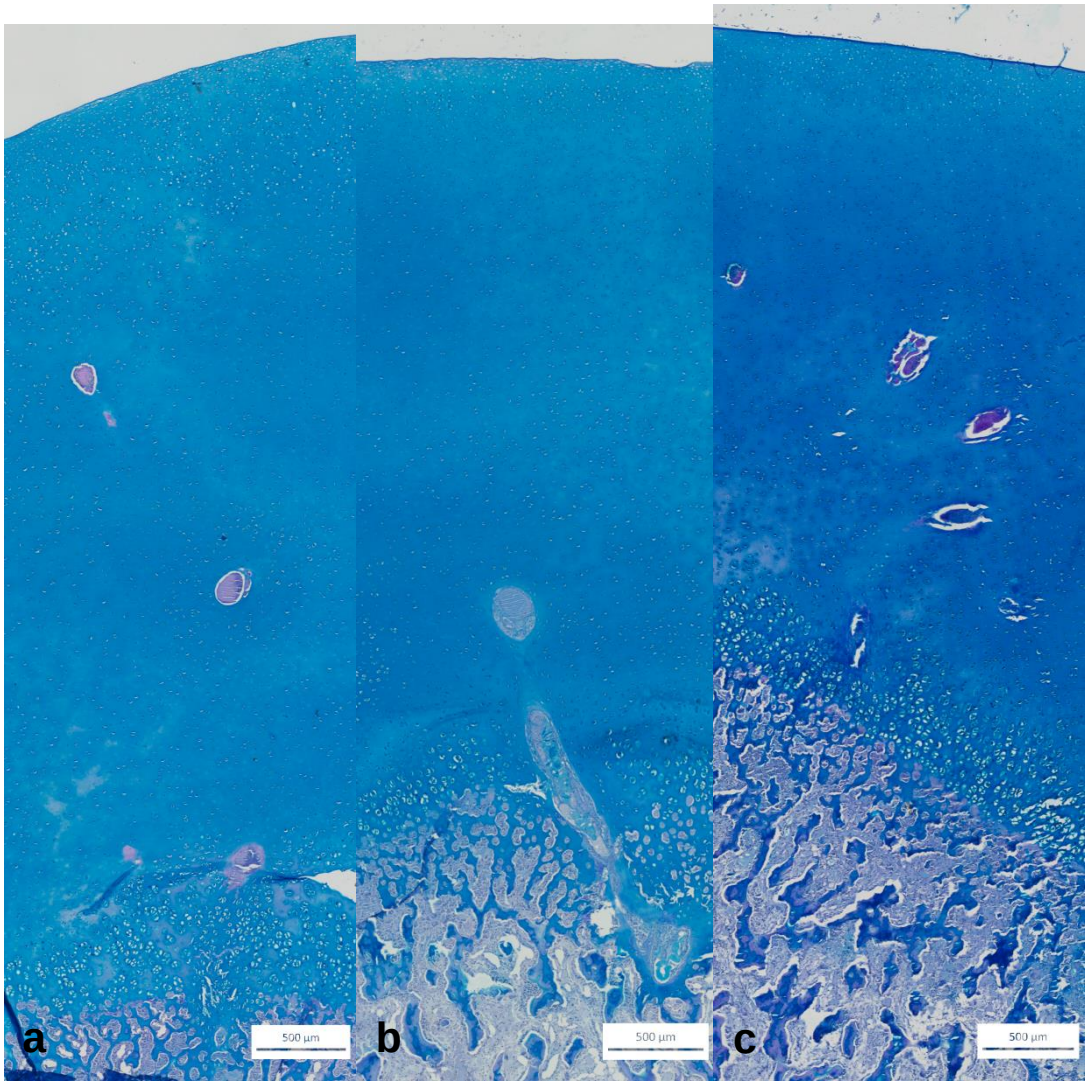

Figure 5.28 Alcian blue stained sections of native immature porcine osteochondral tissues. a) 73 days old, b) 74 days old and c) 77 days old. Scale bars = 500 µm.

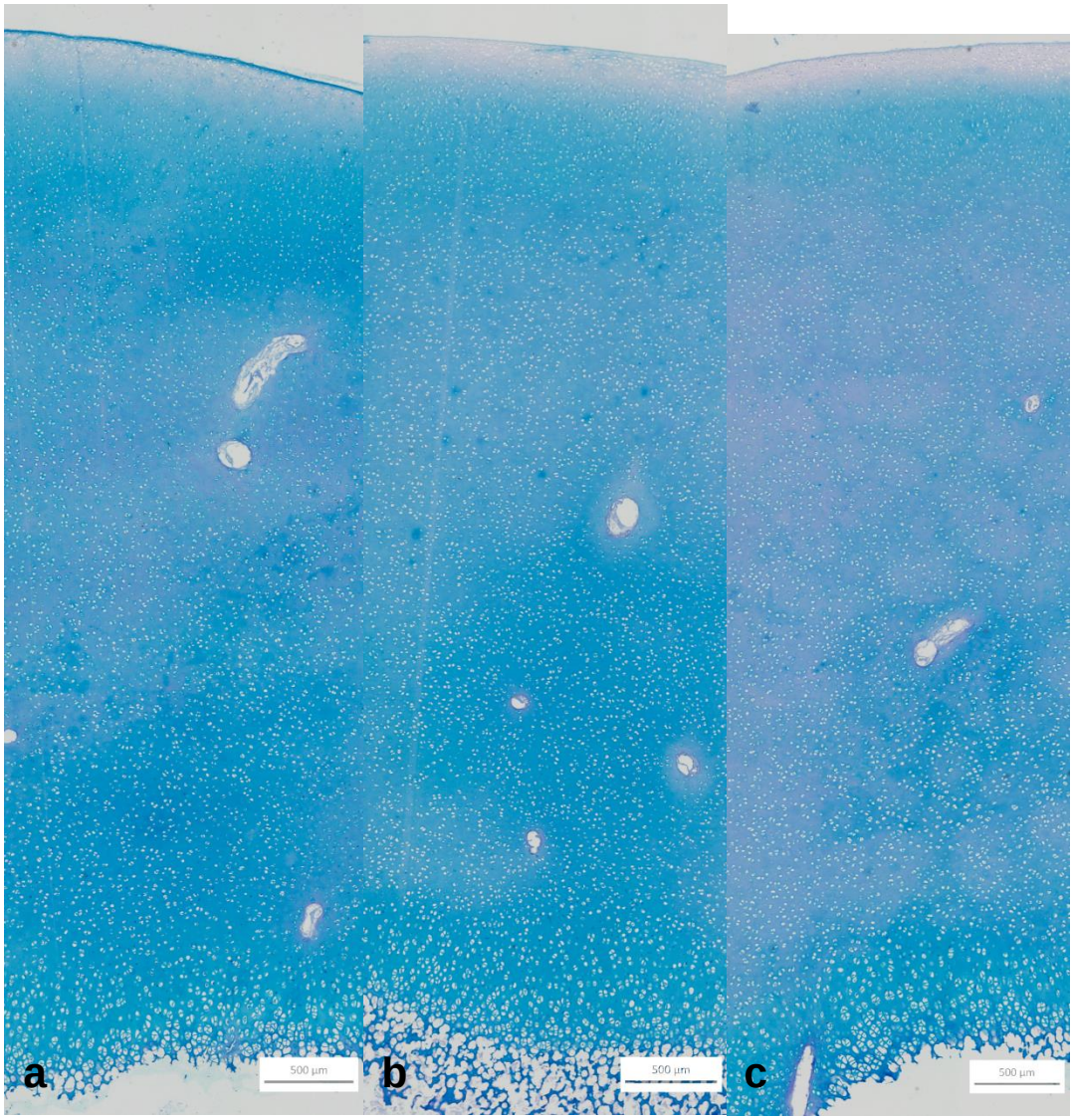

Figure 5.29 Alcian blue stained sections of immature porcine osteochondral tissues following decellularisation with dCELL 3 process at 42 °C. a) 73 days old, b) 74 days old and c) 77 days old. Scale bars = 500 µm.

5.4.3.6 Decellularisation with 1 vs 5 pins per pot

Pins from mature and immature animals showed no sign of cartilage damage, however, they were decellularised 1 pin per pot, as opposed to the usual 2 - 5, so that the pins from each individual pig could be identified. To determine whether the lack of cartilage damage seen in the previous study was due to having a single pin per pot and therefore altering the flow of solutions in each pot during agitation, two further sets of porcine (6 month old) osteochondral pins were decellularised with either one or five pins per pot.

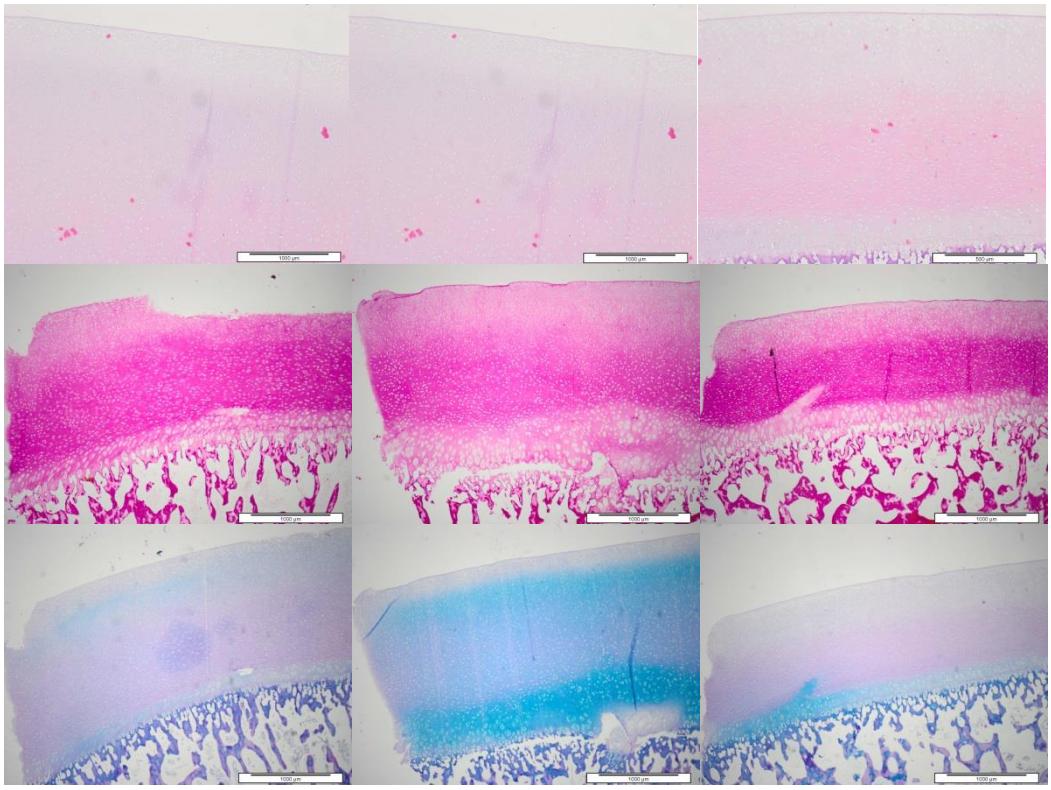

Figure 5.30 Osteochondral pins decellularised using the dCELL 3 protocol at 42 °C with 1 pin per pot. Panel a) H&E stained tissue sections, scale bar = 500 µm, b) van Gieson stained tissue sections, scale bar = 1000 µm, and panel c) alcian blue stained tissue sections, scale bar = 1000 µm.

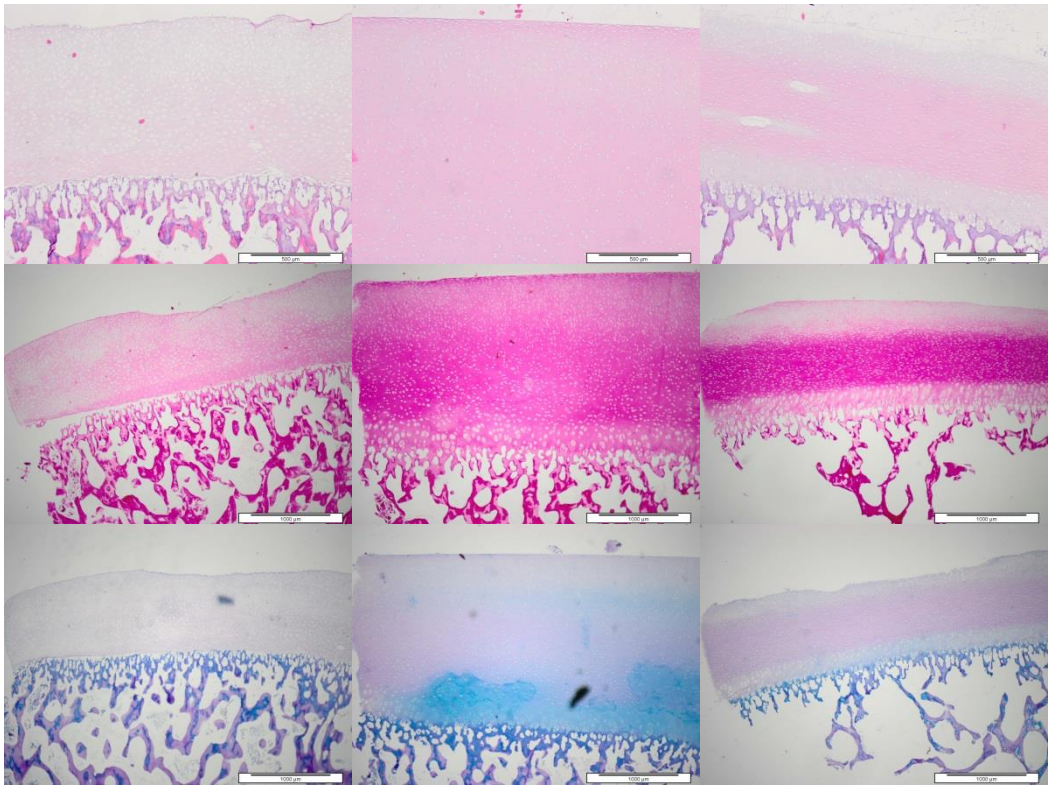

Figure 5.31 Osteochondral pins decellularised using the dCELL 3 protocol 42 °C with 5 pins per pot. Panel a) H&E stained tissue sections, scale bar = 500 µm, b) van Gieson stained tissue sections, scale bar = 1000 µm, and panel c) alcian blue stained tissue sections, scale bar = 1000 µm.

Stained sections of osteochondral pins decellularised with one pin per pot are shown in Figure 5.30. Minimal damage was seen, with the structure appearing normal, but with some loss of GAGs. When 5 pins per pot were decellularised, damage was seen in pins in two of the three pots (Figure 5.31), the cartilage was thinner and the surface had become more rough, complete loss of cartilage GAGs was seen in one of the pins.

5.5 Discussion

As discussed in the previous chapter, the aim of this study was to produce an acellular osteochondral scaffold for use in lesion repair. A protocol was developed to successfully decellularise bovine osteochondral tissues. The aim of the work in this chapter was to optimise the previously developed protocol for decellularisation of porcine osteochondral tissues.

5.5.1 Decellularisation optimisation

Following completion of the basic dCELL 1 protocol it was evident that cells were more easily removed from porcine tissues than bovine. Histologically, far fewer cell nuclei were present in porcine tissues than bovine tissues following decellularisation. The porcine cartilage DNA content was reduced by 77.5 % whereas a non-significant reduction of only 20.9 % was seen for bovine cartilage. The inclusion of two cycles of 0.1 % (w/v) SDS and hypotonic washes in dCELL5 were necessary to fully decellularise bovine tissues, however with the apparent ease of decellularisation of porcine tissue, a shorter protocol was preferred to minimise tissue damage. As use of the water pik and extended PBS end wash were shown to significantly increase cell and DNA removal in bovine tissues compared to the basic protocol, the dCELL 3 protocol was performed on porcine osteochondral pins, and was successful. This was in contrast to a study by Kheir *et al*. (2011) in which 3 cycles of low concentration SDS and hypotonic washes were required to fully decellularise porcine tissues, however this work was performed on large osteochondral cuts, as opposed to 9 mm diameter pins used in the current study.

Loss of cartilage proteoglycans was observed following decellularisation of porcine tissues using dCELL 3, and this adversely affected the mechanical properties of the tissue. Further optimisation with reduced SDS concentration and incubation times were employed to minimise GAG loss, however, following these protocols, cartilage damage was seen, with cartilage detaching from the bone and becoming gelatinous. Further analysis

was required to characterise the cartilage damage and to elucidate the cause.

5.5.2 Cartilage damage

Damaged tissue had a distinct histological appearance as evidenced with multiple staining techniques. The tissue became highly porous, with lacunae of chondrons becoming greatly enlarged and the collagen network between chondrons becoming clumped and net-like as opposed to evenly distributed. The cartilage surface became rough, likely due to a loss of tension in the collagen fibres which run parallel to the surface. Cartilage became very loosely attached to the bone, as lacunae which previously housed hypertrophic chondrons became stretched and enlarged, leaving only thin collagen fibres tying cartilage to the subchondral bone. No GAGs could be quantified in severely damaged tissues (6 h SDS) and there was a significant increase in water content, up to 95 %.

The distinct histological appearance of damaged cartilage was also witnessed by Schwartz *et al*. (2012) when developing acellular nasal septum cartilage. Schwartz *et al*. employed a decellularisation process involving osmotic cell lysis with distilled water, following which sodium hydroxide (> pH 12) was used to inactivate pathogens, denature DNA/RNA and remove cellular debris. Samples were defatted in 70 % (v/v) ethanol and GAGs and other non-collagenous proteins were denatured and removed using a guanidine hydrochloride (1 M) solution containing sodium acetate (0.05 N). Cartilages were finally sterilised using hydrogen peroxide (5% v/v).

The histological appearance of the treated nasal septum cartilage was more pronounced in porcine (7 - 8 months old) compared to human (18 - 74 years old) cartilage. The process resulted in a significant GAG reduction from 4.82 ± 0.94 % to 1.50 ± 0.43 % as a percentage of dry weight, and an almost complete loss of alcian blue staining. They saw an increase in tissue porosity from 19 ± 12 % to 29 ± 12 %. They concluded that loss of GAG and increased porosity were advantageous for cell infiltration during recellularisation.

A study to produce acellular osteochondral tissues by Kheir *et al*. (2011), also used immature porcine tissue (4 months old), and employed a similar protocol to that described in this study, based on that of Stapleton *et al*. (2008). They used 50 mm x 10 mm x 10 mm osteochondral blocks from the porcine femoral groove and found that 6 cycles of hypertonic buffer and SDS in hypertonic buffer (0.1 %, w/v) were required to fully remove all cell nuclei and achieve a 98 % reduction in cartilage DNA, however, no histological damage to cartilage was apparent following this more harsh protocol.

To further assess the cartilage damage seen in the current study, digestion of cartilage with α-chymotrypsin was performed to cleave denatured collagen which could then be quantified using the hydroxyproline assay. This was performed with the aim of identifying whether collagen damage was occurring during the decellularisation process and contributing to the histological appearance and tissue degeneration. No significant increase in denatured collagen was found compared to native tissue, suggesting that collagen fibres had remained intact.

5.5.3 Investigation into cartilage damage

To identify the cause of cartilage damage, many different factors associated with the decellularisation protocol were investigated . Although no collagen denaturation was observed, damage to other non-collagenous proteins may have occurred at high temperatures of incubation. Osteochondral pins decellularised at 45 °C (reaching temperatures of 48 °C) disintegrated more readily than those incubated at 40 °C, however, cartilage damage was still present at lower temperatures. The increased damage at higher temperature may have been as a result of increased diffusion. As temperature had had an effect on the extent of damage, all subsequent protocols were performed at the lower temperature of 42 °C, as this would not range above 45 °C, and would remain at a higher temperature than 37°C, avoiding the optimal temperature for bacterial growth.

As reduction in incubation temperature had not eliminated cartilage damage, each aspect of the decellularisation process was considered and removed from the process to determine the individual effect on cartilage stability.

Many phases of the decellularisation protocol had the potential to cause damage; freeze-thaw cycles create interstitial and intracellular ice crystals, which increase matrix permeability, hypotonic buffer has an osmotic effect on the cells and tissue, SDS denatures proteins and solubilises membranes (Seddon *et al*., 2004) and PAA causes protein damage by oxidative stress (Pruss *et al*., 1999). Although PBS washes alone were not thought to be damaging to the tissue, cartilage disintegration tended to occur during the final end wash, so this was also isolated as a potential damage causing factor. As a negative control, pins were washed in PBS alone. Surprisingly, all protocols, including the PBS alone control resulted in some degree of tissue damage. This indicated that damage was not as a direct result of any particular stage of the decellularisation process, and other protocols based on the same sequence of decellularisation treatments had not resulted in tissue damage (Booth *et al.*, 2002; Stapleton *et al.,* 2008; Kheir *et al*., 2011).

Cartilage damage had occurred when osteochondral pins were incubated in PBS with aprotinin (10 $KUI.ml^{-1}$) for 5 days. Advancing on protocols developed by Stapleton *et al*. (2008) and Kheir *et al*. (2011), EDTA, a matrix metalloproteinase inhibitor had been omitted from the PBS wash buffer in this study, as it also functions to decalcify bone and has been linked to cytotoxicity (Koulaouzidou *et al*., 1999). Pins were incubated in a PBS wash buffer containing EDTA (0.1 %, w/v) and aprotinin (10 $KUI.ml^{-1}$) for 5 days, to see if addition of the MMP inhibitor reduced or prevented the cartilage damage. No damage was seen, however, neither was it seen in the PBS only positive control. Although addition of EDTA did not clarify the role of MMPs in cartilage damage, due to the lack of denatured collagen in damaged samples, it is unlikely that collagenase activity of MMPs was responsible for cartilage degradation.

Another factor associated with the PBS wash buffer to consider was the tonicity. PBS is isotonic for cells, but may not necessarily be isotonic to the cartilage ECM. According to Baumgarten *et al*. (1985), the osmolality of normal synovial fluid is 404 ± 57 $mOsmol.Kg^{-1}$, however following exercise this reduced to isotonic levels, 301 ± 19 $mOsmol.Kg^{-1}$. Synovial fluid from knee joints of individuals suffering from OA and rheumatoid arthritis was found to have reduced osmolality, being 297.3 ± 16.9 $mOsmol.Kg^{-1}$ and

279.6 ± 7.5 mOsmol.Kg^{-1} respectively (Shanfield *et al*., 1988). Having linked reduced osmolality of synovial fluid to arthritic joints, Bloebaum & Magee (1989) developed and patented a modified ringers solution containing mannitol for use as a hypertonic irrigating solution during arthroscopic lavage. In this study the osmolality of porcine synovial fluid was found to be 329 ± 59 mOsmol.Kg^{-}1. To increase the osmolality of the PBS wash buffers used for decellularisation, mannitol was added. A 1 % (w/v, 350 mOsmol. Kg^{-1}) solution was used to match porcine synovial fluid and a 2 % (w/v, 400 mOsmol.kg-1) solution of mannitol in PBS was used to match values stated for human synovial fluid. After incubation at 42 °C with agitation in PBS with mannitol for 5 days, all osteochondral pins appeared histologically undamaged, however as stated before, the PBS only control also did not show signs of damage. Potentially the retention of cells in the tissue was stabilising the structure, so mannitol enhanced PBS wash buffers were used as part of the dCELL 3 protocol. Following decellularisation with the mannitol solutions, both showed slight histological signs of damage, as did the decellularisation using PBS without mannitol. Use of hypertonic PBS did not prevent cartilage damage during decellularisation.

It was noted that although porcine cartilage showed signs of damage following application of the dCELL 3 protocol, bovine tissues did not; the quality of the porcine source material was therefore considered a potential factor in cartilage degeneration. Characterisation of osteochondral tissues from different species in Chapter 3 highlighted differences in the maturity of porcine and bovine tissues. To assess the effect of skeletal maturity on cartilage degeneration, two further age ranges of pigs were selected. As pigs are skeletally mature from 2.5 years (Reinwald & Burr., 2008), a skeletally mature group aged between 2.4 and 3.6 years and a very immature group aged 3 months old were selected for decellularisation. Histologically the native osteochondral tissues from immature pigs showed characteristically thick cartilage with high cell density and indistinct cell orientation and intense alcian blue staining for GAGs (Julkunen *et al*., 2009), vascularisation was also seen throughout the young cartilage, indicative that the tissue was not fully formed and still growing, and the cartilage-bone interface was not clear and appeared full of hypertrophoc cells. Conversely, tissue from the older

pigs was fully mature, with much thinner cartilage, which had a lower cell density and much more defined cell orientation. The tissues from mature pigs showed a defined, thick subchondral bone plate.

Upon decellularisation, neither the immature group nor the mature group showed any signs of cartilage damage. Although cartilage had become detached from the bone of 2/3 pins from immature pigs during washing, this was likely due to the poor attachment originally and shear stress applied to the attachment site during coring of osteochondral pins from the joint, and not due to the decellularisation process. Of interest was the fact that immature tissues appeared to be fully decellularised following application of dCELL 3, however mature porcine tissues (similarly to bovine osteochondral tissues) were not fully decellularised, likely due to inadequate solution infiltration through the dense subchondral bone plate.

To identify which osteochondral pin came from which individual pig when assessing the effect of skeletal maturity on cartilage degradation, each pin was decellularised in a single pot. Usually 3-5 pins are decellularised in one pot at a time. A single pin agitated in a pot of solution will likely have different effect on how the fluid flows, and may affect the mechanical shear forces experienced by that single pin compared to a larger number of pins, explaining why neither mature nor immature porcine osteochondral pins showed cartilage damage. To this end one pin and five pins per pot were decellularised using the dCELL 3 protocol. Damage to varying degrees was seen in both conditions, so the number of pins per pot is not thought to influence cartilage damage.

Of note throughout this study was the variability with which cartilage responded to any of the processes detailed. The presence or absence of damage and extent to which cartilage damage occurred was inconsistent within treatment groups and between processes. This unpredictability made it difficult to conclusively determine the effect of any treatment on porcine cartilage. The lack of consistency may be due to the stage of development of the porcine tissue, as minor variations in pig age could have had pronounced effects on the cartilage stability.

5.5.4 Conclusion

Although initially a protocol was developed to successfully decellularise porcine tissues, further investigation revealed that the cartilage was damaged, which in some cases resulted in the cartilage dissolving completely in the decellularisation solutions, and in other cases resulted in the cartilage becoming devoid of GAGs, having a greatly increased porosity and water content and having drastically reduced biomechanical properties. High temperatures were found to increase the severity of cartilage damage, likely through increased diffusion.

Chapter 6
Biocompatibility of acellular bovine osteochondral scaffolds

6.1 Introduction

A protocol was developed to successfully decellularise bovine osteochondral tissues in Chapter 4. Histological analysis of the acellular scaffold was performed and the DNA, GAG and hydroxyproline content quantified as well as an evaluation of the biomechanical properties. The tissue was found to have severely reduced GAG content, which resulted in reduced mechanical properties. To further characterise the effect of decellularisation on the osteochondral extracellular matrix, immunohistochemistry was used to locate specific matrix constituents.

Furthermore, SDS used in the decellularisation has been reported to have cytotoxic effects when not effectively removed from decellularised tissue matrices (Rieder *et al*., 2004). Residual SDS within the scaffold may prevent ingrowth of cells in vivo and result in graft failure. Residual SDS within the tissue was quantified and the contact cytotoxicity of the acellular scaffold was determined.

6.2 Aims and objectives

Aims:

The aim of the research in this chapter was to investigate changes to specific matrix proteins in bovine osteochondral tissues following decellularisation and to assess the biocompatibility of the acellular scaffold.

Objectives:

- To determine the biocompatibility of the acellular osteochondral matrix.
    - To determine the concentration at which SDS has cytotoxic effects on BHK and 3T3 cell lines.
    - To quantify the SDS removed from the tissues during wash cycles and determine the concentration of residual SDS left in bovine cartilage and bone following decellularisation.
    - To determine biocompatibility of the acellular scaffold in vitro using the contact cytotoxicity technique with BHK and 3T3 cell lines.

Additional objectives were not pursued due to unforeseen issues with the initial biocompatibility testing.

6.3 Methods

6.3.1 SDS quantification

Reagents

In addition to reagents listed in Section 4.4.1, the following reagents were used.

- *^{14}C radiolabelled SDS in hypotonic buffer (0.1 % w/v, 0.01 µCi.ml^{-1})* *750 ml SDS in hypotonic solution 75 µl ^{14}C SDS*
- *MicroScint™-20*

Method

To quantify the SDS washed out of the decellularised tissues in each wash solution (n=3) and also to quantify the residual SDS in the decellularised tissues (n=3), the decellularisation protocol described in Section 4.4.2.14 was performed using SDS in hypotonic solution which had been spiked with ^{14}C radiolabelled SDS, produced as described in Section 6.3.2.1. Solutions and tissues from the decellularisation were collected.

A set of standards were produced from the spiked SDS solution to give SDS concentrations of 1000 µg.ml^{-1}, 750 µg.ml^{-1}, 500 µg.ml^{-1}, 250 µg.ml^{-1}, 125 µg.ml^{-1}, 50 µg.ml^{-1}, 25 µg.ml^{-1}, 10 µg.ml^{-1} and 0 µg.ml^{-1}. Standard (40 µl), test solution (40 µl) or macerated decellularised cartilage or bone (40 mg) were added in triplicate to a flat bottomed 96 well optiplate™ and MicroScint™-20 (160 µl) was added to each well. Counts per minute were measured using Top count ™, with each well being counted for 20 min. A standard curve of counts per minute was produced from the known concentrations of SDS, from which the concentration of SDS in the test solutions and tissue could be interpolated.

6.3.2 Determining the toxic concentration of SDS

To determine the concentration at which SDS had cytotoxic effects on two cell lines, 3T3 and BHK cell lines were incubated with varying concentrations

of SDS solution. Cell culture was performed as described in Section 2.2.6. Cells were seeded at subconfluent numbers onto flat bottomed 96 well culture plates and incubated overnight at 37 °C in 5 % CO_2 (v/v) in air. Once cells had attached, culture medium was aspirated and replaced with 200 µl of medium containing a known concentration of SDS or DMSO positive control (40 %, v/v) in cell culture medium. SDS was dissolved in appropriate cell culture medium for each cell type at concentrations of 750 $\mu g.ml^{-1}$, 500 $\mu g.ml^{-1}$, 250 $\mu g.ml^{-1}$, 100 $\mu g.ml^{-1}$, 50 $\mu g.ml^{-1}$, 25 $\mu g.ml^{-1}$, 10 $\mu g.ml^{-1}$, 5 $\mu g.ml^{-1}$ and 0 $\mu g.ml^{-1}$ and sterilised by passing through a 2 µm filter. Cells were incubated in these test media for 24 h at 37 °C in 5 % CO_2 (v/v) in air. Following incubation cell viability was determined using the ATPLite-M® assay.

6.3.2.1 ATPLite-M® cell viability assay

Cell viability was determined using the ATP-lite M® assay kit, where cellular adenosine triphosphate (ATP; present in all metabolically active mammalian cells) reacts with D-luciferin in the presence of luciferase to produce light which can be quantified using a scintillation counter. In cells which have undergone apoptosis, ATP will rapidly deplete, so little to no light will be detected.

Cell culture medium was aspirated from cells cultured in a 96 well plate and 50 µl of the appropriate cell culture medium was added to each well. Mammalian cell lysis solution (50 µl) from the ATPLite-M® assay kit was added to each well and the plate was shaken for 5 min on a microshaker. The contents from each well was transferred to a 96 well optiplate™ and 50 µl substrate solution was added to each well. The plate was covered in foil and agitated for a further 5 minutes on a microshaker. Any air bubbles were removed by carefully flaming the plate before determining the luminescence of each well using Top count™ scintillation counter.

6.3.3 Contact cytotoxicity

Bovine osteochondral pins (2 pins per pot from n=3 animals) were decellularised using dCELL 5 (Section 4.4.2.14). Each pin was dissected into small pieces as described in Figure 6.1 and 3 pieces from one pin were each placed in a well of a 6 well culture plate and secured using a steri-strip. A drop of cyanoacrylate contact adhesive was applied to the centre of one well on each plate to act as a positive control for cell growth inhibition and a steri-strip adhered to another as a negative control, a final well was left empty to observe normal cell growth.

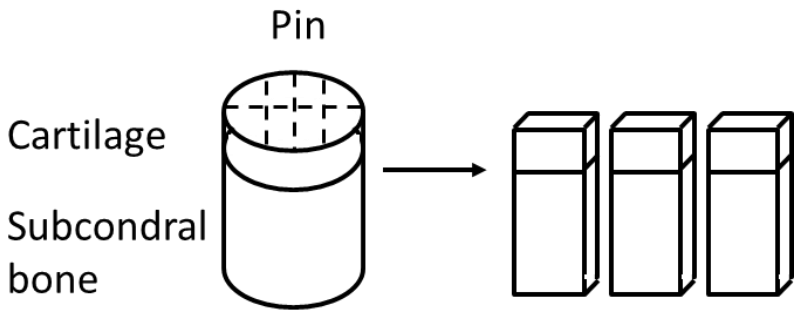

Figure 6.1 Dissection of osteochondral pins for contact cytotoxicity assay. Pins were cut along the dotted lines using a sterile scalpel blade to produce four rectangular osteochondral pieces exposing the innermost part of the pin.

Plates were washed using PBS without calcium or magnesium three times for ten minutes each before being seeded with 3T3 (n=3) or BHK cells (n=3) at numbers appropriate to become confluent after 48 h. Plates were incubated for 48 h at 37 °C in 5 % CO_2 (v/v) in air. Each well was examined microscopically to detect changes in cell morphology, vacuolisation, detachment and cell lysis. The medium was aspirated and each well washed in PBS before fixation of the monolayer with 10 % (v/v) NBF for 10 min. NBF was aspirated and Giemsa stain was applied to each well for 5 min. Excess Giemsa stain was then removed using tap water. Again, changes to the cells were visualised by light microscopy.

6.3.4 Modified protocol for the production of biocompatible bovine osteochondral scaffolds

The protocol developed to decellularise bovine osteochondral pins (Section 4.4.2.14) was augmented to include further PBS end washes, with the intention of improving SDS wash out to produce a biocompatible scaffold. Two extended protocols (7 day and 14 day extended PBS washes) were developed to determine the optimum end wash duration, where sufficient SDS wash out was achieved without unnecessarily extending the protocol. The basic 48 - 60 h weekend end wash protocol (Section 4.4.2.12) was augmented with 4 x 24 h PBS washes after the final weekend wash (7 day PBS end wash) or 4 x 24 h PBS washes, followed by a second 48 – 60 h PBS wash and a further 4 x 24 h PBS washes (14 day PBS end wash). All PBS washes were performed at 42 °C with agitation. The three protocols (2 day, 7 day and 14 day PBS end wash) were performed alongside each other, 2 pins per pot from n=3 animals were used for each protocol.

6.4 Results

6.4.1 SDS quantification

To quantify SDS washed out from tissues during decellularisation and to determine the concentration of residual SDS in the decellularised osteochondral matrix, tissues were decellularised using solutions spiked with radiolabelled SDS. Quantification of radiolabelled SDS was performed by adding scintilant to spiked solutions/ tissues and measuring the activity on a scintillation counter. A standard curve of SDS concentration against counts per minute was produced (Figure 6.2), from which unknown SDS concentrations could be interpolated.

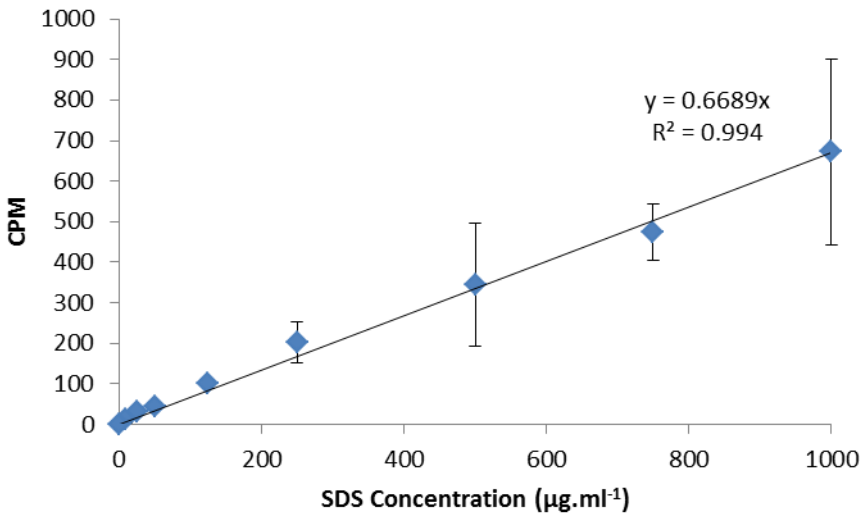

Figure 6.2 Linear relationship between SDS concentration and counts per minute. Data is shown as the mean (n=3) ± 95 % confidence limits.

The concentration of SDS in each wash solution of the decellularisation process is shown in Figure 6.3. High concentrations of SDS were measured in the SDS wash solutions (750 ± 210 µg.ml^{-1}), however this was lower than the 1000 µg.ml^{-1} expected from a 0.1 % (w/v) SDS solution. Error was high in the SDS solutions and some SDS from the solution would have entered the tissues, explaining the lower value. The hypotonic wash (24 h) after the first SDS incubation showed a relatively high concentration of SDS (59 ± 87

µg.ml^{-1}) compared to the PBS wash (10 min) following the second SDS incubation, suggesting a more thorough wash out of SDS during that first 24 h wash period. All solutions showed low concentrations of SDS, suggesting that SDS was still being washed out of the tissue during the last PBS wash.

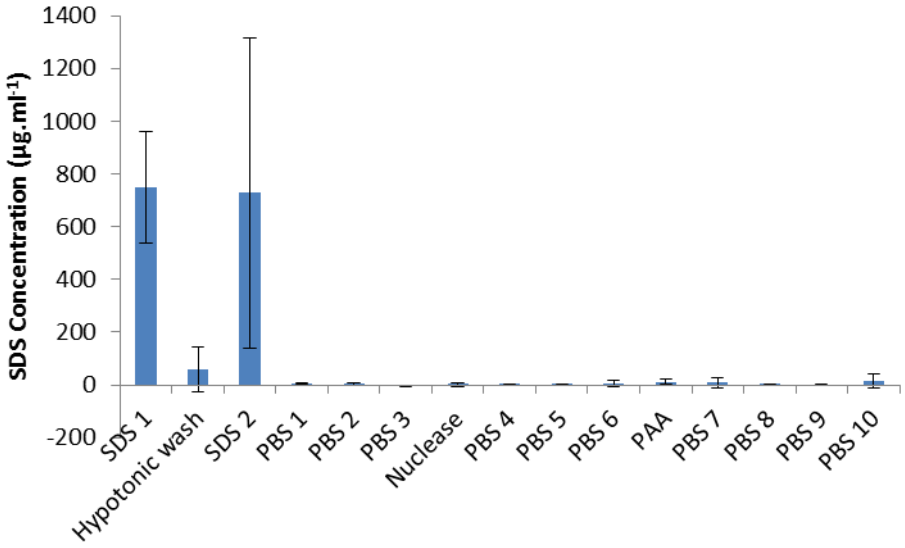

Figure 6.3 Concentration of SDS in decellularisation solutions following quantification of ^{14}C SDS. Data is shown as the mean (n=3)) ± 95 % confidence limits.

Quantification of SDS in the tissue showed that decellularised bovine cartilage contained 364 ± 43 ng.mg^{-1} SDS and decellularised bone contained 374 ± 187 ng.mg^{-1} SDS (Figure 6.4), approximately 0.037 % (w/w) SDS per tissue wet weight.

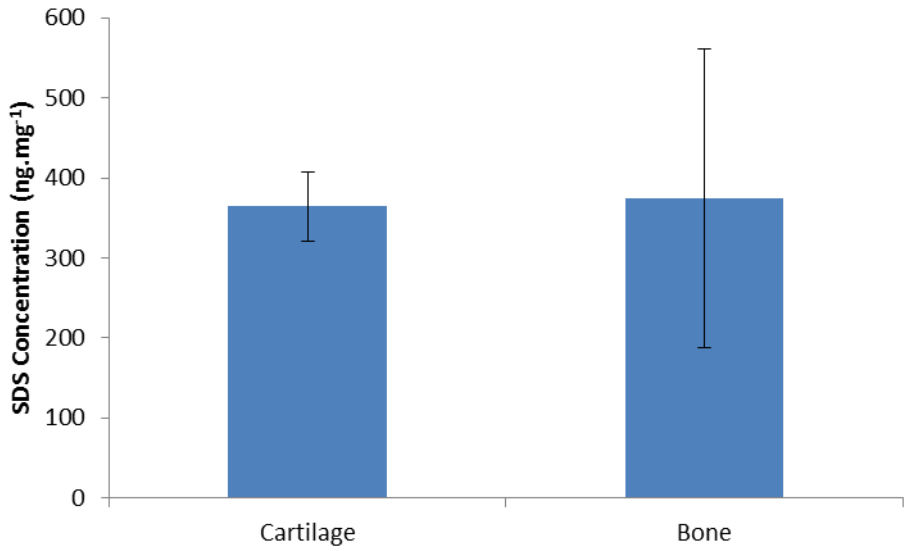

Figure 6.4 Concentration of residual SDS in decellularised bovine cartilage and bone. Data is shown as the mean (n=3)) ± 95 % confidence limits.

6.4.2 SDS toxicity

To determine the concentration at which SDS had cytotoxic effects, cell lines were incubated with varying concentrations of SDS in cell culture medium and incubated overnight. Cell viability was determined using the ATP-lite M® assay.

The cytotoxic effect of varying concentrations of SDS on BHK and 3T3 cell lines can be seen in Figure 6.5. At SDS concentrations of 25 $\mu g.ml^{-1}$ and below, no cytotoxic effect was seen with either cell line. At ≥ 50 $\mu g.ml^{-1}$ SDS, BHK cells showed a significant reduction in counts per minute (CPM), indicating that reduced cell viability had occurred at these concentrations. 3T3 cells only showed a significant reduction in CPM at SDS concentrations ≥ 250 $\mu g.ml^{-1}$ suggesting this cell type had lower sensitivity to SDS cytotoxicity.

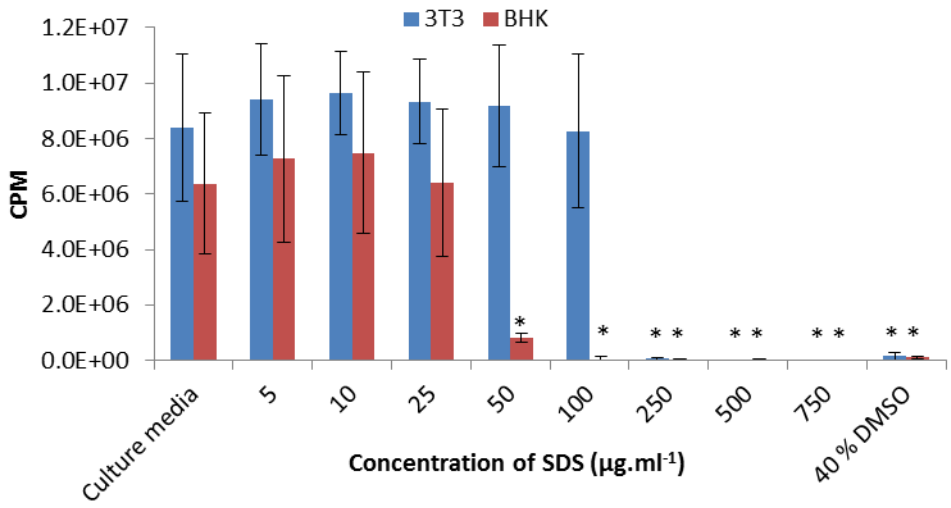

Figure 6.5 Cytotoxicity of varying concentrations of SDS to BHK and 3T3 cell lines. Data is shown as the mean (n=3)) ± 95 % confidence limits. * Significant, p<0.05 (ANOVA).

6.4.3 Contact cytotoxicity

Decellularised tissues were incubated with either 3T3 cells (Figure 6.6) or BHK cells (Figure 6.7) for 48 h to determine contact cytotoxicity. Growth of both cell types appeared normal when seeded into a blank well of the culture plate. Those cultured with a steri-strip negative control also had normal morphology and grew up to and against the strip. Cells cultured with cyanoacrylate positive control did not adhere next to the glue and had a rounded morphology characteristic of dead cells. 3T3 cells cultured with decellularised cartilage and bone had normal morphology and grew up to the tissue. However when BHK cells were cultured with decellularised tissue one of the 3 tissues (Figure 6.7 d & e) showed cytotoxic effects, with cells not adhering next to the tissue and having a rounded ball morphology.

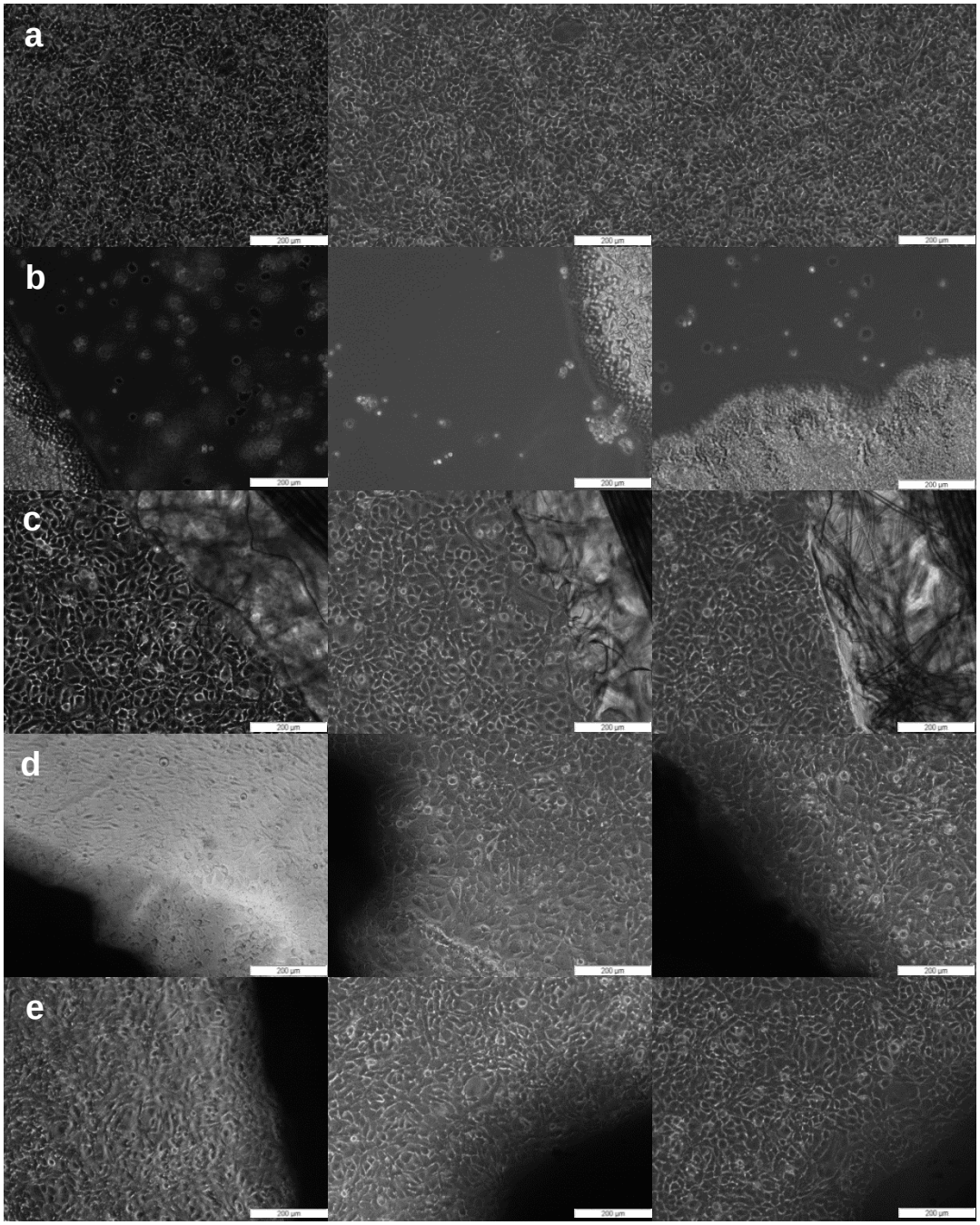

Figure 6.6 Contact cytotoxicity of decellularised bovine osteochondral tissues when cultured for 48 h with 3T3 cells. Panel a) cells only, panel b) cyanoacrylate positive control, panel c) steri-strip negative control, panel d) decellularised bovine bone, panel e) decellularised bovine cartilage. 100 x magnification, scale bars = 200 µm.

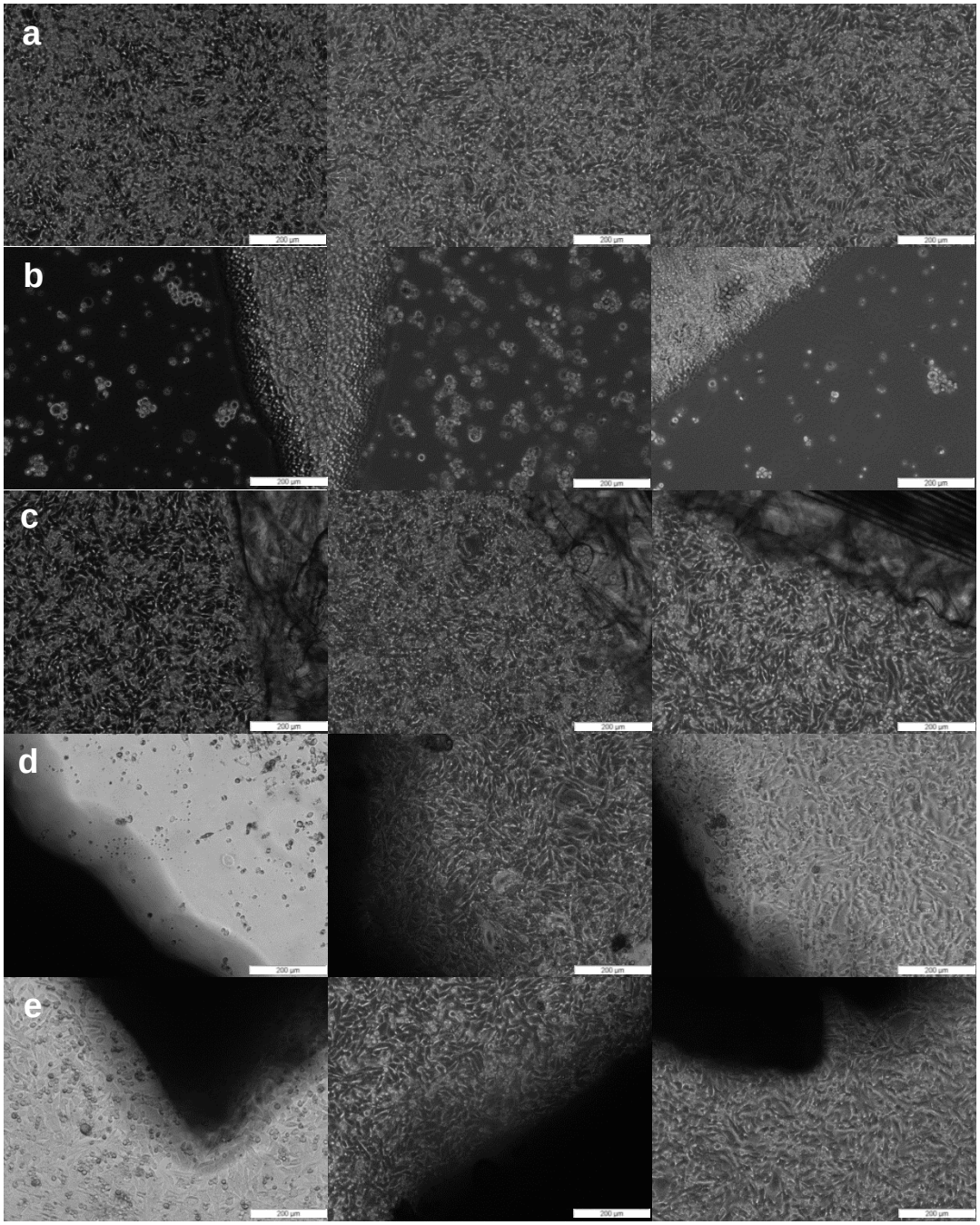

Figure 6.7 Contact cytotoxicity of decellularised bovine osteochondral tissues when cultured for 48 h with BHK cells. Panel a) cells only, panel b) cyanoacrylate positive control, panel c) steri-strip negative control, panel d) decellularised bovine bone, panel e) decellularised bovine cartilage. 100 x magnification, scale bars = 200 µm.

6.4.4 Modified protocol

Following application of the 7 and 14 day PBS wash modified protocols (Section 6.3.5), cartilage damage occurred in all samples between the 4 and 5 day point. The cartilage detached from a number of samples as observed with porcine tissues (Chapter 5). Further analysis could not be performed.

6.5 Discussion

The aim of this study was to further characterise the decellularised bovine osteochondral matrix to identify whether the resultant scaffold was biocompatible.

For acellular scaffolds to be used in patients, it is essential that they are not toxic or harmful. ISO 10993 is in place to ensure thorough and appropriate testing of all medical devices is completed during product development. Initial basic *in vitro* biocompatibility testing should be performed prior to *in vivo* testing and use in animal models to ensure the scaffold has no immediate toxic effects before more advanced immune responses can be investigated.

SDS, a detergent included in the decellularisation process to solubilise cellular membranes has been shown to have cytotoxic effects when not thoroughly removed from dcellularised tissues (Rieder *et al*., 2004). SDS is able to impart a negative charge on proteins, which may inhibit cell attachment and proliferation, it is also able to denature proteins, which may affect cell survival (Seddon, 2004).

Quantification of the residual SDS in the decellularised tissues, found that the majority of SDS was removed during wash steps, and that tissues only contained ~ 370 $ng.mg^{-1}$ SDS per wet weight following decellularisation. However, incubation of cells with varying concentrations of SDS showed concentrations of ≥ 250 $\mu g.ml^{-1}$ to be cytotoxic to 3T3 cells and even lower concentrations of ≥ 50 $\mu g.ml^{-1}$ to be cytotoxic to BHK cells. Assuming 370 $ng.mg^{-1}$ SDS present in tissues is equivalent to 370 $\mu g.ml^{-1}$, the residual SDS in decellularised tissues may have resulted in them being cytotoxic .

Contact cytotoxicity assays with 3T3 cells did not show any cytotoxic effects of the tissues, however, BHK cells, which showed higher sensitivity to SDS did show cytotoxicity with one sample. It may be that, although the concentration of SDS in the tissues was high, it was not immediately accessible from the dense 3D solid tissues to the cell monolayer, as it would be expected that all samples would be cytotoxic with both cell types at this concentration.

As some cytotoxicity was seen, modifications to the protocol were included to increase the number and duration of PBS washes at the end of the process to improve SDS wash out. When additional PBS washes were included, tissue samples began to show signs of damage, as seen in porcine tissue. The cartilage shrivelled in from the bone and in cases became detached. It appeared that the same problem was present with bovine and porcine osteochondral decellularisation.

The potential causes of cartilage damage were thoroughly investigated in Chapter 5, however the size of osteochondral pin decellularised is a common factor in porcine and bovine decellularisation processes which had not been investigated. To conclusively eradicate cartilage damage during the decellularisation process, further methods using larger osteochondral constructs were investigated in the next chapter.

Chapter 7
Decellularisation of large osteochondral constructs

7.1 Introduction

Previously in this study, a protocol was developed for the decellularisation of osteochondral pins from the knee condyles of 6 month old pigs (Chapter 5). A limitation to this process was that the cartilage often became irreversibly damaged during decellularisation. The degree to which cartilage damage occurred varied greatly, resulting in a range of tissue morphologies from slight increase of porosity at the cartilage surface, to shrinkage in from the cut edges, complete loss of GAGs and increase in water content to 95 % (w/w), to the cartilage completely dissolving away in the decellularisation wash solutions. The cause of the damage was thoroughly investigated, however, no protocol could be developed which fully eradicated cartilage damage. Prior to studies with porcine cartilage, it had been shown that bovine cartilage pins from the knee condyles of 18 month old animals could be decellularised without sustaining any overt damage (Chapter 4), however, with increased wash cycles to reduce residual SDS levels in the tissue, the bovine cartilage pins also exhibited similar damage (Chapter 6).

During the course of this study, Schwarz *et al*., (2012) reported upon the decellularisation of porcine and human nasal cartilage. It was of interest to note, that although not recognised by the authors as damaged, the histology images of the decellularised cartilage showed similar morphology to the damaged cartilage found in the present study. A similarity was that Schwarz *et al*. performed decellularisation on cylindrical cuts of cartilage (5 mm diameter discs, 1 mm depth). Collagen fibres in hyaline cartilage are under tension, this tension plays an important role in cartilage structure and function. The collagen network interacts with GAGs to resist repulsion between the negatively charged proteoglycans, holding the ECM together

(Mow *et al*., 2005). It was hypothesised that when extracting cartilage pins and producing a cut edge, a loss of tension in the collagen fibres occurred and this facilitated the decellularisation solutions to cause damage to the tissue. In order to test this hypothesis it was logical to determine whether damage would occur when larger cuts or uncut cartilage (large bovine plates and whole porcine condyles) were subject to the decellularisation process and observing the effect on cartilage structure.

7.2 Aims and objectives

Aims:

The aim of the study presented in this chapter was to apply the decellularisation protocols developed in Chapter 5 for porcine cartilage and Chapters 4 and 6 for bovine cartilage to whole porcine condyles and large bovine osteochondral cuts and to identify any structural damage caused to the cartilage.

Objectives:

- To apply the decellularisation protocol for porcine cartilage pins to whole porcine medial condyles (with the cancellous bone removed).
- To apply the decellularisation protocol for bovine pins to bovine osteochondral plates (40 mm long x 20 mm wide x 10 mm deep).
- To qualitatively assess the decellularised osteochondral tissues using histology, to determine the histoarchitecture, GAG distribution and cellularity.

7.3 Methods

7.3.1 Dissection of porcine medial condyles

Whole porcine (6 months old) right legs (n=3) were dissected as described in Section 2.2.2.1 and 2.2.2.2. Following exposure of the femoral component of the knee, the femur was clamped and a hand saw used to cut into the bone between the two condyles. Another cut was made across the femur, from the base of the femoral groove to the back of the condyle, to release the condyle in its entirety. Using a hand drill with 5 mm diameter drill bit, the cancellous bone was drilled into from the underside and bone cutters used to hollow out the condyle, leaving approximately 10 mm subchondral bone underneath the cartilage surface. Condyles were stored frozen as described in Section 2.2.2.4 until required.

7.3.2 Dissection of bovine medial groove plates

Bovine femurs (n=3) were dissected as described in Section 2.2.2.1 and 2.2.2.2. Using callipers, a plate 20 mm wide x 40 mm long was measured and marked out on the cartilage surface using a scalpel. Using a hand saw, the shape was cut into the groove, and a final cut was made parallel to the cartilage surface through the bone to release the plate. A purpose built clamp was used to hold the plate and the subchondral bone was accurately trimmed to 10 mm depth using a hack saw (Figure 7.1).

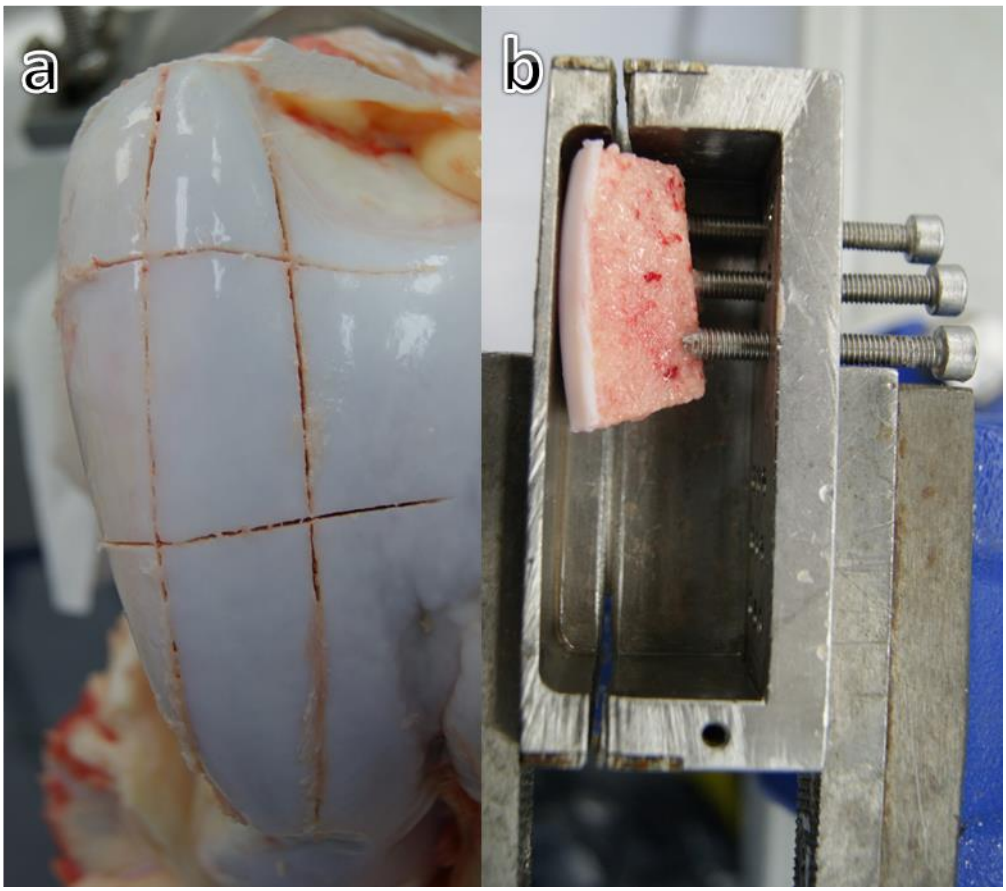

Figure 7.1 Preparation of bovine osteochondral plates. a) a 20 mm x 40 mm rectangle was marked out on the medial femoral groove and cut out using a saw. b) the plate was secured in a purpose deigned holder and the bone was cut to 10 mm deep using a saw.

7.3.3 Porcine condyle decellularisation

Porcine condyles (n=3) were decellularised one per 150 ml pot with 125 ml decellularisation solution as described in Section 5.3.2.2. Condyles were subject to additional 4 x 24 h PBS washes at 42 °C with agitation following the extended 48 - 60 h PBS wash.

7.3.4 Bovine plate decellularisation

Bovine osteochondral plates (n=3) were decellularised one per 150 ml pot with 125 ml decellularisation solution as described in Section 4.4.2.14. Plates were subject to additional 4 x 24 h PBS washes at 42 °C with agitation following the extended 48 - 60 h PBS wash.

7.3.5 Histological analysis

7.3.5.1 Slide preparation

Whole decellularised porcine condyles and bovine plates were fixed in 10 % (v/v) NBF and decalcified as described in Section 2.2.3.1 and 2.2.3.2. A 5 - 8 mm thick slice was taken through the centre of the porcine condyle (medial to lateral side) which was then processed, wax embedded and sectioned as described in Section 2.2.3.3 and 2.2.3.4. Slices (5-8 mm thick) were also taken through the centre of the bovine plate across the plate width which were then processed, wax embedded and sectioned.

7.3.5.2 Reverse processing

Wax embedded bovine tissue blocks were melted in an oven at 60 °C overnight. Under vacuum with agitation in the Lecia TP 120 automated tissue processor, tissues were dewaxed through 2 x 2 h cycles of xylene and dehydrated in 2 x 2 h cycles of 100 % methylated spirits. Tissues were placed in 70 % methylated spirits for 15 min prior to being re-processed as described in Section 2.2.3.3.

7.3.5.3 Wax block decalcification

Wax embedded bovine tissue blocks were trimmed down to expose the sample using a microtome (Leica RM2125RTF). Blocks were then immersed in a 12.5 % (w/v) EDTA solution (Section 2.2.3.2.1) overnight at room temperature without agitation to decalcify the exposed surface to be sectioned.

7.3.5.4 Sectioning and slide preparation

Wax embedded tissues were sectioned and transferred to slides as described in Section 2.2.3.4.

7.3.5.5 Histological staining

Tissue sections were stained with H&E (Section 2.2.4.1), Alcian blue (Section 2.2.4.3), van Gieson (Section 2.2.4.4) and DAPI (Section 2.2.4.6) prior to being mounted and imaged microscopically.

7.4 Results

7.4.1 Porcine whole medial condyles

Porcine whole medial condyles (n=3) were decellularised as described in Section 7.3.3. Macroscopically, following decellularisation, cartilage appeared firm and smooth over the whole surface of the condyle, even following the prolonged PBS washes. The cartilage appeared to be intact. Histologically, the decellularised porcine osteochondral tissues appeared to be largely devoid of cells (Figure 7.2 – 7.7), however, a few isolated nuclei were still present in the calcified cartilage regions of the condyle (Figure 7.7b). The cartilage of all three decellularised condyles did not show the increased porosity characteristic of damaged cartilage (Chapter 5), however a slight increase in chondron lacunae size in the superficial zone and surface roughening could be seen (Figure 7.2 – 7.4). The minimal disruption to collagens at the cartilage surface could be more clearly visualised with van Geison staining (Figure 7.8 – 7.10). Alcian blue staining showed low levels of GAGs throughout the superficial and middle cartilage zones (Figure 7.11 & 7.13) and also in the deep zone (Figure 7.12) across the whole cross section of the condyle.

7.4.2 Bovine osteochondral plates

Bovine osteochondral plates were decellularised as described in Section 7.3.4. Following decellularisation, cartilage appeared smooth, firm and white and appeared to be intact. Initially, as a result of technical error, samples were incompletely processed, attempts were made to reverse process the tissues and correctly reprocess as described in Sections 7.5.3.1 and 7.5.3.2. Incomplete processing rendered the tissues dry, crumbly and difficult to section, so blocks were directly decalcified to ease sectioning (Section 7.3.5.3). Samples were successfully sectioned, however as a result of sample preparation, histological stains appeared more intense than in tissues which had been processed correctly. Histologically, bovine tissues showed incomplete decellularisation, with nuclei remaining in the deep calcified regions (Figures 7.14 – 7.19). The cut edges and cartilage surface

of all three bovine osteochondral cuts appeared porous, showing signs of damage, however the internal middle and deep zones were not damaged as shown by intense van Gieson staining of cartilage collagens (Figure 7.20 – 7.22). The cut edges and surface also showed reduced intensity of alcian blue staining showing loss of GAGs in these regions directly in contact with the decellularisation solutions (Figure 7.23 – 7.25). Bovine osteochondral plates showed larger areas of damage than whole porcine condyles following decellularisation.

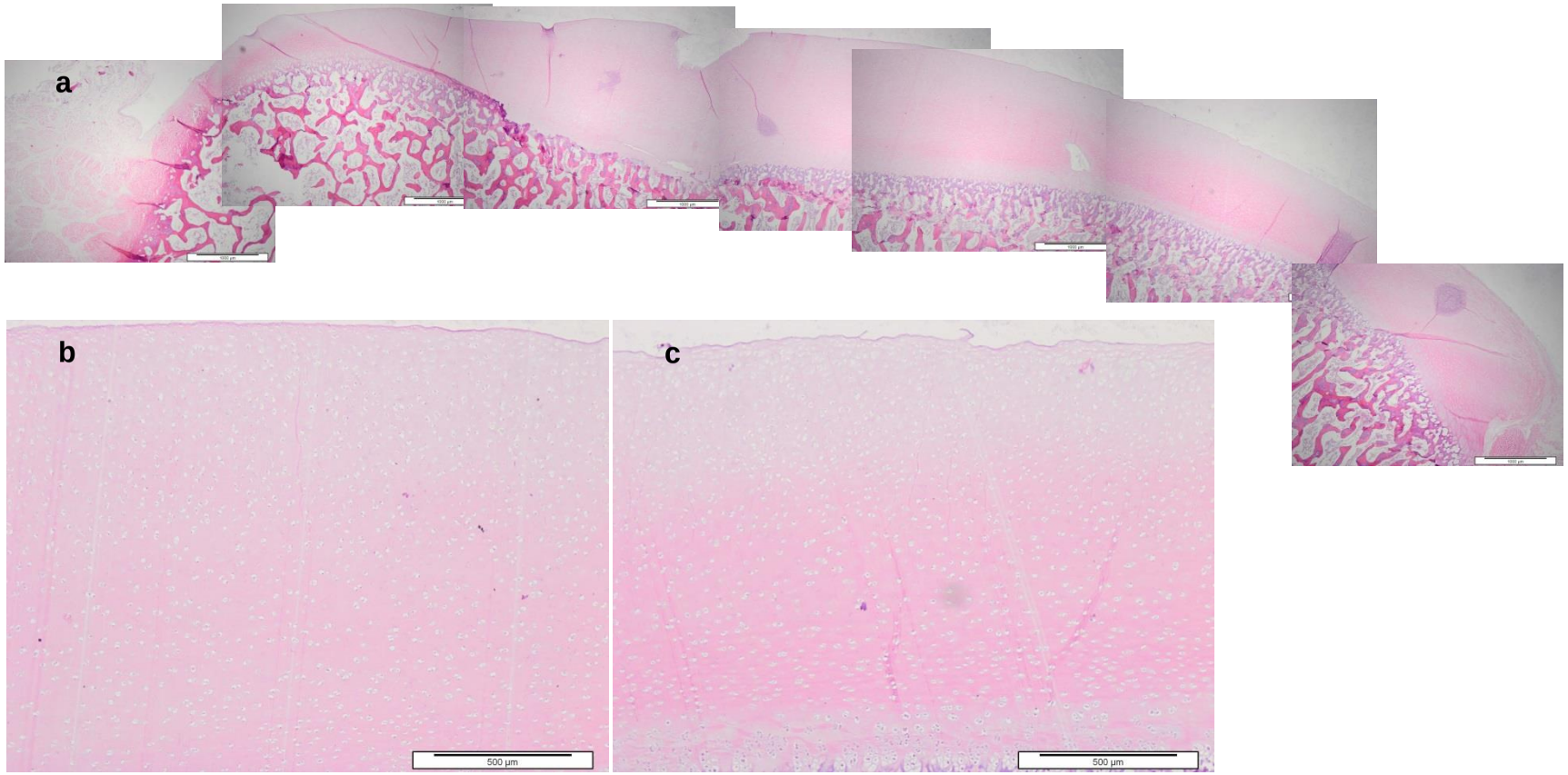

Figure 7.2 H&E stained sections of decellularised porcine condyle 1. a) full condyle, scale bar = 1000 µm, b) and c) scale bar = 500 µm.

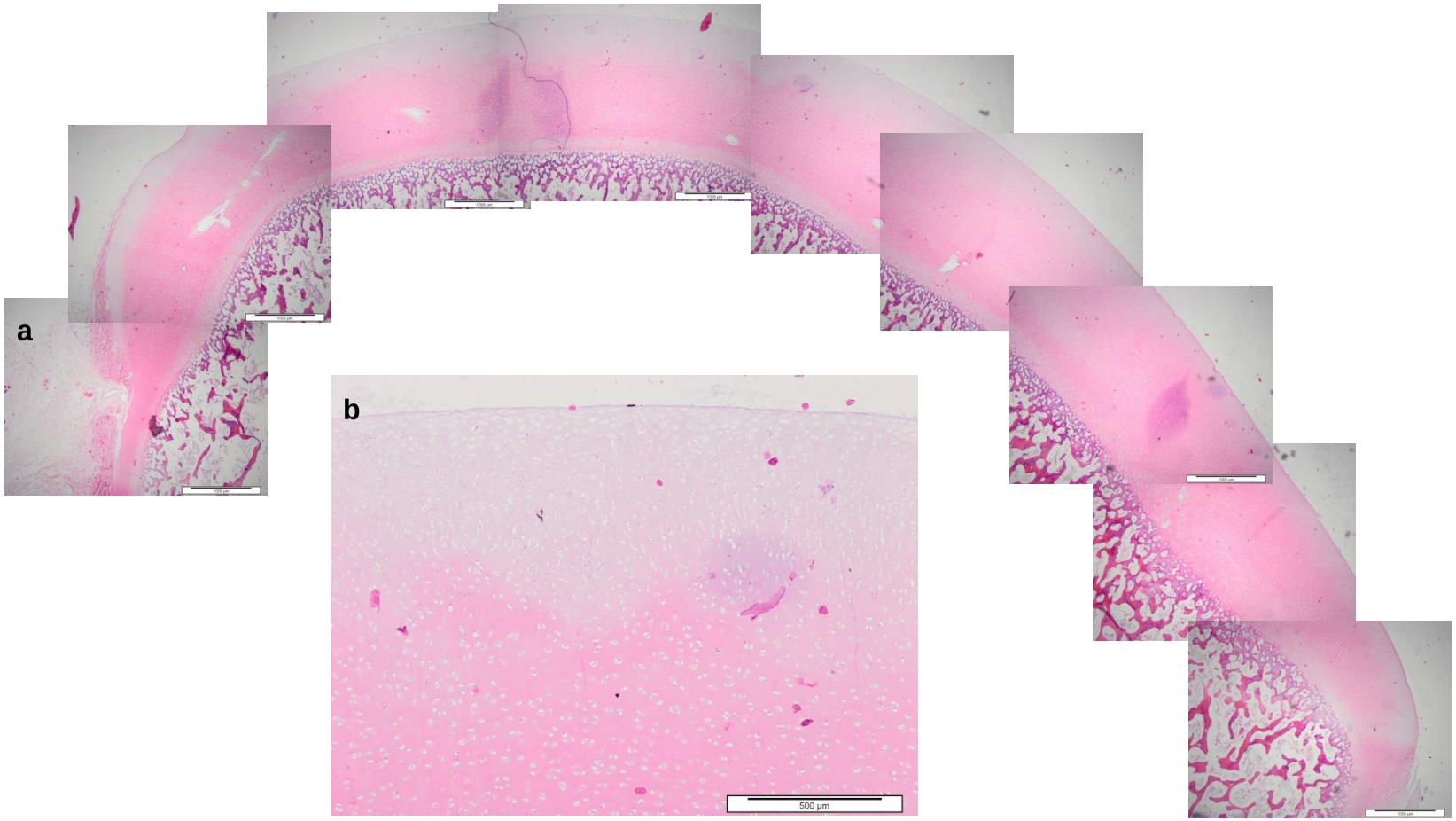

Figure 7.3 H&E stained sections of decellularised porcine condyle 2. a) full condyle, scale bar = 1000 µm, b) scale bar = 500 µm.

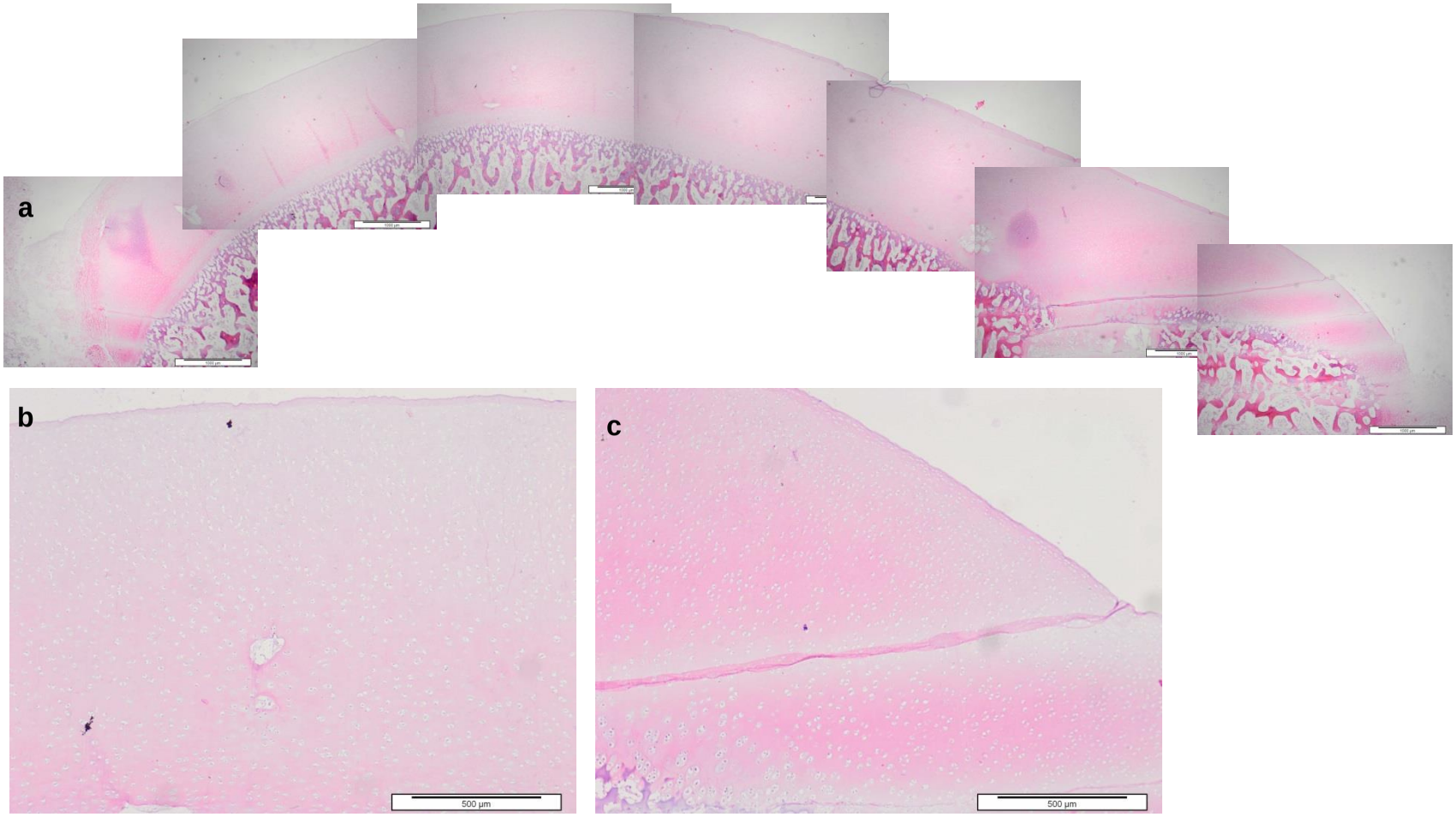

Figure 7.4 H&E stained sections of decellularised porcine condyle 3. a) full condyle, scale bar = 1000 µm, b) and c) scale bar = 500 µm.

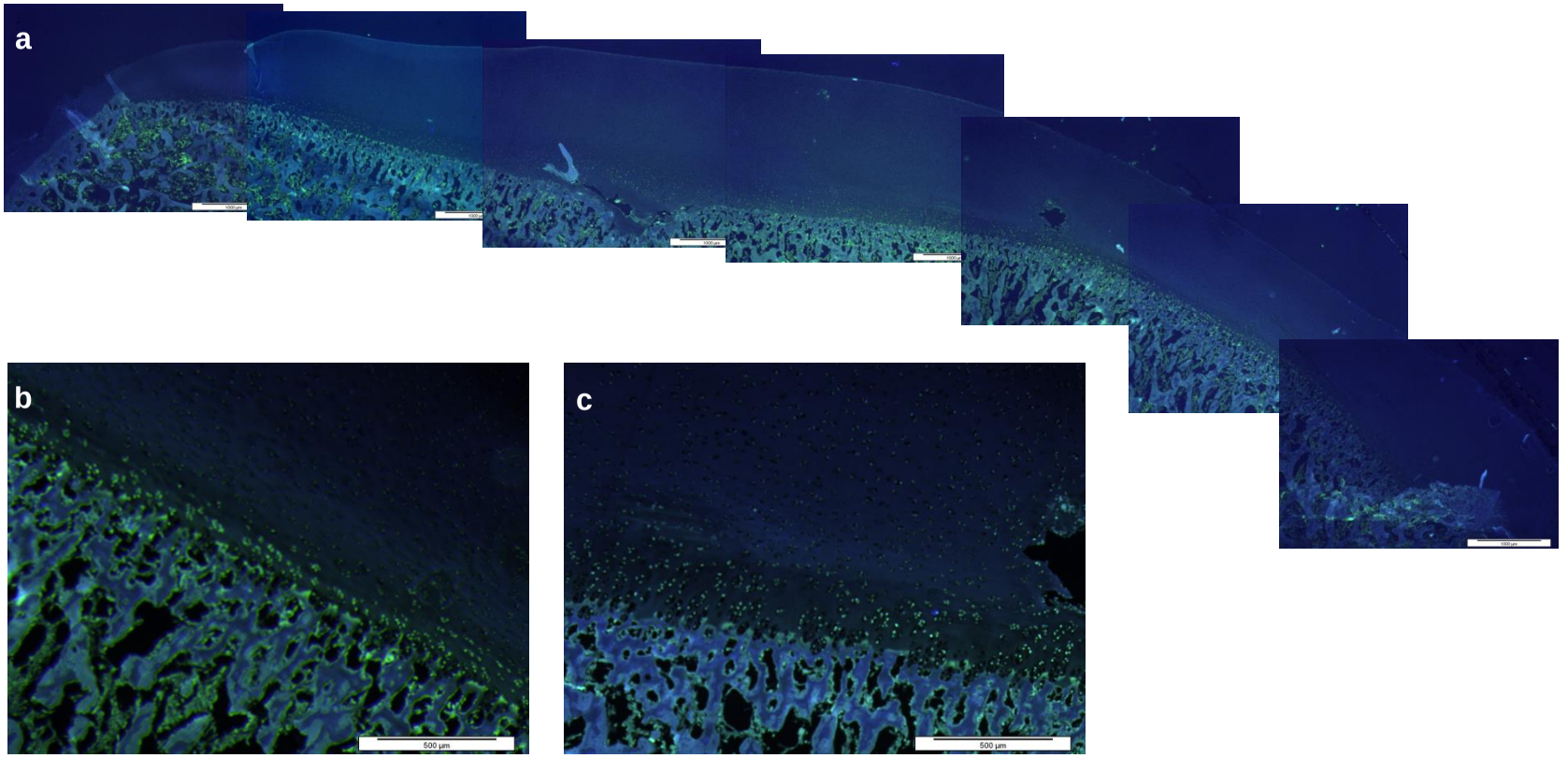

Figure 7.5 DAPI stained sections of decellularised porcine condyle 1. Blue = DAPI. Green = collagen autofluorescence. a) full condyle, scale bar = 1000 µm, b) and c) scale bar = 500 µm.

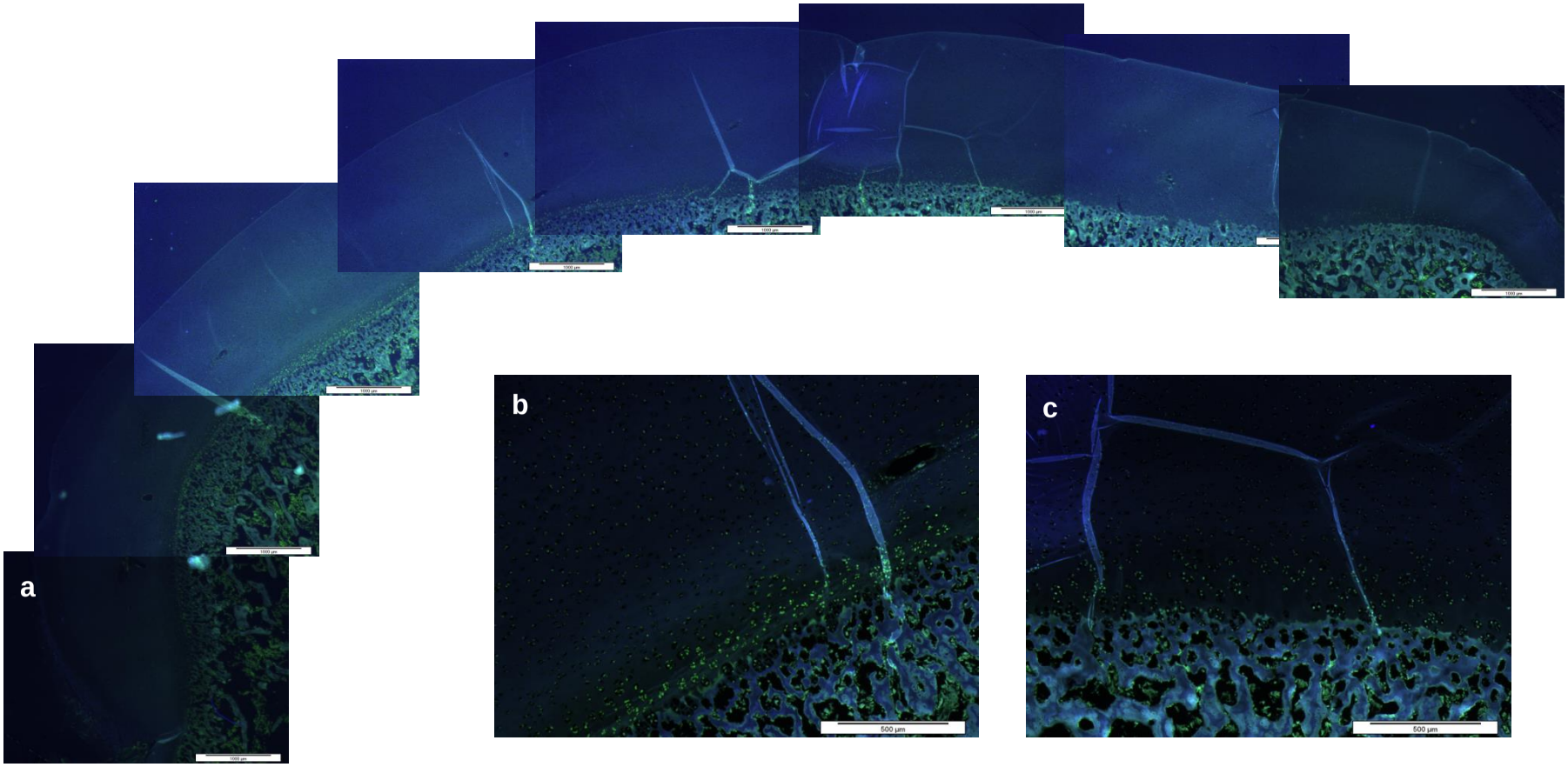

Figure 7.6. DAPI stained sections of decellularised porcine condyle 2. Blue = DAPI. Green = collagen autofluorescence. a) full condyle, scale bar = 1000 µm, b) and c) scale bar = 500 µm.

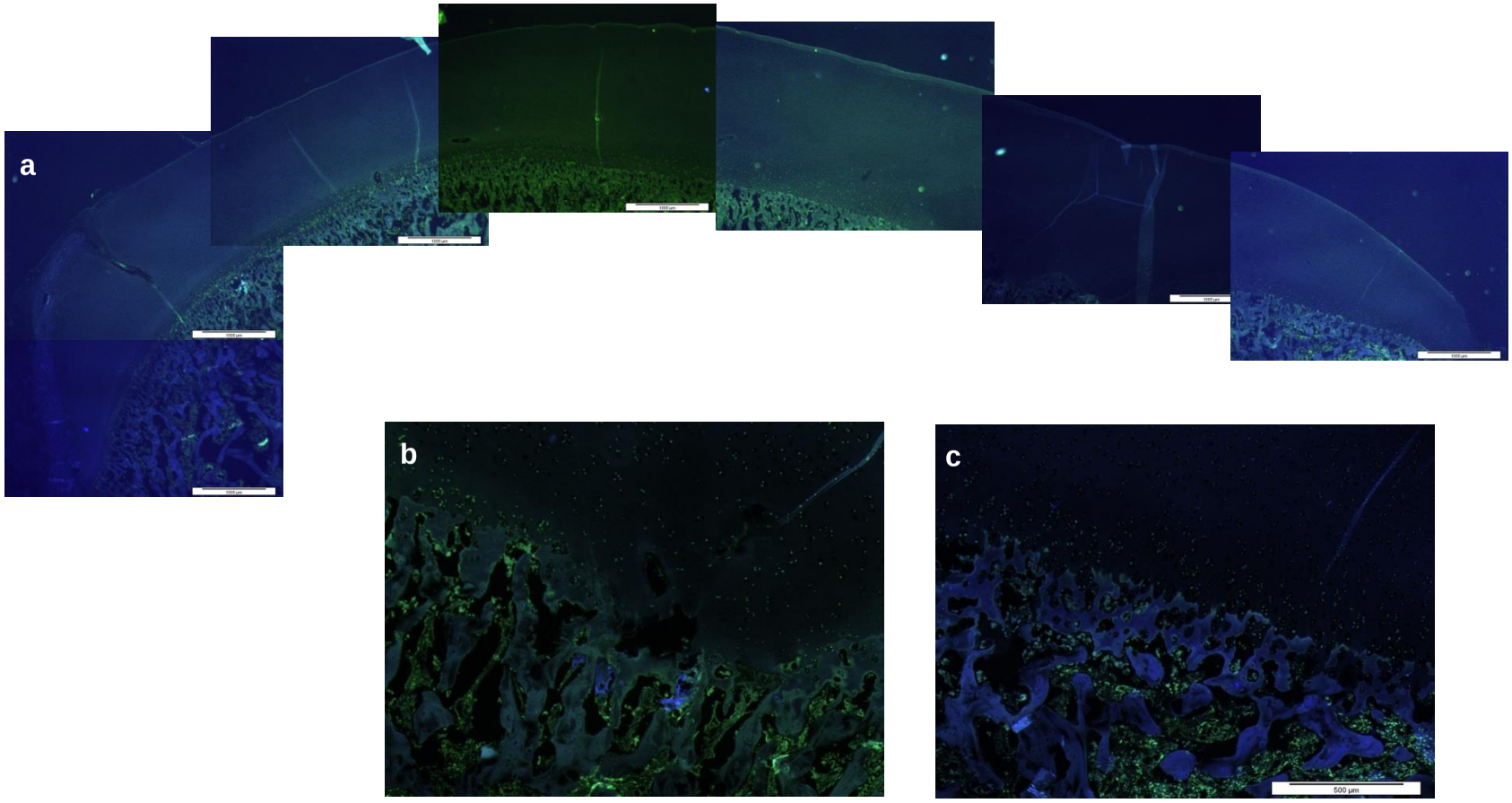

Figure 7.7. DAPI stained sections of decellularised porcine condyle 3. Blue = DAPI. Green = collagen autofluorescence. a) full condyle, scale bar = 1000 µm, b) and c) scale bar = 500 µm.

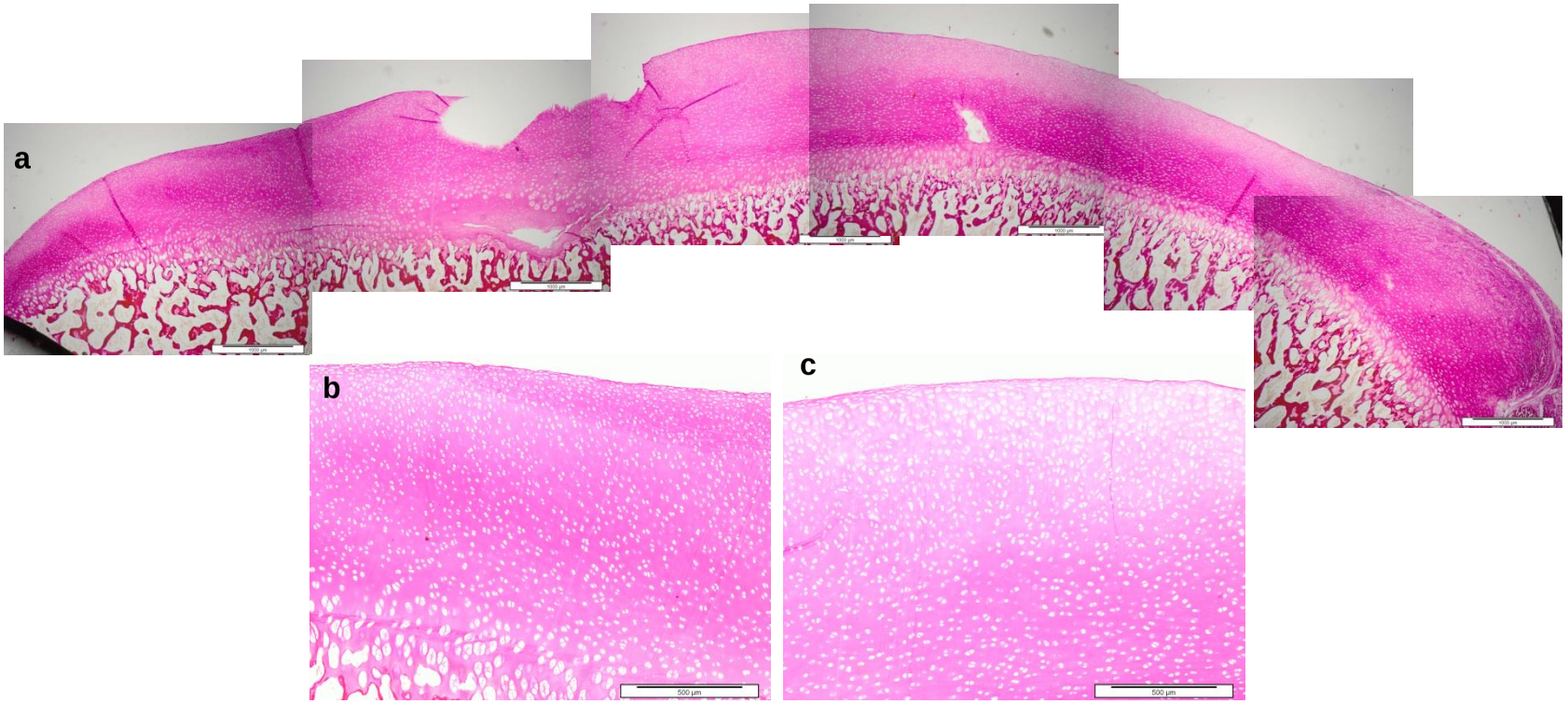

Figure 7.8. van Gieson stained sections of decellularised porcine condyle 1. a) full condyle, scale bar = 1000 µm, b) and c) scale bar = 500 µm.

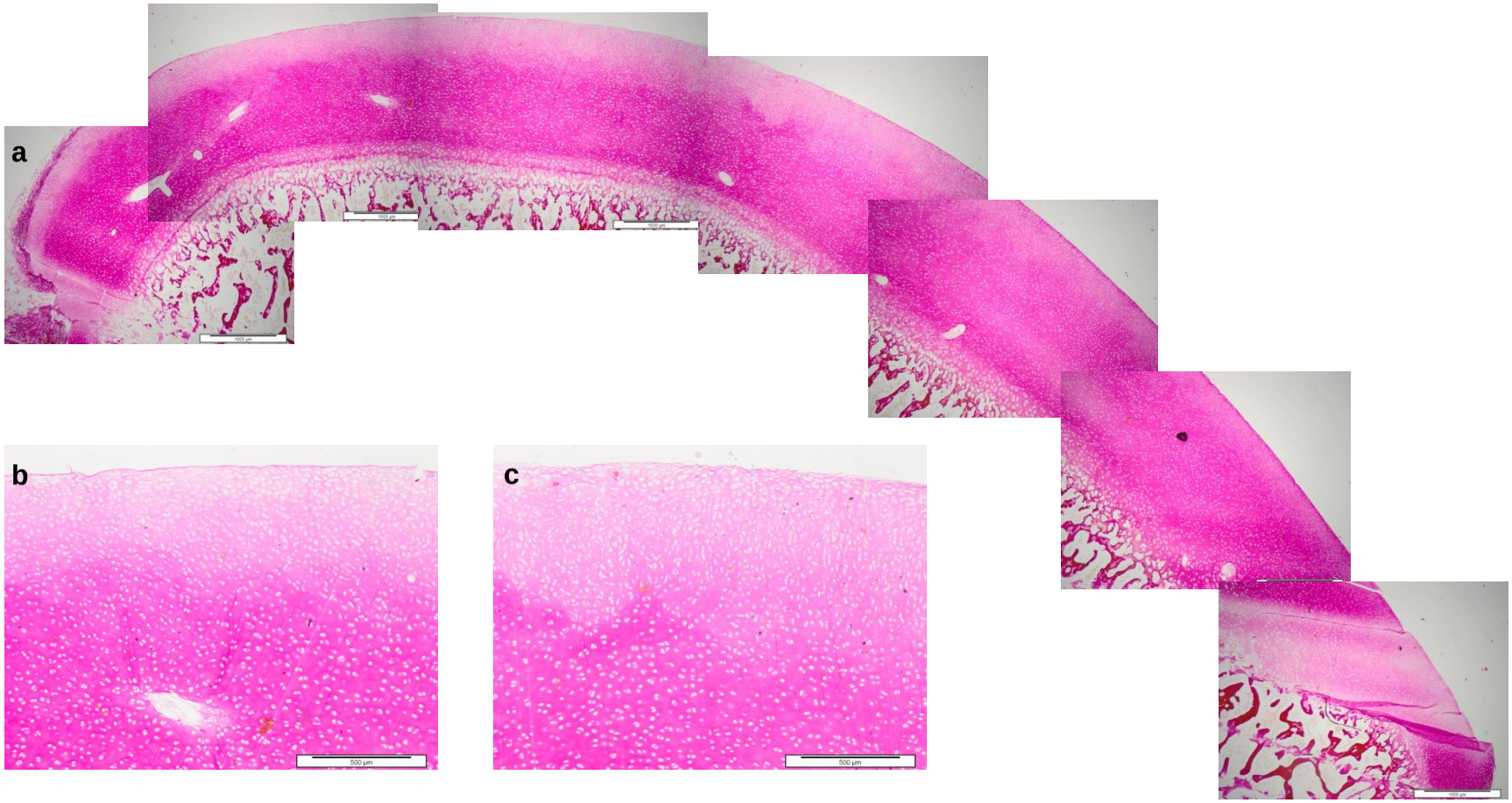

Figure 7.9. van Gieson stained sections of decellularised porcine condyle 2. a) full condyle, scale bar = 1000 µm, b) and c) scale bar = 500 µm.

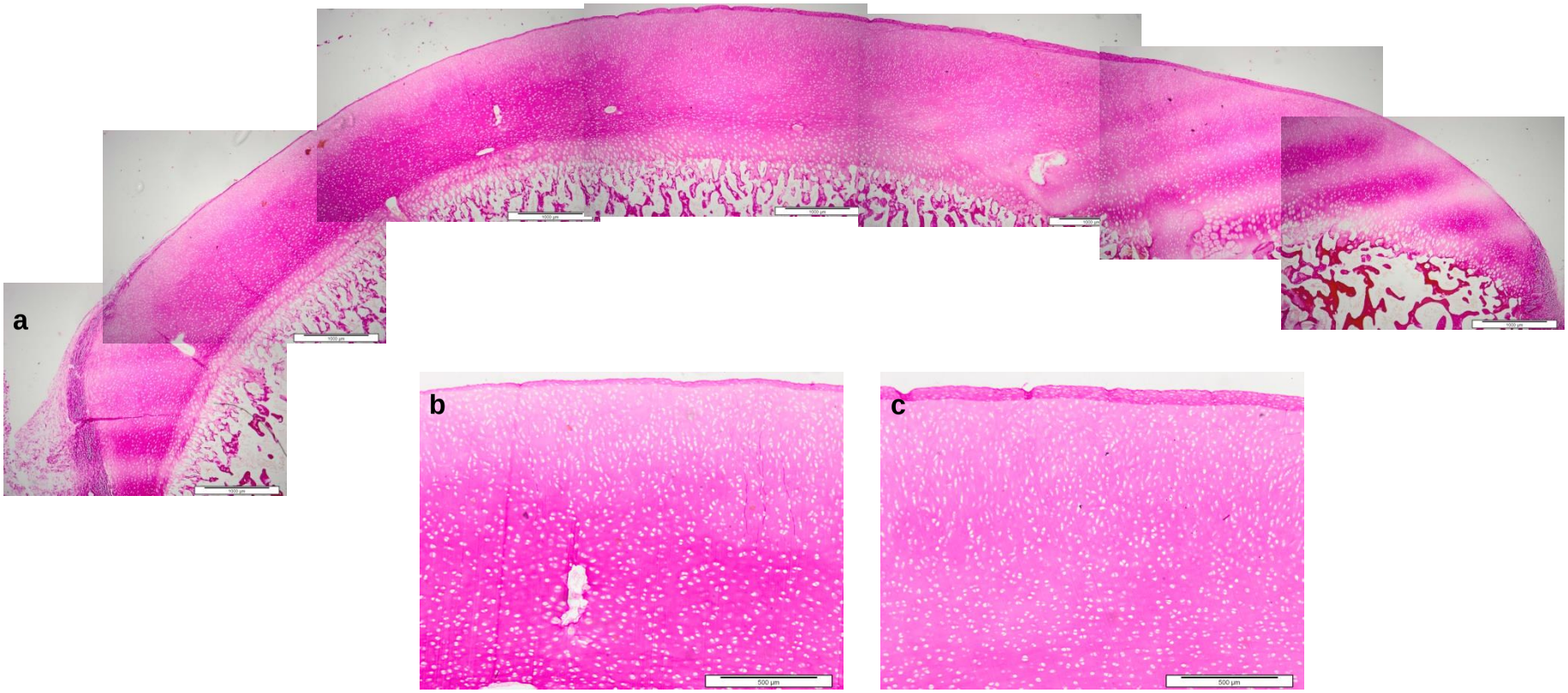

Figure 7.10. van Gieson stained sections of decellularised porcine condyle 3. a) full condyle, scale bar = 1000 µm, b) and c) scale bar = 500 µm.

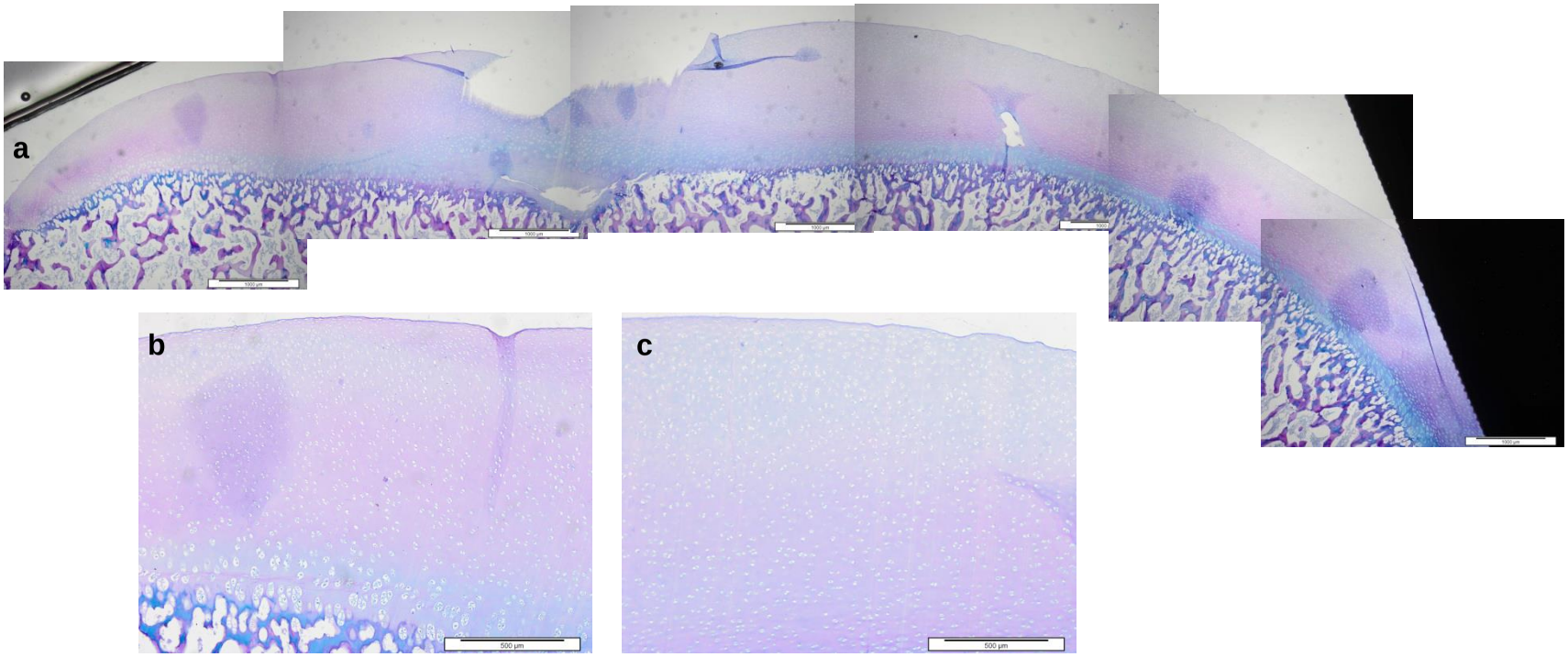

Figure 7.11. Alcian blue stained sections of decellularised porcine condyle 1. a) full condyle, scale bar = 1000 µm, b) and c) scale bar = 500 µm.

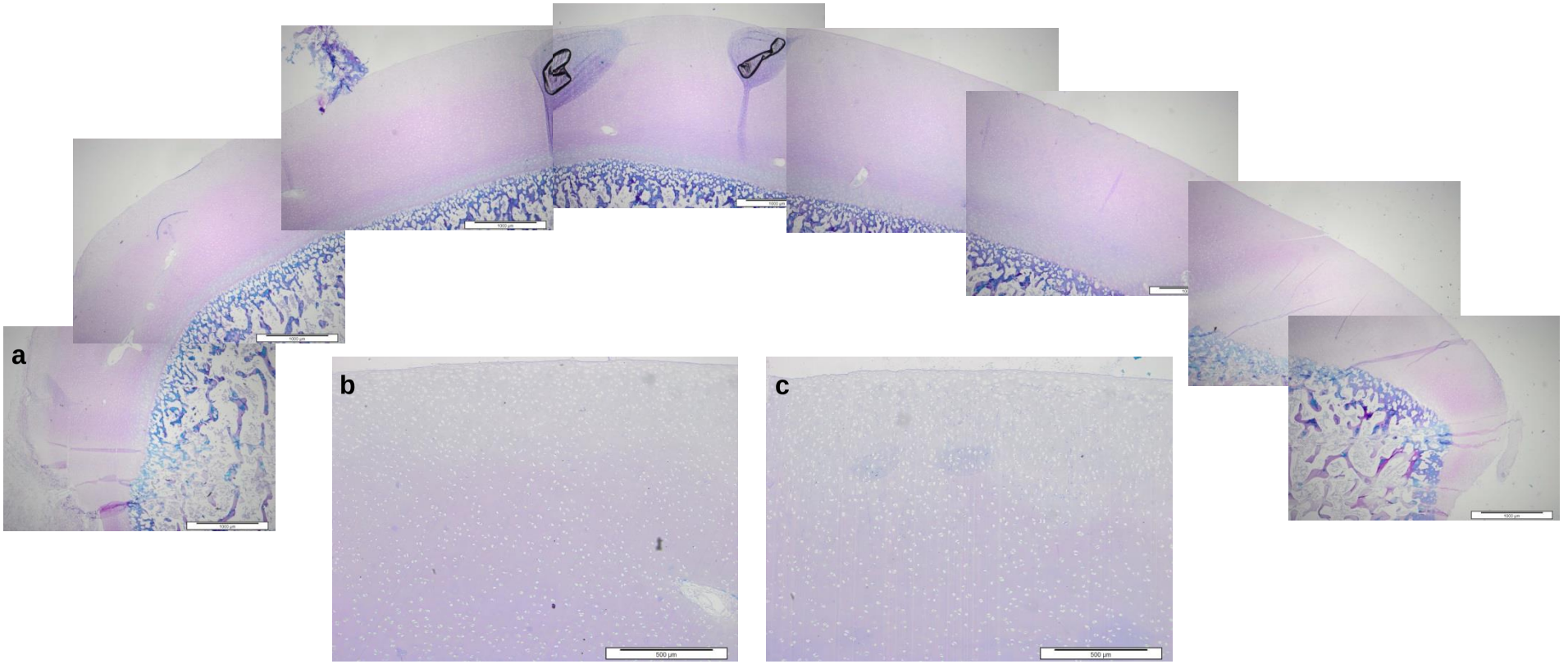

Figure 7.12. Alcian blue stained sections of decellularised porcine condyle 2. a) full condyle, scale bar = 1000 µm, b) and c) scale bar = 500 µm.

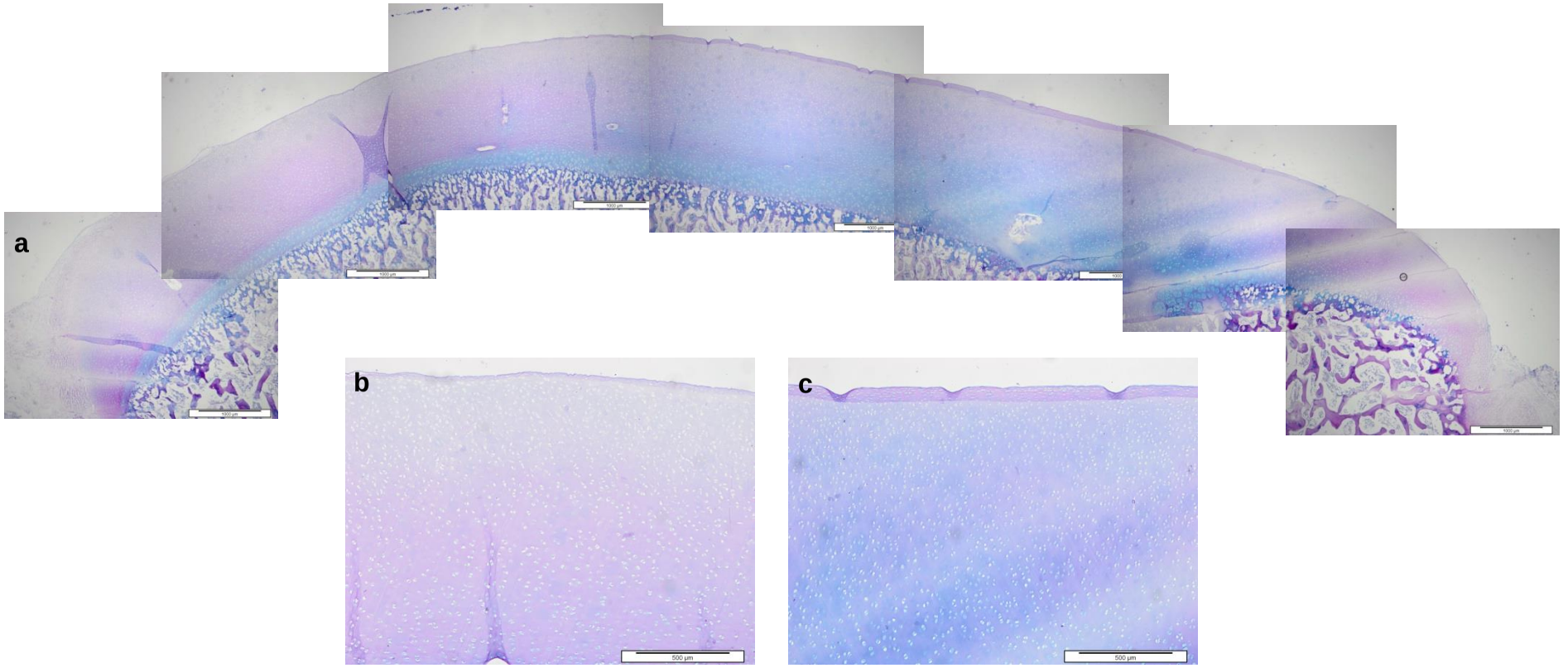

Figure 7.13. Alcian blue stained sections of decellularised porcine condyle 3. a) full condyle, scale bar = 1000 µm, b) and c) scale bar = 500 µm.

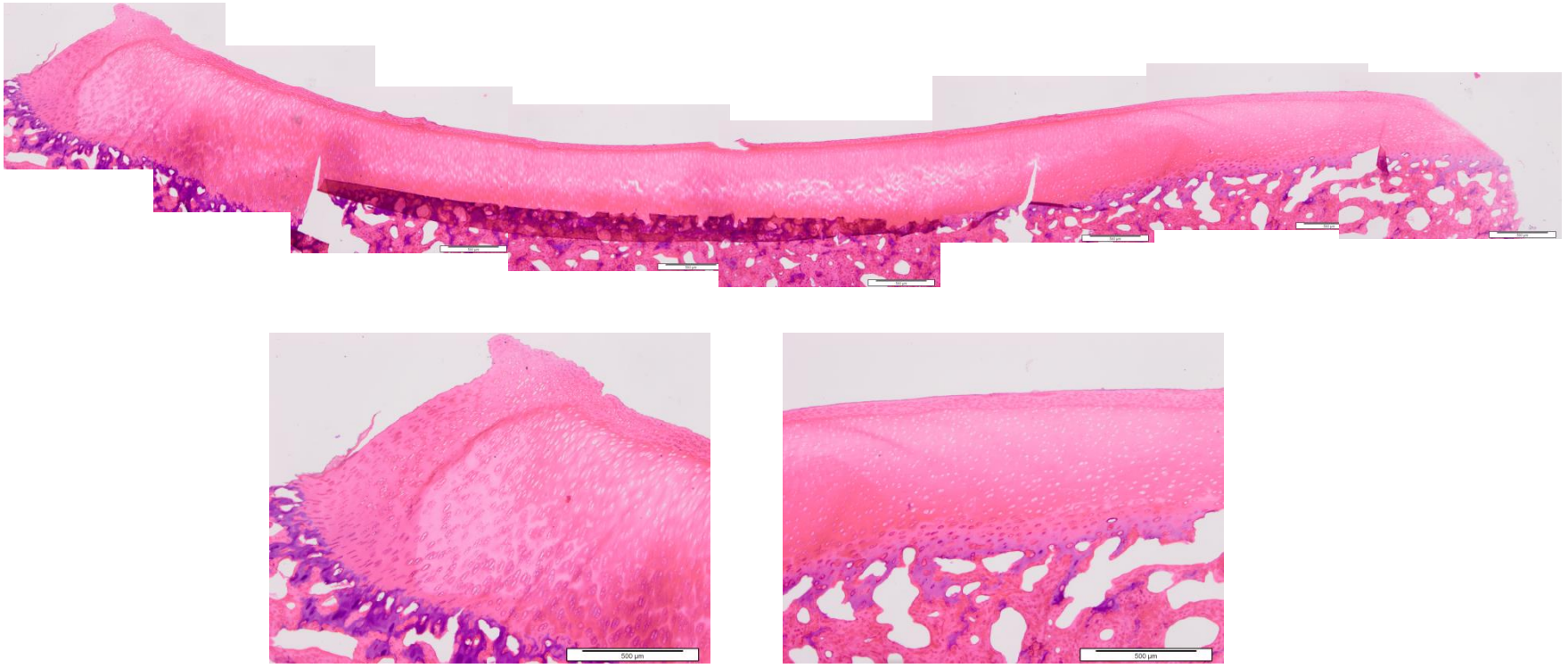

Figure 7.14 H&E stained sections of decellularised bovine groove plate 1. Cross section of plate, scale bar = 500 µm.

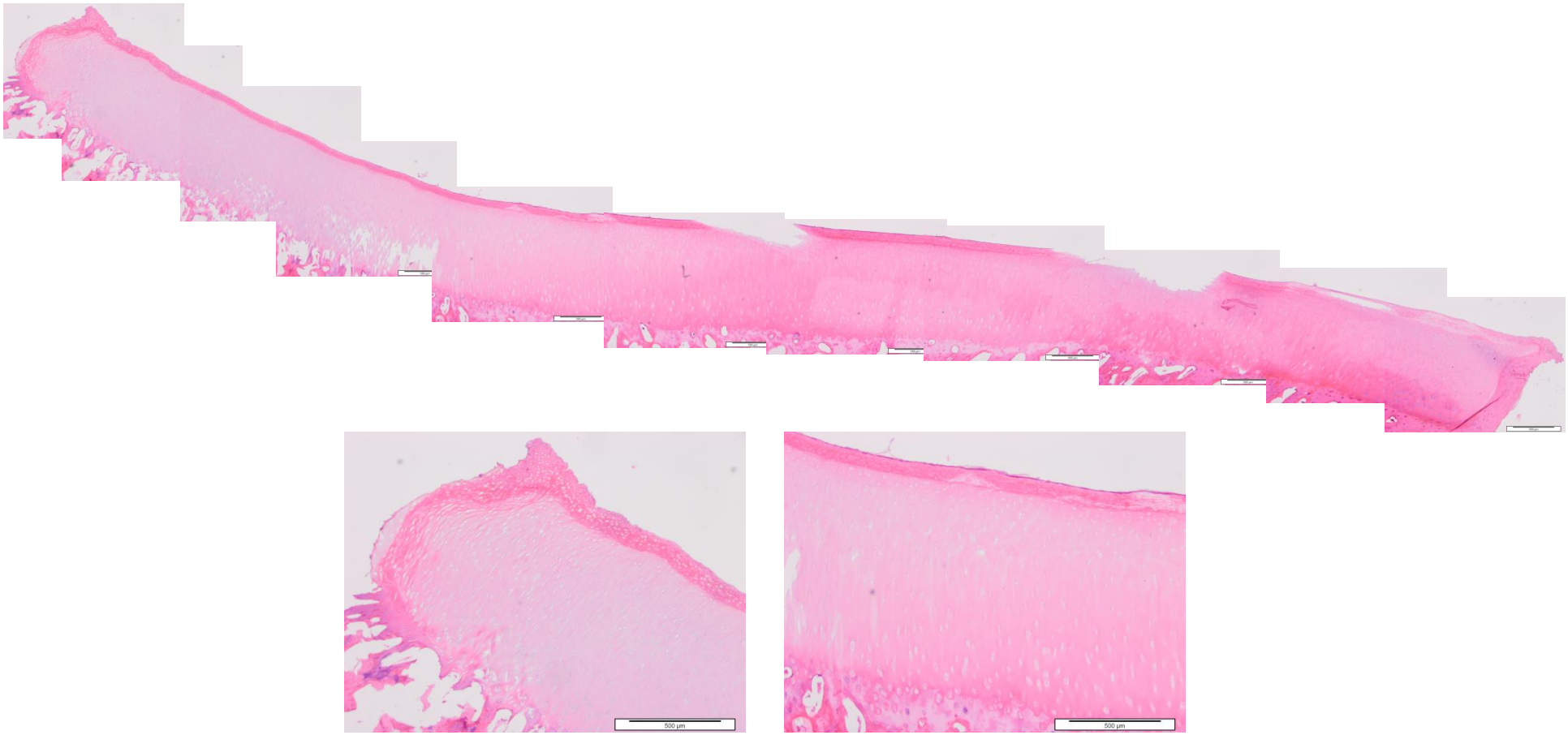

Figure 7.15 H&E stained sections of decellularised bovine groove plate 2. Cross section of plate, scale bar = 500 µm.

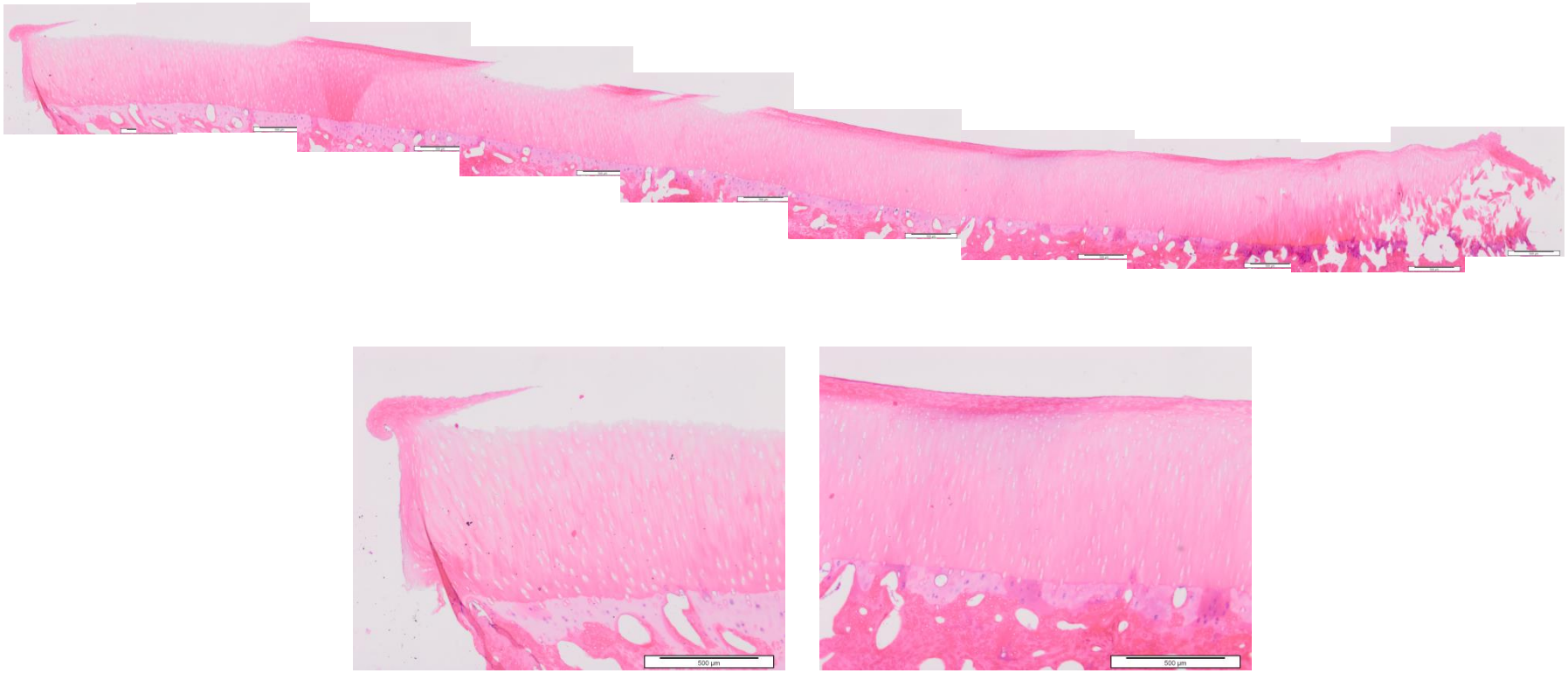

Figure 7.16 H&E stained sections of decellularised bovine groove plate 3. Cross section of plate, scale bar = 500 µm.

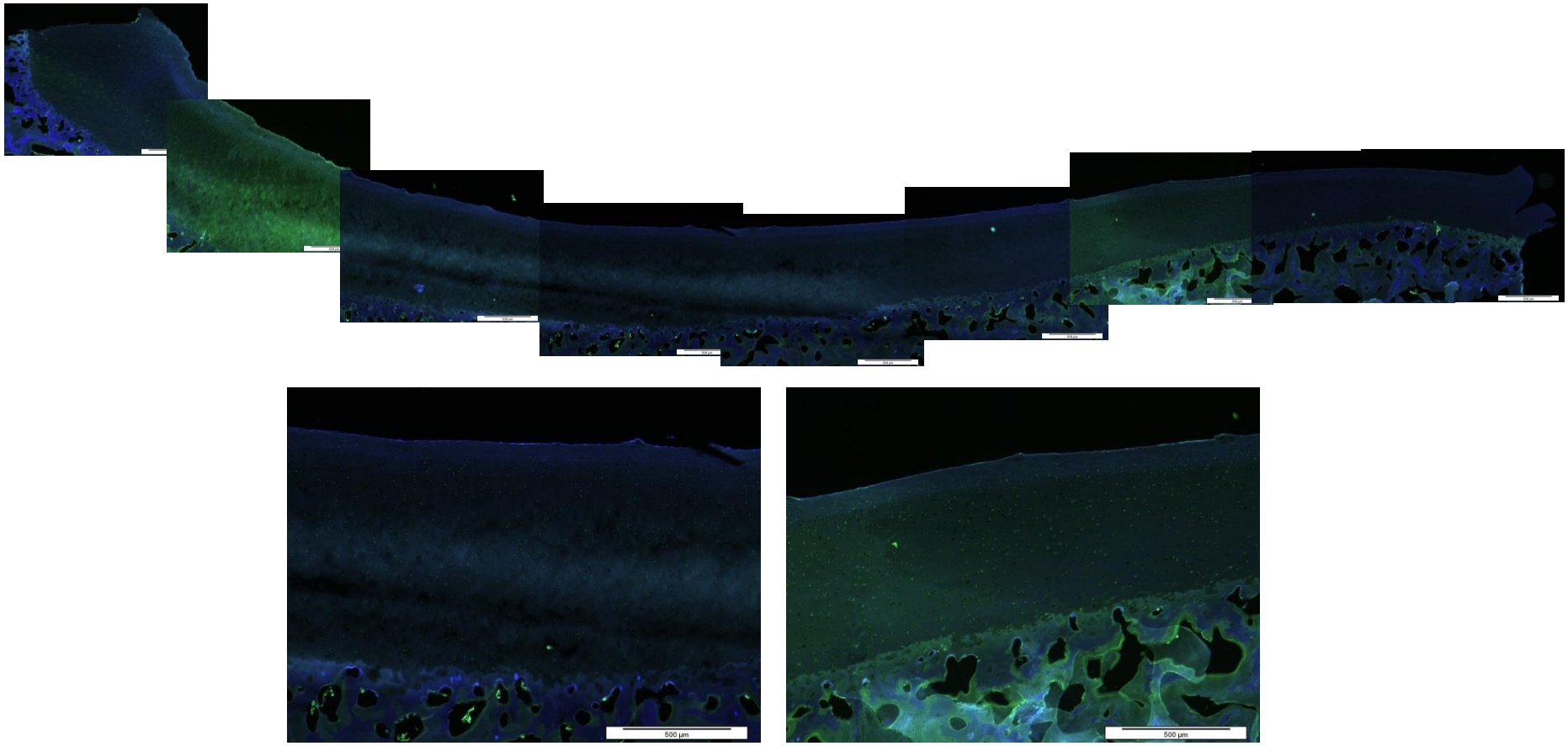

Figure 7.17 DAPI stained sections of decellularised bovine femoral groove plate 1. Cross section of plate, blue = DAPI, green = collagen autofluorescence, scale bar = 500 µm.

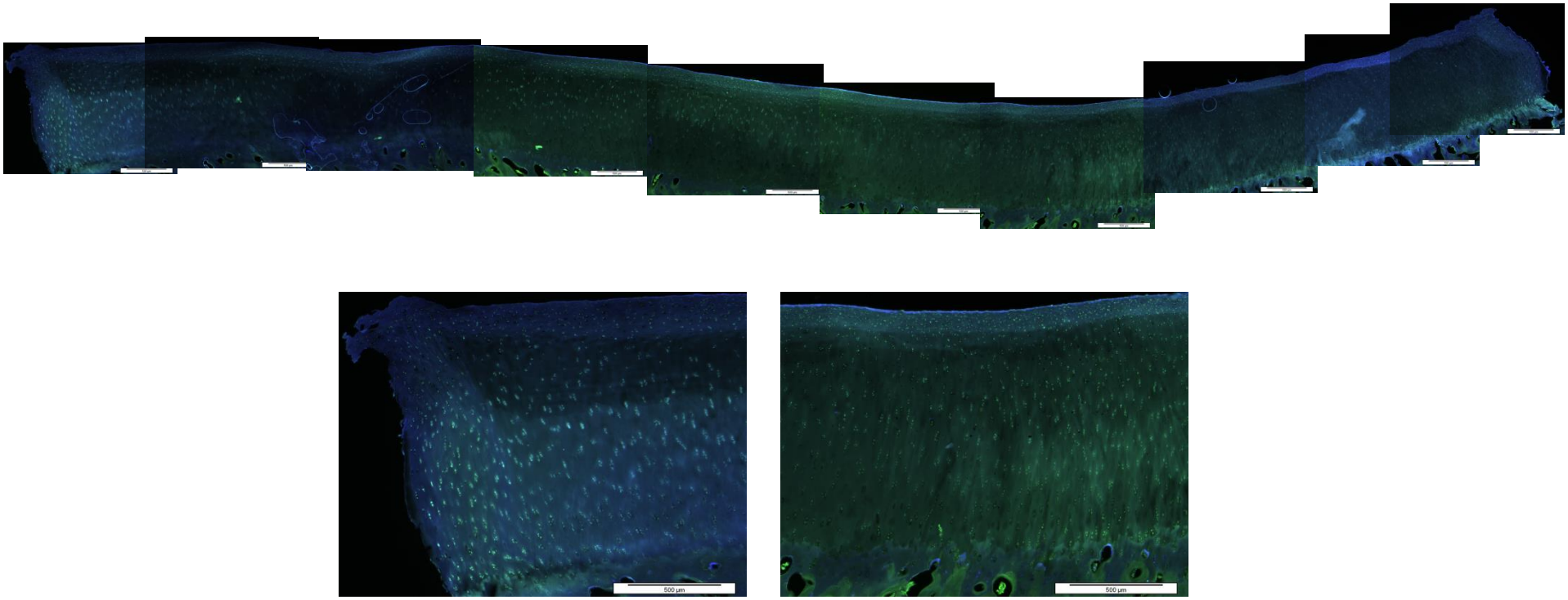

Figure 7.18 DAPI stained sections of decellularised bovine femoral groove plate 2. Cross section of plate, blue = DAPI, green = collagen autofluorescence, scale bar = 500 µm.

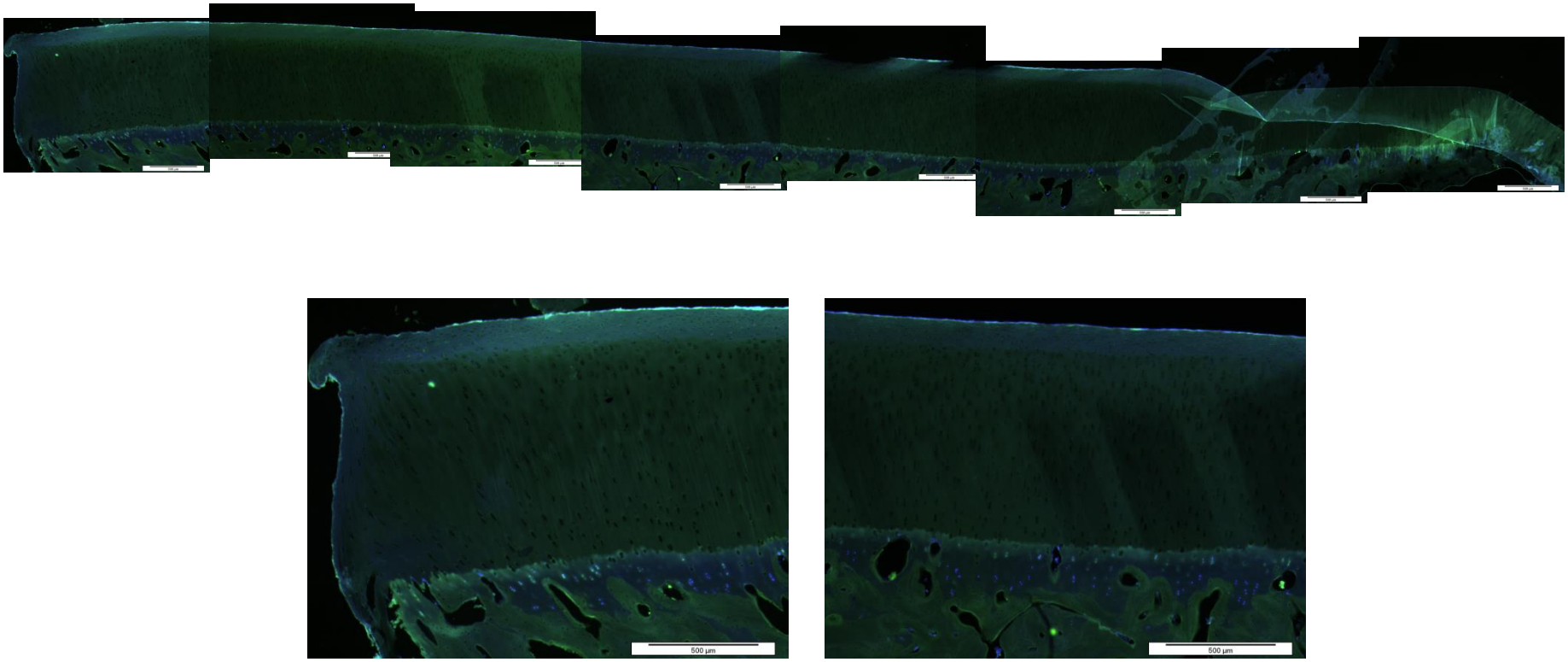

Figure 7.19 DAPI stained sections of decellularised bovine femoral groove plate 3. Cross section of plate, blue = DAPI, green = collagen autofluorescence, scale bar = 500 µm.

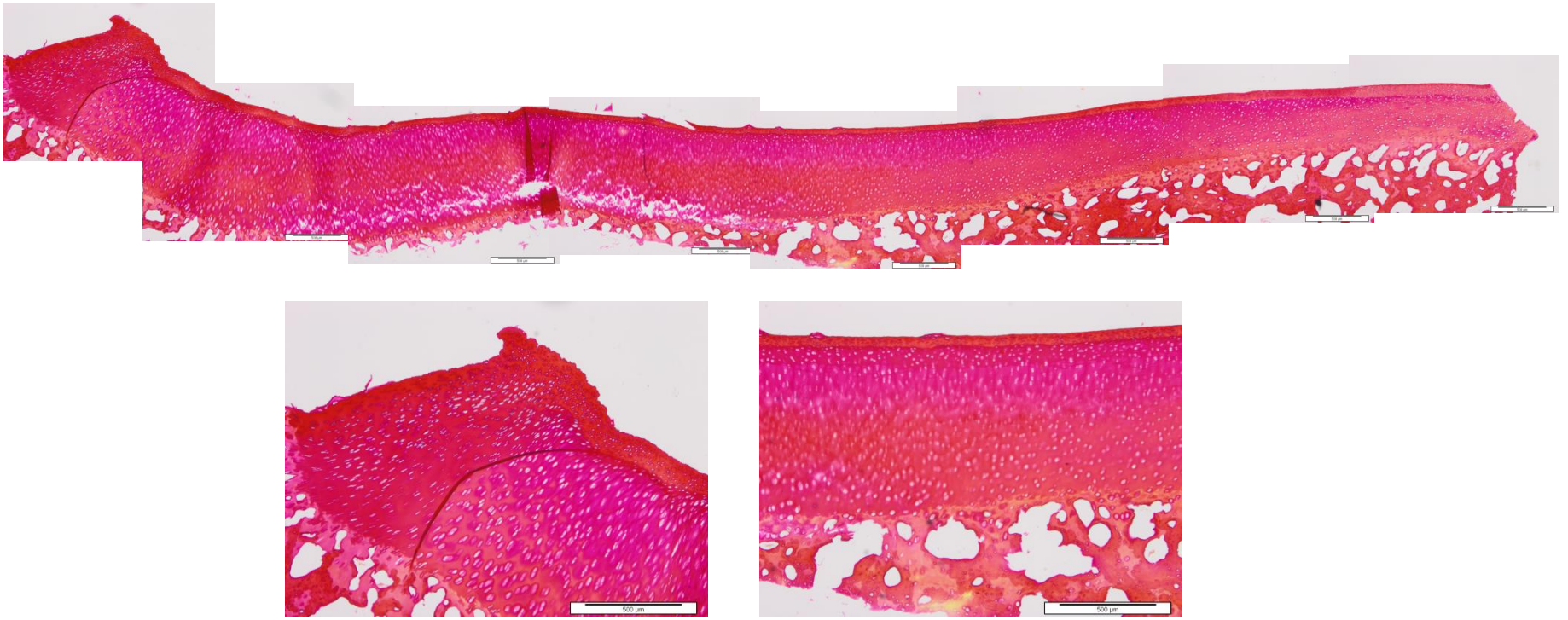

Figure 7.20 van Gieson stained sections of decellularised bovine femoral groove plate 1. Cross section of plate, scale bar = 500 µm.

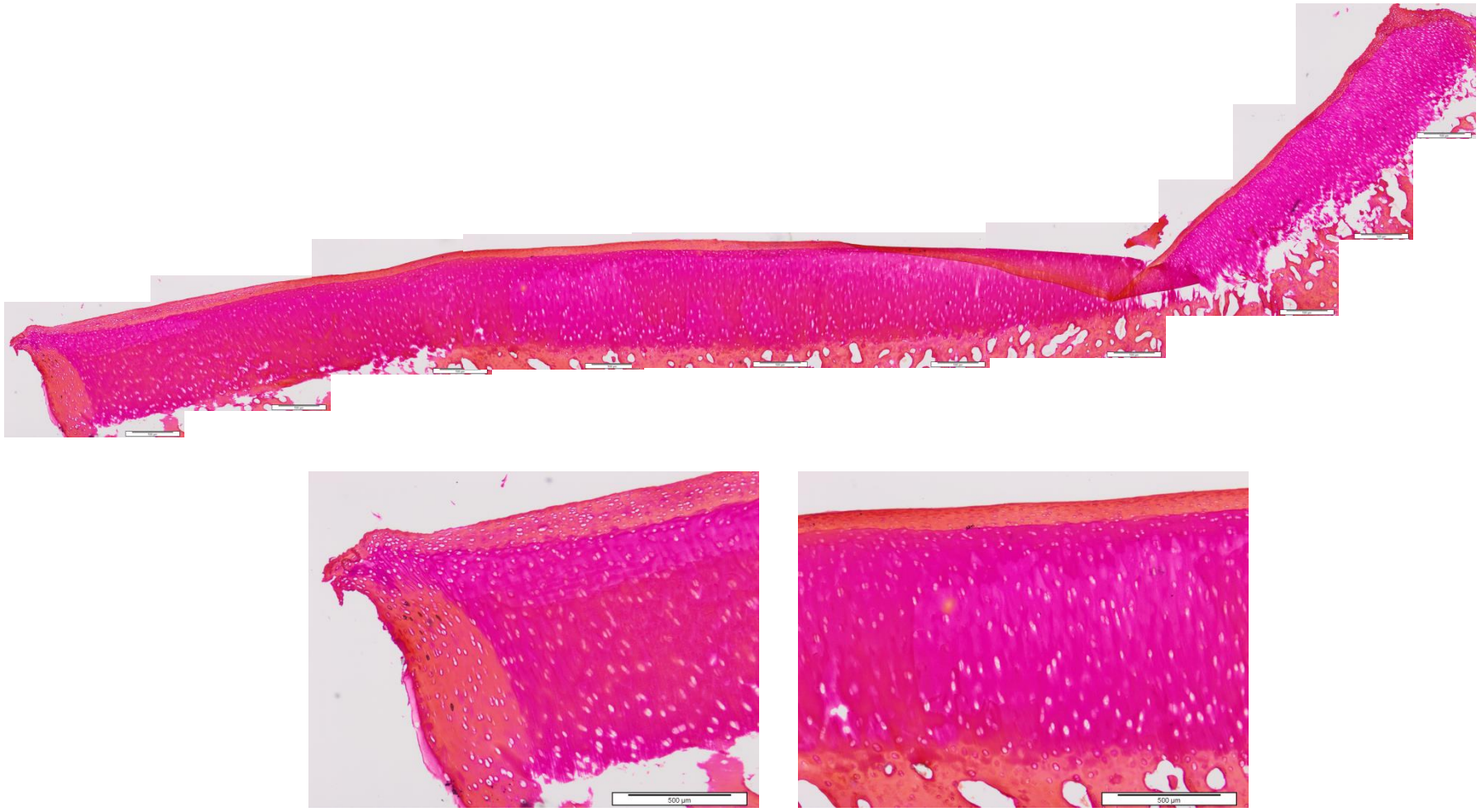

Figure 7.21 van Gieson stained sections of decellularised bovine femoral groove plate 2. Cross section of plate, scale bar = 500 µm.

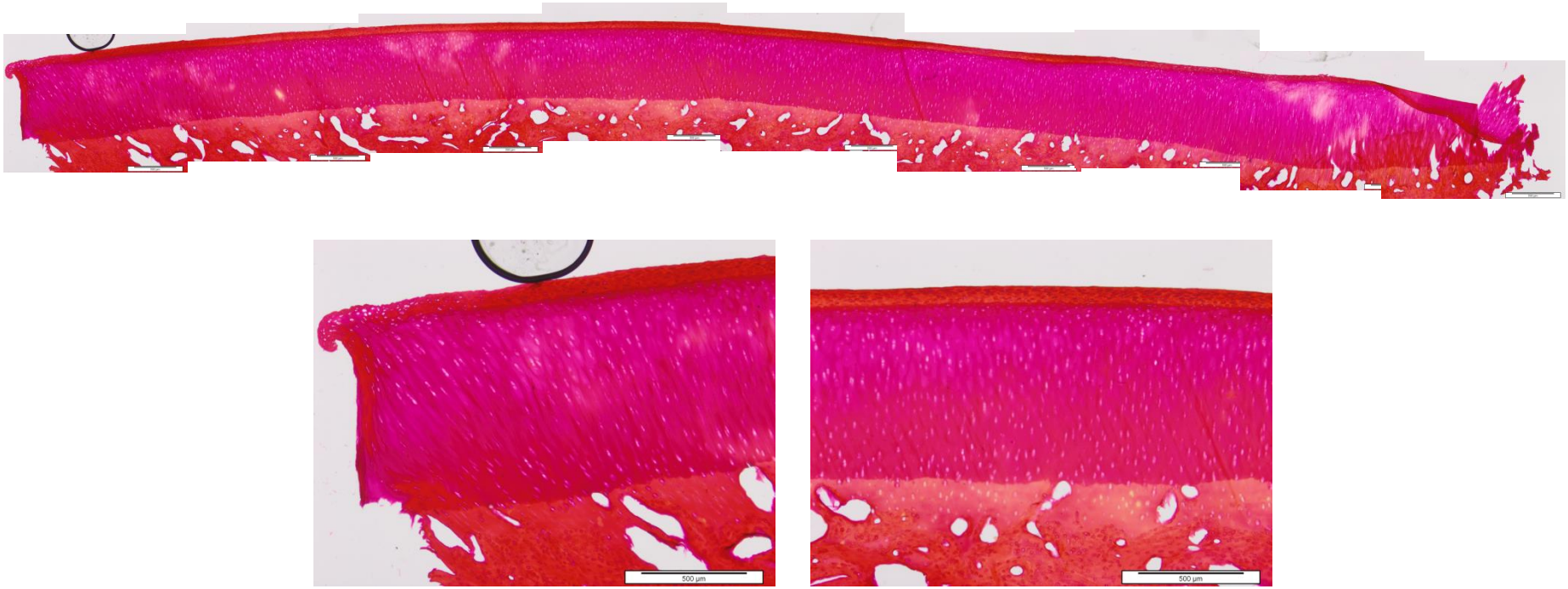

Figure 7.22 van Gieson stained sections of decellularised bovine femoral groove plate 3. Cross section of plate, scale bar = 500 µm.

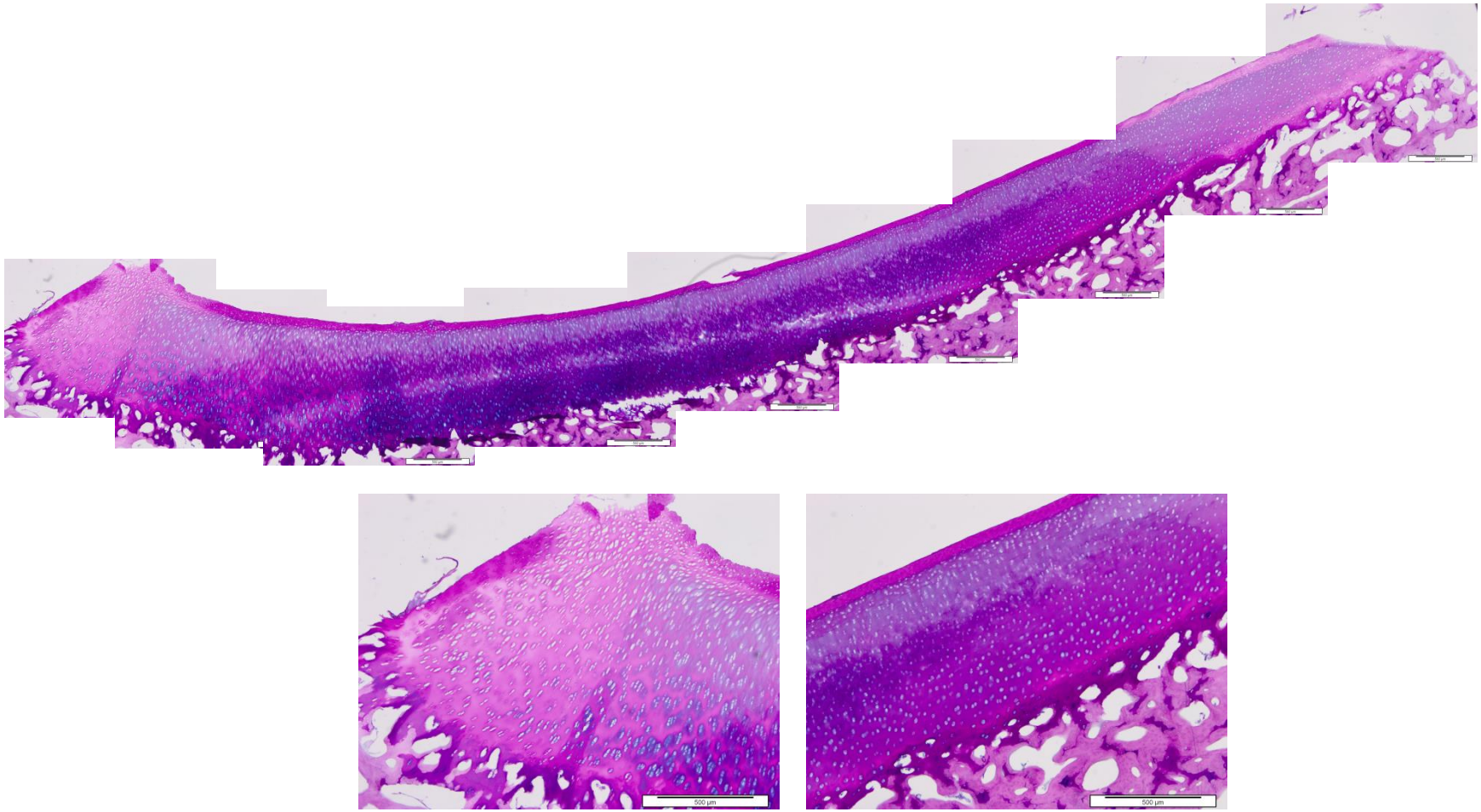

Figure 7.23 Alcian blue stained sections of decellularised bovine femoral groove plate 1. Cross section of plate, scale bar = 500 µm.

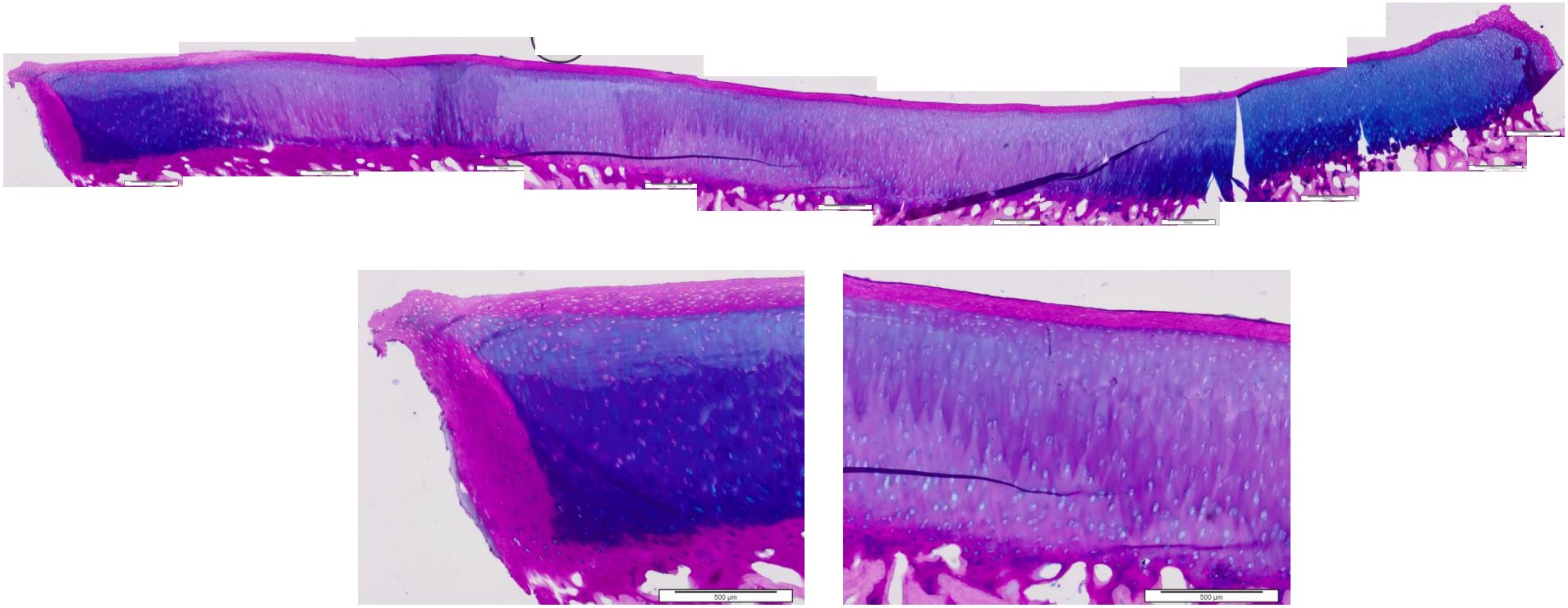

Figure 7.24 Alcian blue stained sections of decellularised bovine femoral groove plate 2. Cross section of plate, scale bar = 500 µm.

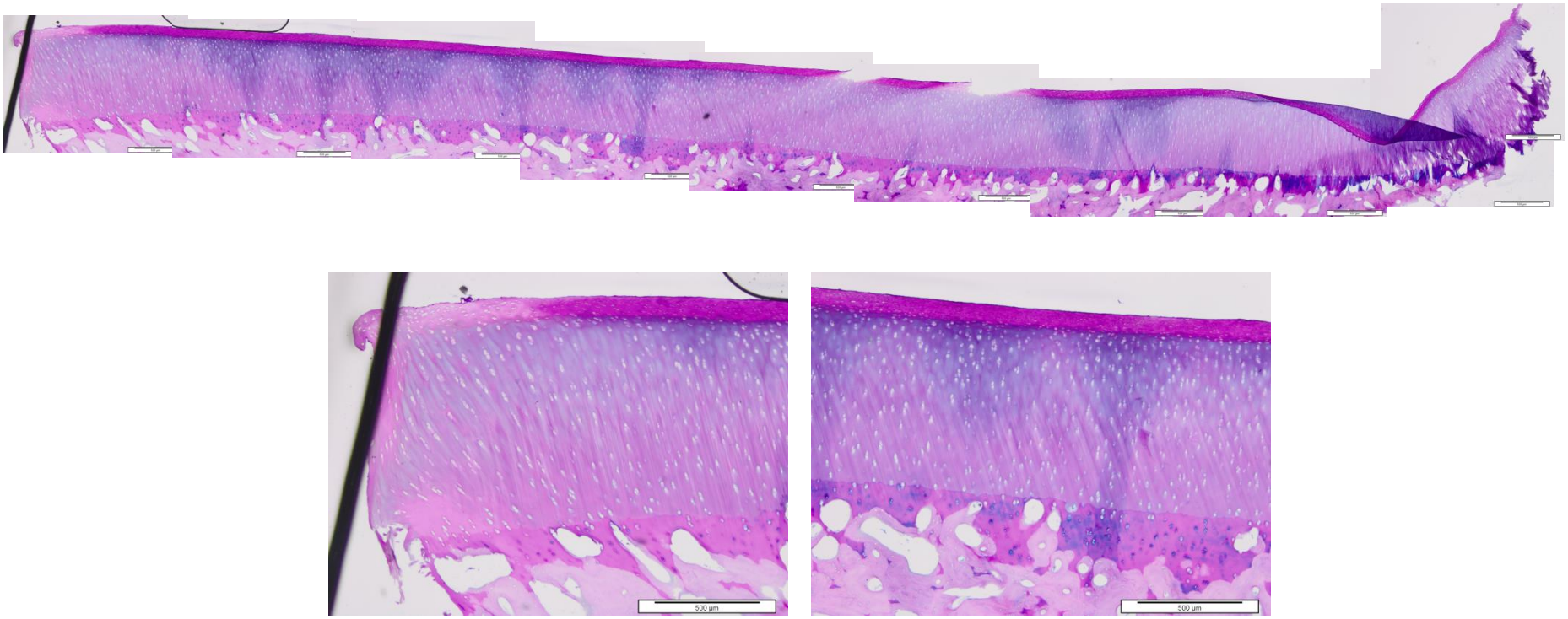

Figure 7.25 Alcian blue stained sections of decellularised bovine femoral groove plate 3. Cross section of plate, scale bar = 500 µm.

7.1 Discussion

Previous attempts to decellularise porcine osteochondral tissues (Chapter 5) resulted in the cartilage becoming damaged, showing a large reduction in GAGs and increase in water content. Macroscopically, damaged tissues appeared soft, shrinking in from the edges of the bone plug and presented with a roughened dull surface. Histologically, cartilage showed increased porosity, with the smooth collagen network becoming a more mesh-like matrix full of holes and the size of chondron lacunae appeared increased. The work in Chapter 5 attempted to systematically elucidate the cause of cartilage damage, the high temperature of incubations in the decellularisation solutions was found to be a contributing factor, but it was not possible to identify a protocol that fully eradicated the cartilage damage. Furthermore, the work carried out in Chapter 6 to determine the biocompatabiliy of decellularised bovine osteochondral scaffolds showed that increasing the duration of the terminal PBS wash cycles to greater than 60 h also resulted in damage to bovine cartilage, which had not previously been seen.

To further investigate the cause of cartilage damage, the preliminary work carried out in this Chapter used large osteochondral plates (2 mm x 4 mm, bovine) or whole condyles (porcine) to investigate the effect of having a reduced ratio of cut edges to cartilage area on cartilage stability during decellularisation. As reviewed in Chapter 1 and by Mow *et al.* (2005) the fibres of the cartilage collagen network have a characteristic orientation (Jeffery *et al*., 1991) and are under tension, providing the tensile strength of the tissue. Proteoglycans are dispersed throughout the collagen network and bind water in the tissue, providing the compressive strength of the tissue (Roughley, 2006). It was hypothesised that preparing osteochondral tissues for decellularisation by cutting around the circumference of the pin had severed collagen fibres and resulted in loss of tension, particularly in fibres orientated parallel to the surface in the cartilage superficial zone. With the loss of tension, the collagen network would have reduced ability to counter the repulsive forces of negatively charged proteoglycans being held in close

proximity to one another, resulting in an increase in porosity allowing GAGs to be removed, more water to enter the tissue and the collagen fibres to therefore clump together.

Porcine osteochondral blocks (50 mm in length, 10 mm in width and 10 mm in depth) with a larger area to cut edge ratio than 9 mm diameter pins were successfully decellularised by Kheir *et al.* (2011) using a similar protocol to that described here. The osteochondral blocks were subject to four cycles of freeze thaw (the final two in hypotonic solution) and then incubated through 6 cycles of 24 h in hypotonic solution followed by 24 h in 0.1 % (w/v) SDS in hypotonic solution, both containing aprotinin and EDTA at 45 °C with agitation. Blocks were than treated with nuclease and sterilised using 0.1 % PAA (v/v). The process was completed by 2 x 30 min PBS washes and a short 24 h final PBS wash. Following use of this protocol, porcine osteochondral tissues were fully decellularised and remained intact. Histological analysis showed full removal of cell nuclei, however GAG content was greatly reduced. No collagen clumping, characteristic of cartilage damage was seen, however some loss of tension could be seen at the surface and superficial zone of cartilage sections stained specifically using an antibody against collagen type II.

In contrast, Shwartz *et al*. (2012) used much smaller 5 mm diameter discs of human and porcine nasal septum cartilage with a large cut edge to area ratio. The decellularised tissue had the characteristic collagen clumping and loss of GAG seen in severely damaged cartilage in this study (Chapter 5), differing greatly to decellularisation results seen by Kheir *et al.* (2011).

The size of osteochondral tissues used for decellularisation in this Chapter was therefore increased to minimise the ratio of cut edge to cartilage area. For bovine osteochondral tissues, the ratio of cut edge to cartilage area was reduced by using larger osteochondral plates (2 mm x 4 mm) as opposed to small pins (9 mm diameter). For porcine osteochondral tissues, only one cut edge was produced when separating the condyle from the groove, all other edges were natural cartilage edges on the condyle.

Following decellularisation the bovine tissues were not fully decellularised and showed some damage, especially at the cut edge and cartilage surface.

The central cartilage regions retained GAG content and did not show the porous structure characteristic of damage histologically. The cartilage did not detach from the bone or appear damaged macroscopically, with the exception of the cut edges.

Porcine tissues did not appear damaged macroscopically following decellularisation, but upon histological analysis, characteristic damage could be seen in the superficial zone of the cartilage and at the surface, however this damage appeared less severe than that seen in bovine cartilage. The tissues were almost completely decellularised apart from a few nuclei still present at the cartilage-bone interface and the tissue remained intact following extended washing in PBS.

It was therefore demonstrated that reducing the ratio of cut edges to cartilage area greatly improved cartilage stability during the decellularisation processes, but did not completely eradicate cartilage damage. Additional steps should be taken to ensure complete decellularisation of porcine whole condyles and bovine blocks. It would then be possible to harvest acellular osteochondral pins of clinically relevant size from the least damaged regions of these decellularised large osteochondral constructs.

Further biochemical and biomechanical testing is required to determine the degree of damage caused to decellularised whole condyles and determine whether the resultant tissues retained adequate biological and biomechanical function for use as a cartilage substitution biomaterial.

Chapter 8
Discussion

8.1 General Discussion

The underpinning hypothesis of this study was that it was possible to generate an acellular xenogeneic osteochondral graft material of future clinical utility in osteochondral lesion repair. A novel regenerative cartilage repair material such as this is required, as joint damage is common in the active population. Osteochondral lesions as a result of trauma can in themselves cause pain, swelling and mechanical problems, reducing the quality of life for patients (Minas & Nehrer, 1997). Furthermore, some instances of osteoarthritis have been found to originate from initially minor cartilage lesions (Ding *et al.*, 2005) which, due to their avascular nature are unable to undergo healing and repair, so degenerate over time with regular joint loading and articulation (Chaing & Jiang, 2009). Currently, for osteoarthritic joints, the only effective treatment is total joint arthroplasty. In the case of osteoarthritis which originates from cartilage lesions, early intervention therapies are available to prevent or delay the disease onset by repair of the initial lesion. Surgical therapies currently performed to preserve cartilage such as lavage and debridement (Chang *et al.*, 1993; Moseley *et al.,* 2002) and marrow stimulation techniques (Steinwachs *et al.,* 2008) however have variable long term outcomes and often result in inferior fibrocartilage like repair materials. Similarly, perichondrial/periosteal grafting, mosaicplasty (Koulalis *et al.,* 2004) and autologous chondrocyte implantation (Grande *et al.,* 1989) may result in donor site morbidity amongst other complications (Minas & Nehrer, 1997; Lützner *et al*., 2009).

As current surgical techniques have been unable to restore fully functional hyaline cartilage, tissue engineering is seen as the way forward in developing adequate cartilage repair therapies with good long term prognosis, by optimising and balancing scaffold biomaterials with bioactive factors and cells (Vinatier *et al*., 2009). Biomaterials can be broadly labelled

as natural or synthetic. Synthetic materials currently being researched include polylactic acid (PLA; Giurea *et al*., 2003) and polyglycolic acid (PGA; Liu *et al*., 2002), they are easy to manufacture and their specific properties can be accurately controlled to mimic the natural ECM. The biomechanical properties of such materials can be tailored, however, often there are issues with tissue integration, a lack of biological cues and detrimental degradation products (Atala, 2007, Puppi *et al*., 2010). Natural biomaterials such as collagens (Frenkel *et al*., 1997) or hyaluronic acid (Grigolo *et al*., 2001) have the advantage of low toxicity and biological signalling, however there are issues regarding batch variation and they do not have adequate biomechanical properties (Puppi *et al*., 2010).

The aforementioned biomaterials, although promising, do not show the same level of structural and biological complexity found in healthy cartilage which is key to the function and regeneration potential of the natural tissue. Recent tissue engineering approaches have been to decellularise or devitalise natural ECM scaffolds, thereby retaining the natural ECM constituents and structure as well as biological cues such as growth factors whilst removing immunogenic materials which would result in graft rejection (Crapo *et al.*, 2011, Benders *et al*., 2013).

This tissue engineered acellular ECM approach is already being used clinically for a number of tissues including heart valves (Bach *et al*., 2005) and trachea (Macchiarini *et al*., 2008). Decellularised small intestinal submucosa (SIS) has been used clinically for over a decade to repair tissues such as skin, muscle and tendon (eg. Restore™, DePuy Orthopaedics; Surgisis®, Cook Biotech Inc.). For musculoskeletal tissue repair, decellularised ECM biomaterials including tendon (Ingram *et al*., 2007; Martinello *et al*., 2012) and meniscus (Stapleton *et* al., 2008) are undergoing development. The current study was performed with the aim of producing a decellularised osteochondral ECM scaffold from xenogeneic tissues which could be used either seeded with cells or as a standalone off-the-shelf product to enable effective long term repair of osteochondral lesions.

This tissue engineered approach for cartilage or osteochondral repair has previously been researched in a number of studies and the current research

position was well summarised by Benders *et al*. (2013). Some approaches have focused on homogenising cartilage tissue by lyophilisation and grinding (Yang, Z *et al*., 2010) or shattering into fragments and centrifuging to produce microfilaments (Yang, Q *et al*., 2008) prior to decellularisation. Scaffolds produced from decellularised homogenised cartilage have the benefit of retaining bioactive cues for cell growth and are also more customisable, however, they lack the 3D architecture and structure of native cartilage and therefore have reduced biomechanical function. Other approaches have been to research the decellularisation of cell derived cartilage ECM (Elder *et al*., 2009). Decellularised cell-derived-ECM scaffolds have no issues of biocompatibility, however the need to culture cells renders the process time consuming and this approach requires cell harvesting from the patient, increasing the number of invasive procedures performed and potentially causing donor site morbidity. Yet another approach has been to develop methods to decellularise intact, native 3D cartilage tissues (Elder *et al*., 2010, Schwarz *et al*., 2012). The decellularisation of intact native cartilage tissues has the potential to produce an ECM with bioactive cues, and with the natural biological, biochemical and biomechanical composition and structure.

Although protocols for whole native 3D cartilage decellularisation are currently under development, there are to date no reports of the clinical relevance/success of such products. Such approaches do not provide a subchondral bone component for integration and stability of a cartilage repair biomaterial upon implantation.

Kheir *et al.* (2011) developed a process to decellularise porcine osteochondral tissues, whereby intact, full thickness, zonal cartilage, subchondral bone plate and trabecular bone were fully acellular and biocompatible and retained similar biological and biochemical composition compared to native tissue. In this decellularisation protocol, osteochondral blocks (50 mm in length, 10 mm in width and 10 mm in depth) were subject to four cycles of freeze thaw (the final two in hypotonic solution) and then incubated through 6 cycles of 24 h in hypotonic solution followed by 24 h in 0.1 % (w/v) SDS in hypotonic solution, both containing aprotinin and EDTA at 45 °C with agitation. Blocks were then treated with nuclease and sterilised

using 0.1 % PAA (v/v). The process was completed by 2 x 30 min PBS washes and a short 24 h final PBS wash. The decellularised matrix had reduced GAG content compared to native cartilage which resulted in inferior biomechanical properties. Additionally the size and shape of the acellular osteochondral matrix was not appropriate for current surgical applications, such as mosaicplasty.

The current study was intended to improve and progress the work of Kheir *et al*. (2011), Firstly by addressing the xenogeneic source material used for decellularisation, to identify a joint region and species which had similar biological, biochemical and biomechanical properties to human cartilage, and potentially find a tissue with high GAG content, to reduce the detrimental effect of GAG loss following decellularisation. The source material would also be shaped to a 9 mm diameter osteochondral pin, to enable the biomaterial to be used with current surgical techniques and equipment. Secondly, alterations to the established decellularisation protocol (Stapleton *et al*., 2008; Kheir *et al*., 2011) were investigated to minimise GAG loss and produce a biologically, biochemically and biomechanically acceptable osteochondral scaffold. The improved decellularised scaffold could then be investigated in terms of biocompatibility and regenerative capacity.

A variety of source tissues have been used for articular cartilage decellularisation including immature 4 week old calf cartilage from the distal femur (Elder *et al*., 2010), 7 – 8 month old pig knee cartilage (Schwartz *et al*., 2012) and osteochondral tissues from the femoral groove of 4 month old pigs (Kheir *et al*., 2011). It has been well documented that the biomechanical properties of cartilage vary topographically (Shepherd & Seedhom, 1999b), as does the cartilage GAG content (Rogers *et al*., 2006) and thickness (Shepherd & Seedhom 1999a). It therefore seems sensible to constrain a decellularisation source cartilage to a specific joint region, rather than taking, for example, distal femoral knee cartilage as a whole, in order to avoid unnecessary variation in the properties of the final scaffold. Similarly, cartilage properties are also known to vary between species (Athanasiou *et al*., 1991; Kääb *et al*., 1998) and with age (Julkunen *et al*., 2009; Rieppo *et al*., 2009; Hamann *et al*., 2013). The properties of a decellularised scaffold will relate to those of the source material, so it was logical that donor

species, age and joint region should be investigated to determine the optimum starting material to produce a scaffold with acceptable properties for use in human patients.

In the current study, cartilage from three common species were investigated; pig (6 month), cow (18 month) and sheep (aged ~12 month or > 4 year). Tissues were compared from the acetabulum and femoral head of the hip and the groove, medial and lateral condyles and medial and lateral tibial plateau of the knee of each species. Ovine cartilage, being from the smallest species, was thinnest (femoral groove cartilage was 0.86 mm in young sheep and 0.63 mm in old sheep) much thinner than values reported for human cartilage (1.76-2.59 mm, Shepherd & Seedhom 1999b). If implanted into a human knee joint, the ovine osteochondral pin would not be able to simultaneously align at the surface and at the cartilage-bone interface with the surrounding human tissue which would be problematic for integration and function. For this reason, ovine tissues were discounted as a potential source material. Additionally, mature ovine tissues showed signs of degeneration, being yellowed and stiffened suggesting the presence of advanced glycation end products (Bank *et al.*, 1998). Both porcine and bovine tissues had comparable cartilage thickness to human (2.04 mm and 1.52 mm respectively), and also showed high levels of sulphated proteoglycans, 78 ± 30 $\mu g.mg^{-1}$ and 68 ± 8 $\mu g.mg^{-1}$ GAG per wet weight cartilage respectively, compared to the 54.7 $mg.g^{-1}$, 38.6 $mg.g^{-1}$ (Vilim *et al.*, 1991) and 25 – 40 $\mu g.mg^{-1}$ (Hollander *et al*., 1991) quoted for human femoral head cartilage. The biomechanical properties of each species differed, with bovine cartilage being stiffer than porcine on the whole, with an equilibrium elastic modulus of 0.66 MPa and 0.81 MPa respectively for cartilage from the lateral condyle, compared to an equilibrium aggregate modulus of 0.70 MPa for human cartilage (Athanasiou *et al*., 1991). The relatively low stiffness of porcine cartilage was in contrast with the high GAG content measured which should infer compressive resistance, this highlighted the possible effects of cartilage maturity. Proteoglycans within the relatively immature porcine cartilage may not be as well developed and functional as those of mature tissues. Differences were seen between the properties of different joint regions, with cartilage from the femoral knee (condyles and

groove) tending to be thickest and having higher GAG content than other areas, the tissue in these regions also tended to be stiffer.

Regrettably, biotribological analysis of cartilage was not performed in the current study. It has been reported that the coefficient of friction of cartilage is increased with GAG depletion (Katta *et al*., 2009), likely due to reduced biphasic and surface lubrication. Varying levels of proteoglycans, therefore, may have an impact on the frictional properties of cartilage from different species and/or joint regions. Information in the literature regarding this is limited for comparison due to the variation in testing conditions.

A major limitation of this aspect of the current study is that animals of different ages were compared. This was due to the restricted availability of animals bred from the food chain for human consumption. In this case, it is difficult to discern which properties can be attributed to the species and which to the stage of cartilage maturation. This raises an intriguing point for consideration, is a mature or immature source tissue more appropriate for an acellular natural ECM scaffold? As highlighted previously, underdeveloped, immature cartilage may not have the same biomechanical function as mature human cartilage, which may restrict the success of such a material upon implantation. However, beneficially, immature cartilage is still undergoing growth and remodelling, it is more metabolically active than fully developed mature cartilage. It stands to reason that the growth factors and biological signals which are present, guiding tissue growth, may be advantageous if retained in a decellularised scaffold, to potentially improve recellularisation and neomatrix deposition by infiltrating host cells. Furthermore, immature porcine cartilage had an underdeveloped subchondral bone plate and vascularisation of the cartilage. These features may aid in the migration of host cells (including mesenchymal stem cells) from the surrounding bone marrow and cartilage.

As the benefits of using a mature versus an immature tissue were unknown, it was decided that two tissues, immature porcine medial condyle and mature bovine medial groove osteochondral tissues should both be taken forward as source materials for the development of a decellularisation

protocol, based on the biological, biochemical and biomechanical properties investigated.

Following a number of iterations, a protocol was optimised to decellularise bovine osteochondral pins. The method, based on that of Stapleton *et al*. (2008) and Kheir *et al*. (2011), comprised a novel incubation of osteochondral pins in PBS with proteinase inhibitors for 18 h followed by use of a water pik to physically remove bone marrow. In accordance with previous methods, tissues underwent four freeze/thaw cycles (two of which were in hypotonic buffer) to produce ice crystals to physically open up the matrix and produce an osmotic tension to lyse cells. Tissues were then subject to two cycles of washing in hypotonic buffer followed by 0.1% (w/v) SDS in hypotonic buffer to again lyse cells and solubilise cellular membranes, all solutions contained aprotinin (10 $KIU.ml^{-1}$)to inhibit protease activity. One cycle of hypotonic and SDS washes was not sufficient to remove cells in the dense calcified cartilage and subchondral bone plate, however only two cycles were required, fewer than that of Kheir *et al*. (2011) and Stapleton *et al*. (2008), likely due to the smaller size of tissue used. Osteochondral pins were then treated with nucleases to digest nucleic acids and sterilised using 0.1% (v/v) PAA. Following a final extended PBS wash the decellularised tissue had no visible whole cell nuclei, and a dry weight cartilage DNA content of 39 $ng.mg^{-1}$. An undesirable effect of the decellularisation process was that the cartilage GAG content of the acellular scaffold was severely reduced from that of the native bovine cartilage. Porcine tissues were also successfully decellularised using the same method, however only a single incubation in SDS was required to fully remove cellular debris and reduce the DNA content to below 50 $ng.mg^{-1}$. Again, GAG loss was seen, but the reduction was only 60 %.

A decellularised matrix, as classified by Crapo *et al.* (2011), should have a DNA content of < 50 $ng.mg^{-1}$. Reduction of DNA content is important as the phosphate backbone of residual nucleic acids can act as a nucleation site for calcification of implants (Schoen & Levy, 2005). Whereas this would not be a problem for the bone component of the composite scaffold, calcification of cartilage may severely alter the equilibrium elastic modulus of the tissue and have detrimental effects on the friction coefficient. Such calcified cartilage

could cause severe damage to the opposing articulating surface and accelerate joint degeneration, rather than prevent or delay cartilage damage, as was the original intention of the cartilage lesion repair.

It is also important to take into account the fragment length of any residual DNA in decellularised matrix. Keane *et al.* (2012), used DNA fragment length as an indication of decellularisation efficacy, to quantify potential residual cellular debris. It was shown that decellularised tissues with a larger residual DNA fragment length (500 – 1500 bp) had tended towards an inflammatory M1 macrophage response from the host. Whereas a constructive M2 macrophage response was seen with more effectively decellularised porcine SIS with residual DNA of < 500 bp fragment length, although values were not significant *in vivo*. There was a significantly higher number of infiltrating macrophages in the SIS with large DNA fragment size. However, the study only used DNA quantification to test decellularisation efficacy and did not make any attempt to quantify other antigenic cell remnants such as intracellular cytoplasmic proteins and membrane components by any other means. Stapleton *et al*. (2008) assessed the fragment length of residual DNA in decellularised porcine meniscal tissue via agarose gel electrophoresis. Fresh tissue showed a clear band around 10,000 base pairs, no band could be seen for DNA extracted from decellularised meniscus. However, they later report a significant reduction in DNA concentration following decellularisation, so the lack of a band present for decellularised tissue may not be that the fragment length is too short to be detected, but that the amount of DNA is too small to be seen, as the same volume of extracted DNA was loaded into the gel, despite the fact that the concentration of DNA differed between native and decellularised tissues.

It is also important to ensure DNA fragment size is minimal so to ensure that functional genomic material is not transferred to the host, which could be problematic, for example, the potential transfer of latent viral DNA. The risks from latent viral DNA are minimal however, as infection-independent horizontal gene transfer of porcine endogenous retrovirus (PERV) from porcine cells to phagocytic human fibroblasts has been shown to be inefficient, with the virus only transmitted to 0.22 % of co-cultured cells, and transient, with no detectable virus after 4 weeks. The virus was unable to

insert into the human genome and no viral replication occurred (Bisset *et al*., 2007). A major concern when using porcine xenogeneic tissues is the transmission of PERV, as pigs are asymptomatic carriers (Bucher *et al*, 2005). Whilst transmission of PERV has been seen *in vitro* (Patience *et al*., 1997), it has not been observed *in vivo* (Irgang *et al*., 2003). As viruses are obligate intracellular parasites, destruction and removal of porcine cells from the xenograft should result in the complete removal of PERV's also.

In the current decellularisation protocol, nucleases (DNase and RNase) were used to cleave nucleic acids exposed following rupture of cytoplasmic and nuclear membranes (Stapleton *et al*., 2008; Kheir *et al*., 2011) . Cleavage of nucleic acids into small fragments enabled effective wash out, and the DNA content of decellularised cartilage was significantly reduced, however the fragment length of residual DNA was not quantified. Initial attempts were made to measure fragment length of residual DNA isolated from decellularised tissues using agarose gel electrophoresis, however potentially due to the low levels of DNA present, no DNA could be detected. It may be necessary in future studies to concentrate DNA extracts to enable better detection.

Sterilisation of the natural scaffold is an important step in the decellularisation process to avoid disease transfer from viral, bacterial and fungal agents.

Another concern regarding the medical use of animal materials is the risk of bovine spongiform encephalopathy (BSE) transmission (Laurencin & Al-Amin, 2008). Transmissible spongiform encephalopathys (TSE) are chronic degenerative diseases characterised by the accumulation of the abnormal cellular glycoprotein known as prion protein. Bovine spongiform encephalopathy appeared in UK cattle in the mid 1980's. This TSE is transmissible between species and the infectious prion protein in humans causes fatal Creutzfeldt-Jakob disease. Transmission has been seen to occur through human consumption of contaminated beef products, and so caution should be taken when using biological materials, especially bovine products for medical applications (Dormont, 1996; Wickham, 1996). Terminal sterilisation techniques currently used for xenotransplants are

ineffective against prion proteins and processes which are able to inactivate the protein would cause damage to delicate biological tissues (Dormont, 1996). It is possible to minimise the risk of spongiform encephalopathy transmission from xenotransplant as different tissues have different levels of infectiousness. The brain and central nervous system are highly infectious, spleen tissue is infectious but 10^6 times less so than the brain. However, other tissues such as heart and bone have not been shown to transmit any TSE agent (Dormont, 1996). Therefore it is unlikely that any bovine osteochondral tissues, even from an animal with BSE, would be capable of transmitting spongiform encephalopathy to humans following transplantation. To eradicate the risk, it is a regulatory requirement to use tissues from certified BSE free cattle, as outlined in the Note for guidance on minimising the risk of transmitting animal spongiform encephalopathy agents via human and veterinary medicinal products (EMEA/410/01 REV 3) published in the official journal of the European Union (2011), however this would greatly increase the manufacturing costs.

Terminal sterilisation is a more viable alternative to screening source tissues and sterile tissue processing. The current protocol used 0.1% (v/v) PAA to sterilise the decellularised osteochondral scaffolds. This method, although shown to be effective for other tissues (Lomas *et al*., 2003), has not been validated for osteochondral tissues. It may be that the dense nature of bone and cartilage inhibits penetration of PAA. Mirsadraee *et al*. (2006) developed a methodology to validate the sporicidal activity of 0.1 % (v/v) PAA on decellularised human pericardium. *Bacillus Atrophaeus* spores were applied directly to the surface of the decellularised tissue, or to filter paper which could only be accessed by permeation of the sterilisation solution through a layer of pericardium. Tissues and filter papers were macerated and cultured on tryptone soya agar plates, the number of colony forming units was compared between PAA treated and untreated tissues. A similar method was performed by Pruss *et al.* (1999) to confirm virus inactivation by PAA in bone. These methods could be modified and used to validate PAA sterilisation of osteochondral tissues. Additionally, sterilised osteochondral tissues could be macerated and cultured on a variety of plates (agar, blood agar etc.) to observe the presence/absence of residual microbes. Other sterilisation methods such as ethylene oxide

treatment or γ irradiation could potentially provide more acceptable results in terms of tissue penetration, however the level of irradiation would need to be optimised in order to minimise tissue damage (Vangsness *et al*., 2003).

Although bovine and porcine osteochondral tissues were successfully decellularised, a significant structural change was seen in the cartilage matrix. The GAG content of porcine cartilage was reduced by 60 %, and bovine cartilage was almost devoid of GAGs, with only 1 % of the original content remaining following decellularisation. SDS has been linked to GAG reduction, as the anionic detergent can disrupt protein-protein interactions (Seddon *et al*., 2004). It is hypothesised that ionic interactions with SDS disrupt link protein, a key attachment protein which links hyaluronan to aggrecan. This link protein disruption essentially would cleave the proteoglycan network of cartilage and enable wash out of aggrecan. The loss of GAGs from the cartilage tissue would lead to increased cartilage deformation as the fluid phase of load support was reduced. The effect of GAG loss on the biotribology of cartilage is currently unknown. It is unclear what the effect of altered biomechanical and biotribological properties of the osteochondral graft would be post implantation. However, previous studies have shown that the reduction of cartilage GAG content had deleterious effects on the coefficient of friction (Katta *et al*., 2009). It may be that ingress of host cells into the biomaterial post implantation would begin to produce proteoglycans to replenish those lost during decellularisation, without the temporarily reduced GAG concentration having adverse effects in the short term. Alternatively, it may be necessary to take a MACI-type approach and recellularise scaffolds prior to implantation with extracted autologous cells, this would potentially begin the production of proteoglycans *ex vivo*, improving or restoring tissue function. Furthermore, to produce an off the shelf product, without the need to culture a patient's own cells, it may be possible to restore cartilage biochemistry using self-assembling peptides.

Many peptides in nature undergo self-assembly; "the spontaneous association of molecules under equilibrium conditions into stable, structurally well-defined aggregates joined by noncovalent bonds" (Whitesides *et al*., 1991). Synthesised, designed self-assembling peptides are not naturally occurring but are produced from natural building blocks. A number of fibrous

self-assembling peptide hydrogels have been identified as potential candidates for use as tissue engineering biomaterials. It is possible to alter the amino acid sequence to control peptide properties such as assembly (to control hydrogel pore size, fibre thickness and mechanical properties), chemical properties (to determine pH and ionic sensitivity and surface properties) or even to include biologically relevant amino acid sequences to alter the biological properties (Maude *et al*. 2013). A set of self-assembling peptides currently undergoing research and development are the P_{11} group of peptides. These peptides are of particular interest in tissue engineering approaches as their assembly can be triggered by a change in pH, ionic strength or, for some peptides, upon addition of a complementary counterpart, so they can be applied as a liquid and undergo gelation *in situ* and some peptides have shown to be cytocompatible (Maude *et al*. 2013). Such peptides in liquid form could be applied to the decellularised cartilage matrix alongside or covalently bonded to chondroitin sulphate or other GAGs, self-assembly could then be triggered, trapping the GAGs in the tissue. Research into such an approach is already underway to restore GAG content in spinal discs (Miles *et al*., 2012).

The biocompatibility of the decellularised osteochondral xenograft required investigation prior to pre-clinical evaluation. ISO 10993 is in place to ensure thorough and appropriate testing of all medical devices is completed during product development. Initial basic *in vitro* biocompatibility testing should be performed prior to *in vivo* testing and use in animal models to ensure the scaffold has no immediate toxic effects before more advanced immune responses can be investigated.

SDS used in the decellularisation process has been reported to have cytotoxic effects when not effectively removed from decellularised tissue matrices (Rieder et al, 2004). Residual SDS within the scaffold may prevent ingrowth of cells in vivo and result in graft failure. Quantification of residual SDS using detection of C^{14} labelled SDS in decellularised bovine osteochondral tissues revealed a relatively high concentration of residual SDS, above cytotoxic levels, even though most SDS had been washed out into the wash solutions. Surprisingly, no cytotoxic effects were observed when decellularised osteochondral tissues were cultured with the 3T3 cell

line, however, when cultured with BHK cells, contact cytotoxicity was seen with one sample. This largely corroborates with the results of Kheir *et al*. (2011), in which three times as many SDS washes were applied to a larger tissue section with the same duration of terminal wash cycles as the current study, but no cytotoxicity was seen. It is likely that the three dimensional dense nature of the osteochondral tissue may give false positives for cytotoxicity and further testing should be performed to assess the biocompatibility of soluble extracts of the scaffold, or attempts to 3D culture cells with the scaffold. It did however appear that the acellular tissue was having some cytotoxic effect and alterations to the decellularisation protocol were required to improve biocompatibility.

As porcine osteochondral tissues required a less extensive protocol for decellularisation, the protocol was altered in an attempt to retain a higher percentage of the cartilage GAG content. Upon changing the duration/concentration of the SDS wash it was found that cartilage was sustaining damage, and in cases completely disintegrating and dissolving away from the bone into the wash solutions. Analysis of damaged tissues revealed quantitatively a huge increase in water content, a large reduction in cartilage GAG content, however collagen denaturation was not occurring. Histologically, tissues appeared highly porous, had a roughened surface and the connection of cartilage to the bone in the hypertrophic cartilage region was stretched and tenuous. Furthermore, upon increasing the duration of the final PBS wash to improve biocompatibility of decellularised bovine cartilage, the same damage was also witnessed in bovine tissues.

Such damage to articular cartilage has not been reported previously using SDS based decellularisation methods (Elder *et al*., 2010; Kheir *et al*., 2011). However, similar characteristics were witnessed when using more harsh protocols on nasal septum cartilage (Schwarz *et al*., 2012). Numerous iterations of the current decellularisation protocol were carried out to elucidate the cause of cartilage damage. None of the individual wash cycles of the protocol were found to be solely responsible for cartilage degradation, and surprisingly, incubation in PBS alone for the duration of the protocol lead to damage. The effect of solution osmolality and protease activity were ruled out, as were the number of pins decellularised per pot and the age/stage of

maturation of the source tissue. Only a decrease in incubation temperature was shown to reduce the extent of cartilage damage, however not to eliminate it.

That porcine cartilage had sustained damage, simply with incubation in PBS with agitation at 42 °C, was surprising. This finding highlighted the relative fragility of cartilage when extracted from its natural environment.

The stretching of the porcine cartilage matrix at the hypertrophic zone and detachment of the cartilage at the interface with bone suggests that this area is a weak spot. The number of large cells in this region makes it highly porous and removal of cells from this region may have further weakened the structure. The difference in structure in this region between porcine and bovine cartilage may provide a possible explanation as to why porcine cartilage was damaged more readily than bovine. Bovine deep cartilage has linear columns of chondrocytes aligned perpendicularly to the bone, with defined areas of cartilage matrix between columns, and has fewer cells, rather than the clusters of large numbers of hypertrophic cells seen in porcine cartilage. Therefore the attachment of cartilage to bone may be stronger in the more mature bovine tissues. It has been widely accepted that collagen fibres are continuous between cartilage and bone to anchor the two tissues securely together (Mow *et al*., 2005). Other studies, however contradict this idea (Clark & Huber, 1990), so it may be that the attachment of cartilage to bone is not as secure as is commonly assumed.

It was unexpected that neither immature porcine cartilage (4 months old), nor mature cartilage (2.4 – 4.2 years old) became damaged during the decellularisation process, whereas cartilage of 6 month old pigs did. Also of note was the relative inconsistency with which 6 month old porcine tissue became damaged. It is possible that at this transitional maturation stage porcine cartilage is comparatively unstable. Rieppo *el al.* (2009) reported that in porcine cartilage during maturation, the collagen structure was altered from fibres being aligned mostly parallel to the surface (4 months old) to developing the characteristic anisotropic fibre orientation of mature (21 month old) cartilage. The current study highlighted other major characteristics of immature cartilage which are lost during maturation;

vascularisation and cartilage thickness. Cartilage also decreases in cellularity following maturation. It is clear that maturing tissues are undergoing major metabolic changes, greatly altering the structure of the tissue (Hamann *et al*., 2013). Following the anabolic processes of tissue formation, catabolic processes ensue to reduce cellularity, vascularisation and cartilage thickness as well as re-orientate collagen fibrils, during this transitional period prior to mature tissue homeostasis, it is possible that the tissue is more susceptible to damage, providing a possible explanation for why cartilage from 6 month old pigs was more readily, yet inconsistently damaged during decellularisation.

It was hypothesised that by decellularising an osteochondral pin, the production of a cut edge was detrimental to cartilage stability; reducing tension in the collagen fibres aligned parallel to the cartilage surface and exposing the middle and deep zones of the cartilage, allowing solutions to enter more freely. This loss of tension in the collagen network would allow for swelling of the tissue with the ingress of decellularisation solutions. This would result in the subsequent wash out of proteoglycans, which are no longer confined and compressed by the collagen matrix. This would explain the hugely increased water content and absolute loss of GAGs seen in damaged tissues.

If this theory is correct, a further explanation for the differences seen between the damage to porcine and bovine cartilage could be the relative permeability of each tissue. Despite having a higher GAG content, porcine cartilage was shown to be more permeable than bovine, so the rate at which solutions entered the structure and washed out the GAGs may have been higher.

In an attempt to test this theory, larger osteochondral blocks (bovine) and entire condyles (porcine) were decellularised. Bovine tissues sustained damage at the cut edge, showing increased porosity and GAG loss, but did retain GAGs within the central region. Porcine condylar cartilage did still show some GAG reduction, as seen in successful pin decellularisation, however the structure appeared mainly intact, with only a slight increase in

matrix porosity seen at the cartilage surface, suggesting that the cut edge effect is important to consider during osteochondral decellularisation.

Future work to fully elucidate the cause of cartilage damage should be undertaken if osteochondral decellularisation is to be further optimised. It would not be acceptable to put a decellularised product into large scale manufacture for clinical use without understanding the reason behind the damage highlighted in this study and having appropriate safeguards put in place to avoid damage occurring. To this end, it will be necessary to find improved, more definitive methods of detecting whether damage has occurred, either by quantitative analysis of tissues themselves, or by quantification of components lost into wash solutions. Additionally, more in depth immunohistochemical analysis may identify specific factors which are lost which can then potentially be quantified using ELISA or other quantitative means. Once such methods are applied, it may be possible to more accurately follow damage progression and identify when/how it is initiated.

What is clear is that some level of structural alteration will occur with decellularisation, and it will be necessary to identify the tissue condition at which damage has occurred, but will not progress and is not detrimental to the cartilage function. It may therefore also be useful to characterise human osteochondral tissues, to identify the range of tissue properties with which the decellularised graft will need to be compatible, if it is to function correctly within the host post implantation.

8.2 Further future work

Prior to *in vivo* testing, methods of graft rejection should be considered to reduce chances of failure. Intracellular cytoplasmic proteins and membrane components of cells in allografts and xenografts may elicit an immune response and lead to graft rejection. Xenogeneic grafts additionally have a cell surface sugar, galactose α1-3 galactose (α-gal), which is present in all mammals except for humans and old world monkeys (Galili *et al*., 1987). Due to the presence of a sugar similar in shape to α-gal on some human gut bacteria, humans have a high titre of pre-formed antibodies reactive against α-gal. Implantation of a graft material containing cells presenting α-gal results in hyperacute rejection of the graft (Bucher *et al*., 2005). Usually, initial exposure to circulating anti-α-gal antibodies occurs with endothelial cells of vascularised xenogafts. The binding of antibodies to α-gal on endothelial cells results in activation of the complement cascade; this recruits neutrophils and macrophages to the site and results in inflammation and blood clotting. Blood vessels in the xenograft become blocked, resulting in hypoxia and necrosis of the implanted tissue (Janeway, *et al*., 2005; Knight & Ingham, 2006).

Acellular xenografts will not undergo the same mechanism of rejection as cellular vascularised grafts as described above, as hypoxia and necrosis are not relevant, however the presence of α-gal may well negatively impact on the degradation/remodelling of the implanted scaffold. Antibody binding to the α-gal epitope may activate the classical complement cascade, and soluble α-gal may also activate the alternative complement pathway. Complement triggered release of C5a and C3a will recruit polymorphonuclear cells (PMNs; such as neutrophils) and monocytes to the xenograft. PMNs perform phagocytosis as well as releasing pro-inflammatory mediators and reactive oxygen species (ROS) which may result in destruction of the scaffold matrix. Monocytes recruited to the implanted material may differentiate into proinflammatory (M1) macrophages which will release pro-inflammatory cytokines (IL-1β and TNF-α), degradative enzymes and ROS (Boehler *et al.* 2011; Franz *et al.* 2011). The

continued release of proinflammatory cytokines may perpetuate the response and continued destruction of the implant.

A further mechanism of adverse scaffold degradation is ‘frustrated phagocytosis’. As macrophages are unable to phagocytose particles larger than 5 μm, a number of cells can fuse to form foreign body giant cells (FBGCs) in response to foreign biomaterials. If unable to phagocytose the foreign material, FBGCs display a change in activity, with reduced phagocytosis activity and enhanced degradative capacity. The increased release of enzymes and ROS may result in the scaffold being resorbed, and only once all foreign material is remodelled will the inflammatory response subside (Franz *et al.* 2011). This adverse remodelling of acellular xenografts would impair functionality and minimise the regenerative capacity of such medical devices. Furthermore, indiscriminate release of degradative products could damage surrounding healthy host tissues and exacerbate the original tissue disorder.

Immunohistochemical analysis of α-gal in osteochondral tissues by Kheir *et al.* (2011) revealed that chondrocytes of porcine cartilage did not positively stain for the epitope, however α-gal was present on cells of the subchondral bone. Stone *et al*. (1997) quantified low levels of α-gal in porcine and bovine cartilage.

Due to the avascular nature of cartilage and the tissue density, cartilage is relatively immunoprivileged, so exposure of α-gal to circulating antibodies would be minimal with xenogeneic cartilage implantation. Stone *et al.* (1997) have reported that hyperacute rejection of porcine and bovine cartilage does not occur when implanted into old world monkeys, however tissues were subject to chronic inflammatory rejection. Upon implantation, the primate immune system increased the anti-α-gal activity 10 – 300 fold in response to α-gal containing cartilage tissues (Galili *et al*., 1997). Treatment of cartilages with α-galactosidase to remove the epitope resulted in anti-α-gal titres less than two fold greater than basal levels upon implantation (Stone *et al.*, 1998), however an immune response was still seen to other cartilage-specific antigens. Of note was that these cartilage tissues were not implanted *in situ* into the avascular joint space, but into a suprapatellar

pouch, so would have had higher exposure to vascularisation and therefore circulating antibodies/lymphocytes.

Analysis of the immune response to acellular porcine small intestinal submucosa (SIS) containing high levels of α-gal implanted into α1,3 galactosyltransferase knockout mice was performed by Raeder *et al.* (2002). They found that the presence of α-gal delayed tissue remodelling and increased the inflammation duration in mice without the α1,3 galactosyltransferase gene (GTKO mice), however the tissue was effectively remodelled to the same degree. A small number of acute inflammatory cells did remain in implants in the knockout mice. The time frame for complete tissue remodelling may well be increased in dense cartilage tissues from that seen with SIS, and inflammation may not subside as quickly. Therefore, it is imperative to ensure that the α-gal epitope is thoroughly removed from tissues to avoid adverse tissue damage as a result of prolonged inflammatory reactions. Tests to determine α-gal within the decellularised osteochondral tissues should be performed in future, prior to *in vivo* testing, if the scaffold is to be considered biocompatible.

To overcome the issues with α-gal and afore mentioned BSE transmission, it may be possible to use human cadaveric osteochondral tissues as an allogeneic source material for decellularisation in the future. A protocol developed for mature bovine tissue would likely be successful for mature human tissue also. It would require careful selection of donor material, as stiffened, aged cartilage may not be a suitable repair material for young active patients.

After the removal of α-gal from decellularised osteochondral tissues has been confirmed, *in vivo* testing should be performed to assess the immunogenicity of the scaffold. The approach commonly used is to subcutaneously implant small pieces of the decellularised tissue into a mouse model. Histological and immunohistochemical analysis of explants could then be performed to determine the presence or absence of immune cells (Stapleton *et al*. 2010)

Prior to clinical trials in humans, the acellular osteochondral graft should be implanted *in situ* into a large animal model, such as a sheep or goat. This

would give a better indication of the immune response to the graft when it is implanted into the appropriate environment, and would also reveal whether integration of the graft with the surrounding recipient tissue has been successful.

8.3 Detailed approach to future work

Four key objectives should be met in the further development of an acellular osteochondral graft in order to enable progress to a clinical therapy. Firstly, the mechanism of cartilage damage should be fully elucidated. Secondly, human host tissues should be characterised to determine the acceptable range of properties which an acellular graft may possess. Thirdly, the decellularisation process should be further optimised for use with large osteochondral tissue segments to produce a scaffold with levels of damage acceptable for implantation. Finally, the regenerative capacity of the scaffold should be investigated *in vitro* and *in vivo* prior to the commencement of human clinical trials.

8.3.1 Mechanism of cartilage damage

To fully understand the mechanism of cartilage damage it will first be necessary to further understand the damage which occurs during the decellularisation process by performing more in depth characterisation of damaged tissues. Analysis of collagen loss/damage could be achieved through immunohistochemical (IHC) analysis of minor collagens. Transmission electron microscopy (TEM) and atomic force microscopy (AFM) would allow more detailed qualification of the tissue collagens and differential scanning calorimetry (DSC) would enable quantitative assessment of collagen denaturation.

The solutions used for decellularisation could be assessed using quantitative biochemical assays and TEM to determine what is being removed from tissues during damage development. Additionally, biomechanical testing and analysis of cartilage biotribology would potentially provide sensitive detection of subtle changes in tissue function due to low levels of structural damage.

Once sensitive and quantitative methods for tissue damage detection and monitoring have been developed, the progression of damage over time could be observed and by determining the nature and progression of damage, the mechanism could potentially be elucidated. Once the mechanism is understood, alterations to the decellularisation process to avoid damage could be made accordingly.

8.3.2 Human tissue characterisation

An acellular osteochondral scaffold should ideally mimic the structure and function of the surrounding recipient tissue to provide a successful repair material. Therefore it will be necessary to characterise human osteochondral tissues from appropriately aged donors using the biological, biochemical and biomechanical methods described in Chapter 3. Furthermore, assessment of cartilage biotribology using methods such as pin on plate friction testing or, preferably, whole natural joint friction testing would give further understanding of host tissue biomechanical properties. The properties of acellular osteochondral tissues produced using variations of the decellularisation process could then be compared to the range of properties observed for human tissues to determine which process, if any, provides an acceptable cartilage substitute biomaterial.

8.3.3 Decellularisation of large osteochondral tissue segments

Once the mechanism of cartilage damage has been determined, the processes to decellularise large osteochondral tissue segments could be optimised, as described in Chapter 4 and 5, to fully decellularise tissues whilst minimising damage. Such a process should produce a scaffold with acceptable levels of damage and properties comparable to those determined for human recipient cartilage.

8.3.4 Regenerative capacity of acellular osteochondral scaffolds

Before the acellular osteochondral scaffold could be tested in clinical trials, the biocompatibility and regenerative capacity of the biomaterial would require assessment *in vitro* and *in vivo*.

8.3.4.1 *In vitro* assessment

The methods described in Chapter 6 could be used for basic *in vitro* compatibility testing. The presence of residual cytotoxic SDS in the tissue should be quantified either using radiolabelled SDS or using a colourimetric assay with Stains-all dye. Contact cytotoxicity of the scaffold should be determined and the cytotoxicity of scaffold extracts could be measured by culturing with appropriate cell lines and their proliferative capacity measured using, for example, the ATPLite-M® assay.

In addition, as discussed previously, methods to assess the sterility of tissue scaffolds should be employed, such as incubating sterilised scaffold samples on agar plates or in nutrient broth. The scaffolds should also be inoculated with *Bacillus atrophaeus* spores and the efficacy of PAA for effectively killing the microbes determined.

To predict the detrimental effects of α-gal on the *in vivo* response to the implanted scaffold, qualitative immunohistochemistry and quantitative antibody absorption assays followed by ELISA to detect α-gal in decellularised scaffolds should be performed. The capacity of the scaffold to bind antibodies to α–gal in human sera and activate complement could be determined. If the scaffold is found to be cytotoxic, non-sterile or to contain unacceptable levels of α-gal the decellularisation process will need to be re-optimised to address these issues before *in vivo* studies are performed.

Other *in vitro* predictions of scaffold performance could be performed. The presence of growth factors such as TGF-β within the scaffold could be assessed using ELISA and IHC to indicate how inductive the scaffold might be to recellularisation and regeneration. Testing of the scaffold in a whole natural joint simulator could give an idea of how the graft would perform biomechanically/biotribologically upon implantation.

8.3.4.2 *In vivo* assessment

Subcutaneous implantation of the acellular osteochondral scaffold into mice would allow assessment of the immune response to the biomaterial. Histological and immunohistochemical analysis of explants would allow characterisation of cell infiltrates. If there is an adverse response to the tissue, further alterations to the decellularisation protocol should be made to produce an immune-compatible scaffold.

A proof of concept study should be performed in an appropriate large animal model, such as the sheep, to predict the clinical performance of the scaffold. Implantation of the scaffold *in situ* should give a more accurate representation of the local immune response and regeneration of the scaffold following histological and IHC analysis of explants. Furthermore, implantation into the joint using the appropriate surgical procedures would

provide details on the clinical utility of the scaffold and the performance of the implant in terms of joint function could be observed.

Subject to acceptable performance in the proof of concept study, the acellular osteochondral scaffold could then be taken forward to pre-market medical device clinical trials to assess safety and clinical utility in humans.

8.4 Conclusion

In conclusion, this study represents a major step forward in the understanding of cartilage decellularisation. The methods presented here are currently the most effective known for decellularisation of intact bovine cartilage, with no visible cell nuclei present and a residual DNA content of < 50 $ng.mg^{-1}$ in the decellularised cartilage matrix. However issues with cartilage disintegration need to be better understood and fully overcome before further necessary testing of the biocompatibility and regenerative capacity of such a scaffold material can be performed. This study has increased knowledge and understanding of the effects of decellularisation on osteochondral tissues which will form the basis for future development of a bioactive, acellular, natural tissue engineered repair material for osteochondral lesions to prevent or delay the onset of osteoarthritis.

Chapter 9
References

Altman, R.D. (1987) Overview of osteoarthritis. *Am J Med*, 83, 65-69.

Antonsson, P., Heinegird, D., Oldberg, A. (1989) The keratan sulfate-enriched region of bovine cartilage proteoglycan consists of a consecutively repeated hexapeptide motif. *J Biol Chem*, 264, 16170-16173.

Arden, N.K., Jordan, K.M., Thomas, L., Hassan, A., Ledingham, J. (2008) A randomised controlled trial of tidal irrigation vs corticosteroid injection in knee osteoarthritis: the KIVIS study. *Osteoarthr Cartil*, 16, 733-739.

Arthritis Care. (2012) OA Nation 2012 [Online]. [Accessed 19th September 2013]. Available from: http://www.arthritiscare.org.uk/Livingwith Arthritis/oanation-2012.

Atala, A. (2007) Engineering tissues, organs and cells. *J Tissue Eng Regen Med*, 1, 83-96.

Ateshian, G.A. (2009) The role of interstitial fluid pressurization in articular cartilage lubrication. *J Biomechanics*, 42, 1163-1176.

Athanasiou, K.A., Rossenwasser, M.P., Buckwalter, J.A., Malinin, T.I. Mow, V.C. (1991) Interspecies comparisons of in situ intrinsic mechanical properties of distal femoral cartilage. *J Orthop Res* 9, 330-40.

Bach, D.S., Kon, N.D., Dumesnil, J.G., Sintek, C.F., Doty, D.B. (2005) Ten-year outcome after aortic valve replacement with the freestyle stentless bioprosthesis. *Ann Thorac Surg*, 80, 480 –487.

Badylak, S., Liang, R., Tullius, R., Hodde, J. (1999) Endothelial cell adherence to small intestinal submucosa: an acellular bioscaffold. *Biomaterials*, 20, 2257-2263.

Bae, D.K., Song, S.J., Yoon, K.H., Heo, D.B., Kim, T.J. (2013) Survival analysis of microfracture in the osteoarthritic Knee - minimum 10-year follow-up. *Arthroscopy*, 29, 244-250.

Bank, R.A., Bayliss, M.T., Lafeber, F.P.J.G., Maroudas, A., TeKoppele, J.M. (1998) Ageing and zonal variation in post-translational modification of collagen in normal human articular cartilage. *Biochem. J*, 330, 345-351.

Barry, F.P., Gaw, J.U., Young, C.N., Neame, P.J. (1992) Hyaluronan-binding region of aggrecan from pig laryngeal cartilage: amino acid sequence, analysis of N-linked oligosaccharides and location of the keratan sulphate. *Biochem. J*, 286, 761-769.

Bauer, M., Jackson, R.W. (1988) Chondral lesions of the femoral condyles: a system of arthroscopic classification. *Arthroscopy*, 4, 97-102.

Baumgarten, M., Bloebaum, R.D., Ross, S.D.K., Campbell, P., Sarmiento, A. (1985) Normal human synovial fluid: osmolality and exercise-induced changes. *J Bone Joint Surg Am*, 67, 1336-1339.

Benders, K.E.M., van Weeren, P.R., Badylak, S.F., Saris, D.I.B.F., Dhert, W.J.A., Malda, J. (2013) Extracellular matrix scaffolds for cartilage and bone regeneration. *Trends Biotechnol*, 31, 169-176.

Bisset, L.R., Böni, J., Lutz, H., Schüpbach, J. (2007) Lack of evidence for PERV expression after apoptosis-mediated horizontal gene transfer between porcine and human cells. *Xenotransplantation*, 14, 13–24.

Bloebaum, R.D., Magee, F.P. (1989) Hypertonic solution for arthroscopic surgery. US4872865.

Boehler, R. M., Graham, J. G., & Shea, L. D. (2011) Tissue engineering tools for modulation of the immune response. *Biotechniques*, 51, 239-254.

Bolland, F., Korossis, S., Wilshaw, S.P., Ingham, E., Fisher, J., Kearney, J.N., Southgate, J. (2007) Development and characterisation of a full-thickness acellular porcine bladder matrix for tissue engineering. *Biomaterials*, 28, 1061-1070.

Bolton, M.C., Dudhia, J., Bayliss, M.T. (1999) Age-related changes in the synthesis of link protein and aggrecan in human articular cartilage: implications for aggregate stability. *Biochem J*, 337, 77-82.

Bornstein, P., Sage, E.H. (2002) Matricellular proteins: extracellular modulators of cell function. *Curr Opin Chem Biol*, 14, 608–616.

Bouwmeester, P.S.J.M., Kuijer, R., Homminga, G.N., Bulstra, S.K., Geesink, R.G.T. (2002) A retrospective analysis of two independent cartilage repair studies: autogenous perichondrial grafting versus subchondral drilling 10 years post-surgery. *J Orthop Res*, 20, 267-273.

Brooks, P.M. (2006) The burden of musculoskeletal disease - a global perspective. *Clin Rheumatol*, 25, 778–781.

Brown, B.N., Valentin, J.E., Stewart-Akers, A.M., McCabe, G.P., Badylak, S.F. (2009) Macrophage phenotype and remodeling outcomes in response to biologic scaffolds with and without a cellular component. *Biomaterials*, 30, 1482–1491.

Bucher, P., Morel, P., Bühler, L.H. (2005) Xenotransplantation: an update on recent progress and future perspectives. *Transplant Int*, 18, 894–901.

Buckwalter, J.A., Mankin, H.J. (1998) Articular cartilage. Part I: Tissue design and chondrocyte matrix interactions. *J Bone Joint Surg Am*, 79, 600-611.

Burton-Wurster, N., Borden, C., Lust, G., MacLeod, J.N. (1998) Expression of the (V+C)- fibronectin isoform is tightly linked to the presence of a cartilaginous matrix. *Matrix Biol*, 17, 193-203.

Butnariu-Ephrat, M., Robinson, D., Mendes, D.G., Halperin, N., Nevo, Z. (1996) Resurfaacing of goat articular cartilage by chondrocytes derived from bone marrow. *Clin Orthop Relat Res*, 330, 234-243.

Cao, E., Chen, Y., Cui, Z., Foster, P.R. (2003) Effect of freezing and thawing rates on denaturation of proteins in aqueous solutions. *Biotechnol Bioeng*, 82, 684-690.

Cassetta, L., Cassol, E., Poli, G. (2011) Macrophage Polarization in Health and Disease. *ScientificWorldJournal*, 11, 2391–2402.

Cebotari, S., Mertsching, H., Kallenbach, K., Kostin, S., Repin, O., Batrinac, A., Kleczka, C., Ciubotaru, A., Haverich, A. (2002) Construction of autologous human heart valves based on an acellular allograft matrix. *Circulation*, 106, 63-68.

Chaing, H., Jiang, C.C. (2009) Repair of articular cartilage defects: review and perspectives. *J Formos Med Assoc*, 108, 87-101.

Chang, C.H., Lin, F.H., Lin, C.C., Chou, C.H., Liu, H.C. (2004) Cartilage tissue engineering on the surface of a novel gelatine-calcium-phosphatebiphasic scaffold in a double-chamber bioreactor. *J Biomed Mater Res*, 71, 313–321.

Chang, R.W., Falconer, J., Stulberg, S.D., Arnold, W.J., Manheim, L.M., Dyer, A.R. (1993) A randomised controlled trial or arthroscopic surgery versus closed-needle joint lavage for patients with osteoarthritis of the knee. *Arthritis Rheum*, 36, 289-296.

Chen, C.H., Yeh, M.L., Geyer, M., Wang, G.J., Huang, M.H., Heggeness, M.H., Höök, M., Luo, Z.P. (2006) Interactions between collagen IX and biglycan measured by atomic force microscopy. *Biochem Biophys Res Commun*, 339, 204-208.

Chen, F.H., Thomas, A.O., Hecht, J.T., Goldring, M.B., Lawler, J. (2005) Cartilage oligomeric matrix protein/thrombospondin 5 supports chondrocyte attachment through interaction with integrins. *J Biol Chem*, 280, 32655-32661.

Chen, R.N., Ho, H.O., Tsai, Y.T., Sheu, M.T. (2004) Process development of an acellular dermal matrix (ADM) for biomedical applications. *Biomaterials*, 25, 2679-2686.

Chu, C.R., Dounchis, J.S., Yoshioka, M., Sah, R.L., Coutts, R.D., Amiel, D. (1996) Osteochondral repair using perichondrial cells – a one year study in rabbits. *Clin Orthop Relat Res*, 340, 220-229.

Clark, J.M., Huber, J.D. (1990) The structure of the human subchondral plate. *J Bone Joint Surg Br*, 72, 866-873.

Cohen, S.B., Meirisch, C.M., Wilson, H.A., Diduch, D.R. (2003) The use of absorbable co-polymer pads with alginate and cells for articular cartilage repair in rabbits. *Biomaterials*, 24, 2653-2660.

Courtman, D.W., Pereira, C.A., Omar, S., Langdon, S.E., Lee, J.M., Wilson, G.J. (1995) Biomechanical and ultrastructural comparison of cryopreservation and a novel cellular extraction of porcine aortic valve leaflets. *J Biomed Mater Res*, 29, 1507-1516.

Cox, B., Emili, A. (2006) Tissue subcellular fractionation and protein extraction for use in mass-spectrometry-based proteomics. *Nat Protoc*, 1, 1872 – 1878.

Crapo, P.M., Gilbert, T.W., Badylak, S.F. (2011) An overview of tissue and whole organ decellularization processes. *Biomaterials*, 32, 3233-3243.

Cremer, M.A., Rosloniec, E.F., Kang, A.H. (1998) The cartilage collagens: a review of their structure, organization, and role in the pathogenesis of experimental arthritis in animals and in human rheumatic disease. *J Mol Med*, 76, 275–288.

Cronklin, B.S., Richter, E.R., Kreutziger, K.L., Zhong, D.S., Chen, C. (2002) Development and evaluation of a novel vascular xenograft. *Med Eng Phys*, 24, 173-183.

Daheshia, M., Yao, J.Q. (2008) The interleukin 1β pathway in the pathogenesis of osteoarthritis. *J Rheumatol* 35, 2306-2312.

Danielson, K.G., Baribault, H., Holmes, D.F., Graham, H., Kadler, K.E., Lozzo R.V. (1997) Targeted disruption of decorin leads to abnormal collagen fibril morphology and skin fragility. *J Cell Biol*, 136, 729-742.

Dausse, Y., Grossin, L., Miralles, G., Pelletier, S., Mainard, D., Hubert, P., Baptiste, D., Gillet, P., Dellacherie, E., Netter, P., Payan, E. (2003) Cartilage repair using new polysaccharidic biomaterials: macroscopic, histological and biochemical approaches in a rat model of cartilage defect. *Osteoarthr Cartil*, 11, 16-28.

DiCesare, P.E., Carlson, C.S., Stolerman, E.S., Hauser, N, Tulli, H., Paulsson, M. (1996) Increased degradation and altered tissue

distribution of cartilage oligomeric matrix protein in human rheumatoid and osteoarthritic cartilage. *J Orthop Res*, 14, 946-955.

DiCesare, P.E., Morgelin, M., Carlson, C.S., Pasumarti, S., Paulsson, M. (1995) Cartilage oligomeric matrix protein: isolation and characterization from human articular cartilage. *J Orthop Res*, 13, 422-428.

Ding, C., Garnero, P., Cicuttini, F., Scott, F., Cooley, H., Jones, G. (2005) Knee cartilage defects: association with early radiographic osteoarthritis, decreased cartilage volume, increased joint surface area and type II collagen breakdown. *Osteoarthr Cartil*, 13, 198-205.

Ding, C., Garnero, P., Cicuttini, F., Scott, F., Cooley, H., Jones, G. (2005) Knee cartilage defects: association with early radiographic osteoarthritis, decreased cartilage volume, increased joint surface area and type II collagen breakdown. *Osteoarthr Cartil*, 13, 198-205.

Doege, K.J., Coulter, S.N., Meek, L.M., Maslen, K., Wood, J.G. (1997) A human-specific polymorphism in the coding region of the aggrecan gene. *J Biol Chem*, 272, 13974-13979.

Dormont, D., (1996) How to limit the spread of Creutzfeldt-Jakob disease. *Infect Control Hosp Epidemiol*, 17, 521-528.

Dowson, D. (1995) Elastohydrodynamic and micro-elastohydrodynamic lubrication. *Wear*, 190, 125-138.

Du, L., Wu, X., Pang, K., Yang, Y. (2010) Histological evaluation and biomechanical characterisation of an acellular porcine cornea scaffold. *Br J Ophthalmol*, 95, 410-414.

Dudhia, J. (2005) Aggrecan, aging and assembly in articular cartilage. *Cell Mol Life Sci*, 62, 2241–2256.

Edwards, C.A., O'Brien, J.R. (1980) Modified assay for determination of hydroxyproline in a tissue hydrolyzate, *Clinica Chemica Acta*, 104, 161-167.

Elder, B.D., Eleswarapu. S.V., Athanasiou, K.A. (2009) Extraction techniques for the decellularization of tissue engineered articular cartilage constructs. *Biomaterials*, 30, 3749–3756.

Elder, B.D., Kim, D.H., Athanasiou, K.A. (2010) Developing an articular cartilage decellularisation process toward facet joint cartilage replacement. *Neurosurgery*, 66, 722-727.

European Commission (EMA) No, 410/01 rev.3 of 5 March 2011 Note for guidance on minimising the risk of transmitting animal spongiform encephalopathy agents via human and veterinary medicinal products.

Farndale, R.W., Sayers, C.A., Barrett, A.J. (1982) AQ direct spectrophotometric microassay for sulphated glycosaminoglycans in cartilage structures. *Connect Tissue Res*, 9, 247-248.

Felson, D.T. (2009) Developments in the clinical understanding of osteoarthritis. *Arthritis Res Ther*, 11, 203-214.

Felson, D.T., Zhang, Y. (1998) An update on the epidemiology of knee and hip osteoarthritis with a view to prevention. *Arthritis Rheum*, 41, 1343-1355.

Forster, H., Fisher, J. (1996) The influence of loading time and lubricant on the friction of articular cartilage. *Proc IMechE Part H: J Engineering in Medicine*, 210, 109-119.

Forster, H., Fisher, J. (1999) The influence of continuous sliding and subsequent surface wear on the friction of articular cartilage. *Proc IMechE Part H: J Engineering in Medicine*,, 213, 329-345.

Franz, S., Rammelt, S., Scharnweber, D., & Simon, J. C. (2011) Immune responses to implants–A review of the implications for the design of immunomodulatory biomaterials. *Biomaterials*, 32, 6692-6709.

Fraser , J.R.E., Laurent, T.C., Laurent, U.B.G. (1997) Hyaluronan: its nature, distribution, functions and turnover. *J Intern Med*, 242, 27–33.

Frenkel, S.R., di Cesare, P.E. (2004) Scaffolds for articular cartilage repair. *Ann Biomed Eng*, 32, 26-34.

Frenkel, S.R., Toolan, B., Menche, D., Pitman, M.I., Pachence, J.M. (1997) Chondrocyte transplantation using a collagen bilayer matrix for cartilage repair, *J Bone Joint Surg Br*, 79, 831-836.

Freytes, D.O., Badylak, S.F., Webster, T.J., Geddes, L.A., Rundell, A.E. (2004) Biaxial strength of multilaminated extracellular matrix scaffolds. *Biomaterials*, 25, 2353–2361.

Funamoto, S., Nama,K., Kimura, T., Murakoshi, A., Hashimoto, Y., Niwaya, K., Kitamura, S., Fujisato, T., Kishida, A. (2010) The use of high-hydrostatic pressure treatment to decellularize blood vessels. *Biomaterials*, 31, 3590–3595.

Gabriel, S.G., Michaud, K. (2009) Epidemiological studies in incidence, prevalence, mortality and comorbidity of the rheumatic diseases. *Arthritis Res Ther*, 11, 229.

Galili, U., Clarks, M.R., Shohet, S.B., Buehler, J., Macher, B.A. (1987) Evolutionary relationship between the natural anti-Gal antibody and the Galα1->3Gal epitope in primates. *Proc Natl Acad Sci USA*, 84, 1369-1373.

Galili, U., LaTemple, D. C., Walgenbach, A. W., & Stone, K. R. (1997) Porcine and bovine cartilage transplants in cynomolgus monkey. *Transplantation*, 63, 646-651.

Gerwin, N., Hops, C., Lucke, A. (2006) Intraarticular drug delivery in osteoarthritis. *Adv Drug Deliv Rev*, 58, 226-242.

Getgood, A., Bhullar, T.P.S., Rushton, N. (2009) Current concepts in articular cartilage repair. *J Orthop Trauma*, 23, 189-200.

Getgood, A.M.J., Kew, S.J., Brooks, R., Aberman, H., Simon T., Lynn, A.K., Rushton, N. (2012) Evaluation of early-stage osteochondral defect repair using a biphasic scaffold based on a collagen–glycosaminoglycan biopolymer in a caprine model. *The Knee*, 19, 422–430.

Gilbert, T.W., Wognum, S., Joyce, E.M., Freytes, D.O., Sacks, M.S., Badylak, S.F. (2008) Collagen fiber alignment and biaxial mechanical

behavior of porcine urinary bladder derived extracellular matrix. *Biomaterials*, 29, 4775–4782.

Gille, J., Behrens, P., Volpi, P., de Girolamo, L., Reiss, E., Zoch, W., Anders, S. (2013) Outcome of Autologous Matrix Induced Chondrogenesis (AMIC) in cartilage knee surgery: data of the AMIC Registry. *Arch Orthop Trauma Surg*, 133, 87–93.

Giurea, A., Kleain, T.J., Chen, A.C., Goomer, R.S., Coutts, R.D., Akeson, W.H., Amiel, D., Sah, R.L. (2003) Adehsion of Perichondrial cells to a polylactic acid scaffold. *J Orthop Res*, 21, 584-589.

Goldring, M.B. (1999) The role of cytokines as inflammatory mediators in osteoarthritis: Lessons from animal models. *Connect Tissue Res*, 40, 1-11.

Grande, D.A., Pitman, M.I., Peterson, L., Menche, D., Klein, M. (1989) The repair of experimentally produced defects in rabbit articular cartilage by autologous chondrocyte transplantation. *J Orthop Res*, 7, 208-218.

Grauss, R.W., Hazekamp, M.G., Oppenhuizen, F., van Munsteren, C.J., Gittenberger-de Groot, A.C. DeRuiter, M.C. (2005) Histological evaluation of decellularised porcine aortic valves: matrix changes due to different decellularisation methods. *Eur J Cardiothorac Surg*. 27, 566–571.

Gray, H. (2000). Anatomy of the human body. [Online]. 20th edition. New York: Bartleby.com. [Accessed 19th September 2013]. Available from: www.bartleby.com/107/

Grigolo, B., Roseti, L., Fiorini, M., Fini, M., Giavaresi, G., Aldini, N.N., Giardino, R., Facchini, A. (2001) Transplantation of chondrocytes seeded on a hyaluronan derivative (Hyaff®-11) into cartilage defects in rabbits. *Biomaterials*, 22, 2417-2424.

Halstead, J., Bergin, D., Keenan, A., Madden, J., McGonagle, D. (2010) Ligament and bone pathologic abnormalities more frequent in neuropathic joint disease in comparison with degenerative arthritis of the foot and ankle. *Arthritis Rheum*, 62, 2353–2358.

Hamann, N., Zaucke, F., Dayakli, M., Brüggemann, G.P., Niehoff, A. (2013) Growth-related structural, biochemical, and mechanical properties of the functional bone-cartilage unit. *J Anat*, 222, 248-259.

Hartmann, C. (2006) A wnt cannon orchestrating osteoblastogenesis. *Trends Cell Biol*, 16, 151-158.

Hecht, J.T., Hayes, E., Haynes, R., Cole, W.G. (2005) COMP mutations, chondrocyte function and cartilage matrix. *Matrix Biol*, 23, 525-533.

Hedlund, H., Hedbom, E., Heinegård, D., Mengarelli-Widholm, S., Reinholt, F.P., Svensson, O. (1999) Association of the aggrecan sulphate-rich region with collagen in bovine articular cartilage. *J Biol Chem*, 274, 8777-8781

Hedlund, H., Mengarelli-Widholm, S., Heinegård, D., Reinholt, F.P., Svensson, O. (1994) Fibromodulin distribution and association with collagen. *Matrix Biol*, 14, 227-232.

Hendrickson, D.A., Nixon, A.J., Grande, D.A., Todhunter, R.J., Minor, R.M., Erb, H., Lust, G. (1994) Chondrocyte-fibrin matrix transplants for resurfacing extensive articular cartilage defects. *J Orthop Res*, 12, 485-497.

Herrero-Beaumont, G., Roman-Blas, J.A., Castañeda, S., Jimenez, S.A. (Primary osteoarthritis no longer primary: three subsets with distinct etiological, clinical, and therapeutic characteristics. *Semin Arthritis Rheum*, 39, 71-80.

Hoemann, C.D., Légaré, A., Buschmann, M.D. (2005) Tissue engineering of cartilage using an injectable and adhesive chitosan-based cell-delivery vehicle. *Osteoarthr Cartil*, 13, 318-329.

Hofmann, S., Garcia-Fuentes, M. (2011). Bioactive scaffolds for the controlled formation of complex skeletal tissues, regenerative medicine and tissue engineering - cells and biomaterials, Eberli, D. Ed., ISBN: 978-953-307-663-8, InTech, Available from: http://www.intechopen.com/books/regenerative-medicine-and-tissue-engineering-cells-andbiomaterials/bioactive-scaffolds-for-the-controlled-formation-of-complex-skeletal-tissues

Hollander, A.P., Atkins, R.M., Eastwood, D.M., Dieppe, P.A., Elson, C.J. (1991) Human cartilage is degraded by rheumatoid arthritis synovial fluid but not by recombinant cytokines in vitro. *Clin Exp Immunol*, 83, 52-57.

Homandberg, G.A., Wen, C., Hui, F. (1998) Cartilage damaging activities of fibronectin fragments derived from cartilage and synovial fluid. *Osteoarthr Cartil*, 6, 231-244.

Homminga, G.N., Bulstra, S.K., Bouwmeester, P.M., van der Linden, A.J. (1990) Perichondrial grafting for cartilage lesions of the knee. *J Bone Joint Surg Br*, 72, 1003-1007.

Hopkinson, A., Shanmuganathan, V.A., Gray, T., Yeung, A.M., Lowe, J., James, D.K., Dua, H.S. (2008) Optimization of amniotic membrane (AM) denuding for tissue engineering. *Tissue Eng*, 14, 371-381.

Hubbard, M.J.S. (1996) Articular debridement versus washout for degeneration of the medial femoral condyle – a five year study. *J Bone Joint Surg Br*, 78, 217-219.

Hui, W., Rowan, A.D., Richards, C.D., Cawston, T.E. (2003) Oncostatin M in combination with tumour necrosis factor α induced cartilage damage and matrix metalloproteinase expression in vivo and in vitro. *Arthritis Rheum*, 38, 3404-3418.

Ingram, J., Korossis, S., Howling, G., Fisher, J., Ingham, E. (2007) The use of ultrasonication to aid recellularization of acellular natural tissue scaffolds for use in anterior cruciate ligament reconstruction. *Tissue Eng*, 13, 1561-1572.

Irgang, M., Sauer, I.M., Karlas, A., Zeilinger, K., Gerlach, J.C., Kurth, R., Neuhaus, P., Denner, J. (2003) Porcine endogenous retroviruses: no infection in patients treated with a bioreactor based on porcine liver cells. *J Clin Virol*, 28, 141-154.

Iwanaga, T., Shikichi, M., Kitamura, H., Yanase, H., Nozawa-Inoue, K. (2000) Morphology and functional roles of synoviocytes in the joint. *Arch Histol Cytol*, 63, 17-31.

Janeway, C.A., Travers, P., Walport, M., Shlomchik, M. (2005) Immunobiology: the immune system in health and disease. 6th edition. Hampshire, UK: Thompson Publishing Services.

Jeffery, A.K., Blunn, G.W., Archer, C.W., Bently, G.(1991) Three-dimensional collagen architecture in bovine articular cartilage. *J Bone Joint Surg Br*, 73, 795-801.

Johnson, K., Farley, D., Hu, S.I., Tarkeltaub, R. (2003) One of two chondrocyte-expressed isoforms of cartilage intermediate-layer protein functions as an insulin-like growth factor 1 antagonist. *Arthritis Rheum*, 48, 1302-1314.

Julkunen, P., Harjula, T., Iivarinen, J., Marjanen, J. Seppänen, K. Nähri K., Arokoski, J., Lammi, M.J., Brama, J.S., Jurvelin, J.S., Helminen, H.J. (2009) Biomechanical, biochemical and structural correlations in immature and mature rabbit articular cartilage, *Osteoarthr Cartilage*, 17, 1628-1638.

Kääb, M.J., Gwynn, I.A.P., Nötzli, H.P. (1998) Collagen Fibre arrangement in the tibial plateau articular cartilage of man and other mammalian species. *J Anat*, 193, 23-34.

Katta, J., Jin, Z., Ingham, E., Fisher, J. (2008) Biotribology of articular cartilage – a review of the recent advances. *Med Eng Phys*, 30, 1349-1363.

Keane, T.J., Londono, R., Turner, N.J., Badylak, S.F. (2012) Consequences of ineffective decellularization of biologic scaffolds on the host response. *Biomaterials*, 33, 1771-1781.

Kheir, E., Stapleton, T., Shaw, D., Jin, Z., Fisher, J., Ingham, E. (2011) Development and characterization of an acellular porcine cartilage bone matrix for use in tissue engineering. *J Biomed Mater* Res, 99, 283–294.

Kim, B.S., Yoo, J.J., Atala, A. (2004) Peripheral nerve regeneration using acellular nerve grafts. *J Biomed Mat Res*, 68, 201-209.

Kim, T.K., Sharma, B., Williams, C.G., Ruffner, M.A., Malik, A., McFarland, E.G., Elisseeff, J.H. (2003) Experimental model for cartilage tissue

engineering to regenerate the zonal organization of articular cartilage. *Osteoarthr Cartil*, 11, 653-664.

Kirkley, A., Birmingham, T.B., Litchfield, R.B., Giffin, J.R., Willits, K.R., Wong, C.J., Feagan, B.G., Donner, A., Griffin, S.H., D'Ascanio, L.M., Pope, J.E., Fowler, P.J. (2008) A randomized trial of arthroscopic surgery for osteoarthritis of the knee. *N Engl J Med*, 359, 1097-1107.

Kiviranta, I., Jurvelin, J., Tammi, M., Säämänen, A., Helminen, H.J. (1987) Weight bearing controls glycosaminoglycan concentration and articular cartilage thickness in the knee joints of young beagle dogs. *Arthritis Rheum*, 30, 801-809.

Knight, R., Ingham, E. (2006). Allogeneic cells and tissues. In: Akay, M. ed. Wiley Encyclopedia of Biomedical Engineering. John Wiley & Sons, Inc.

Knudson, C.B., Knudson, W. (2001) Cartilage proteoglycans. *Semin Cell Dev Biol*, 12, 69-78.

Kon, E., Gobbi, A., Filardo, G., Delcogliano, M., Zaffagnini, S., Marcacci, M. (2009) Arthroscopic second-generation autologous chondrocyte implantation compared with microfracture for chondral lesions of the knee: prospective nonrandomized study at 5 years. *Am J Sports Med*, 37, 33-41.

Korossis, S.A., Booth, C., Wilcox, H.E., Watterson, K.G., Kearney, J.N., Fisher, J., Ingham, E. (2002) Tissue engineering of cardiac valve prostheses II: Biomechanical characterisation of decellularised porcine aortic heart valves. *J Heart Valve Dis*, 11, 463-471.

Koulalis, D., Schultz, W., Heyden, M., König, F. (2004) Autologous osteochondral grafts in the treatment of cartilage defects of the knee joint. *Knee Surg Sports Traumatol Arthrosc*, 12, 329-334.

Koulaouzidou, E.A., Margelos, J., Beltes, P., Kortsaris, A.H. (1999) Cytotoxic effects of different concentrations of neutral and alkaline EDTA solutions used as root canal irrigants. *J Endod*, 25, 21-23.

Kreuz, P.C., Müller, S., Ossendorf, C., Kaps, C., Erggelet, C. (2009) Treatment of focal degenerative cartilage defectswith polymer-based

Autologous chondrocyte grafts: four year clinical results. *Arthritis Res Ther*, 11, 33-44.

Kvist, A.J., Johnson, A.E., Mörgelin, M., Gustafsson, E., Bengtsson, E., Lindblom, K., Aszódi, A., Fässler, R., Sasaki, T., Timpl, R., Aspberg, A. (2006) Chondroitin sulphate perlecan enhances collagen fibril formation: implications for perlecan chondrodysplasias, *J Biol Chem*, 128, 33127-33139.

Lai, W.M., Hou, J.S., Mow, V.C. (1991) A triphasic theory for the swelling and deformation behaviours of articular cartilage. *J Biomech Eng*, 113, 245-258

LaPrade, R.F., Botker, J., Herzog, M., Agel, J. (2009) Refrigerated osteoarticular allografts to treat articular cartilage defects of the femoral condyles. A prospective outcomes study. *J Bone Joint Surg Am*, 91, 805-811.

Laurencin, C.T., Saadiq, F. (2008) Xenotransplantation in orthopaedic surgery. *J Am Acad Orthop Surg*, 16, 4-8.

Lawrence, R.C., Felson, D.T., Helmick, C.G., Arnold, L.M., Choi, H., Deyo, R.A., Gabriel, S., Hirsch, R., Hochberg, M.C., Hunder, G.G., Jordan, J.M., Katz, J.N., Kremers, H.M., Wolfe, F. (2008) Estimates of the prevalence of arthritis and other rheumatic conditions in the United States. *Arthritis Rheum*,28, 26-35.

Lee, D.K. (2008) A preliminary study on the effects of acellular tissue graft augmentation in acute achilles tendon ruptures. *J Foot Ankle Surg*, 47, 8-12.

Lefebvre, V., Behringer, R.R., de Crombrugghe, B. (2001) L-Sox5, Sox6 and Sox9 control essential steps of the chondrocyte differentiation pathway. *Osteoarthr Cartil*, 9, S96-S75.

Liu, Y., Chen, F., Liu, W., Cui, L., Shang, Q., Xia, W., Wang, J., Cui, Y., Yang, G., Liu, D., Wu, J., Xu, R., Buonocore, S.D., Cao, Y. (2002) Repairing Large Porcine Full-Thickness Defects of Articular Cartilage Using Autologous Chondrocyte-Engineered Cartilage. *Tissue Eng*, 8, 709-721.

Lomas, R.J., Cruse-Sawyer, J.E., Simpson, C., Ingham, E., Bojar, R., Kearney, J.N. (2003) Assessment of the biological properties of human split skin allografts disinfected with peracetic acid and preserved in glycerol. *Burns*, 29, 515-525.

Lotz, M., Moats, T., Villiger, P.M. (1992) Leukaemia inhibitory factor is expressed in cartilage and synovium and can contribute to the pathogenesis of arthritis. *J Clin Invest*, 90, 888-896.

Lützner J, Kasten P, Günther KP, Kirschner S (2009) Surgical options for patients with osteoarthritis of the knee. *Nat Rev Rheumatol*, 5, 309-316.

Macchiarini, P., Jungebluth, P., Go, T., Asnaghi, M.A., Rees, L.E., Cogan, T.A., Dodson, A., Martorell,J., Bellini, S., Parnigotto, P.P., Dickinson, S.C., Hollander, A.P., Mantero, S., Conconi, M.T., Birchall, M.A. (2008) Clinical transplantation of a tissue-engineered airway. *Lancet*, 372, 2023–2030.

Marijnissen, W.J.C.M., van Osch, G.J.V.M., Aigner, J., van der Veen, S.W., Hollander, A.P., Verwoerd-Verhoef, H.L., Verhaar, J.A.N. (2002) Alginate as a chondrocyte-delivery substance in combination with a non-woven scaffold for cartilage tissue engineering. *Biomaterials*, 23, 1511-1527.

Martel-Pelletier, J., Boileau, C., Pelletier, J.P., Roughley, P.J. (2008) Cartilage in normal and osteoarthritis conditions. *Best Pract Res Clin Rheumatol*, 22, 315-384.

Martinello, T., Bronzini, I., Volpin, A., Vindigni, V., Maccatrozzo, L., Caporale, G., Bassetto, F., Patruno, M. (2012) Successful recellularization of human tendon scaffolds using adipose-derived mesenchymal stem cells and collagen gel. *J Tissue Eng Regen Med*, http://dx.doi.org/10.1002/term.1557

Maude, S., Ingham, E., & Aggeli, A. (2013) Biomimetic self-assembling peptides as scaffolds for soft tissue engineering. *Nanomedicine*, 8, 823-847.

McCullen, S.D., Autefage, H., Callanan, A., Gentleman, E., Stevens, M.M. Anisotropic fibrous scaffolds for articular cartilage regeneration. *Tissue Eng*, 18, 2073- 2083.

McGonagle, D., Tan, A.L., Carey, J., Benjamin, M. (2010) The anatomical basis for a novel classification of osteoarthritis and allied disorders. *J Anat*, 216, 279–291.

McLure, S.W.D., Fisher, J., Conaghan, P.G., Williams, S. (2012) Regional cartilage properties of three quadruped tibiofemoral joints used in musculoskeletal research studies. *Proc IMechE Part H: J Engineering in Medicine*, 226, 652–656.

Melrose, J., Hayes, A.J., Whitelock, J.M., Little, C.B. (2008) Perlecan, the “jack of all trades” proteoglycan of cartilaginous weight-bearing connective tissues. *BioEssays*, 3, 457-469.

Mendler, M., Eich-Bender, S.G., Vaughan, L., Winterhalter, K.H., Bruckner, P. (1989) Cartilage contains mixed fibrils of collagen types II, IX, and XI. *J Cell Biol*, 108, 191-197.

Miles, D. E., Mitchell, E., Kapur, N., Wilcox, R. K., & Aggeli, A. (2012) Design of self-assembling peptide/glycosaminoglycan hydrogels for spinal therapies. *J Tissue Eng Regen Med*, 6, 40.

Mills, C.D., Kincaid, K., Alt, J.M., Heilman, M.J., Hill, A.M. (2000) M-1/M-2 macrophages and the Th1/Th2 paradigm. *J Immunol*, 164, 6166-6173.

Minas, T. (2001) Autologous chondrocyte implantation for focal chondral defects of the knee. *Clin Orthop Relat Res*, 391, 349-361.

Minas, T., Nehrer, S. (1997) Current concepts in the treatment of articular cartilage defects. *Orthopedics*, 20, 525-538.

Mirsadraee, S. (2006) Tissue Engineering of Pericardium. PhD, University of Leeds.

Moradi, B., Schönit, E., Nierhoff, C., Hagmann, S., Oberle, D., Gotterbarm, T., Schmitt, H., Zeifang, F. (2012) First-generation autologous chondrocyte implantation in patients with cartilage defects of the

knee: 7 to 14 years' clinical and magnetic resonance imaging follow-up evaluation. *Arthroscopy*, 12, 1851-1861.

Moseley, J.B., O'Malley, K., Petersen, N.J., Menke, T.J., Brody, B.A., Kuykendall, D.H., Hollingsworth, J.C., Ashton, C.M., Wray, N.P. (2002) A controlled trial of arthroscopic surgery for osteoarthritis of the knee. *N Engl J Med*, 347, 81-88.

Mow, V.C., Gu, W.Y., Chen, F.H. (2005) Structure and function of articular cartilage and meniscus. In: Family name, Mow, V.C., Huiskes, R. eds. Basic orthopaedic biomechanics and mechano-biology. Philadelphia: Lippincott Williams & Wilkins,181-258.

Mow, V.C., Holmes, M.H., Lai, W.M. (1984) Fluid transport and mechanical properties of articular cartilage: a review. *J Biomechanics*, 17, 377-394.

Muir, H. Bullough, P., Maroudas, A. (1970) The distribution of collagen in human ar,ticular cartilage with some of its physiological implications. *J Bone Joint Surg Br*, 52, 554-63.

Müller, F.A., Müller, L., Hofmann, I., Greil, P., Wenzel, M.M., Staudenmaier, R. (2006) Cellulose-based scaffold materials for cartilage tissue engineering. *Biomaterials*, 27, 3955-3963.

National Institute for Health and Care Excellence. (2008) The use of autologous chondrocyte implantation for the treatment of cartilage defects in knee joints. [TA89]. London: National Institute for Health and Care Excellence.

Nikitovic, D., Katonis, P., Tsatsakis, A., Karamanos, N.K., Tzanakakis, G.N. (2008) Lumican, a small leucine-rich proteoglycan. *IUBMB Life*, 60, 818-823.

O'Driscoll, S.W., Keeley, F.W., Salter, R.B. (1988) Durability of regenerated articular cartilage produsedby free autogenous periosteal grafts in major full-thickness defects in joint surfaces under the influence of continuous passive motion. A follow up report at one year. *J Bone Joint Surg Am*, 70, 595-606.

Oliveira, J.T., Martins, L., Picciochi, R., Malafaya, P.B., Sousa, R.A., Neves, N.M., Mano, J.F., Reis, R.L. (2010) Gellan gum: a new biomaterial for cartilage tissue engineering applications. *J Biomed Mater Res*, 93, 852-863.

Outerbridge, R.E. (1961) The etiology of chondromalacia patellae. *J Bone Joint Surg Br*, 43, 752-757.

Pan, Y., Xiong, D. (2009) Friction properties of nano-hydroxyapatite reinforced poly(vinyl alcohol) gel composites as an articular cartilage. *Wear*, 266, 699-703

Patience, C., Takeuchi, Y., Weiss, R.A., (1997) Infection of human cells by an endogenous retrovirus of pigs. *Nat Med*, 3, 282-286.

Paul, J.P. (1976) Force actions transmitted by joints in the human body. *P Roy Soc Lond B Bio*, 192, 163-72.

Pawaskar, S.S., Fisher, J., Jin, Z. (2010) Robust and general method for determining surface fluid flow boundary conditions in articular cartilage contact mechanics modelling, *J Biomech Eng-T ASME*, 132, 1-8.

Pawaskar, S.S., Grosland, N.M., Ingham, E., Fisher, J., Jin, Z. (2011) Hemiarthroplasty of hip joint: An experimental validation using porcine acetabulum. *J Biomechanics*, 44, 1536–1542.

Pettenger, M.F., Mackay, A.M., Beck, S.C., Jaiswal, R.K., Douglas, R., Mosca, J.D., Moorman, M.A., Simonetti, D.W., Craig, S., Marshak, D.R. (1999) Multilineage potential of adult human mesenchymal stem cells. *Science*, 284, 143-147.

Poole, C.A. (1997) Articular cartilage chondrons: form, function and failure. *J Anat*, 191, 1-13.

Pruss, A., Kao, M., Kiesewetter, H., von Versen, R., Pauli G. (1999) Virus safety of avital bone tissue transplants: evaluation of sterilization steps of spongiosa cuboids using a peracetic acid–methanol mixture. *Biologicals*, 27, 195–201.

Puppi, D., Chiellini, F., Piras, A.M., Chiellini, E. (2010) Polymeric materials for bone and cartilage repair. *Prog Polym Sci*, 35, 403–440.

Raeder, R. H., Badylak, S. F., Sheehan, C., Kallakury, B., & Metzger, D. W. (2002) Natural anti-galactose α1, 3 galactose antibodies delay, but do not prevent the acceptance of extracellular matrix xenografts. *Transpl Immunol*, 10, 15-24.

Reing, J.E., Brown, B.N., Daly, K.A., Freund, J.M., Gilbert, T.W., Hsiong, S., Huber, A., Kullas, K.E., Tottey, S., Wolf, M., Badylak, S.F. (2010) The effects of processing methods upon mechanical and biologic properties of porcine dermal extracellular matrix scaffolds. *Biomaterials*, 31, 8626–8633.

Reinwald, S., Burr, D. (2008) Review of nonprimate, large animal models for osteoporosis research. *J Bone Miner Res*, 23, 1353–1368.

Rhee, D.K., Marcelino, J., Baker, M., Gong, Y., Smits, P., Lefebvre, V., Jay, G.D., Stewart, M., Wang, H., Warman, M.L., Carpten, J.D. (2005) The secreted glycoprotein lubricin protects cartilage surfaces and inhibits synovial cell overgrowth. *J Clin Invest*, 115, 622-631.

Rieder, E., Kasimir, M., Silberhumer, G., Seebacher, G., Wolner, E., Simon, P., Weigel, G. (2004) Decellularization protocols of porcine heart valves differ importantly in efficiency of cell removal and susceptibility of the matrix to recellularization with human vascular cells. *J Thorac Cardiovasc Surg*, 127, 399-405.

Rieppo J., Hyttinen, M.M. Halmesmaki, E., Ruotsalainen, H., Vasara, A., Kiviranta, I., Jurvelin, J.S., Helminen, H.J. (2009) Changes in spatial collagen content and collagen network architecture in porcine articular cartilage during growth and maturation. *Osteoarthr Cartil*, 17, 448-455.

Rogers, B. A., Murphy, C. L., Cannon, S. R., Briggs, T. W. R. (2006) Topographical variation in glycosaminoglycan content in human articular cartilage. *J Bone Joint Surg Br*, 88,1670-1674.

Roughley, P.J. (2001) Articular cartilage and changes in arthritis, noncollagenous proteins and proteoglycans in the extracellular matirx of cartilage. *Arthritis Res*, 3, 342-347.

Roughley, P.J., (2006) The structure and function of cartilage proteoglycans. *Eur Cell Mater*, 12, 92-101.

Roughley, P.J., White, R.J. (1980) Age-related changes in the structure of the proteoglycan subunits from human articular cartilage. *J Bio Chem*, 255, 217-24.

Samouillan, V., Lamure, A., Maurel, E., Dandurand, J., Lacabanne, C., Ballarin, F., Spina, M. (2000) Characterisation of elastin and collagen in aortic bioprostheses. *Med Biol Eng Comput*, 38, 226-231.

Saxne, T., Heinegård, D. (1992) Cartilage oligomeric protein: a novel marker of cartilage turnover detectable in synovial fluid and blood. *Br J Rheumatol*, 31, 583-591.

Schaefer, D., Martin, I., Jundt, G., Seidel, J., Heberer, M., Grodzinsky, A., Bergin, I., Vunjak-Novakovic, G., Freed, L.E. (2002) Tissue engineered composites for the repair of large osteochondral defects. *Arthritis Rheum*, 46, 2524-2534.

Schindler, O.S. (2011) Current concepts of articular cartilage repair. *Acta Orthop Belg*, 77, 709-726.

Schoen, F.J., Levy, R.J. (2005) Calcification of tissue heart valve substitutes: progress toward understanding and prevention. *Ann Thorac Surg*, 79, 1072– 80.

Schwarz, S., Koerber, L., Elsaesser, A.F., Goldberg-Bockhorn, E., Seitz, A.M., Dürselen, L., Ignatius, A., Walther, P., Breiter, R., Rotter, N. (2012) Decellularized cartilage matrix as a novel biomatrix for cartilage tissue-engineering applications. *Tissue Eng*, 18, 2195-2209.

Scott, J.E. (1992) Supramolecular organization of extracellular matrix proteoglycans, in vitro and in the tissues. *FASEB J*, 6, 2639- 2645.

Seddon, A.M., Curnow, P., Booth, P.J. (2004) Membrane proteins, lipids and detergents: not just a soap opera. *Biochim Biophys Acta*, 1666, 105–117.

Segat, D., Paulsson, M., Smyth, N. (2001) Matrillins: structure, expression and function. *Osteoarthr Cartil*, 9, S29-S35.

Shanfield, S., Campbell, P., Baumgarten, M., Bloebaum, R.D., Sarmiento, A. (1986) Synovial fluid osmolality in osteoarthritis and rheumatoid arthritis. *Clin Orthop Relat Res*, 235, 289-295.

Shen, G. (2005) The role of type X collagen in facilitating and regulating endochondral ossification of articular cartilage. *Orthod Craniofacial Res*, 8; 11–17.

Shepherd, D.E.T., Seedhom, B.B. (1999a) Thickness of human articular cartilage in joints of the lower limb. *Ann Rheum Dis*, 58, 27-34.

Shepherd, D.E.T., Seedhom, B.B. (1999b) The 'instantaneous' compressive modulus of human articular cartilage in joints of the lower limb. *Rheumatology*, 38, 124-132.

Simon, W.H., Freidenberg, S., Richardson, S., (1973) Joint congruence: a correlation of joint congruence and thickness of articular cartilage in dogs. *J Bone Joint Surg Am*, 55, 1614-1620.

Sinnatamby, C.S. (2011). Last's anatomy: regional and applied. 11th edition. London: Churchill Livingsone.

Sokal, R.R., Rohlf, .F.J. (1995) Biometry: the principals and practice of statistics in biological research. 3rd edition. New York: W.H. Freeman and company.

Solheim, E., Hegna, J., Øyen, J., Austgulen O.K., Harlem T., Strand, T. (2010) Osteochondral autografting (mosaicplasty) in articular cartilage defects in the knee: Results at 5 to 9 years. *The Knee*, 17, 84–87.

Solheim, E., Hegna, J., Øyen, J., Harlem T., Strand, T. (2013) Results at 10 to 14 years after osteochondral autografting (mosaicplasty) in articular cartilage defects in the knee. *The Knee*, 20, 287–290.

Stapleton, T. (2008b) Development and characterisation of an acellular porcine medial meniscus for use in tissue engineering. PhD, University of Leeds.

Stapleton, T., Ingram, J., Fisher, J., Ingham, E. (2010) Investigation of the regenerative capacity of an acellular porcine medial meniscus for tissue engineering applications. *Tissue Eng*, 17, 231–242.

Stapleton, T., Ingram, J., Katta, J., Knight, R., Korossis, S., Fisher, J., Ingham, E. (2008) Development and characterization of an acellular porcine medial meniscus for use in tissue engineering. *Tissue Eng*, 14, 505-518.

Steadman, J.R., Briggs, K.K., Rodrigo, J.J., Kocher, M.S., Gill, T.J., Rodkey, W.G. (2003) Outcomes of microfracture for traumatic chondral defects of the knee: average 11-year follow-up. *Arthroscopy*, 19, 477-484.

Steinwachs, M.R., Guggi, T.H., Kreuz, P.C. (2008) Marrow stimulation techniques. *Injury*, 39, 26-31

Steplewski, A., Hintze, V., Fertala, A. (2007) Molecular basis of organization of collagen fibrils. *J Struct Biol*, 157, 297–307.

Stockwell, R.A. (1971) The interrelationship of cell density and cartilage thickness in mammalian articular cartilage, *J Anat*, 109, 411-421.

Stockwell, R.A. (1976) The cell density of human articular and costal cartilage. *J Anat*, 101, 753-763.

Stone, K. R., Ayala, G., Goldstein, J., Hurst, R., Walgenbach, A., & Galili, U. (1998) Porcine cartilage transplants in the cynomolgus monkey: III. Transplantation of [alpha]-galactosidase-treated porcine cartilage. *Transplantation*, 65, 1577-1583.

Stone, K. R., Walgenbach, A. W., Abrams, J. T., Nelson, J., Gillett, N., & Galili, U. (1997) Porcine and bovine cartilage transplants in cynomolgus monkey: I. A model for chronic xenograft rejection. *Transplantation*, 63, 640-645.

Takahashi, K., Tanabe, K., Ohnuki, M., Narita, M., Ichisaka, T., Tomoda, K., Yamanaka, S. (2007) Induction of pluripotent stem cells from adult human fibroblasts by defined factors. *Cell*, 131, 861-872.

Taylor, S.D., Tsiridis, E., Ingham, E., Jin, Z., Fisher, J., Williams, S. (2011) Comparison of human and animal femoral head chondral properties and geometries. *Proc IMechE Part H: J Engineering in Medicine*, 226, 55-62.

Teichtahl, A.J., Wluka, A.E., Proietto, J., Cicuttini, F.M. (2005) Obesity and the female sex, risk factors for knee osteoarthritis that may be attributable to systemic or local leptin biosynthesis and its cellular effects. *Med Hypotheses*, 65, 312-315.

Thambya, A., Nather, A., Goh, J. (2006) Mechanical properties of articular cartilage covered by the meniscus. *Osteoarthr Cartilage*, 14, 580-588.

Unsworth, A. (1991) Tribology of human and artificial joints. *Proc IMechE Part H: J Engineering in Medicine*, 205, 163-172.

Valderrabano, V., Miska, M., Leumann, A., Wiewiorski, M. (2013) Reconstruction of osteochondral lesions of the talus with autologous spongiosa grafts and autologous matrix-induced chondrogenesis. *Am J Sports Med*, 41, 519-527.

van Susante, J.L.C., Buma, P., Homminga, G.N., van den Berg, W.B., Veth, R.P.H. (1998) Chondrocyte-seeded hydroxyapatite for repair of large articular cartilage defects. A pilot study in the goat. *Biomaterials*, 19, 2367-2374.

Vangsness, C.T., Garcia, I.A., Mills, C.R., Kainer, M.A., Roberts, M.R., & Moore, T.M. (2003) Allograft transplantation in the knee: tissue regulation, procurement, processing, and sterilization. *Am J Sports Med*, 31, 474-481.

Vavken, P., Joshi, S., Murray, M.M, (2009) Triton-X Is most effective among three decellularization agents for ACL tissue engineering. *J Orthop Res*, 27, 1612–1618.

Verzjil, N., DeGroot, J, Zaken C.B., Braun-Benjamin, O., Maoudas, A., Bank, R.A., Mizrahi, J., Schalkwijk, C.G., Thorpe S.R., Baynes J.W.,

Bijlsma, J.W., Lafeber, F.P.J.G., TeKoppele, J.M. (2002) Crosslinking by advanced glycation end products increases the stiffness of the collagen network in human articular cartilage. *Arthritis Rheum*, 46, 114–123.

Vilim, V., Krajickova, J. (1991) Proteoglycans of human articular cartilage. *Biochem J*, 273, 579-85.

Vinatier, C., Mrugala, D., Jorgensen, C., Guicheux, J., Noël, D. (2009) Cartilage engineering: a crucial combination of cells, biomaterials and biofactors. *Trends Biotechnol*, 27, 307-314.

Vuolteenaho, K., Moilanen, T., Knowles, R.G., Moilanen, E. (2007) The role of nitric oxide in osteoarthritis. *Scand J Rheumatol*, 36, 247-258.

Wagener, R., Ehlen, H.W.A., Koa Y., Kobbe, B., Mann, H.H., Sengle, G., Paulsson, M. (2005) The matrilins – adaptor proteins in the extracellular matrix. *FEBS Lett*, 579, 3323–3329.

Wakayama, T., Tabar, V., Rodriguez, I., Perry, A.C.F., Studer, L., Mombaerts, P. (2001) Differentiation of embryonic stem cell lines generated from adult somatic cells by nuclear transfer. *Science*, 292, 740-742

Wakitani, S., Goto, T., Pineda, S.J., Young, R.G., Mansour, J.M., Caplan, A.I., Goldberg, V.M. (1994) Mesenchymal cell-based repair of large, full-thickness defects of articular cartilage. *J Bone Joint Surg Am*, 67, 579-592.

Walker, P.S., Dowson, D., Longfield, M.D., Wright, V. (1968) “Boosted lubrication” in synovial joints by fluid entrapment and enrichment. *Ann Rheum Dis*, 27, 512-520.

Whitesides, G.M., Mathias, J.P., & Seto, C.T. (1991) Molecular self-assembly and nanochemistry: a chemical strategy for the synthesis of nanostructures. *Science*, 254, 1312-1319.

Wickham, E.A. (1996) Potential transmission of BSE via medicinal products. *BMJ*, 312, 988.

Woods, T., Gratzer, P.F. (2005) Effectiveness of three extraction techniques in the development of a decellularized bone–anterior cruciate ligament–bone graft. *Biomaterials*, 26, 7339–7349.

Wu, S., Liu, Y., Bharadwaj, S., Atala, A., Zhang, Y. (2011) Human urine-derived stem cells seeded in a modified 3D porous small intestinal submucosa scaffold for urethral tissue engineering. *Biomaterials*, 32, 1317-1326.

Yang, Q., Peng, J., Guo, Q., Huang, J., Zhang, L., Yao, J., Yang, F Wang, S., Xu, W., Wang, A., Lu, S. (2008) A cartilage ECM-derived 3-D porous acellular matrix scaffold for in vivo cartilage tissue engineering with PKH26-labeled chondrogenic bone marrow-derived mesenchymal stem cells. *Biomaterials*, 29, 2378-2387.

Yang, Z., Shi, Y., Wei, X., He, J., Yang, S., Dickson, G., Tang, J., Xiang, J., Song, C., Li, G. (2010) Fabrication and repair of cartilage defects with a novel acellular cartilage matrix scaffold. *Tissue Eng*, 16, 865-876.

Appendix A
Materials

Table 1 Equipment used throughout the study.

Equipment	Model	Supplier
Automatic Pipettes	Gilson P2-P1000	Anachem Ltd
Balances (Accuracy: 0.01g/0.0001g)	GR200/GX2000	Jencons PLC
Bench top centrifuge	5415R	Eppendorf
Class II safety cabinet	Heraeus 85	Kendro
CO_2 Incubator	MCO-20AIC	SANYO Biomedical Europe BV
Freeze drier	Modulyod-230	Thermo Savant
Freezer (-20 °C)	Electrolux 3000	Jencons PLC
Fridge	Electrolux ER8817C	Jencons PLC
Fume cupboard/Fume hood	-	Whiteley
Histology cassettes	CMB-160-030R	Thermo Fisher Scientific Ltd
Histology water bath	MH8515	Barnstead
Hot plate	E18.1 hotplate	Raymond A Lamb
Hot wax dispenser	E66 was dispenser	Raymond A Lamb
Incubator	Heraeus	Jencons PLC
Instron material testing machine	3365	Instron
Linear variable differential transformer (LVDT)	RDP DS-200H	Electrosence
Liquid nitrogen Dewar	BIO65	Jencons PLC
Luminescence counter and liquid scintillation counter	Packard TopCount NX	Perkin Elmer
Magnetic stirrer	Stuart SB161	Scientific Laboratory Systems Ltd
Micro- osmometer	3MO Plus Freezing Point Osmometer	Advanced Instruments
Micro-plate	Multiscan Spectrum 1500	Thermo Scientific

spectrophotometer		
Microscope (Inverted)	Olympus IX71	Microscopes, Medical Diagnostics Systems and Olympus Patient Systems Ltd
Microscope (upright)	Olympus BX51	Microscopes, Medical Diagnostics Systems and Olympus Patient Systems Ltd
Microtome	RM2125 RTR	Leica Microsystems
Nanodrop Spectrophotometer	ND-1000	Labtech Int
Neubauer haemocytometer	MNK-420-010N	Fischer scientific
Orbital Shaker	IKA KS130 basic	Jencons PLC
Oven (hot air)		
pH meter	Jenway 3010	VWR International
Piezo-electric force transformer	060-1896-02	Electrosence
Pipette boy	Acu	Integra biosciences
Plate Shaker	IKA KS130 basic	Jencons PLC
Slide holder	E102	Raymond A Lamb
Tissue Processor	TP11020	Leica Microsystems
Vortexer	Topmix FB15024	Fisher Scientific
Water Bath	Grant	Jencons PLC
Water Pik Ultra Water Flosser	WP100	WaterPik
Water purifier	Option 7	ELGA
Wax oven	Windsor E18/31	Scientific Laboratory Supplies

Table 2 Chemicals/reagents used throughout the study.

Chemical/Reagent	Supplier
1,9 dimethylene blue	Sigma-Aldrich
^{14}C labelled SDS	Hartmann Analytical
Acetic Acid	Thermo Fisher Scientific Ltd
Acetone	European Bios
Alcian blue	Atom Scientific
Aprotinin (10,000 KUI)	Mayfair house
ATP-Lite-M® assay	Perkin Elmer Ltd
Bovine Serum Albumin	Sigma-Aldrich
Calcium Chloride	VWR International
Calf thymus DNA	Sigma-Aldrich
Chloramine T	Sigma-Aldrich
Chondroitin sulphate B	Sigma-Aldrich
Citric acid	VWR International
Cyanoacrylate	Sigma-Aldrich
DABCO	Sigma-Aldrich
DABCO	Sigma-Aldrich
DAPI	Sigma-Aldrich
Dimethyl sulfoxide (DMSO)	Sigma-Aldrich
di-sodium hydrogen orthophosphate	VWR International
DMSO	Sigma-Aldrich
Dnase	Sigma-Aldrich
DNase	Sigma-Aldrich
Dneasy blood & tissue kit	Qiagen
DNeasy blood and tissue kit	Qiagen
DPX mountant	Thermo Fisher Scientific Ltd
Dulbecco's modified Eagle's medium (DMEM)	Gibco Life Technologies Ltd.
Dulbecco's modified Eagles medium	Invitrogen Ltd
Dulbecco's PBS tablets	Oxoid
Eosin	VWR International
Ethanol	Thermo Fisher Scientific Ltd
Ethylenediaminetetraacetic acid (EDTA)	VWR International
Fast green	Sigma
Foetal bovine serum	Lonza

Formic acid	Sigma-Aldrich
Gentamycin	Sigma-Aldrich
Glasgows modified Eagle's medium (GMEM)	Gibco Life Technologies Ltd.
Glycerol	Sigma-Aldrich
Glycerol	Sigma-Aldrich
Haematoxylin (Gill's no. 3)	Sigma-Aldrich
Haematoxylin (Mayers)	Thermo Fisher Scientific Ltd
Haematoxylin (Weigert's)	Atom Scientific
Hirudin	Sigma-Aldrich
Hydrochloric acid	VWR International
Hydrogen peroxide	Sigma-Aldrich
ImmEdge Hydrophobic Barrier Pen	Vector laboratories
Isopropanol	Thermo Fisher Scientific Ltd
L-cystine hydrochloride	Sigma-Aldrich
L-glutamine	Lonza
Magnesium Chloride	Thermo Fisher Scientific Ltd
Mannitol	Sigma-Aldrich
Methanol	Vichers Laboratories
MicroScint™-20	Perkin Elmer Ltd
Miller'S STAIN	Raymond A Lamb
Monosodium citrate	Sigma-Aldrich
Neutral buffered formalin (10% v/v)	Genta Medical
Oxalic acid	Thermo Fisher Scientific Ltd
Papain	Sigma-Aldrich
Paraffin wax	Thermo Fisher Scientific Ltd
PBS with Ca^{2}/Mg^{2+}	lonza
PBS without Ca^{2}/Mg^{2+}	Lonza
p-dimethylaminobenzaldehyde	Sigma-Aldrich
Penicillin	Lonza
Peracetic acid	Sigma-Aldrich
Perchloric acid	BDH
Periodic acid	Sigma-Aldrich
pH standards (4, 7, 10)	Scientific Laboratory Supplies Ltd
Piric acid	Sigma-Aldrich
Potassium permanganate	Thermo Fisher Scientific Ltd

Propan-1-ol	VWR International
rans-4-hydroxy-L-proline	Sigma-Aldrich
RNAse	Sigma-Aldrich
RNase	Sigma-Aldrich
Safranin O	Acros
Schiff's Reagent	Sigma-Aldrich
Sirius red	Raymond A Lamb
Sodium acetate	Thermo Fisher Scientific Ltd
Sodium azide	G Biosciences
Sodium chloride	Thermo Fisher Scientific Ltd
sodium di-hydrogen orthophosphate	VWR International
Sodium dodecyl sulphate (SDS)	Sigma-Aldrich
Sodium formate	VWR International
Sodium hydrogen carbonate	VWR International
Sodium Hydroxide	VWR International
Steri-Strip	Medisave
Streptomycin	Lonza
Sulphuric acid	Sigma-Aldrich
Trigene	Scientific Laboratory Supplies Ltd
Trizma base	Sigma-Aldrich
Trypan blue	Sigma-Aldrich
Trypsin	Sigma-Aldrich
Trypsin/EDTA solution	Sigma-Aldrich
Tryptone phosphate broth (TPB)	Sigma-Aldrich
Tween 20	Sigma-Aldrich
Ultra Vision One detection system, HRP polymer	Thermo Fisher Scientific Ltd
Ultra Vision One Large Volume Detection System, DAB plus substrate System	Thermo Fisher Scientific Ltd
Virkon	Scientific Laboratory Supplies Ltd
Xylene	Genta Medical
α-chymotrypsin	Sigma-Aldrich

Table 3 General consumables used throughout the study.

Item	Model/Size	Supplier
Cryovials	Cryolife™	Nunc International Corporation
Glass coverslips	MIC3228	Scientific Laboratory Supplies Ltd
Microtome Blades	SD3050835	Fisher Scientific
Parafilm M	-	Sigma-Aldrich
Scalpel blade	Size 22A	Fisher Scientific
Superfrost Plus microscope slide	MIC3022	Scientific Laboratory Supplies Ltd
Syringe needles	-	Thermo Fisher Schientific Ltd

Table 4 Plasticware used throughout the study.

Item	Model/Size	Supplier
Bijous	5 ml	Scientific Laboratory Supplies Ltd
Cell culture flasks	T75, 75 cm^2	Thermo Fisher Scientific Ltd
Disposable plastic syringes	1 ml, 2 ml, 5 ml, 10 ml, 20 ml, 50 ml	Scientific Laboratory Supplies Ltd
Pipette tips (filtered and non-filtered)	10 µl, 20 µl, 200 µl, 1000 µl	Star Labs
OptiplateTM	96-well	PerkinElmerTM
Sterile containers	60 ml, 150 ml, 250 ml	Scientific Laboratory Supplies Ltd
Stripette (disposable pipettes)	1 ml, 2 ml, 5 ml, 10 ml, 25 ml	Sigma-Aldrich Ltd
Universals	25 ml	Scientific Laboratory Supplies Ltd
Well plates, Nunc® (flat bottomed)	6-well, 12-well, 24-well, 48-well, 96-well plates	Nunc International Corporation

Appendix B
Publications

- Fermor, H.L., McLure, S.W.D., Taylor, S.D., Russell, S.L., Williams, S., Fisher, J., Ingham, E. Biological, biochemical and biomechanical characterisation of articular cartilage from the porcine, bovine and ovine hip and knee. *Bio-Med Mater Eng,* In press.

- Fermor, H.L., McLure, S.W.D., Taylor, S.D., Russell, S.L., Williams, S., Fisher, J., Ingham, E. (2012) Biological, biochemical and biomechanical characterisation of cartilage from the porcine, bovine and ovine hip and knee. *J Tissue Eng Regen Med*, 6, 66-66. (Published abstract)

- Hasan, J., Jones, G., Fermor, H.L., Fisher, J., Ingham, E. Priority date 4th September 2013. Filed UK Patent – Composite connective tissue and bone implants. No. GB1215725.1.

Appendix C
Presentations

- Fermor, H.L., Russell, S.L., Williams, S., Fisher, J. Ingham, E. (2011) Engineering of natural cartilage substitution biomaterials. TCES, Leeds, UK.

- Fermor, H.L., McLure, S.W.D., Taylor, S.D., Russell, S.L., Williams, S., Fisher, J., Ingham, E. (2011) Biological, biochemical and biomechanical characterisation of articular cartilage from the porcine, bovine and ovine hip and knee. BiTEG, York, UK.

- Fermor, H.L., McLure, S.W.D., Taylor, S.D., Russell, S.L., Williams, S., Fisher, J., Ingham, E. (2012) Biological, biochemical and biomechanical characterisation of articular cartilage from the porcine, bovine and ovine hip and knee. Regener8, Gateshead, UK.

- Fermor, H.L., McLure, S.W.D., Taylor, S.D., Russell, S.L., Williams, S., Fisher, J., Ingham, E. (2012) Biological, biochemical and biomechanical characterisation of articular cartilage from the porcine, bovine and ovine hip and knee. TERMIS, Vienna, Austria.

- Fermor, H.L., Russell, S.L., Williams, S., Fisher, J., Ingham, E. (2013) Development of an acellular xenogenic osteochondral biomaterial. ORS, San Antonio, TX, USA.